

Berichte

zur Polar-
und Meeresforschung

621
2010

Reports
on Polar and Marine Research



The Expedition of the Research Vessel "Polarstern"
to the Arctic in 2010 (ARK-XXV/3)

Edited by
Volkmar Damm
with contributions of the participants



ALFRED-WEGENER-INSTITUT FÜR
POLAR- UND MEERESFORSCHUNG
in der Helmholtz-Gemeinschaft
D-27570 BREMERHAVEN
Bundesrepublik Deutschland

ISSN 1866-3192

Hinweis

Die Berichte zur Polar- und Meeresforschung werden vom Alfred-Wegener-Institut für Polar- und Meeresforschung in Bremerhaven* in unregelmäßiger Abfolge herausgegeben.

Sie enthalten Beschreibungen und Ergebnisse der vom Institut (AWI) oder mit seiner Unterstützung durchgeführten Forschungsarbeiten in den Polargebieten und in den Meeren.

Es werden veröffentlicht:

- Expeditionsberichte (inkl. Stationslisten und Routenkarten)
- Expeditionsergebnisse (inkl. Dissertationen)
- wissenschaftliche Ergebnisse der Antarktis-Stationen und anderer Forschungs-Stationen des AWI
- Berichte wissenschaftlicher Tagungen

Die Beiträge geben nicht notwendigerweise die Auffassung des Instituts wieder.

Notice

The Reports on Polar and Marine Research are issued by the Alfred Wegener Institute for Polar and Marine Research in Bremerhaven*, Federal Republic of Germany. They appear in irregular intervals.

They contain descriptions and results of investigations in polar regions and in the seas either conducted by the Institute (AWI) or with its support.

The following items are published:

- expedition reports (incl. station lists and route maps)
- expedition results (incl. Ph.D. theses)
- scientific results of the Antarctic stations and of other AWI research stations
- reports on scientific meetings

The papers contained in the Reports do not necessarily reflect the opinion of the Institute.

The „Berichte zur Polar- und Meeresforschung“
continue the former „Berichte zur Polarforschung“

* Anschrift / Address

Alfred-Wegener-Institut
für Polar- und Meeresforschung
D-27570 Bremerhaven
Germany
www.awi.de

Editor in charge:
Dr. Horst Bornemann

Assistant editor:
Birgit Chiaventone

Die "Berichte zur Polar- und Meeresforschung" (ISSN 1866-3192) werden ab 2008 ausschließlich als Open-Access-Publikation herausgegeben (URL: <http://epic.awi.de>).

Since 2008 the "Reports on Polar and Marine Research" (ISSN 1866-3192) are only available as web based open-access-publications (URL: <http://epic.awi.de>)

The Expedition of the Research Vessel "Polarstern" to the Arctic in 2010 (ARK-XXV/3)

**Edited by
Volkmar Damm
with contributions of the participants**

**Please cite or link this publication using the identifier
hdl:10013/epic.36297 or <http://hdl.handle.net/10013/epic.36297>**

ISSN 1866-3192

ARK-XXV/3



1 August - 9 October 2010

Reykjavik - Bremerhaven

**Chief scientist
Volkmar Damm**

**Coordinator
Eberhard Fahrbach**

CONTENTS

Summary	1
Zusammenfassung	3
1. Preface	4
2. Scientific programme	6
2.1 Geological and tectonic framework	6
2.2 Previous surveys and existing data	7
2.3 Objectives	9
2.4 Work at Sea	10
3. Cruise narrative	14
4. Navigation and data management	23
5. Multi-beam bathymetry	26
6. Sediment echosounding	33
6.1 Method and instrument control	33
6.2 Processing	38
6.3 Example results	40
6.4 Testing of different SLF frequencies	43
7. Gravimetry	44
7.1 Method and instrument	44
7.2 Data processing	46
7.3 Gravity ties to land stations	47
7.4 Data quality and preliminary results	51
7.5 Gravity data: description and preliminary results	53

8. Magnetics	64
8.1 Marine magnetometer systems and operation	64
8.2 Data acquisition	67
8.3 Data processing and calibration	70
8.4 Preliminary results	74
9. Seismics	81
9.1 Methods	81
9.2 Marine mammal observation to comply with environmental regulations	81
9.3 Seismic equipment and survey setup	83
9.4 Processing of multi-channel reflection data	95
9.5 Preliminary results of MCS data	109
9.6 Processing and preliminary results of wide-angle sonobuoy data	113
9.7 Processing of refraction/wide-angle OBS data and landstations	116
9.8 Review of refraction/wide-angle OBS data	119
10. Heat flow measurements	126
10.1 Method and instrument	126
10.2 Station work and preliminary results	129
11. Sediment coring	132
11.1 Instrumentation and procedures	132
11.2 Core description	133
12. Gas geochemistry	135
12.1 Methods and material	135

13. Biogeochemistry and geomicrobiology	136
13.1 Methods and instruments	137
13.2 Processing of core material	138
14. Onshore rock sampling	140
14.1 Objectives	140
14.2 Methods and materials	140
15. Joint interpretation of key profiles and discussion	142
15.1 Profile BGR10-306a	142
15.2 Profile BGR10-307/-307a	144
15.3 Profile BGR10-302/-302a	146
15.4 Profile BGR10-309	148
15.5 Profile BGR10-311	149
16. Conclusions and future work	154
17. Acknowledgements	155
18. References	156
A.1 Teilnehmende Institute / participating institutions	160
A.2 Fahrtteilnehmer / cruise participants	162
A.3 Schiffsbesatzung / ship's crew	163
A.4 Stationsliste / station list PS 76	164
A.5 Geophysical profile list	189
A.5A Exemplary processing work flow	192
A.6 OBS station list, profile BGR10-3r1	195
A.7 OBS station list, profile BGR10-3r2	196
A.8 OBS station list, profile BGR10-3r3	197

Contents

A.9 OBS station list, profile BGR10-3r4	198
A.10 List of land stations	199
A.11 Sonobuoy station list	200
A.12 Heat flow station list	201
A.13 Coring station list	202
A.14 Gas geochemistry sampling list	204
A.15 Onshore rock sampling list	205
A.16 Summary of helicopter operations	208
A.17 Weekly marine mammal observation reports	209
A.18 List of figures and tables	223

SUMMARY

Volkmar Damm

Bundesanstalt für Geowissenschaften und Rohstoffe

The multidisciplinary marine geoscientific expedition ARK-XXV/3 was focused on the Greenland part of northern Baffin Bay and was aimed to acquire new geoscientific data to be used for modelling the evolution of the Greenland continental margin and the hydrocarbons in the area. The cruise was performed under the lead of the Federal Institute for Geosciences and Natural Resources Hannover in cooperation with the Alfred Wegener Institute for Polar and Marine Research, Bremerhaven. Using 70 days of ship time onboard the research icebreaker R/V *Polarstern*, a comprehensive data set was acquired along profiles extending from the deep oceanic basin in the central part of North Baffin Bay onto the Greenland continental margin in an area which was bordered by the Kane Basin in the North and Disko Island in the South. By means of multi-channel seismic, wide angle seismic, gravimetric and magnetic methods, the structural inventory of the crust in the NW Baffin Bay was investigated. Additionally, heat flow data and sediment cores were collected along lines crossing the Greenland continental margin. The cores were extracted for geochemical and geomicrobiological analysis to be used for basin modelling and studying the hydrocarbon genesis, including their degradation by microorganisms under polar conditions. Geological sampling in the coastal area was done between Melville Bay and Washington Land. The collected rock material will be used to derive constraints on the erosion history of the coastal area. Aeromagnetic data was acquired covering a substantial part of the marine survey area to investigate magnetic signatures of the oceanic crust and the continental margin.

This report summarizes the working programme and contains the documentation of acquired data and first results of the expedition.

Summary

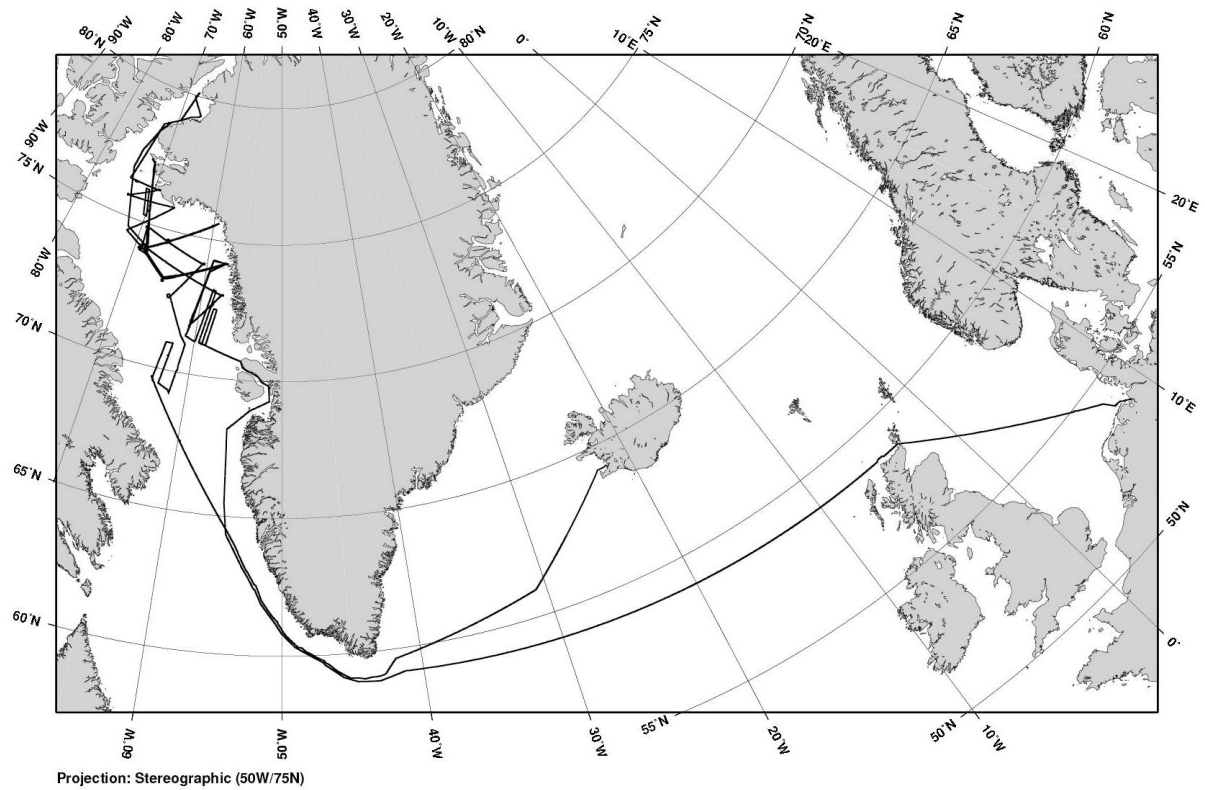


Fig. 1: Cruise track of Polarstern during ARK-XXV/3 from Reykjavik to the survey area North Baffin Bay and back to Bremerhaven

Abb.1. Fahrtverlauf von F/S Polarstern während ARK-XXV/3 von Reykjavik ins Messgebiet nördliche Baffinbay und Transit nach Bremerhaven

ZUSAMMENFASSUNG

Die Forschungsfahrt ARK-XXV/3 führte in den grönländischen Teil der nördlichen Baffin Bay. Schwerpunkt des wissenschaftlichen Programms bildeten multidisziplinäre marine Forschungsarbeiten zur Klärung der tektonischen Entwicklung des grönländischen Teils der Baffin Bay und der Entstehung von Kohlenwasserstoffen. Das Projekt wurde unter Federführung der Bundesanstalt für Geowissenschaften und Rohstoffe Hannover in Kooperation mit dem Alfred-Wegener-Institut, Bremerhaven, durchgeführt. Während der 70-tägigen Forschungsfahrt an Bord des F/S *Polarstern* wurde ein umfangreicher Datensatz entlang von Messprofilen akquiriert, die den Bereich vom Zentralteil der nördlichen Baffin Bay bis auf den grönländischen Kontinentrand und von Disko Island im Süden bis zum Kane Basin im Norden abdecken. Mit Hilfe von Mehrkanalseismik, Weitwinkelseismik, gravimetrischen und magnetischen Messverfahren wurde das strukturelle Inventar der Kruste in der nordwestlichen Baffin Bay untersucht. Zusätzlich wurden an mehr als 30 ausgewählten Lokationen entlang von Profilen über den grönländischen Kontinentrand Wärmestrommessungen vorgenommen und Sedimentkerne entnommen. Das Probenmaterial wird nachfolgend geochemisch und geomikrobiologisch analysiert. Die Ergebnisse fließen in Modellierungen der Beckenbildungsprozesse ein und werden für das Verständnis der Kohlenwasserstoffentstehung in der Region und der Kohlenwasserstoffzersetzung durch Mikroorganismen unter polaren Bedingungen verwendet. Geologische Beprobungen von Aufschlüssen der küstennahen Region zwischen Melville Bay und Washington Land wurden vorgenommen, um die Erosionsgeschichte des grönländischen Kontinentrandes zu rekonstruieren. Aeromagnetische Befliegungen in weiten Teilen des Arbeitsgebietes flankierten das marine Arbeitsprogramm zur Untersuchung magnetischer Signaturen der ozeanischen Kruste und des grönländischen Kontinentrandes.

Im vorliegenden Bericht werden Arbeitsprogramm und erste Ergebnisse der Forschungsfahrt dokumentiert.

1. PREFACE

Volkmar Damm
Bundesanstalt für Geowissenschaften und Rohstoffe

The focus of the original scientific programme of ARK-XXV/3 was on multidisciplinary geoscientific investigations to explain the structural and tectonic evolution of the crust in the Northern Baffin Bay and the adjacent continental margins at both the Canadian continental margin (from Northern Baffin Island as far as Ellesmere Island, including the eastern part of the Lancaster Sound), and the Greenland margin of North Baffin Bay. The expedition programme was planned as a cooperation project between the Federal Institute for Geosciences and Natural Resources, Hannover, the Alfred Wegener Institute for Polar and Marine Research, Bremerhaven, and National Resources of Canada, Earth Science Sector, Geological Survey of Canada, Dartmouth as part of an overall endeavour of international polar research to understand the geological history of the Arctic. Following a review of the environmental compatibility of the research activities, the Canadian and Greenland authorities had approved the expedition. The Canadian permit stipulated additional mitigation measures in order to minimize impacts on life in the oceans during the conduct of marine seismic surveys, e.g. that marine mammal observers have to be on board and that the safety zone around the centre of the air source array has to be increased from 500 metres to at least 1,000 metres. All the environmental regulations and restrictions that were stated by Canadian and Greenland authorities in their approvals have been followed and complied with. The Geological Survey of Canada had originally planned to utilise the scientific data gathered during the expedition in Canadian territory as a contribution to their national scientific projects. For example, it was foreseen that a very small part of the overall scientific research to be carried out during ARK-XXV/3 in Canadian waters was to be analysed also in the context of the Eastern Canadian Arctic Seismic Experiment (ECASE) project. However, since planning the joint cruise, local Inuit communities had expressed concerns about the ECASE project, and the project had become more and more the core of an inner-Canadian debate.

R/V *Polarstern* departed the port of Reykjavik Aug. 1, 2010 heading for the survey area shortly after the Canadian research permission was granted. Arriving in the Baffin Bay on Aug. 8, the ship's master and chief scientist were informed that following an application for an injunction by the Qikiqtani Inuit Association (QIA), the Canadian regional Nunavut Court of Justice had issued an Interlocutory Order restraining Natural Resources Canada from proceeding to conduct seismic testing pursuant to the Eastern Canadian Arctic Seismic Experiment. As a consequence of the court decision, the GSC stopped all activities within the joint cruise and ordered their scientists off *Polarstern*. BGR and AWI, in consultation with the German Foreign Office, the ship's master and the scientific coordinator of R/V *Polarstern*, decided to

cancel all intended operations in Canadian territorial waters during ARK-XXV/3. An alternative research programme had to be elaborated, which focused on the Greenland continental margin only. In total, 50% of the original planned working time within the survey area had to be adjusted. The final alternative programme was a slight modification of the original programme with more focus to study the variability of the crust along the Greenland margin and to analyse the sediment structures and basins along the Greenland margin than previously planned. Following the investigations in 2001 and 2008 the newly acquired data will close the still existing data gaps. The extended survey area of the ARK-XXV/3 expedition covers an area from the Kane Basin in the North to Disko Island in the South. Additionally, aeromagnetic surveying and geological sampling of the near-coastal outcrops were included into the survey programme.

2. SCIENTIFIC PROGRAMME

Volkmar Damm

Bundesanstalt für Geowissenschaften und Rohstoffe

2.1 Geological and tectonic framework

The Baffin Bay is an ocean basin with sediment thicknesses up to 12 km in its northern part (Reid & Jackson 1997). The opening of Baffin Bay developed in several stages of tectono-magmatic activity. After initial stretching from Late Triassic to Late Jurassic, stretching and thinning from the Late Jurassic to the Early Cretaceous, and further thinning developed during the Paleogene. Spreading was active in Paleocene and Eocene times, when the Greenland plate separated from North America (Larsen et al., 2009).

There is no consensus about the nature of the underlying crust in Baffin Bay. Evidence indicating that the deep sea area of the Baffin Bay crust is oceanic has been provided by Keen and Barrett (1972) based on seismic refraction data. They showed that the crust underlying the deeper part of Baffin Bay is very thin and they interpreted their velocity model as a layered oceanic crust consisting of oceanic layer 2 with velocities of 5.0 - 6.3 km/s and layer 3 with 6.5 - 6.9 km/s. However, Reid and Jackson (1997) did not find evidence for oceanic layer 2 and interpreted the layer with a velocity of 6.8 km/s as serpentinized mantle material. They suggest that rifting was amagmatic and separation of passive continental margins was comparable to ultra-slow spreading ridges. Linear magnetic anomaly patterns in this region were not clearly identified. The position of the extinct spreading axis was defined by a northwest-trending linear gravity anomaly of central Baffin Bay (Fig. 2.1; Chalmers and Pulvertaft, 2001). It is suggested that the northwestern part of the hypothesized spreading axis runs east-west into the Lancaster Sound and terminates there in a fault rift structure. Spreading in the Baffin Bay took obviously place in Paleocene and Eocene times in two phases which may be distinguished by a reorientation of the directions of plate motion of Greenland starting about 55 Ma ago (Chalmers and Pulvertaft, 2001). A recent model suggests a northwesterly orientation during Paleocene times, parallel to the bounding continental margins of Baffin Island and West Greenland, and a transecting central segment of Eocene age trends westerly and terminates east of Devon Island (Oakey and Chalmers, 2005). The initial break-up and reorientation of spreading axis is probably related to volcanic activity originated by the Greenland-Iceland plume (Larsen and Saunders, 1998). According to Storey et al. (1998) two phases of volcanism were active in Paleocene-Eocene times which might be related to the Iceland plume. Palaeogene volcanics crop out at Disko Island and Cape Dyer of Baffin Island. Flood basalts are widely distributed offshore in Nuussaq area at the Greenland margin (Whitakker et al., 1997). The total

width of the oceanic crust between the Canadian and Greenland margins in North Baffin Bay is at least 260 km (Harrison, 2006). Due to lack of data the plate boundary between the North American plate and the Greenland plate is not well defined and the nature of the continent-ocean transition zone is widely unknown. The northern segment of the plate boundary which coincides with the Nares Strait is supposed to have acted as a transform fault with sinistral movement of Ellesmere Island with respect to Greenland. It is not fully explained how this postulated Wegener transform fault accommodated the northward movement of Greenland following the opening of the Baffin Bay and where this transform fault is located south of Kane Basin. The contact between the continental shield and the sediments in Northwater Basin area lies west of the available geophysical profiles and could be either an unconformity or a basement-rooted reverse fault (Neben et al., 2006). There is geological evidence for no significant strike slip motion in Smith Sound as far as to Kane Basin (Tessensohn et al., 2006; Harrison, 2006; Dawes, 2009), but there is not much geophysical data available for the offshore area. To account for the absence of the Wegener Fault in this area Harrison (2006) locates the plate boundary in the Arctic Islands following a system of faults on southwestern Ellesmere Islands running to Lancaster Sound.

Flanking the deep water area of Baffin Bay are half-graben basins developed on the West Greenland continental crust and separated from the Baffin Bay basins by basement highs. They have been defined from the northern limit of the Paleogene flood basalts off Nuussaq as far as North of Carey Islands in the Smith Sound (Whittaker et al., 1997). The largest basin structure in this part of the Greenland margin is the Melville graben. Most basins are filled up with several kilometres of Cenozoic sediments. The Kane Basin further north has only received very little geophysical exploration. The depressions of Lancaster Sound and Jones Sound and probably the Smith Sound provided significant transport routes for sediments since Paleogene times. This material was deposited in the central part of North Baffin Bay and formed the extended Baffin Bay Fan with several kilometres thick sediments. The thick pre-Cenozoic and Cenozoic sedimentary basins in the area were formed and influenced by crustal extension and compression in their temporal sequence and are sparsely analysed.

2.2 Previous surveys and existing data

In 2001 during a collaborative marine geophysical programme between BGR Hannover, GSC Calgary and Dartmouth and GEUS Copenhagen data were collected with the support of the Canadian Coast Guard icebreaker *Louis S. St. Laurent* to tie geophysical data to onshore geology to understand the deformation of the region. The investigations included multichannel reflection seismics, refraction seismics, an aeromagnetic survey and geodetic and geological fieldwork onshore. The multi-fold marine reflection seismic data acquired as part of this 2001 Nares Strait geoscientific cruise totals 1,201 kilometers. Marine reflection seismic acquisition parameters were varied due to operating limitations in high Arctic waters. Interpretation suggests a number of fault-bound NE-SW trending Tertiary rift basins containing at least 4 km of sediments subdivided into at least three stratigraphic sequences. The limited data

acquired in Nares Strait has shown no continuous fault (Wegener fault), which could explain crustal displacements in Baffin Bay (Tessensohn et al., 2006).

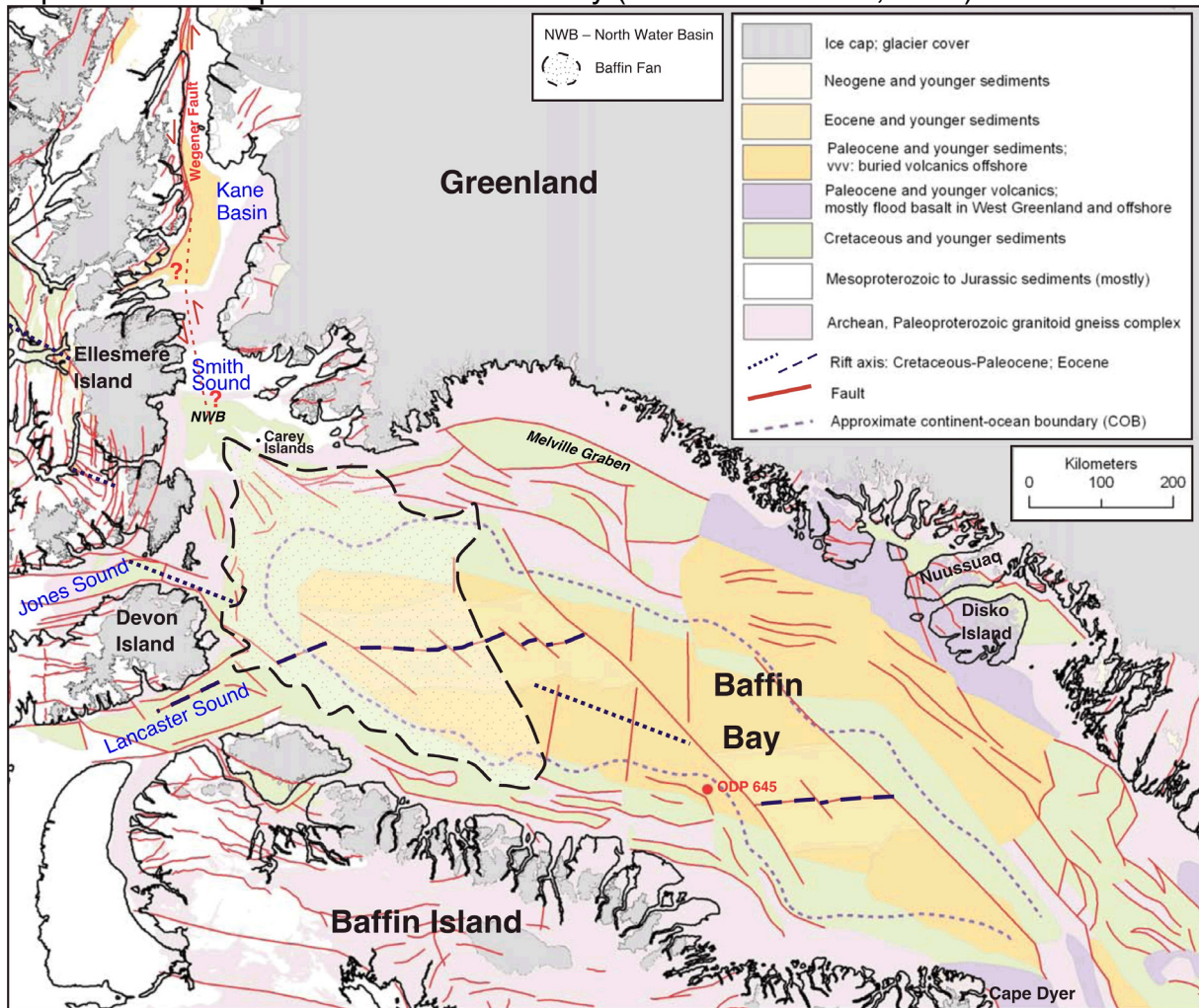


Fig. 2.1: Geological map of northern Baffin Bay (after Harrison et al., 2010)

In 2008 a cooperative geoscientific project between the Alfred Wegener Institute for Polar and Marine Research (AWI), the Federal Institute for Geosciences and Natural Resources (BGR), the Geological Survey of Denmark and Greenland (GEUS) was conducted to survey the areas of Baffin Bay and Davis Strait between Greenland and the Canadian Baffin Island. This project was aimed to develop a tectonic and sedimentary reconstruction of the opening process and to construct a set of gridded detailed paleotopographic maps for a complete geodynamic reconstruction of the gateway Baffin Bay and Davis Strait. With a set of three seismic refraction profiles, using ocean-bottom seismometers on 62 stations, as well as multi-channel reflection seismic recordings with a 3,000-m long streamer, data were acquired from the sedimentary cover to the deep crust and even from parts of the uppermost mantle. Additional seismic data supplement these profiles and provide insights into the structures of the basement and dominant fault zones such as the Ungava fault. A parallel running magnetic survey aimed to resolve the temporal evolution of the

oceanic crust of Baffin Bay. The extension and subsidence of the continental and transitional crust in the Davis Strait and the evolution of oceanic crust in the Labrador Sea and Baffin Bay could be investigated with this dataset, supported by continuously recorded gravity and sub-bottom profiler data.

In 1992, seismic profiles have been acquired by a consortium of six oil companies and the Greenland Nunaoil company as the operator on the West Greenland continental shelf from Nuussuaq through Melville Bay to as far north as the Carey Islands. The data of this KANUMAS project revealed several northwesterly-trending horst and graben structures on the shelf, the largest being Melville Bay Graben with more than 13 km sediment infill. Based on this data Whittaker et al. (1997) interpreted seven distinct phases of basin evolution, and Eocene transpressive inversion structures in the northern Melville Bay area.

In 2000 the Greenland Bureau of Minerals and Petroleum (BMP) and Nunaoil conducted another seismic survey in the Melville Bay to acquire regional seismic data in an area that based on previous exploration might offer a suitable structure for reservoir formation. The data was collected to provide a closer grid than previously available with higher quality data.

More recently TGS NOPEC did regional surveys in 2008 and 2010 with dense line spacing in an area between 73°N and as far as Cape York in the North to provide high quality data for applying oil companies within the recent licensing round.

2.3 Objectives

The North Baffin Bay is a key area to understand the pre-drift position of Greenland and consequently important in plate reconstructions and the formation of the North Atlantic and the Arctic ocean basins. Information on crustal structures and evolution of sedimentary basins along the Greenland continental margin during the opening process will contribute to develop a complete model for the geodynamic reconstruction and separation of the Greenland from North America. The northern segment of the Baffin Bay along the Greenland shelf has been recently surveyed by extensive seismic exploration surveys, but only a few data are available north of Smith Sound.

The primary objective of the marine programme of ARK-XXV/3 was to collect new geophysical data to improve the understanding of the deep crustal structure of the Baffin Bay, the geometry of the plate boundaries and stratigraphy within the sedimentary basins. By means of multi-channel seismic, wide angle seismic, gravimetric and magnetic methods the structural inventory of the crust in the Greenland continental margin in NW Baffin Bay was investigated. Data were acquired along profiles extending from the deep oceanic basin in the central part of North Baffin Bay onto the Greenland continental margin in an area, which is bordered by the Kane Basin in the North and Disko Island in the South. Additionally, heat flow data and sediment cores were collected at selected positions along lines across the Greenland continental margin. The extracted cores were planned for geochemical and geomicrobiological analysis to be used for basin modeling and studying the hydrocarbon generation and microbial hydrocarbon degradation. Aeromagnetic and

2 Scientific programme

marine magnetic data were acquired to investigate magnetic signatures of the oceanic crust and the Greenland continental margin. Main questions and tasks are:

- What is the nature of the West Greenland continental margin?
- Is a segmentation into volcanic and non-volcanic margins observable?
- What is the origin and evolution of possible margin segments?
- How and when have the crustal structures and sedimentary processes evolved along the Greenland continental margin?
- Can we detect pre- and synrift sediments and/or distinct phases of rifting?
- Has the extensional crustal thinning of the central segment in Baffin Bay led to the formation of true oceanic crust?
- Can we detect seafloor spreading anomalies?
- Where is the continent-ocean-transition in the northeastern Baffin Bay?

The subsequent compilation of all acquired data is aimed to:

- derive a crustal evolution model for the Baffin Bay since Paleocene times,
- reconstruct the plate-tectonic motion between Greenland and Canada,
- derive a model for the evolution of thick sedimentary basins in the area and estimate the presence of hydrocarbons.

The results of the multi-disciplinary survey work will be integrated into a regional synthesis of the Greenland rifted margin, sedimentary basin development and evolution.

2.4 Work at Sea

The plan of operations comprises marine geophysical profile work including aeromagnetic surveying and soft sediment coring plus geological sampling in near-coastal areas.

The survey area was bordered by the Kane Basin in the North and Disko Island in the South and limited to Greenland territorial waters only. For location of survey data see Figure 2.2.

Summary statistics of acquired data:

- Reflection seismic profiles: 26 lines with 3,994 km of line data
- Refraction seismic profiles: 4 lines with 1,253 km of line data
- Gravity surveying: 45 lines with 11,215 km of line data
- Magnetic surveying: 40 lines with 6,050 km of line data with shipborne magnetometers, plus
- 10,830 km of line data with helicopter aeromagnetics
- Single-beam echosounder: 14,000 km of line data
- Multibeam bathymetry: Continuous measurements with 19,215 km of data
- CTD measurements: 4 stations
- Heat flow probing: 32 stations
- Sediment coring: 34 stations
- Geological sampling of near coastal outcrops: 87 locations

Structural investigations to study the crustal architecture and basin evolution

The four refraction seismic lines combined with all geophysical data were designed to investigate the deep crustal structures and variations of structural parameters along the western Greenland continental margin. A total of 35 ocean bottom seismometers were available to be deployed along survey lines.

The primary method to improve the understanding of the development and evolution of the sedimentary basins was multi-channel reflection seismics using a 3,900 m streamer. Wide-angle seismic data acquisition was conducted using sonobuoys along reflection seismic profiles to provide additional velocity information of sediment layers. A G-gun array of 51 l expandable to 68 l was used as seismic source. Profile data were acquired along profiles extending from the deep oceanic basin in the central part of North Baffin Bay onto the Greenland continental margin.

Strategies for designing the survey were:

- to cross the Greenland margin and the suggested COB with profiles preferably in perpendicular direction at typical locations of the Greenland margin between Smith Sound in the North and Disko Island in the South
- to allow for seismostratigraphic correlation along the Greenland margin
- to tie seismic lines to profiles acquired during previous BGR/AWI expeditions in 2001 and 2008
- to get first seismic data of the eastern part of Kane Basin.

Seismic data of Kane Basin are of special importance to track the Wegener Fault in a totally underexplored area.

Seismic data recording was complemented by simultaneously magnetic and gravity data acquisition along all profiles. Additionally, heat flow data and sediment cores were collected at selected positions along the refraction seismic lines. The cores were extracted for geochemical and geomicrobiological analysis to be used for subsequent basin modelling and microbial hydrocarbon degradation. Appropriate locations for coring were pre-selected based on multibeam and sediment echosounding data.

Magnetic surveying to identify volcanic and magmatic phases during the crustal evolution

The aeromagnetic data cover part of the marine survey area to investigate magnetic signatures of the oceanic crust and the Greenland continental margin. The main targets were the deep water parts of the Baffin Bay where crust of oceanic origin can be expected. The possible identification of magnetic lineations in these areas will help to constrain the timing and the direction of plate tectonic motions during the opening of the Baffin Bay. The data can also be used to delineate tectonic structures and e.g. volcanic provinces in the Greenland shelf areas. For marine magnetic measurements two towed systems were used: a gradiometer and a vector magnetometer. Additionally, aeromagnetic surveying was done using a Caesium-airborne magnetometer towed below the helicopter of *Polarstern*. The line spacing of 5 to 10 nm was selected to meet the demands for correlation and to allow for optimum coverage of the survey area. Both the aeromagnetic and marine datasets complement each other.

Heat flow measurements

At 32 locations along the 4 refraction seismic profiles heat flow measurements were conducted using a special hard ground heat flow probe. The data will assist in restraining age estimates of the crust in northern Baffin Bay and to identify the areal extent of oceanic or stretched continental crust. The data will also be used for basin modelling and assessment of hydrocarbon generation.

Soft sediment coring

A total number of 34 short piston cores were taken by means of a gravity corer at selected locations along the refraction seismic profiles. The sampling material will be used to study the quantity, the chemical and the isotopic composition of gases adsorbed by the surface sediments. These compositional data will be intergrated into a model of hydrocarbon generation and migration. Additionally, the sampling material will be used to analyse geomicrobiological sedimentary features and hydrocarbon degradation potential of indigenous microbial communities. Samples for molecularbiological studies of the quantitative and qualitative microbial community composition were collected, processed on board and preserved for subsequent analysis.

Geological field work and rock sampling of coastal outcrops

Helicopter-supported onshore fieldwork was done to collect samples for:

- a) thermochronologic techniques (apatite and zircon fission track and (U-Th-Sm)/He analyses)
- b) for organic geochemistry and organic petrography of potential petroleum source rocks.

Both types of analyses will provide important clues to basin models that will form the basis of the subsequent numerical petroleum systems analysis for the northeastern margin of Baffin Bay and along the southeastern Nares Strait.

The results of thermochronologic methods will contribute to a better understanding of the exhumation history on the northeastern margin of Baffin Bay and along the southeastern Nares Strait.

Organic geochemical/petrography results are important parameters for modelling petroleum generation and migration, such as we intend to perform for the target area.

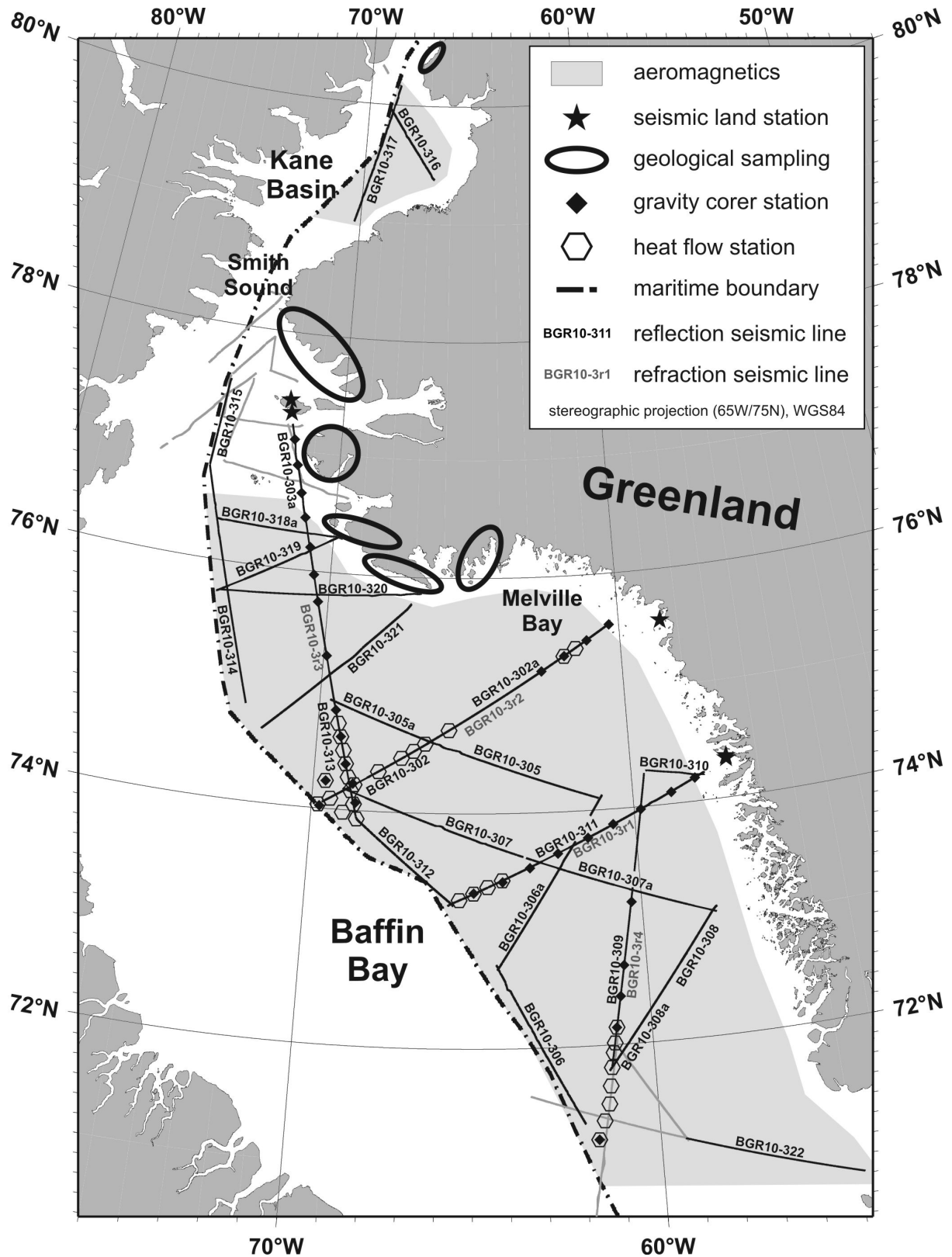


Fig. 2.2: Location of seismic reflection and refraction lines, land based seismic stations, aeromagnetic surveying, heat flow measurements and geological sampling during Polarstern expedition ARK-XXV/3. Grey lines indicate previous BGR cruises MSM09/3 (south) and NARES01 (north).

3. CRUISE NARRATIVE

Volkmar Damm
Bundesanstalt für Geowissenschaften und Rohstoffe

Week 31 (August 1 – August 8, 2010)

Polarstern arrived in Reykjavik on July 29 after completion of her operations during leg 2 of cruise ARK-XXV. Whereas the first two legs of the 2010 Arctic voyage were focused on the North Atlantic, *Polarstern* was ready to leave on August 1 for the northern Baffin Bay during the 3rd leg of her 25th Arctic voyage. The crew change took place the day before and all 34 scientists from Hannover, Bremerhaven and Leipzig including the three Canadian guest scientists embarked on July 31. The day before was already used to start mobilisation activities and to install the geophysical equipment onboard.

After completing bunkering in the evening of August 1, *Polarstern* left the port of Reykjavik and headed off towards the southern tip of Greenland. Eight days of transit were used for preparational work on geophysical equipment and in the geological laboratories, testing of all the instruments and the obligatory safety instructions as usual. Although most of the scientific crew members have never been or have not been for a long time onboard *Polarstern*, everybody felt like home in a very short time thanks to the comfortable conditions and the friendly and helpful ship's crew. After completing almost all preparational work the continuous bathymetric data acquisition was started and a first magnetic profile was recorded.

Polarstern passed the first icebergs after entering the Baffin Bay and stopped at a position of 69°40'N, 64°12'W, approximately 100 nm off the Canadian coast, where the last test runs of some scientific instruments were carried out. On Sunday a marine mammal observer (MMO) was picked up by helicopter with good flight conditions from Clyde River. The MMO was to carry out continuous observation of marine mammals during the geophysical programme. By this means we fulfilled a requirement of the research permission given for our project by the Canadian government and assured that our planned work complied with the specific restrictions given by the autonomous Nunavut authorities. Although all documents about our research work were submitted on time and permission granted after careful screening by the appropriate Canadian authorities, including Nunavut institutions, we were at that time not sure whether we could carry out our survey as planned. Even though there was no port call planned during our 10-week cruise, we hoped there would be a chance to meet with representatives of the local Inuit communities and to inform them, as appropriate on board, in more detail.

Week 32 (August 9 - August 15, 2010)

The second week of our research cruise was influenced by a decision of the regional Nunavut Court of Justice. The court issued an Interlocutory Order restraining Natural Resources Canada (NRCan) from proceeding to conduct seismic acquisition within its project ECASE. This project of our cooperation partner partly relied on seismic data, which acquisition was planned in Nunavut Territory during our research cruise from aboard *Polarstern*.

All necessary research permissions had been granted for these measurements. In the context of the usual application procedure, Canadian authorities, including the regional Nunavut authorities, also carried out an environmental impact assessment. Therefore, we were surprised by the interlocutory order, preventing us from completing our research project as planned. The court decision against the ECASE project had created a complicated legal situation, which could not be resolved quickly. Consequently, we had to focus on the Greenland part of Baffin Bay only for our marine seismic research activities. All necessary applications for work in this region were submitted well in advance and approved by the Greenland authorities.

We were very concerned not to be able to continue our scientific operations as planned, despite the fact that our project had been peer-reviewed and declared as scientifically important. Moreover, scientific and logistic preparation of the project took 6 years. About half of our comprehensive programme was planned for Canadian waters. The situation then demanded a re-organization of our research programme, so that the work would contribute as much as possible to answering our scientific questions, even though we were limited to one half of the original survey area. We started intensive scientific discussions on board, and an alternative / supplementary science plan was set up.

All planned research activities not affected by the above were under way. We successfully collected the first sediment cores, conducted heat flow measurements and acquired geophysical potential field data along survey lines.

After *Polarstern* left Canadian waters, we began seismic data acquisition in Greenland waters at position 71°12'N, 61°38'W. The MMO, a licensed biologist of RPS England supported us in complying with all regulations for environmental protection.

Operation of all scientific outboard equipment and the continuous measurements with shipboard systems was normal.

Week 33 (August 16 - August 22, 2010)

Due to the unexpected situation that our survey area was limited to the Greenland part of Baffin Bay, we modified our original survey plan and started our survey operations in week 32 in reverse order with seismic lines in the northeastern part of Baffin Bay.

After arrival in Greenland territorial waters on August 11, we had started continuous operations along survey lines on the way north using our geophysical outboard systems. With the first refraction seismic line, running from the deep central part of Baffin Bay towards the Greenland coast at Melville Bay, we aimed to study the deep crustal structures in the central and northeastern part of Baffin Bay. Shortly before

3 Cruise narrative

starting data acquisition we were contacted by an exploration vessel operating in the area to coordinate further activities. Since the Norwegian seismic exploration vessel *M/V Bergen Surveyor* (Fig. 3.1) had a crew change and interrupted its activities for a few days we were able to acquire all data in the Melville Bay as per schedule and in good quality. The station work to deploy ocean bottom seismometers along the 180 nm profile was combined with heat flow measurements and sediment coring using a gravity corer. After minor problems in getting sufficient amounts of sampling material we extracted sediment cores of more than 3 m length. The samples were then under processing and were analysed by our geologist and geomicrobiologists. At the end of the profile we were excited by the impressive coastal landscape of Melville Bay with high rock escarpments and surrounding glaciers draining the Greenland icecap. In prolongation of our refraction seismic line we deployed a land seismic station. This gave opportunity for some colleagues to go ashore by helicopter.

Later on, we continued geophysical data acquisition along survey lines heading towards Upernavik at the Greenland coast 230 nm away to drop off our three Canadian and two German colleagues, who had to depart from the little airport there to return home. Since the decision of the regional Nunavut Court of Justice stopped all NRCan activities within its ECASE project the Canadian project partner also decided to halt activities within our BGR project.

The departure of our Canadian colleagues also resulted in additional work for the onboard scientific crew since all guest scientists had been fully integrated into shift schedules on all onboard activities. But we were also very sorry not to continue this fruitful cooperation with these highly experienced and friendly colleagues.



Fig. 3.1: The seismic exploration vessel M/V Bergen Surveyor in the Melville Bay - Seismic operations of this vessel and Polarstern had to be coordinated to prevent interferences in seismic data.

Week 34 (August 23 - August 29, 2010)

After the disembarkation of our five colleagues by helicopter in Upernavik *Polarstern* continued scientific operations by acquiring reflection seismic data. A next profile heading to the SW crossed the outer part of the Palaeogene Disko Island volcanic complex and terminated at the northern end of a refraction line. This line was previously measured during a research cruise by the *Maria S. Merian* in 2008. Starting from this point it was intended to extend the pre-measured profile towards the Greenland continental shelf. Using all geophysical methods it is aimed to better define the location of the geological boundary between oceanic and continental crust and to find out whether this part of the Greenland coast was influenced by volcanism during the initial stages of break-up. Volcanic rocks were partly found along the Canadian continental margin. Since there is no way to apply all geophysical systems at the same time, operations along this line were split up into two parts. Refraction seismics were done in a later stage to guarantee undisturbed data acquisition. Seismic data acquisition in our survey area was partly influenced by interferences generated by the activities of a Norwegian exploration vessel operating in the same region. Their signals remarkably reduced the quality of the refraction seismic data. We decided to complete our operations here in the time slot, when the M/V *Bergen Surveyor* departed for a 2 days crew change at the end of September. Therefore, within the next few weeks we focussed our operations to the northern part of our survey area.

The main objectives in the second half of this week had been the retrieval of the ocean bottom seismometers and station work along our first refraction seismic line in the Melville Bay area. Perfect weather conditions with 24 hour sunshine, temperatures of up to 10 degrees and calm seas allowed for the retrieval of all 25 instruments without any problem and much faster than expected. Heat flow measurements were performed at selected locations along the line. Unfortunately, we could not use the ideal flying conditions for aeromagnetic surveying using the ship based helicopter. The intention was to study the magnetic signatures of the oceanic crust in the nearby Canadian waters. However due to the decision of the regional Canadian court drawn 2 weeks ago it was decided to completely cancel the activities of our cruise which were planned in Canadian territorial waters. Nevertheless, we were able to conduct several helicopter trips to the Greenland coast for geological sampling in the coastal area of Melville Bay. The rock material collected will be analysed at home to derive constraints on the erosional history of the coastal area. For our geologists this was a good opportunity to step onto Greenland ground and for all the others on board to enjoy the picturesque panorama of the Melville Bay coastline for a second time after a couple of foggy days.

Since Friday at midnight we were doing reflections seismic and magnetic data acquisition along lines heading towards Northumberland Island in Smith Sound in the north of our survey area.

All systems were operating without technical problems.

Week 35 (August 30 - September 5, 2010)

As per schedule, *Polarstern* arrived on Monday evening at position 77°13'N, 71°56'W at the northern end of a north heading profile. After completing this line with reflection seismics, magnetics and gravity methods, *Polarstern* headed south again deploying 28 ocean bottom seismometers at equidistant positions. At preselected locations, heat flow measurements were conducted. This profile extended from old Proterozoic crust in the North to the suspected extinct spreading axis in the central part of Baffin Bay. It crossed thick sediment layers deposited on top of the Palaeozoic basement. Based on seismic and potential field data we aimed to better define the transition zone between continental crust in the North and oceanic crust in the South. Refraction seismic investigations are the main tool to get information on the deeper crust, whereas high resolution reflection seismic data will be used to analyze the internal structure of sedimentary basins for subsequent modelling of basin evolution. On Tuesday we got the expected research permission from the Danish Ministry of Foreign Affairs to conduct the extended research programme in Greenland waters. On Thursday *Polarstern* arrived at position 73°56'N, 68°35'W, the southern end of the refraction seismic line. Weather conditions were perfect while sailing north again acquiring geophysical data along the same line, which terminated a few miles off Northumberland Island. Part of the track was in the near-coastal waters along Steensby Land in the Northwest of Greenland. Good weather conditions and the short distance to the coast made it possible to further continue the geological sampling programme using the helicopter. On Friday after two days of recording refraction seismic data the 400 km long N-S line was completed. Only one break interrupted the seismic signal generation the night before. A rope for towing our airgun array had damaged the high pressure air umbilicals. Our technicians fixed the problem within 2 hours and then we continued to work along the profile. Since noon on Friday *Polarstern* had been retrieving OBS instruments heading south again. A special situation happened when we discovered that a large iceberg covered the expected position where an OBS was planned to be retrieved. But after careful calculations we were sure that a small distance between the iceberg and the OBS would remain when we released the OBS anchor. All calculations were perfect and we finally retrieved the instrument 50 m in front of the iceberg.

Week 36 (September 6 - September 12, 2010)

During this week the onboard operations were focused on seismic work in Kane Basin. Before *Polarstern* headed north, all ocean bottom seismometers (OBS) had to be retrieved which were deployed along the second, 400 km long N-S trending refraction seismic line. With moderate seas, all instruments had been recovered by the crew very quickly and routinely. A first quality control demonstrated that the noise created by the simultaneous operations of the seismic vessel *M/V Bergen Surveyor* in the nearby Melville Bay caused only minor interferences which were of less influence on our data than earlier expected. All operations along the second refraction seismic line were successfully completed. During OBS retrieval, sediment cores were extracted by the gravity corer at 11 selected locations along the line. The sampling material was used for geochemical and microbiological analysis.

The subsequently derived geochemical parameters will support modelling evolution processes of sedimentary basins. This modelling will be accompanied by microbiological investigations of the hydrocarbon degradation by microorganisms in the North Baffin Bay. Such investigations were only sparsely done in the past in the Arctic coastal seas and there is not much known about microbial hydrocarbon degradation activities and communities under these special polar conditions. The extracted core material was processed in the onboard laboratories and prepared for subsequent analysis at home.

In the second half of the week *Polarstern* headed north doing reflection seismics along a profile parallel to the Canadian maritime boundary. After 2 weeks of fine weather a meteorological low caused strong northerly winds and rough seas with 4 m waves. The sea calmed down when the vessel reached the Smith Sound. According to weather forecasting and ice reports the expected conditions were sufficiently good to conduct reflection seismic operations in the Kane Basin. It was planned to acquire for the first time ever MCS data along two profiles in this area to better analyse transform faults and sediment structures between Baffin Bay and Lincoln Sea and to extend the recent database of this underexplored area. Ice coverage was 3/10 to 5/10 in Kane Basin and because of the numerous icebergs a shortened streamer with 60 channels was used for the seismic operation. In the evening of September 10 *Polarstern* reached 80°09'N the northernmost position of this cruise leg. After the completion of reflection seismic work in Kane Basin and geological sampling of selected coastal parts, *Polarstern* headed south. Starting on Sunday morning MCS operations in the Smith Sound are being continued using a 3,900 m seismic streamer. The acquired data will fill up a still existing gap between data recorded during a previous expedition to the Nares Strait in 2001 and the recent survey area in Baffin Bay.

Week 37 (September 13 - September 19, 2010)

The reflection seismic data acquisition along the predominantly E-W trending profiles in the Smith Sound that had started the Sunday before was continued in the first half of the week. We wanted to study the internal structure of the thick sedimentary sequences to define the extension of pre-Cenozoic sediment basins and Proterozoic rock units in the north Baffin Bay. Very hard sediments occurred in particular areas of less than 500 m water depth, obviously due to the load of overlaying icebergs. Changing sea levels in the Earth's history and the influence of tides may produce this high density of near surface sediments. Their reflectivity of seismic energy is very high and strong multiple surface reflections mask reflections from the deeper structures. Special and careful data processing is necessary before interpretation. A first step was done by the onboard processing. In addition to the normal processing sequence, it is of great benefit to consider seismic velocities of individual layers which were derived from sonobuoys data. Besides the multi-channel reflection seismic data we were able to record wide-angle reflection data by means of such one-way sonobuoy instruments. The data were radio transmitted up to a distance of 30 km and provide information on propagation velocities in the sediment layers.

Close to the end of a seismic line off Cape York *Polarstern* navigated into an area with numerous icebergs. With the increasing amount of icebergs ahead and the risk of damage to the 3,900 m long seismic cable it was decided to stop data acquisition along this profile. The highly skilled and routineous navigation officers navigated *Polarstern* safely through the labyrinth of icebergs without any collision with the seismic outboard systems during the line change.

The newly recorded seismic data in Smith Sound extends the already existing data base acquired during a previous research cruise of BGR in 2001. The comprehensive data set will be used to map sediment basins in the area and help to understand the tectonic processes of their formation.

Besides the marine geophysical investigations, numerous aeromagnetic survey flights were conducted during that week. Due to good flying conditions up to three helicopter flights per day were possible. The aeromagnetic data with a line spacing of 12 km supplement the marine magnetic data. The whole data set already covers a substantial part of the Greenland side of northern Baffin Bay. The data will be used to study the nature of the crust underlying the thick sediments and identify possible oceanic crust.

During that time ocean bottom seismometers were deployed along the last two refraction seismic lines of our expedition. Following one of these lines *Polarstern* was heading south for another 150 nm of deploying ocean bottom seismometers to the end of profile at position 71°30'N. The sea was calm and temperatures in the South Baffin Bay were with 5°C remarkable milder than last week in the North.

Week 38 (September 20 - September 26, 2010)

That week's operations were focused on the last two refraction seismic lines. In addition the onboard processing of reflection seismic data was continued and the first results of data interpretation were discussed with all scientists.

The deployment of the 33 ocean bottom seismometers along the two refraction seismic lines with a total length of 680 km was combined with heatflow measurements. This operation had to be completed by Sept. 18 in the afternoon to be well prepared for using a predefined time window for data recording. The exploration vessel *M/V Bergen Surveyor* had preannounced a two and a half day interruption of their reflection seismic activities due to a necessary crew change. This gave us the opportunity to record our refraction seismic data along the two lines without any noise or interference and under optimum conditions. The airguns were deployed and operation started well in time. After 60 hours of operation data recording was completed without any technical problems. Shortly after, all outboard systems were brought back on deck and the recovery of ocean bottom seismometers was started. Additionally, it was planned to extract surface sediments using the gravity corer at 13 locations in total. According to pre-calculations we expected to spend three days for these operations. Another two days were pre-booked as spare time in case of waiting for the preset anchor release time of instruments which did not return to the sea surface by the acoustic anchor release. Recovery was started on Tuesday under perfect weather conditions, bright sunshine and calm seas. Also the deployed land seismic stations could be brought back to the ship easily and without

any problem under these conditions. Additional aeromagnetic survey flights were done by the helicopter. Thanks to the highly experienced ship navigators, deck crew, and all involved colleagues who worked very efficiently. They managed to save a substantial amount of time while working along the first line and it became clear that the operation would be completed ahead schedule. All ocean bottom seismometers were completely collected by Thursday evening. The planned spare time remained untouched and was not needed anymore.

The last section of our working programme before heading home was a reflection seismic data acquisition line along a 180 km long profile off Disko Island. This line extended a pre-measured seismic profile of the 2008 survey. The whole research programme was to be completed after finishing this last seismic line on Monday noon, 27 of September. We hoped not to be disturbed during our last operations by the subsidaries of a meteorological low located further south.

On Saturday, the traditional Polar inauguration ceremony was held for all colleagues who had entered the Arctic waters by ship for the first time.

Week 39 (September 27 - October, 2010)

On Sunday morning at 6:00 a.m. the streamer was deployed on time at position 71°12'N, 59°45'W to measure the last seismic profile of the working programme. It extends a seismic line, which was measured during a previous survey in 2008 onto the Greenland continental margin and terminates close to the coastline off Disko Island. The line started in the vicinity of an area which was already licensed to oil companies for exploration and drilling operations. Not far away several exploration and supply vessel were passed, among them the special vessel *Stena Forth* contracted by the Scottish oil company Cairn Energy, which successfully drilled a first exploration well here. Seismic data acquisition along the last profile was completed exactly 24 hours later at position 70°41'N, 54°52'W, a few miles off the Greenland coast. There was no further seismic surveying planned because of the limitation by the exploration activities in the area. The whole survey programme was completed and all outboard equipment was retrieved. Unfortunately, the cable of the magnetic sensor got tangled up with the seismic streamer and it took longer than usual to get all equipment onboard while *Polarstern* was sailing along the east side of Disko Island and heading for Ilulissat. The last obligation before heading home was to drop off the contracted marine mammal observer of RPS Energy, UK. After completing the last seismic line she was carried to Ilulissat by helicopter well in time to return home to the US the following day.

After *Polarstern* navigated through the channel between Disko Island and the mainland and between numerous icebergs for the whole day the vessel got into more icefree seas in the evening. The icebergs emerging the Ilulissat Icefiord were produced by the Jakobshavn Glacier, one of the most active glaciers in the World with flow velocities between 20 and 50 m per day. From now on *Polarstern* returned directly home. The following days were filled up with data interpretation, processing of sampling material, writing the necessary expedition reports and packing all instruments and equipment.

3 Cruise narrative

A last magnetic test survey was done on Friday to compare the sensitivities of the towed marine magnetometer with the new vector aeromagnetic sensor installed in the helicopter. As the most appropriate area the well surveyed magnetic anomalies west of the Mid-Atlantic ridge between 42°W and 35°W were selected for this equipment test.

Week 40 (October 4 - October 9, 2010)

After another 5 days of transit under moderate weather conditions *Polarstern* arrived in the German Bight and was moored up the harbour of Bremerhaven. The 10-weeks research cruise was completed. After a 17 years' break BGR was given the opportunity to use *Polarstern* for a marine geoscientific research project in the polar regions. We experienced an excellent cooperation with the ship's master and crew, were perfectly assisted during our research operations and made use of an exemplary service. Many thanks go to the master and crew of *Polarstern* for their support to successfully complete our research programme and for making our stay onboard convenient and comfortable.

4. NAVIGATION AND DATA MANAGEMENT

Hans-Otto Bargeloh, Bernd Schreckenberger, Ingo Heyde
Bundesanstalt für Geowissenschaften und Rohstoffe

The ship's system for navigation and track planning (NACOS-55-3) with integrated nautical charts receives navigation data from the speed logs, the radar systems and the integrated navigation system (MINS, Marine Inertial Navigation System). All sensors are integrated in the central data acquisition and distribution system PODAS. The MINS provides the main navigation data, like position, velocity and course over ground, heading, pitch and roll. The reference point for the ship's position is the location of the MINS (F-deck, approximately centre of the ship). The positions are filtered by the MINS and are provided continuously every second. The accuracy of the positions amounts to about +/- 5 m. This accuracy is sufficient for our survey and thus no DGPS causing additional costs was used. For more information on the ship's navigation system see

http://www.awi.de/en/infrastructure/ships/polarstern/handbook_polarstern/

A shipboard computer (DShip-E530) in the dry lab 4 provided the following data from the data acquisition and management system (DShip) once per second:

- position, speed and course from MINS
- heading from the gyro
- speed from the Doppler-sonar (DO-Log)
- water depth values from the Atlas DS-II Hydrosweep multibeam echosounder (centre beam) and from PARASOUND
- MINS: Roll, Pitch, Yaw
- weather data
- gravity data

The locations of used ship's and BGR equipment is shown in Figure 4.1. The positions of ship's reference point (MINS-1), gravity meter KSS31 and onboard vector magnetometer, BGR GPS antenna, magnetometer winch and outrigger port are annotated. Magnetometer towfish distances from the ship's GPS position follow from the sketch, taking cable length on the winch, cable path along the outrigger, and GPS antenna position into account.

In addition to the shipboard computers, BGR provided several desktop and laptop computers to perform the acquisition and storage of the collected reflection seismic and potential field data (Fig. 4.2). Computers were installed in the registration lab (acquisition of seismic data), in the dry lab 4 and the gravimeter room.

4 Navigation and data management

The PC (PC0433) used for the acquisition of navigation data, shotpoint data, gravity data, magnetic gradiometer data, time in UTC, depth, and water sound velocity is equipped with a large number of serial and other ports. Each of the data strings were written into the memory of the data acquisition PC by real time programmes developed under LabView software. The PC is connected to a BGR-provided Meinberg GPS-clock, by which a uniform time reference to all collected data is realized.

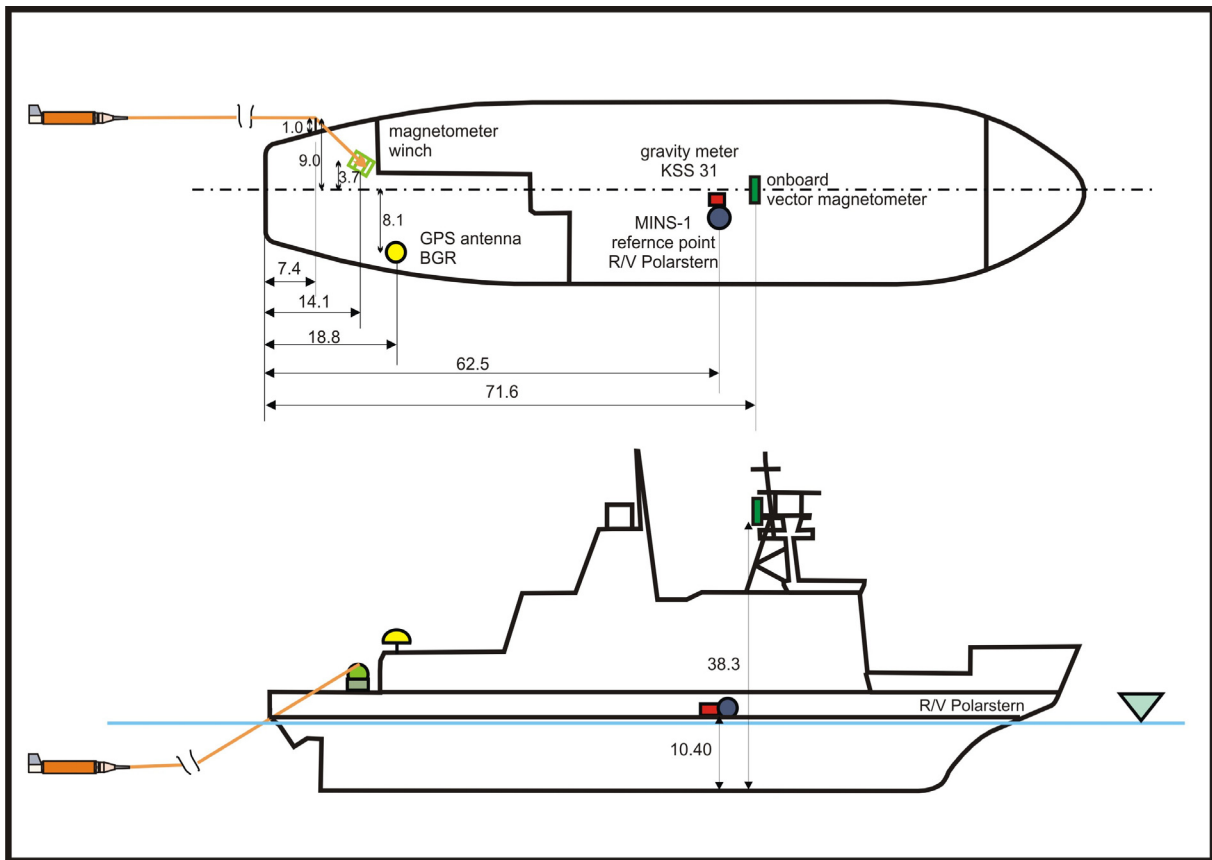


Fig. 4.1: Sketch of Polarstern with the locations of relevant equipment. (distances in meter)

The control of all seismic instruments (G-Guns and streamer) is managed by BGR-developed and industrial software installed on PCs, which were set up in the deck lab. All seismic data are stored intermittently on hard-disk and sequentially transferred onto tape. Shotpoint data are transferred to the data acquisition system discussed above.

PC6945 was used to control the operation of the SeaSpy marine gradiometer and to display the collected magnetic data. The Magson vector magnetometers have no real time data transmission to the ship. Its data are stored on a flash card installed in the

instrument. A notebook computer was installed in the dry lab to provide a visual display of the ship's position in relation to the profile network by a navigation programme (FUGAWI 4.5). This programme permanently displayed the ship's position on a nautical map on which the planned and the already finished profiles are plotted. In addition, analog recordings were produced for the magnetic total intensity and the gradient.

The data pre-processing was performed on various computers. All data which are part of BGR's standard operations were transformed into a special data format with a procedure that checks, reformats, and collects the data items to one data set each 20 seconds on PC1420.

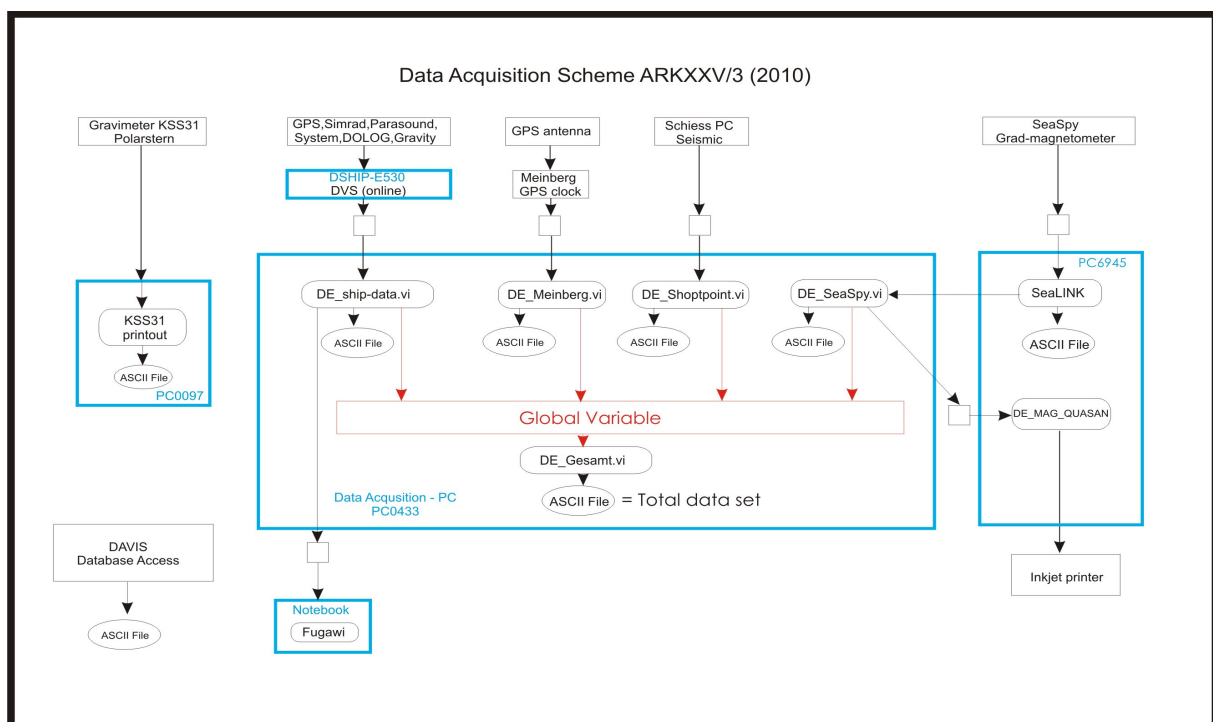


Fig. 4.2 Scheme of the data acquisition installed during ARK-XXV/3

5. MULTI-BEAM BATHYMETRY

Tanja Dufek, Ann-Kathrin Rohardt, Patricia Slabon
Alfred-Wegener-Institut

Objectives

The main task of the bathymetric group was to operate the multibeam echo sounder Hydrosweep DS-2 (Atlas Hydrographic) and monitor the data acquisition to ensure high resolution depth information throughout the cruise. Besides data processing and generating bathymetric survey track planning was carried out along the four seismic profiles where ocean bottom seismometers were deployed to gain depth information of a larger area.

The data will be a valuable contribution to the bathymetric datasets IBCAO (International Bathymetric Chart of the Arctic Ocean) and GEBCO (General Bathymetric Chart of the Ocean).

Data Acquisition

Data acquisition was carried out from 2 of August at 11:10 UTC before leaving Icelandic EEZ until the 7 of October at 6:20 UTC before leaving the British EEZ.

The deep-sea multi-beam echo sounder Hydrosweep DS-2 from Atlas Hydrographic was run in hardbeam mode with a resolution of 59 depth points (preformed beams) per ping. The frequency is 15.5 kHz. The aperture angle of the sonar fan can be set to 90° or 120°. During ARK-XXV/3 an opening angle of 90° was used most of the time, due to low resolution and poor data quality associated with an angle of 120°. In shallow waters between 100 and 350 m a larger swath of 120° was chosen. In very shallow waters (less than 100 m) the system showed systematic errors in the outer beams while operated with a larger sonar fan. These errors could be reduced by using an angle of 90°.

Approaching areas of very shallow waters of less than 100 m the data quality was poor. About 60 % of the data had to be rejected. This problem was mentioned in previous *Polarstern* cruise reports.

Data acquisition was conducted using HYDROMAP ONLINE provided by Atlas Hydrographic. The recorded data was stored in eight hour blocks in the Atlas raw data format SURF (sensor independent raw data format). Using HYDROMAP OFFLINE each block was checked for navigational errors. The data was then converted into dux-format and blunders and spikes in the depth information were removed manually using CARIS HIPS & SIPS 6.1. The cleaned data was converted into ASCII format (longitude, latitude, depth) for generating maps with GMT (Generic Mapping Tool).

In the area of the eastern end of profile BGR10-3r1 the system lost depth regularly and changed into search mode due to shallow water and strong variation in

topography. In Figure 5.1 bathymetric data with IBCAO data in the background of this area are shown. The differences between the high resolution sonar data and the global dataset which derives from the prediction of bathymetry from satellite altimetry can clearly be seen.

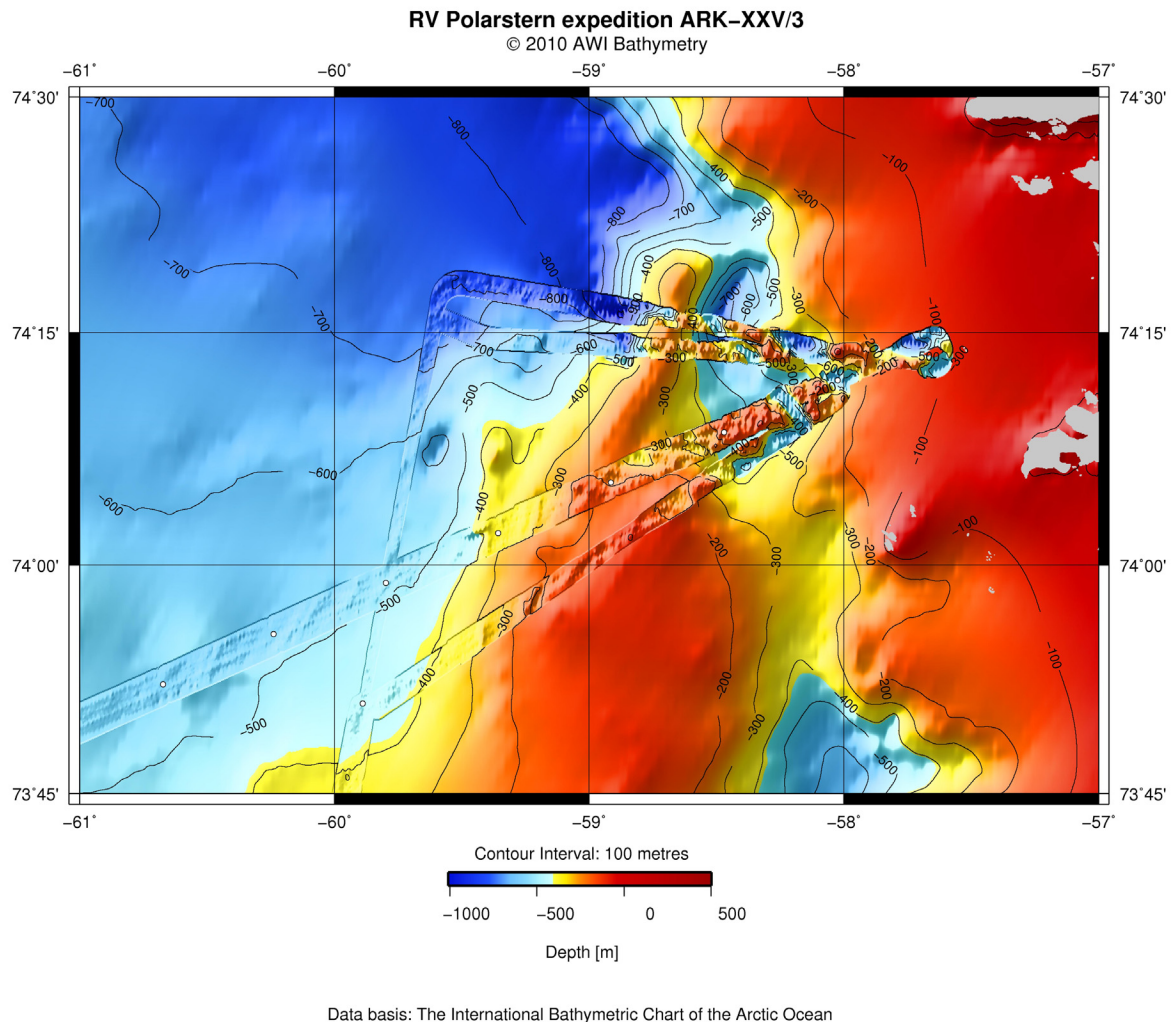


Fig. 5.1: Multi-beam data of the eastern part of BGR10-3r1 with IBCAO data in the background; OBS locations are marked with white points

Sound Velocity Profiles

Echo sounders compute the water depth from the travel time of the acoustic signal from the transducer to the sea floor and back. Therefore it is very important to know the exact sound velocity in the water column. It is influenced by the density and compressibility. These two parameters depend on the pressure, the temperature and the salinity. The mean water sound velocity is 1,500 m/s. This value is used for echo sounder measurements if the exact sound velocity profile is not available. Due to the regional and local variations of the already mentioned physical parameters the sound velocity in the water can also vary strongly depending on the area.

Hydrosweep DS-2 can perform a crossfan calibration to estimate the mean sound velocity within water column. During the cruise the system was mainly running on “standard” calibration mode, accomplishing a crossfan calibration every two nautical miles. In areas with strongly changing water characteristics and thus fast changing water sound velocity the calibration mode was set to “alternate” for a short period of time. This occurred on steep slopes or when approaching the coast for example.

A more precise technique to determine the water sound velocity is to perform CTD measurements. CTD stands for Conductivity, Temperature and Depth. It is a device to measure these physical parameters which are used to determine the sound velocity in the water column. Due to the quickly changing water characteristics (already mentioned previously) the sound velocity profiles won by CTD measurements could not be used for long time in a larger area.

CTD: Data Acquisition and Processing

The CTD equipment on board of *Polarstern* was developed by Sea-Bird Electronics Inc. (SBE). It consists of three different components: a deck unit (SBE11), an underwater unit (SBE911plus) and the data acquisition PC with SBE-Software.

Throughout the cruise ARK-XXV/3 four stations with CTD measurements were carried out. In Figure 5.2 the locations of CTD stations are shown. In the Baffin Bay CTD locations were chosen in the basin covering the whole research area. Table 5.1 shows further information about the four stations.

Tab. 5.1: Statistics of CTD measurements

Name of CTD File	Date Time (UTC)	Longitude	Latitude	Depth [m]	Name of sound velocity profile
ps76_248_03.cnv	08-08-2010 13:18	64° 14.43' W	69° 41.59' N	1926	ps76_248_03.txt
ps76_323_02.cnv	27-08-2010 12:53	61° 31.59' W	75° 22.82' N	1179	ps76_323_02.txt
ps76_401_01.cnv	06-09-2010 23:18	69° 47.89' W	74° 1.98' N	1708	ps76_401_01.txt
ps76_491_01.cnv	23-09-2010 21:47	61° 10.94' W	71° 48.54' N	1629	ps76_491_01.txt

During a station the underwater unit is deployed in the seawater and sends the data continuously to the deck unit via cable. The software Seasave V7 visualizes the data during the whole profile. After the deployment of the CTD the acquired data was processed using SBE Processing V7. Afterwards the software ManageCTD is used to organize the data processing and calculate the sound velocity profile with the utility “SV Hydrosweep”. It selects a number of points which best represent the sound velocity profile with an accuracy chosen by the operator.

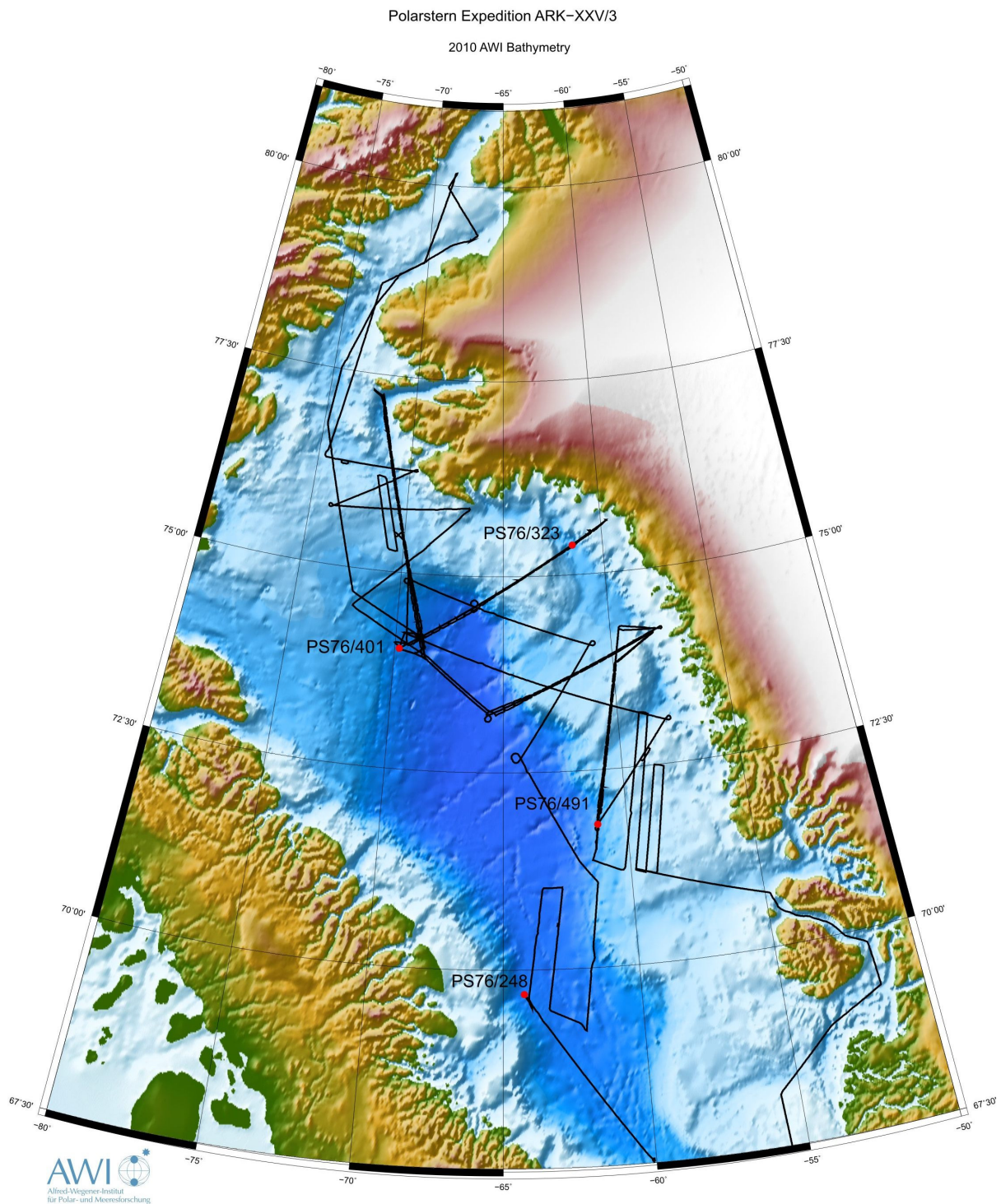


Fig. 5.2: CTD stations during expedition ARK-XXV/3

ManageCTD creates a text file containing the water depth and the matching sound velocity. This file can be directly imported into Hydrosweep DS-2. The system can read sound velocity profiles containing up to 20 points. In Figure 5.3 the CTD acquisition and processing steps are visualised.

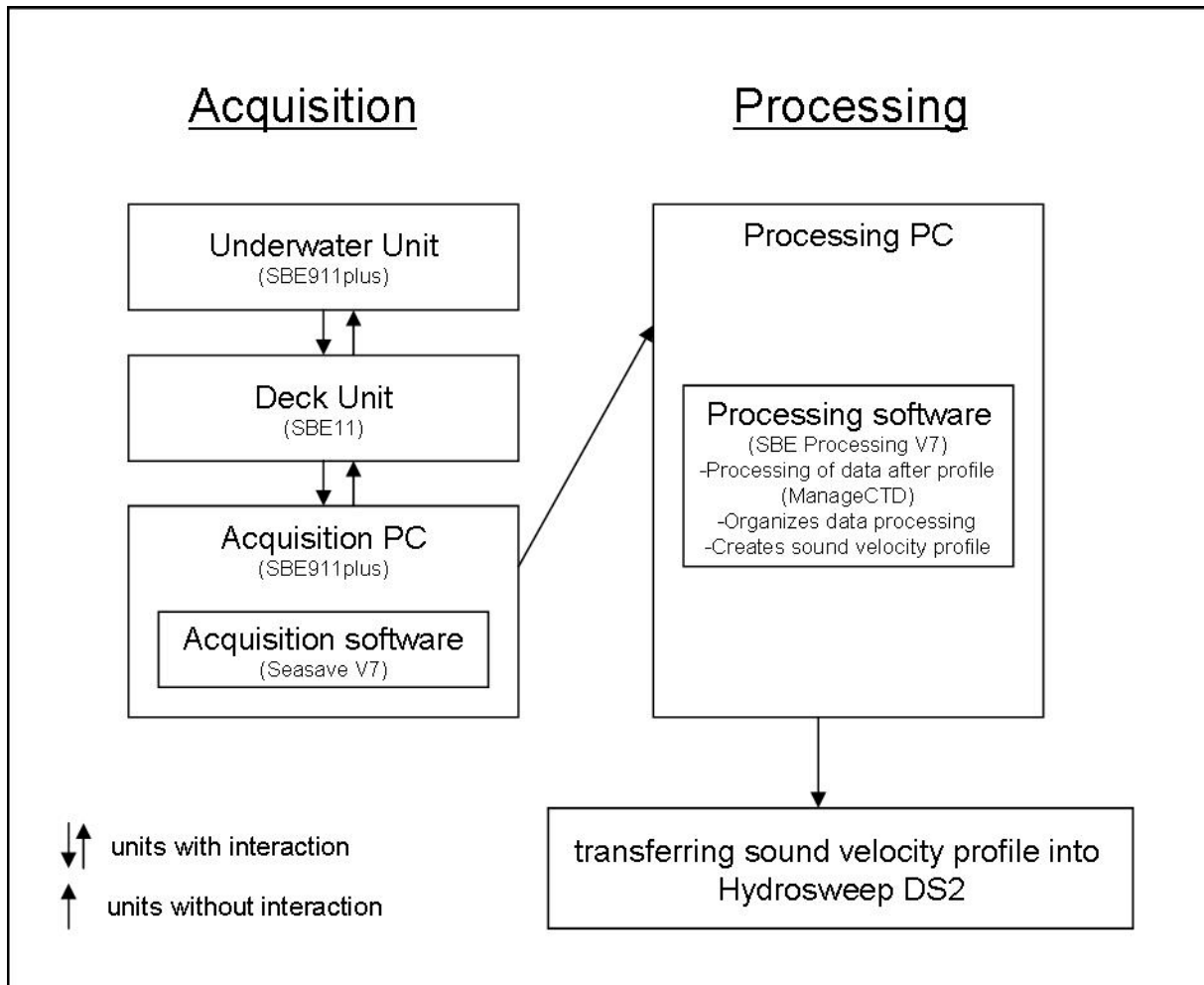


Fig. 5.3: CTD-workflow process on board Polarstern

Preliminary Results

During the cruise a continuous recording of data was achieved, except for data gaps due to unexpected system errors and shutdowns. All data were processed by the end of the cruise. During 67 days a track length of 10,376 nm (19,215 km) was surveyed with 970,055 pings and 57,132,054 beams (before editing). The raw data volume is 6.15 GB with 408 separate files. In the main research area the observed minimum water depth was 46 meters (eastern part of BGR10-3r1) and the maximum water depth 2447 meters (Baffin Bay Basin).

During deployment and recovery of ocean bottom seismometers along four seismic profiles systematic bathymetric surveys parallel to the profile were carried out. Thus the width of the acquired data stripe along profile BGR10-3r2 (312.9 km) is twice as wide and along profiles BGR10-3r1(260.2 km), BGR10-3r4 (302.7 km) and BGR10-3r3 (377.4 km) three times as wide as swath width. In Figure 5.4 the locations of these four seismic profiles are shown. Figure 5.5 shows the result of the bathymetric survey of profile BGR10-3r3.

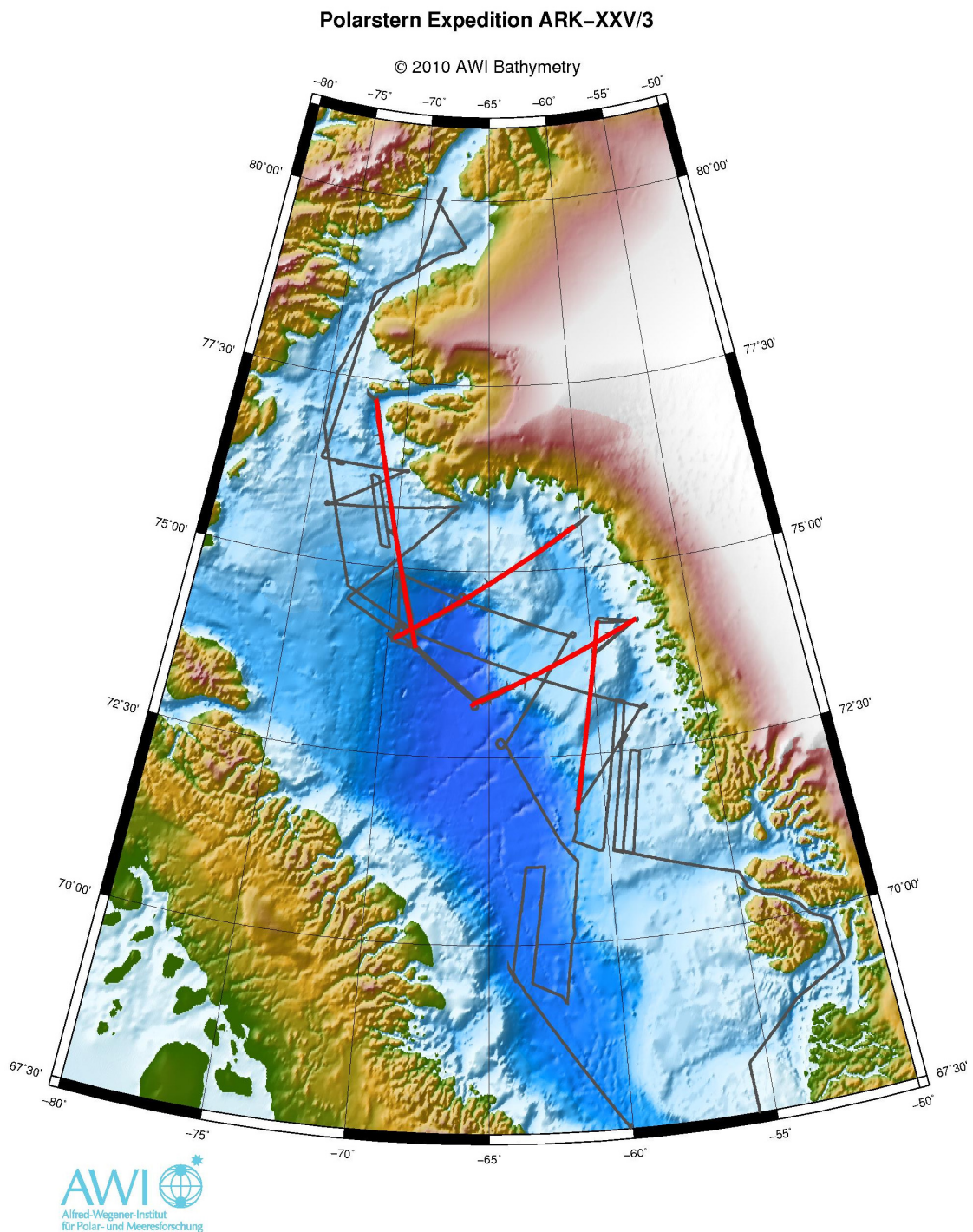


Fig. 5.4: Main research area of Northern Baffin Bay with track plot. The four OBS-profiles where systematic bathymetric survey was carried out are highlighted in red

5 Multi-beam bathymetry

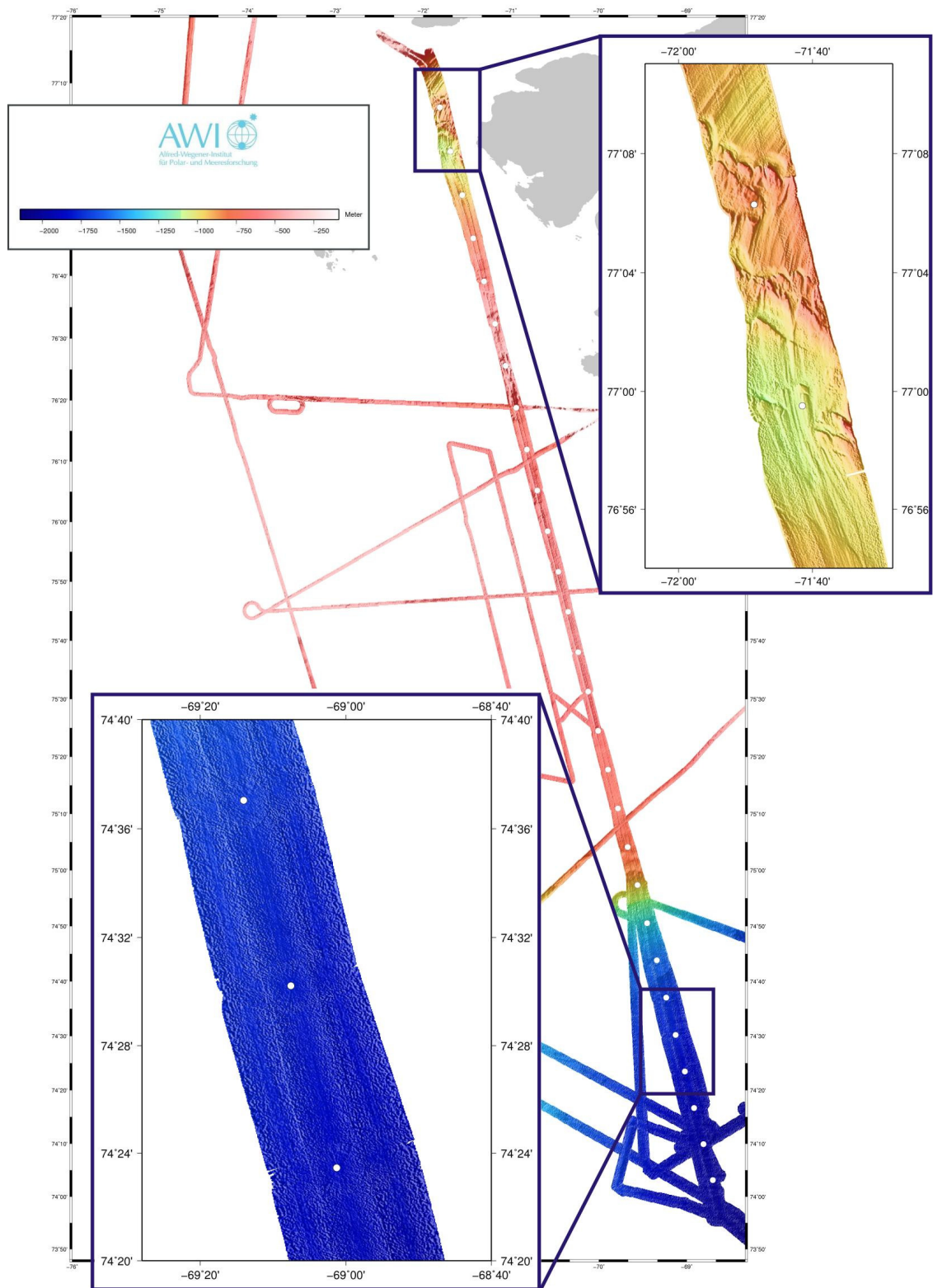


Fig. 5.5: Bathymetric data of profile BGR10-3r3; white points represent the OBS locations; depth range: -2,100 m (dark blue) to -250 m (light red)

6. SEDIMENT ECHOSOUNDING

Kai Berglar

Bundesanstalt für Geowissenschaften und Rohstoffe

6.1 Method and instrument control

The PARASOUND P70 system (Atlas Hydrographic, Bremen) installed on *Polarstern* combines a high-frequency deep-sea echosounder (NBS, narrow-beam system) for water depth sounding with a low-frequency sediment echosounder (SBP, sub-bottom profiler). Because the shipboard multi-beam HYDROSWEEP system was used for water depth sounding, only the SBP capabilities and settings of the PARASOUND system are described here.

The PARASOUND sediment echosounder simultaneously emits two independent pulse-modulated harmonic signals. The two frequencies (16 and 20 kHz), primary low and primary high frequency (PLF and PHF), are emitted and generate a signal (secondary low frequency, SLF) corresponding to the difference (4 kHz) of the PLF and PHF signals.

The SLF signal travels within the emission cone of the primary waves, which are emitted within an angle of only 4 - 5°. The resulting footprint diameter (7% of the water depth) is much smaller than that of conventional single frequency systems thus leading to better vertical and lateral resolutions. A disadvantage of this small footprint is the loss of a return signal over slopes steeper than 4°, where the reflected signal is not captured by the ship's detectors.

The hull-mounted transducer array has 128 individually triggered elements on an area of 1 m². This allows for compensation of pitch and roll of the ship and for the emission of a horizontal wave front. Up to 70 kW of electric power is required due to the low degree of efficiency of the parametric effect.

During this cruise the SLF signal was acquired in Quasi-Equidistant Transmission mode. The PARASOUND system automatically adjusts the time interval between pulses in a way that no pulses are sent out during reception of the returning signal.

PARASOUND settings during cruise ARK-XXV/3

On *Polarstern* two computers running ATLAS Hydromap Control are used for controlling the echo sounder. For acquisition, visualization and storage of the data the software ATLAS Parastore is available. Software versions installed during ARK-XXV/3 were: ATLAS Hydromap Control, v. 2.2.4 and ATLAS Parastore, v. 3.3.6.

Main settings in ATLAS Hydromap Control:

- Frequencies (Fig. 6.1)
- Mode of signal emission (Fig. 6.1)
- Amplification (Fig. 6.2)

6 Sediment echosounding

- Sampling rate (Fig. 6.3)
- Recording window length (Fig. 6.4)

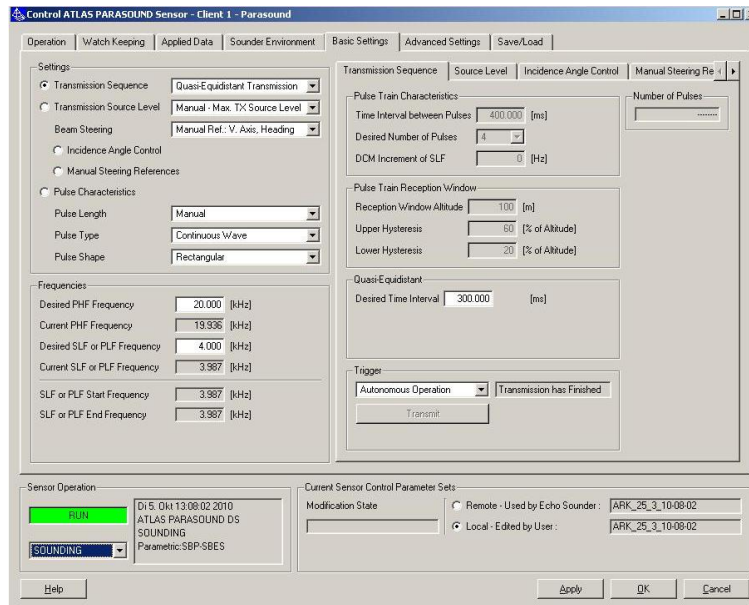


Fig. 6.1: The “Basic Settings” tab in the Control PARASOUND Sender window allow to control frequencies and transmission sequence. We used a PHF of 20 kHz and SLF of 4 kHz. Transmission sequence was set to “Quasi-Equidistant” mode.

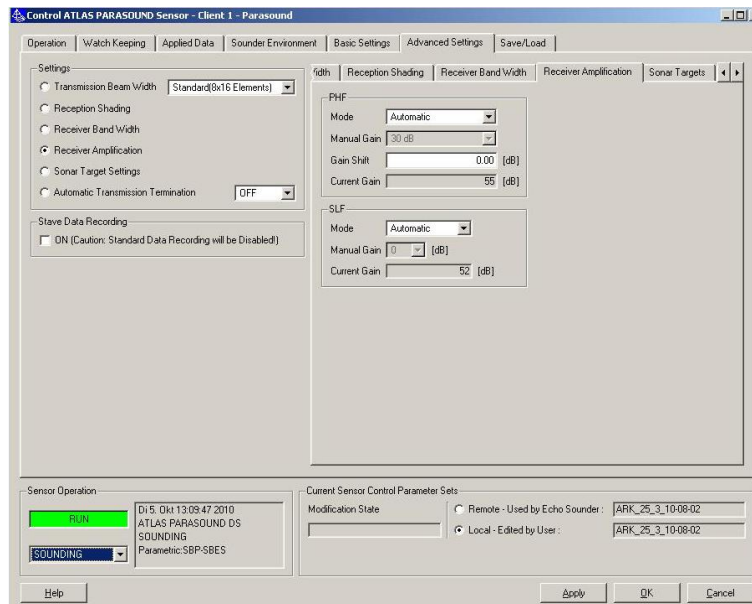


Fig. 6.2: The “Advanced Settings” → “Receiver Amplification” tab in the Control PARASOUND Sensor window allows to control amplification of the received signal. Gain was set to automatic for all frequencies.

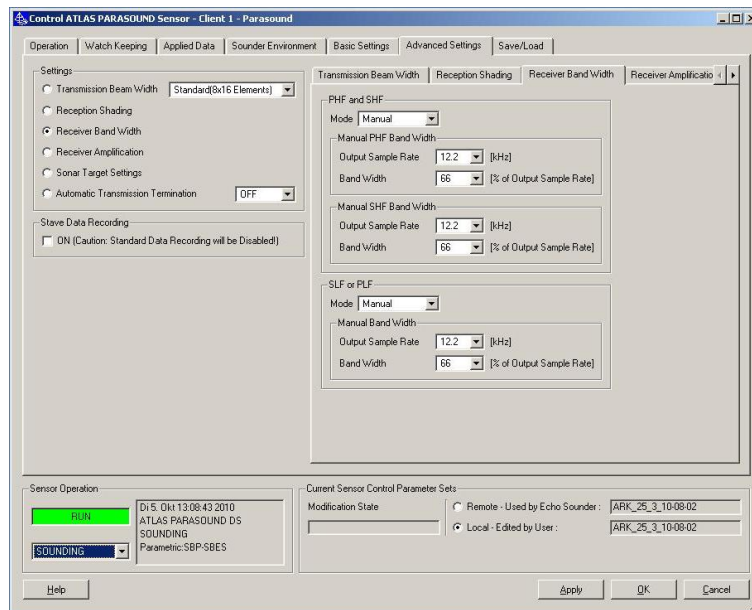


Fig. 6.3: The “Advanced Settings” → “Receiver Band Width” tab enables to control the output sampling rate. We chose 12.2 kHz for the SLF signal (see chapter 6.2(3)).

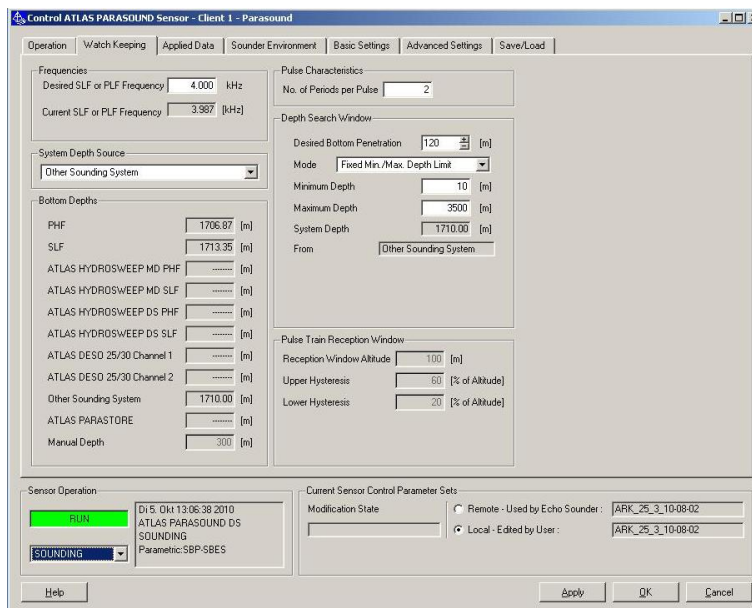


Fig. 6.4: The “Watch Keeping” tab in the Control PARASOUND Sender window is commonly displayed during system operation. We used the shipboard HYDROSWEEP signal to determine the System Depth Source and set the corresponding field to “Other Sounding System”. We used 120 m penetration (with 20% water column resulting in 150 m / 200 ms recording time; also see Figure 6.7).

6 Sediment echosounding

Main settings in ATLAS Parastore:

- Acquired signals (Fig. 6.5)
- Open SLF echogram window (Fig. 6.6)
- Depth determination, recording window length (Fig. 6.7)
- Stored signals and data formats (Fig. 6.8)
- Printing

The online printing resulted in several system crashes, due to printer buffer overflow. After shutting down online print on September 7, the system worked stable.

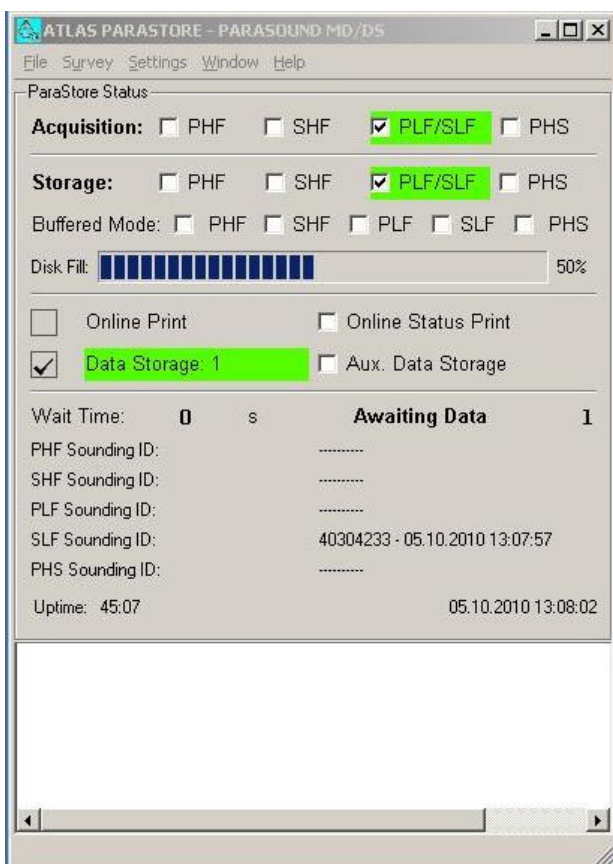


Fig. 6.5: The main Window in PARASTORE gives an overview about the running system. The operator should make sure that "Acquisition" and "Storage" for SLF are activated (green). Additionally, the PHF can be set to acquisition and used for depth determination if the shipboard HYDROSWEEP system is down.

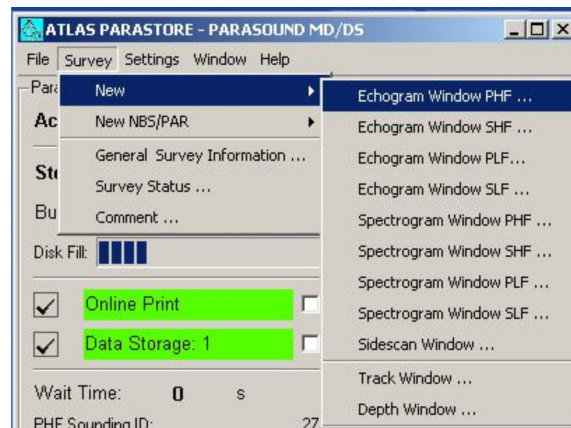


Fig. 6.6: To open a new Acquisition Window choose : Survey→ New → Echogram Window.

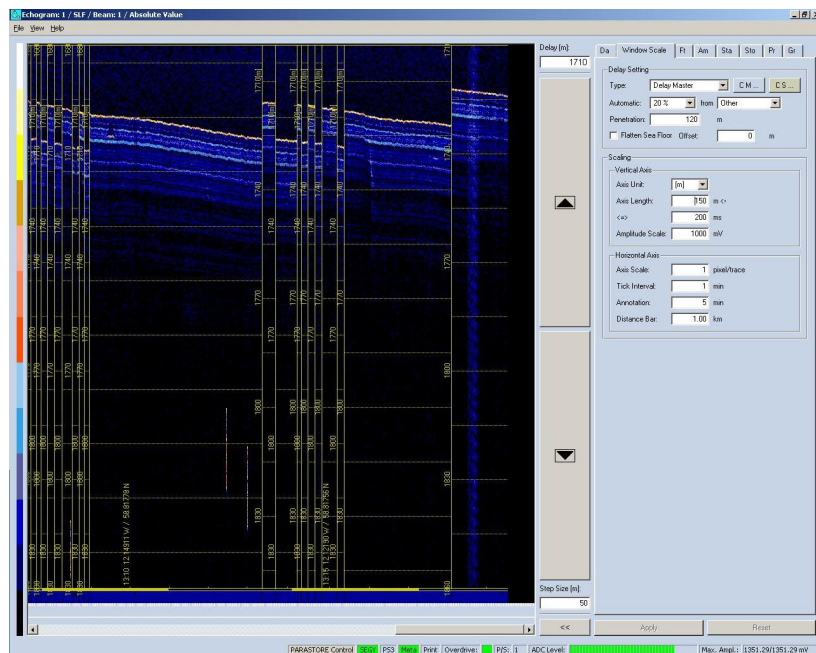


Fig. 6.7: In the SLF echogram the tab „Wi“ (Window Scale) was chosen. Type was set to “Delay Master” and Automatic to 20%, i.e. that the delay value will change when the seafloor is closer to the top or bottom than 20% of the window length (150 m). During this cruise the automatic mode worked flawless. In the “from:” field Other can be chosen, i.e. the HYDROSWEEP depth is used. Alternatively PHF can be used, which is the PARASOUND depth, if the HYDROSWEEP system is down.

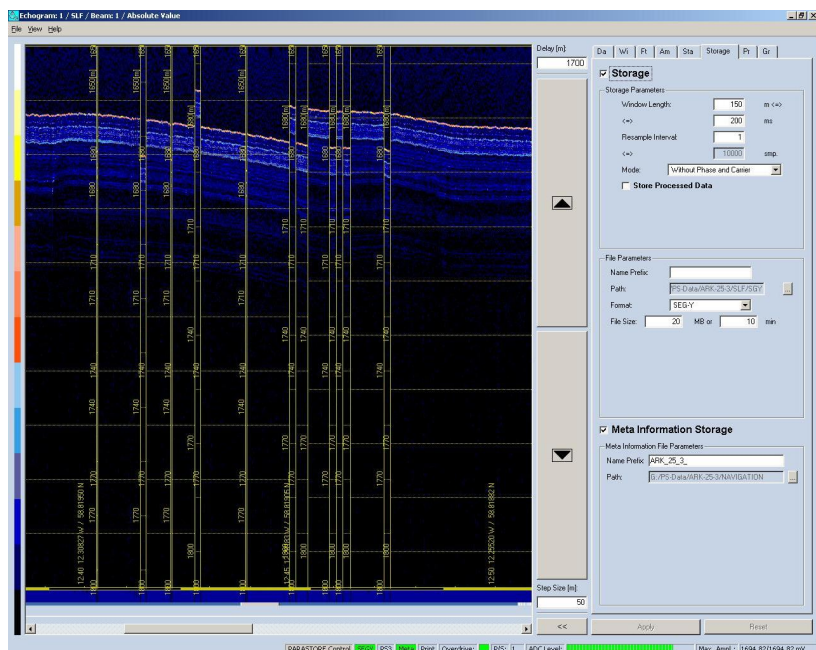


Fig. 6.8: In the SLF window St” (Storage) was chosen (Note: “Storage” and “Meta Information Storage” need to be highlighted, paths for data storage need to be checked). We stored data in SEG-Y format for further processing. IMPORTANT: Do NOT check “Store processed data”. If this option is checked, only the data from the display window are stored, including filtering, amplification, etc.

6.2 Processing

Goal of the data processing was to prepare the echosounder data in a way that it could be loaded as a data class into the GeoFrame system for a combined interpretation with the multi-channel seismic lines, i.e. the traces had to be interpolated at the CDP distances of the MCS lines.

Main processing steps were:

- (1) Data import and coordinate conversion to UTM
- (2) Interpolation of equidistant traces (6.25 m)
- (3) Resampling (0.1 ms)
- (4) Data export, loading into GeoFrame and tying to the MCS data

Processing of the data was done using the 2D-data-analysis module of the software REFLEXW v5.5.1.

(1) Data import and coordinate conversion to UTM

Selection of segy files according to the start and end date and time of the respective seismic profile (see profile list) using the setup shown in Figure 6.9.

Definition of start and end trace of the PARASOUND profile according to start and end coordinates of the MCS profile using the early provided MCS shotpoint tables

File → Edit

TraceHeader → TraceHeaderTabella

Extraction of selected trace range
Processing → Edit traces/traceranges → Extract

Conversion of the navigation data to UTM

File → EditTraceHeader → TraceHeader-Menu → type:UTM-conversion

(2) Interpolation of equidistant traces

The trace interpolation tool of REFLEXW requires the calculation of the distance of each trace along the profile. This can be done via

File → EditTraceHeader → TraceHeaderTabella → update distances button

but proved to calculate different lengths than that of the MCS profiles, because the distances between the single traces are calculated and summed up. As the ships

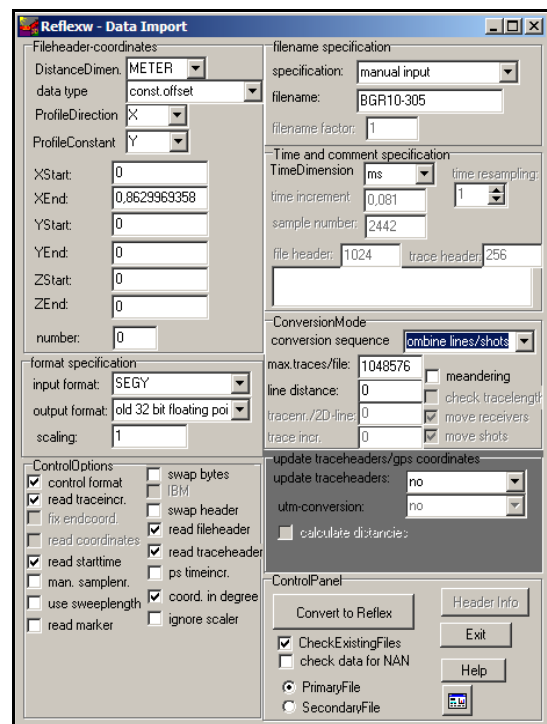


Fig. 6.9: REFLEXW menu, Import of raw SEGY files.

course is never a straight line (see Figure 6.10), the error can sum up to a difference of about 10 % depending on weather conditions. Better results are achieved, if the distances of the traces along the profile are calculated relative to the position of the first trace. Here, it is important, that end of turns have to be omitted and the profile runs along a relatively straight line. The trace header table is exported via **File→EditTraceHeader→TraceHeaderTabella→export** and distance calculation done in Microsoft Excel.

After import of the calculated distances, equidistant traces are interpolated every 6.25 meter which is the CDP distance of the MCS data.

**Processing->
TraceInterpolation/Resorting->
Make equidist.traces**

Note: for transit (i.e. no MCS shooting), curved lines or turns the internal REFLEXW algorithm of distance calculation should be used.

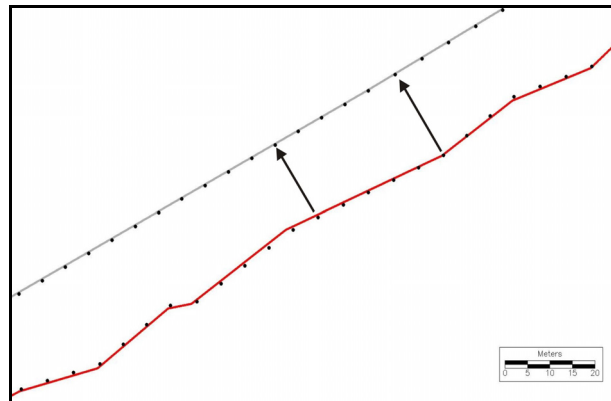


Fig. 6.10: GeoFrame IESX basemap, projection of PARASOUND profile (red) on binned MCS profile (gray). The PARASOUND profile follows the true ship track

(3) Resampling to 10 kHz

The SEGY trace-delay header word is in ms and must be a multiple of the sample rate which header word is in μs , otherwise the data for that depth will be rejected by the GeoFrame interpretation system. In order to stay above the Nyquist frequency of the 4 kHz data, a sample rate of 0.1 ms is chosen.

Processing->1D-Filter->Resampling

(4) Data export, loading into GeoFrame and tying to the MCS data

Processed data are exported from REFLEXW via **File->Export (seg)**

Import into GeoFrame was done with the IESX data manager module. In a first step the equidistantly interpolated PARASOUND data were loaded into a temporary survey. This way they were available early during the cruise and could be used to check on planned OBS, gravity corer and heat flow station positions. After processing and loading of the multi-channel seismic data, trace numbers of the PARASOUND profile and CDP numbers of the equally spaced MCS profile were compared (Fig. 6.10) and the PARASOUND data loaded as a seismic class to the MCS profile. The temporary profile was removed afterwards.

6 Sediment echosounding

6.3 Example results

Along all seismic profiles and additionally on transits and magnetic profiles high-resolution sub-bottom profiles were collected during cruise ARK-XXV/3 using the PARASOUND system. Some general observations from the obtained records within the survey area are depicted below in Figs. 6.11 to 6.16:

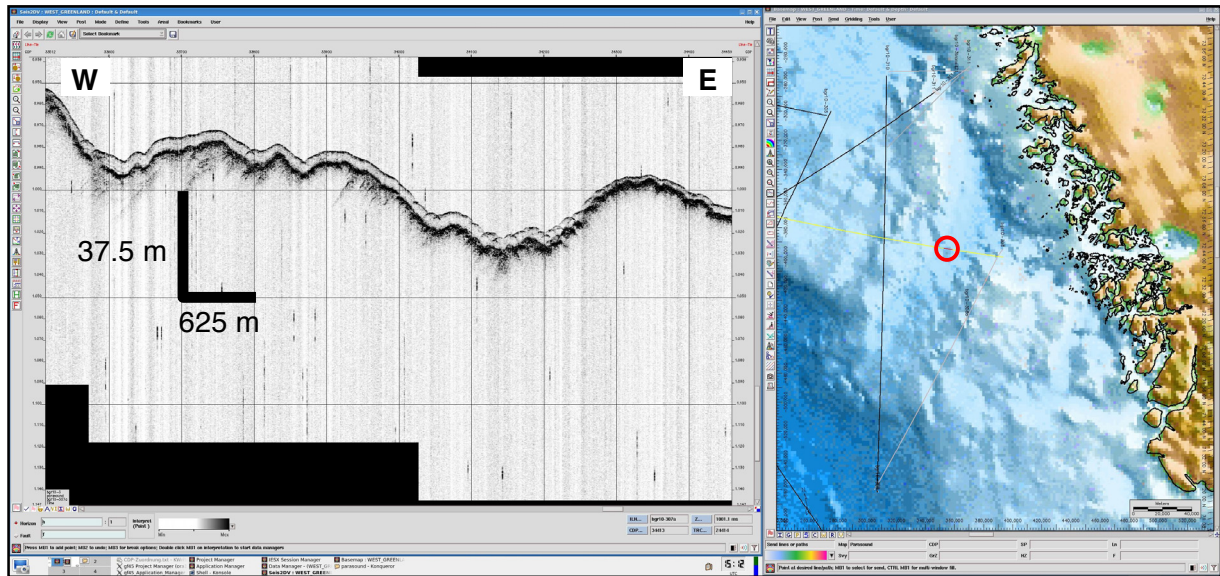


Fig. 6.11: Toplap structures due to glacial erosion in the eastern Baffin Bay.

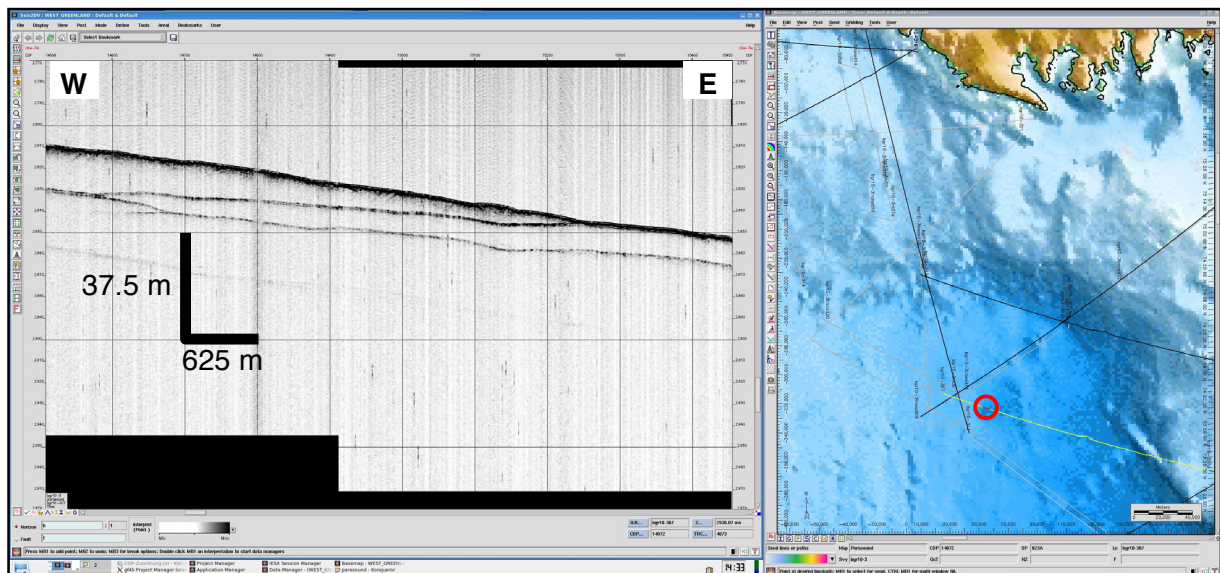


Fig. 6.12: Cross-bedding structures in the distal Baffin Fan.

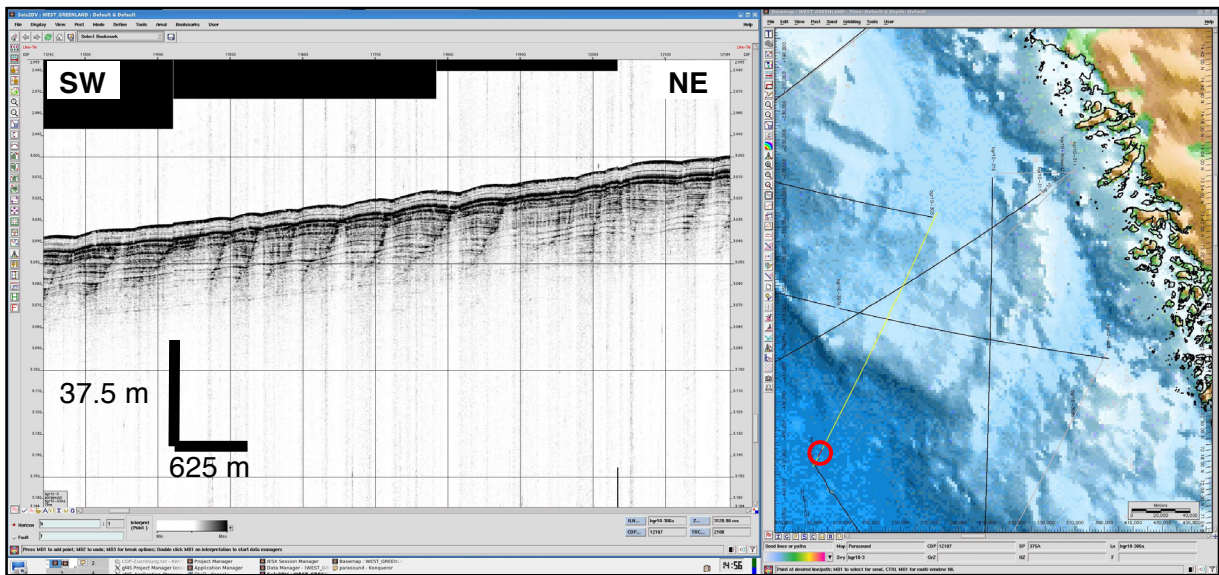


Fig. 6.13: Slope instability and gravitational sliding in the eastern Baffin Bay

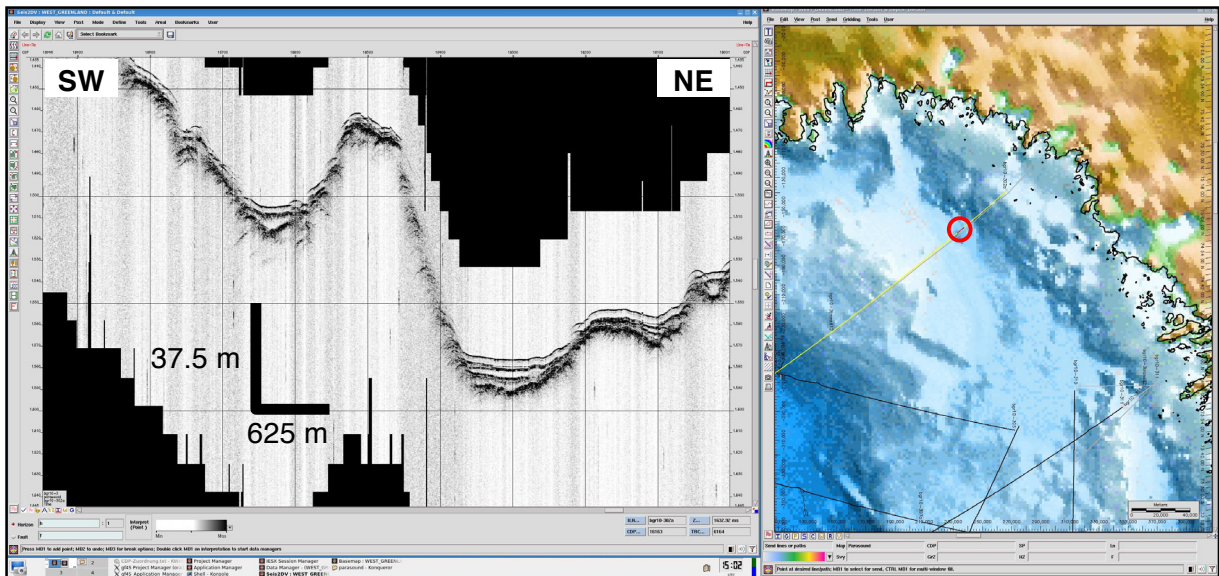


Fig. 6.14: Small basin infills in the Melville Trough

6 Sediment echosounding

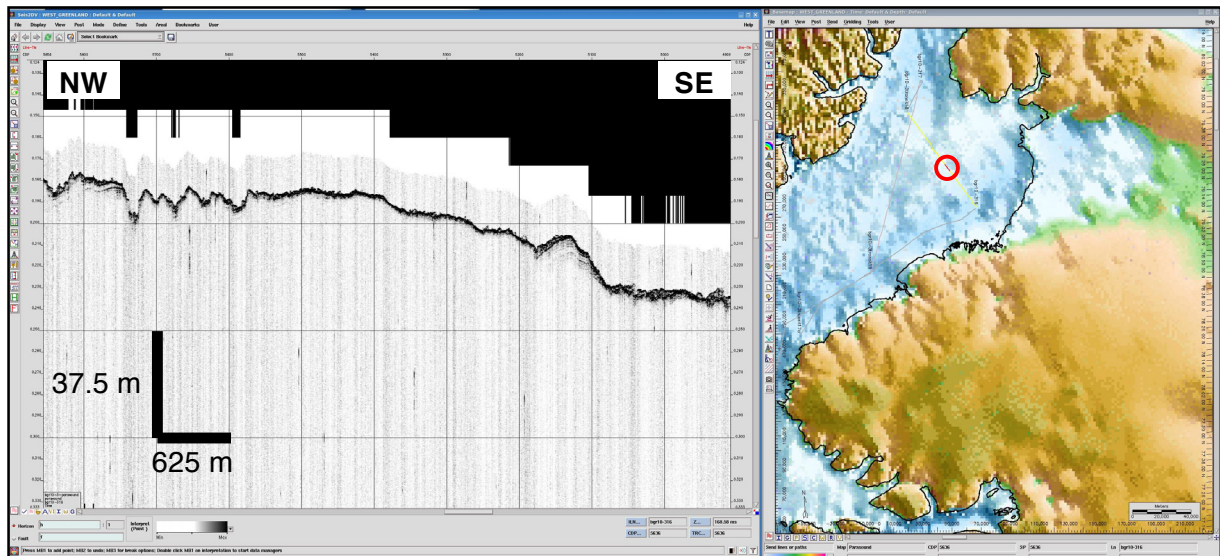


Fig. 6.15: Erosion and overcompacted sediments with little to no reflectivity in the Kane Basin.

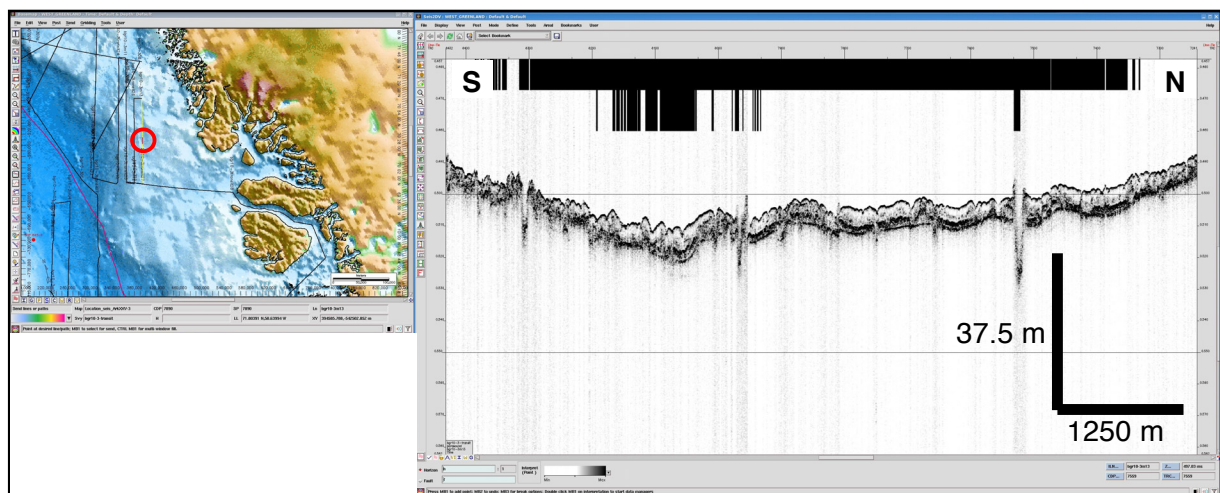


Fig. 6.16: Incisions northwest of Disko Island, possibly iceberg scour marks.

6.4 Testing of different SLF frequencies

OBS-Profiles BGR10-3r2 and BGR10-3r3 offered the possibility to test the PARASOUND system with other frequencies, as they were acquired at 4 kHz during shooting of reflection seismic lines. The maximum possible SLF frequency of 6 kHz was chosen to achieve a higher resolution in the uppermost sediments. This testing showed no significant improvement of resolution or signal quality in the uppermost sedimentary layers when a higher frequency than 4 kHz is used with the PARASOUND system (Fig. 6.17).

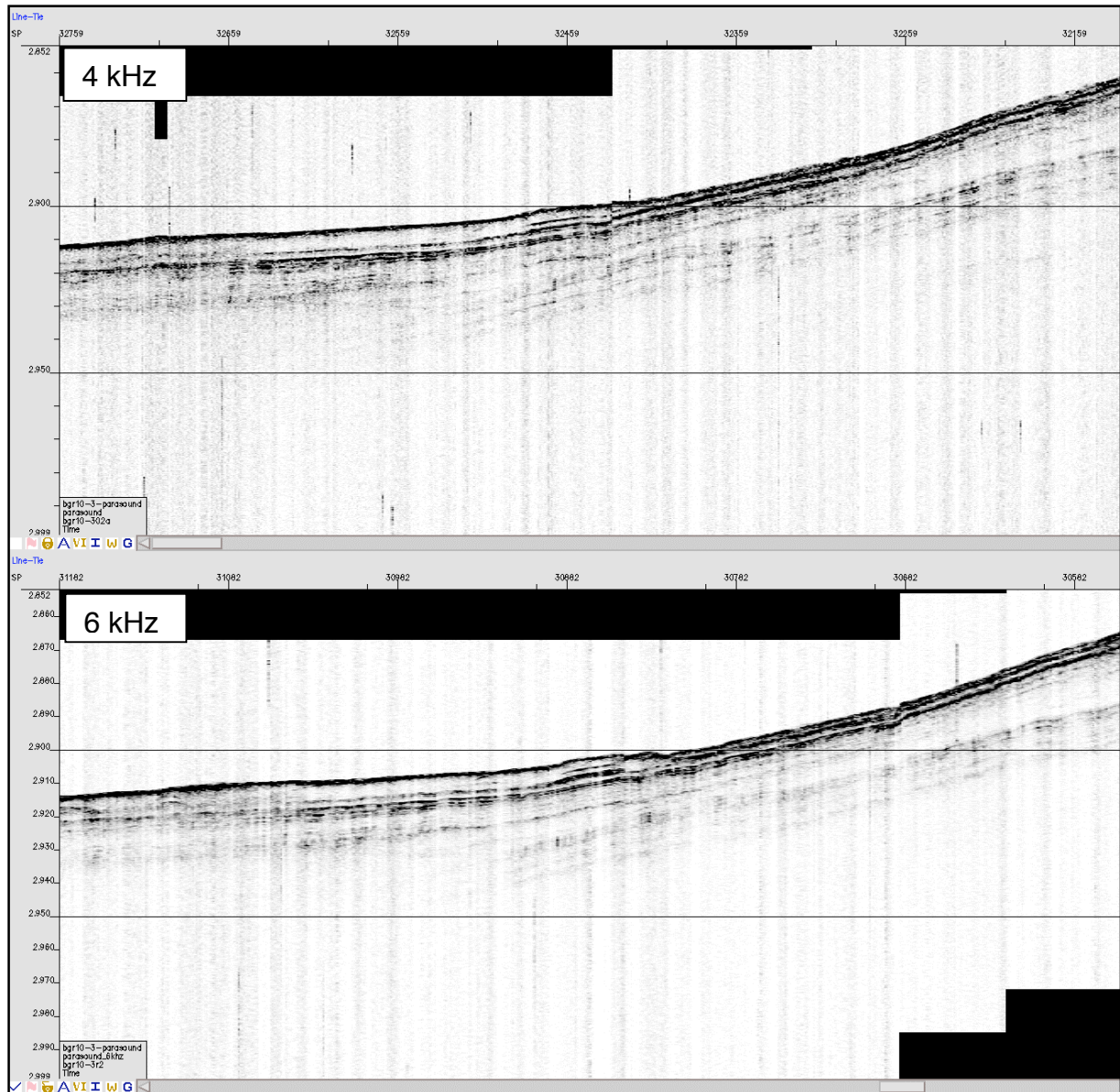


Fig. 6.17: Testing of different frequencies. The 6 kHz data show no significant improvement of resolution in the uppermost sedimentary layers.

7. GRAVIMETRY

Ingo Heyde, Hans-Otto Bargeloh, Bernd Schreckenberger, Michael Zeibig
Bundesanstalt für Geowissenschaften und Rohstoffe

7.1 Method and instrument

During the cruise ARK-XXV/3 the AWI owned sea gravimeter system KSS31, serial No. 25, was used. The KSS31 is permanently installed on *Polarstern* in the gravimeter room one level below the main deck (Fig. 7.1). The sea gravimeter is located 11.26 m above the vessel's keel, 0.88 m to portside from the centerline, and 53.20 m forward of the stern (see Figure 4.1).

The gravimeter system KSS31 is a high-performance instrument for marine gravity measurements, manufactured by Bodenseewerk Geosystem GmbH. While the sensor is based on the Askania type GSS3 sea gravimeter designed by Prof. Graf in the 60ties, the horizontal platform and the corresponding electronic devices were developed at Bodenseewerk Geosystem in the second half of the 70ties. The KSS31 system consists of two main assemblies: the gyro-stabilized platform with the gravity sensor and a rack with the power supply, the system electronics and the data handling subsystem.

The gravity sensor GSS30 (Fig. 7.2) consists of a tube-shaped mass that is suspended on a metal spring and guided frictionless by 5 threads. It is non-astatic and in particular designed to be insensitive to horizontal accelerations. This is achieved by limiting the motion of the mass to the vertical direction. Thus it is a straight line gravity meter avoiding cross coupling effects of beam type gravity meters. The main part of the total gravity acceleration is compensated by the mechanical spring, but gravity changes are compensated and detected by an electromagnetic system. The displacement of the spring-mass assembly with respect to the outer casing of the instrument is measured using a capacitance transducer.

The leveling subsystem consists of a platform stabilized in two axes by a vertical, electrically erected gyro. The stabilization during course changes can be improved by providing the system with online navigation data. The control electronics and the power supply of the platform are located in the data handling subsystem unit. Functions like gyro run-up and -down sequences and the automatic platform caging are performed by the system controller unit located in the data handling subsystem, too. The stabilized platform will keep the sensor in an upright position with an accuracy of leveling in the order of 0.5 minutes of arc. This is particularly important as the sensor is very sensitive to tilting. Vertical acceleration, however, cannot be eliminated. Luckily on a ship the vertical acceleration oscillates periodically around the zero level with a period of some seconds. This signal can be eliminated easily by means of low pass filtering.

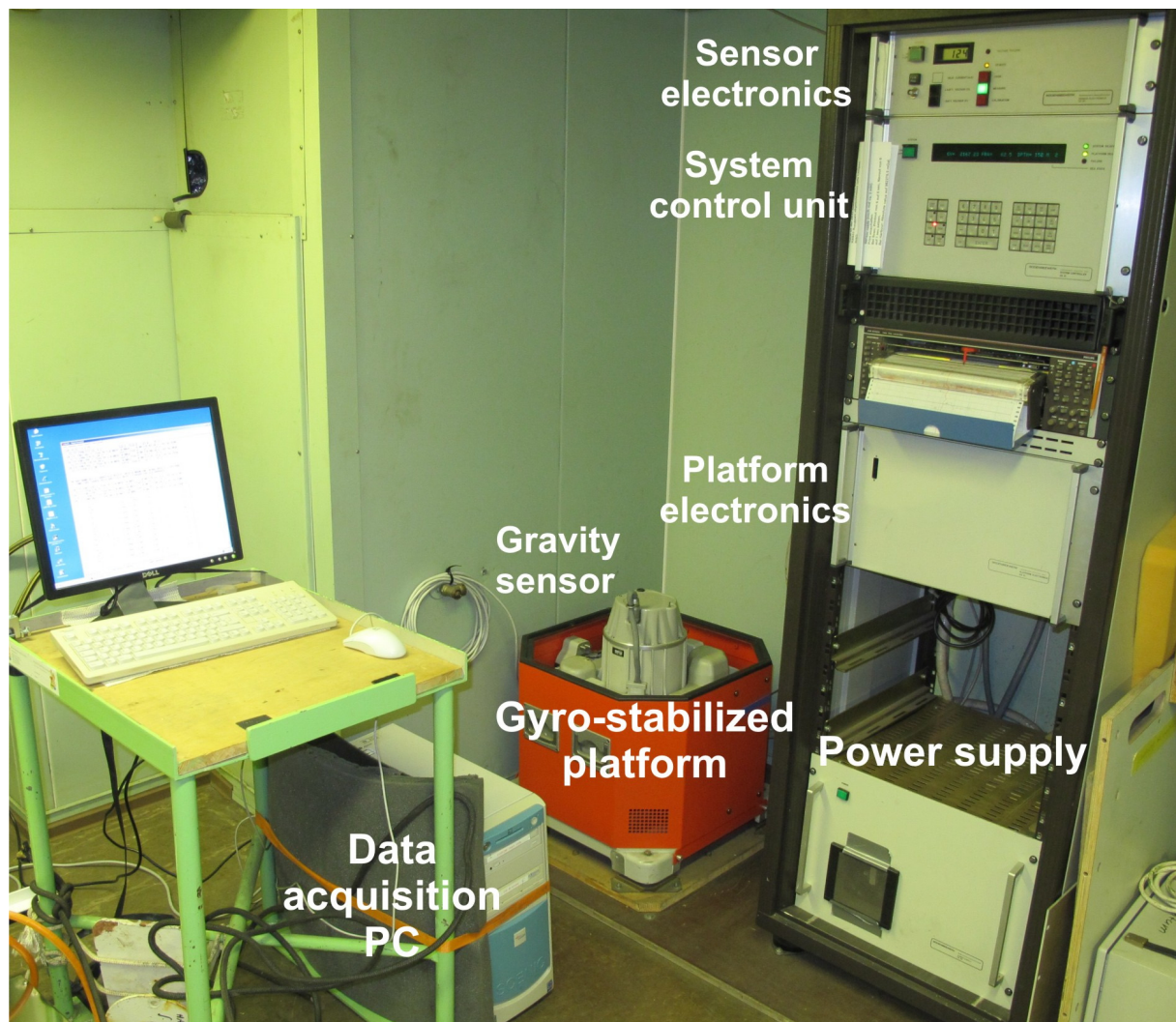


Fig. 7.1: KSS31 gravimeter system (platform with sensor and electronics rack) in the gravimeter room on Polarstern

The data are transmitted to the DSHIP system and online navigation data from this system are sent with a rate of 1 Hz to support the stabilizing platform. The support is realized as follows: The horizontal position of the gyro-stabilized platform is controlled by two orthogonal horizontal accelerometers. The platform is leveled in such a manner that the horizontal accelerations are zero. If the ship describes a curve, the additional horizontal acceleration will cause the platform to be leveled according to the resulting apparent vertical axis. This axis may differ substantially from the true vertical axis and will result in reduced gravity values and additionally in an effect of horizontal accelerations on the measured gravity. The latter effect is eliminated by supplying the system with online navigation data. A microprocessor calculates the leveling errors from this input and enters them into the platform electronics which corrects the platform accordingly.

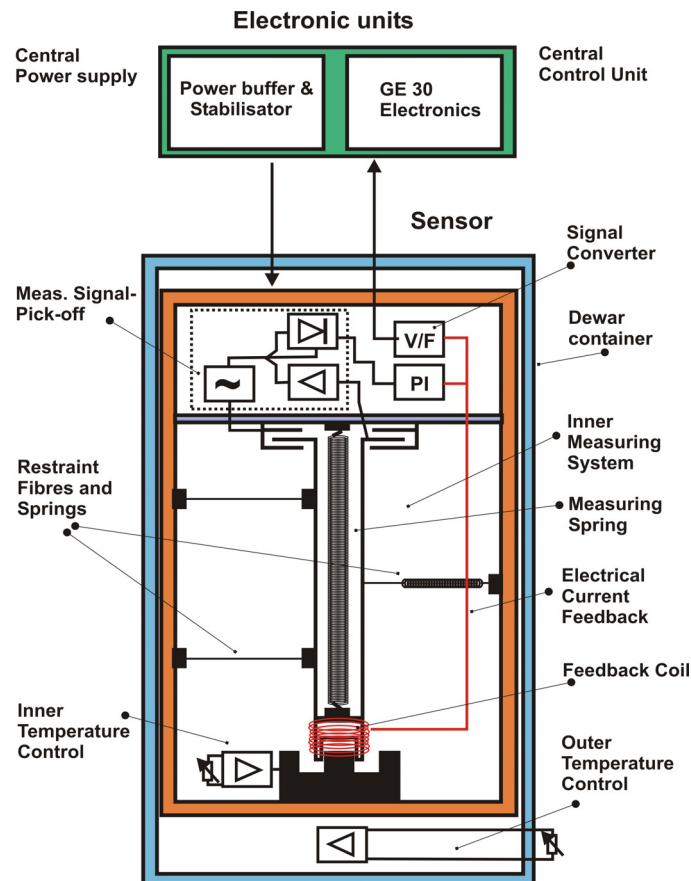


Fig. 7.2: Principle sketch of the gravity sensor GSS30 of the gravimeter system KSS31M

7.2 Data processing

The raw gravity data from the DAVIS-SHIP (DSHIP) system are recorded and processed by the BGR data acquisition system installed in the dry lab no. 4.

Processing of the gravity data consists essentially of the following steps:

- a time shift of 76 seconds due to the overcritical damping of the sensor,
- conversion of the output from reading units (r.u.) to mGal by applying a conversion factor of 0.8969 mGal/r.u. On this cruise this was done in the system itself by hardware settings
- connection of the harbour gravity value to the world gravity net IGSN 71,
- correction for the Eötvös effect using the navigation data,
- correction for the instrumental drift (not performed until completion of the cruise),
- subtraction of the normal gravity (WGS67).

As a result, we get the so-called free-air anomaly (FAA) which in the case of marine gravity is simply the Eötvös-corrected, observed absolute gravity minus the normal gravity. According to the selectable time interval of the BGR data acquisition system, gravity values are available every 20 seconds. These anomalies are named BEARB anomalies in the following.

The gravity anomalies, which are provided directly by the data handling subsystem of the KSS31, were additionally recorded with a separate computer installed in the gravimeter room. Free-air gravity anomalies are obtained when the KSS31 is supplied with the necessary navigation data (geographical latitude and longitude, speed, course over ground and heading). These KSS31 anomalies are available every 5 seconds. The BEARB anomalies show short-wavelength oscillations in the order of 1 mGal. These oscillations are slightly suppressed in the KSS31 data (Fig. 7.3). The reason is that the Eötvös correction values of the KSS31 are filtered the same way as the gravity data, whereas the Eötvös correction values of BEARB are not filtered. The filtered free-air anomalies provided by the KSS31 were used for display and interpretation.

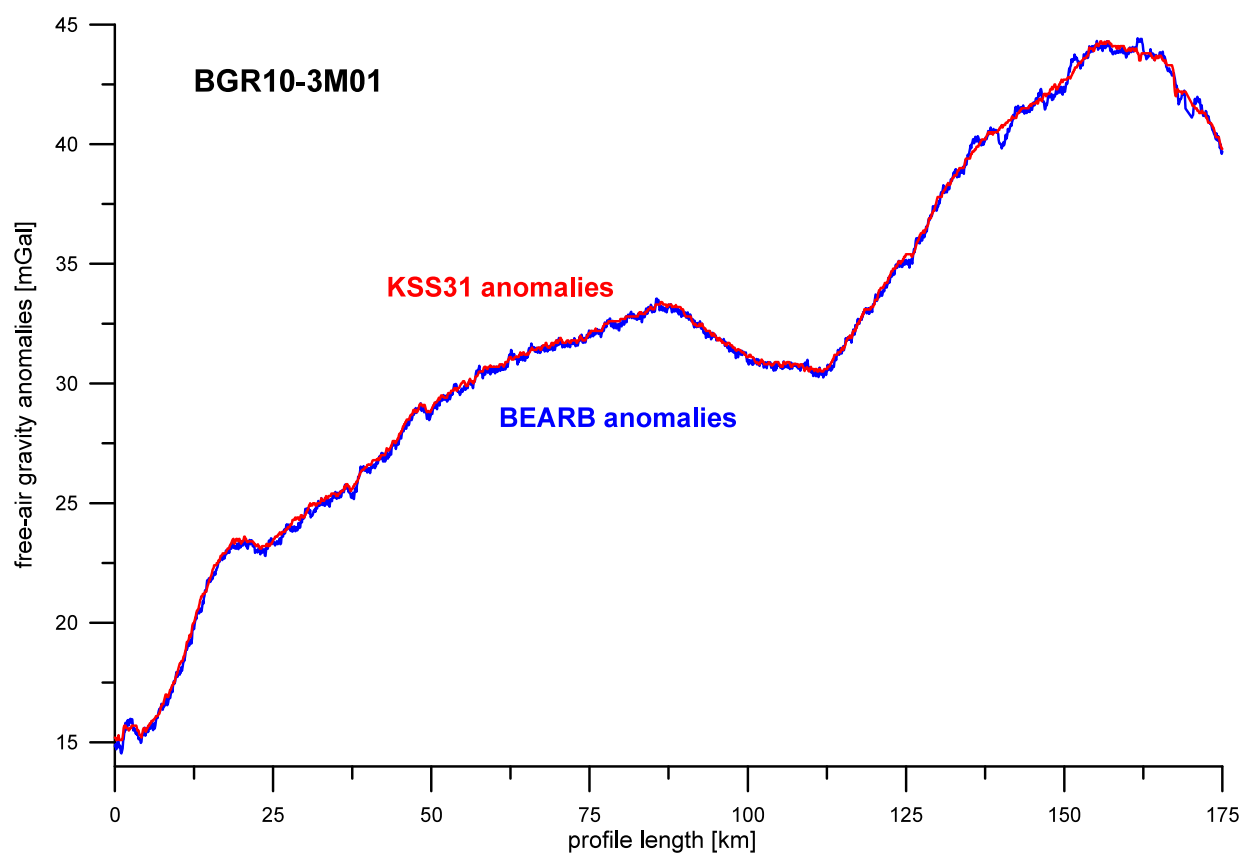


Fig. 7.3: Comparison of BEARB and KSS31M unfiltered free-air gravity anomalies along profile BGR10-3M01 measured during medium to rough sea state conditions and a ship's velocity of 10 knots.

Outliers were removed manually in both data sets. Additional low pass filtering was not necessary in the survey area. During the transit across the North Atlantic, however, the data had to be low pass filtered due to rougher seas.

7.3 Gravity ties to land stations

To compare the results of different gravity surveys the measured data have to be tied to a world-wide accepted reference system. This system is represented by the International Gravity Standardization Net IGSN71 (Morelli, 1974). The IGSN71 was

7 Gravimetry

established in 1971 by the International Union of Geodesy and Geophysics (IUGG) as a set of world-wide distributed locations with known absolute gravity values better than a few tenths of mGal. According to the recommendations of the IUGG, every gravity survey, marine or land, should be related to the datum and the scale of the IGSN71.

Therefore, gravity measurements on land have to be carried out to connect the gravity measurements at sea with the IGSN71. The marine geophysical group of BGR uses a LaCoste&Romberg gravity meter, model G, no. 480 (LCR G480) for the gravity connections. In Bremerhaven the AWI gravity meter (LCR G1031) was used since the BGR instrument had to be stored in the container before arrival. The point descriptions and absolute gravity values of 3 reference stations in Reykjavik were kindly provided by the Bureau Gravimetrique International (BGI) in Toulouse.

Polarstern moored at the NW-SE oriented Skarfabakki berth in Sundahöfn harbour in Reykjavik (Fig. 7.4). On July 31, tie measurements to point A on the pier opposite the gravimeter room on *Polarstern* have been made. Point A is located near the 7th bollard from the southeastern end of the pier (distance: about 60 m). The connection measurements from reference stations 01 and 03 resulted in an average absolute gravity value of 982276.496 mGal (with water level –2.0 m and ship's draught of 10.4 m) for point A at the level of the sea gravimeter. Reference station 01 was preferred as the location of this station is most reliable and has undergone no changes with regard to the BGI description. The difference of -0.29 mGal using reference station 02 results from the fact that the absolute gravity value is given for the top of a 1 m high pillar which has been removed. Thus the connection measurement was done on the ground above the still visible foundation of the pillar. The reading of the KSS31 at the same time (July 31, 2010, 9:55 UTC) was 2030.43 mGal.

Tab. 7.1: Observation report of the gravity tie measurements in Reykjavik and Bremerhaven

Station	Observer	Instrument	Date	Time UTC	Reading units	Gravity value [mGal]
A	H	LCR-G480	31.07.10	09:55	5805.01	5906.133
01	H	LCR-G480	31.07.10	10:15	5787.95	5888.731
02	H	LCR-G480	31.07.10	10:37	5791.83	5892.691
03	H, A	LCR-G480	31.07.10	11:00	5794.00	5894.905
A	H, A	LCR-G480	31.07.10	11:30	5804.97	5906.092
B	H	LCR-G877	09.10.10	07:20	4895.42	5010.349
04	H	LCR-G877	09.10.10	07:45	4895.42	5010.349
B	H	LCR-G877	09.10.10	08:07	4895.74	5010.677

Observer: H = Heyde. A= Altenbernd,

Gravity in mGal was calculated using LCR-G480/-G877 scaling tables.

Reference Stations:

01:	Reykjavik, Monument in front of Hallgrimskirkja, (IGSN71)	982258.79	mGal
	(BGI Station No. 21941B)		
02:	Reykjavik, Catholic Church Landakotskirkja (IGSN71)	982262.46	mGal
	(BGI Station No. 21941C)		
03:	Reykjavik, Main building University of Iceland, (IGSN71)	982264.96	mGal
	(BGI Station No. 21941A)		
04:	Bremerhaven, AWI building, Room 0082 (IGSN71)	981356.72	mGal

Gravity stations:

- A: Reykjavik, Sundahöfn harbour, Skarfabakki berth, 60 m from the southeastern end of the pier (64°09.241'N, 21°51.589'W)
 B: Bremerhaven harbour, Dalbenpier at Lloyd shipyard

Differences between reference and gravity stations:

01 – A	= -17.402 mGal
02 – A	= -13.442 mGal
03 – A	= -11.187 mGal

Absolute gravity at A: 982276.192 mGal from 01
 982275.902 mGal from 02
 982276.147 mGal from 03

Absolute gravity for A (reduced to sensor level –1.14 m) 982276.496 mGal (IGSN71 system) used for the gravity tie on 31.07.2010 (10:00 UTC).
 Reading of sea gravimeter KSS31 at that time: 2030.43 mGal.

Difference between reference and gravity station:

$$04 - B = 0.16 \text{ mGal}$$

Absolute gravity at B: 981356.88 mGal

Absolute gravity for B (reduced to sensor level –1.24 m) 981357.21 mGal (IGSN71 system) used for the gravity tie on 09.10.2010 (08:05 UTC).
 Reading of sea gravimeter KSS31 at that time: 1102.54 mGal.

7 Gravimetry

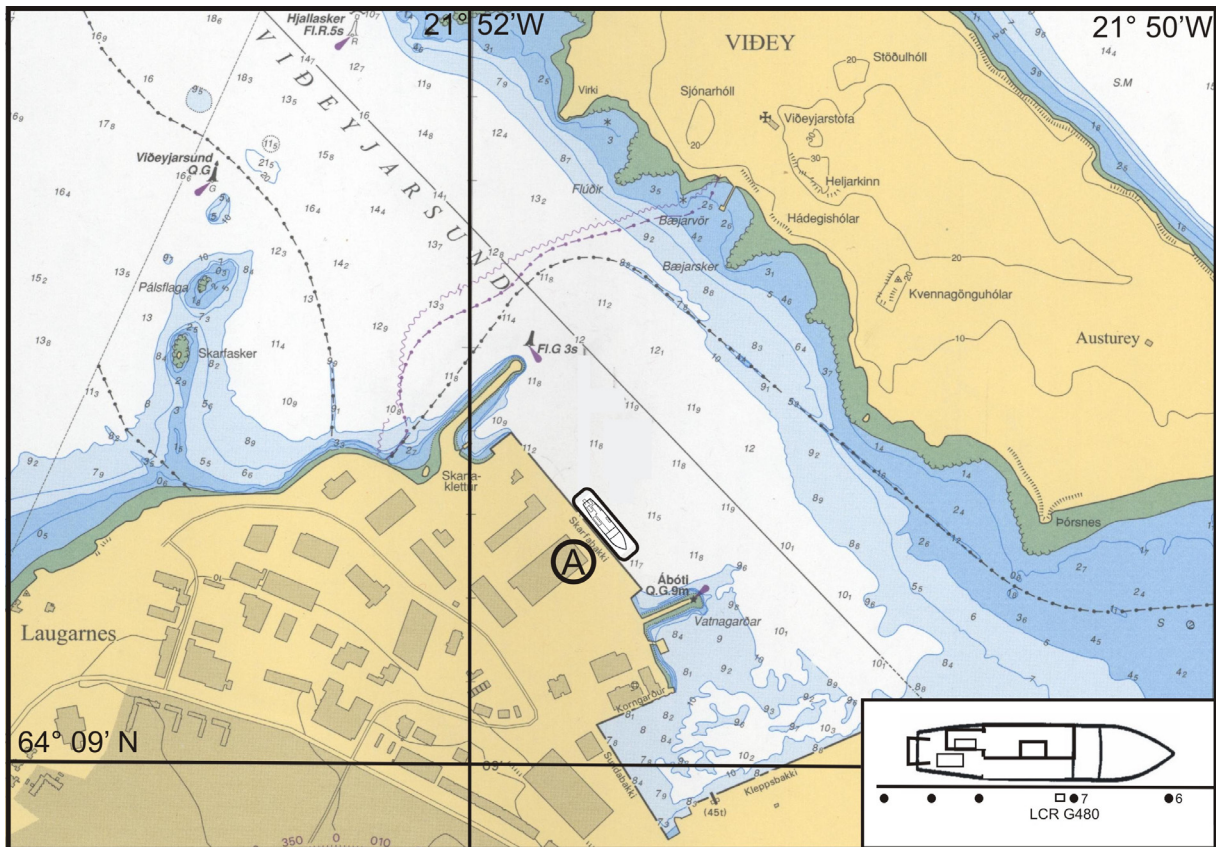


Fig. 7.4: Location of the mooring site of *Polarstern* at the Skarfabakki berth of Sundahöfn harbour in Reykjavik (A).

On September e, measurements with both BGR's LCR G-480 and AWI's LCR G-877 at two reference stations in Qaanaaq were carried out. But while these measurements were successful it proved to be impossible to perform reasonable readings on board *Polarstern* even during station work at calm seastate conditions. At the end of the cruise *Polarstern* moored at the Dalbenpier at Lloyd shipyard in Bremerhaven near the second bollard 60 about 100 m from the southern end of the pier (Fig. 7.5). On October 9, tie measurements to point B on the pier opposite the gravimeter room on *Polarstern* have been made. Point B was 1.7 m above the water level with a ship's draught of 10.8 m.

The connection measurements resulted in an average absolute gravity value of 981357.21 mGal (reduced to sensor level -1.24 m, IGSN71) for point B. The reading of the KSS31 at the same time (October 9, 2010, 08:05 UTC) was 1102.45 mGal. The instrumental drift for the cruise can be derived from the readings in Reykjavik and Bremerhaven to -8.60 mGal / 69.9 days or -0.123 mGal/day. This drift rate is rather large but lies within the normal drift range of marine gravity measurements with the KSS31. It will be applied to the data. Marine gravity measurements were recorded from 01.08.10 (23:00 UTC) till 09.10.10 (1:30 UTC), i.e drift started with -0.190 mGal and ended with -8.567 mGal.

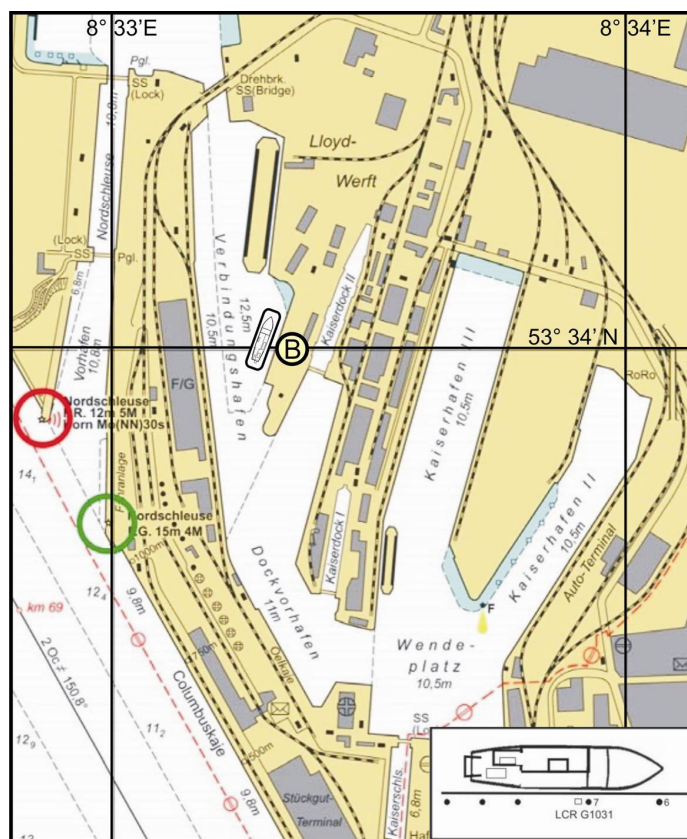


Fig. 7.5: Location of the mooring site of Polarstern at the Dalbenpier at the Lloyd shipyard in Bremerhaven (B).

7.4 Data quality and preliminary results

In order to check the accuracy of the data quantitatively, the values along repeatedly measured profiles and at crossovers of gravity profiles were compared. During the cruise gravity data along 4 profiles were measured twice. Figure 7.6 shows exemplary the comparison for profiles BGR10-302/302a and BGR10-3r2.

The coincidence is nearly perfect and the differences amount to less than 1 mGal. Figure 7.7 shows a map of the ARK-XXV/3 profiles together with the crossover errors (COE). The average COE in the KSS31 data for the 45 crossovers along the track is 1.03 mGal ($1\sigma = 0.72$ mGal). The biggest difference found was 2.48 mGal. The general accuracy, however, is about 1 mGal. Possibly the COE will become smaller applying the drift correction after the tie measurements in Bremerhaven.

7 Gravimetry

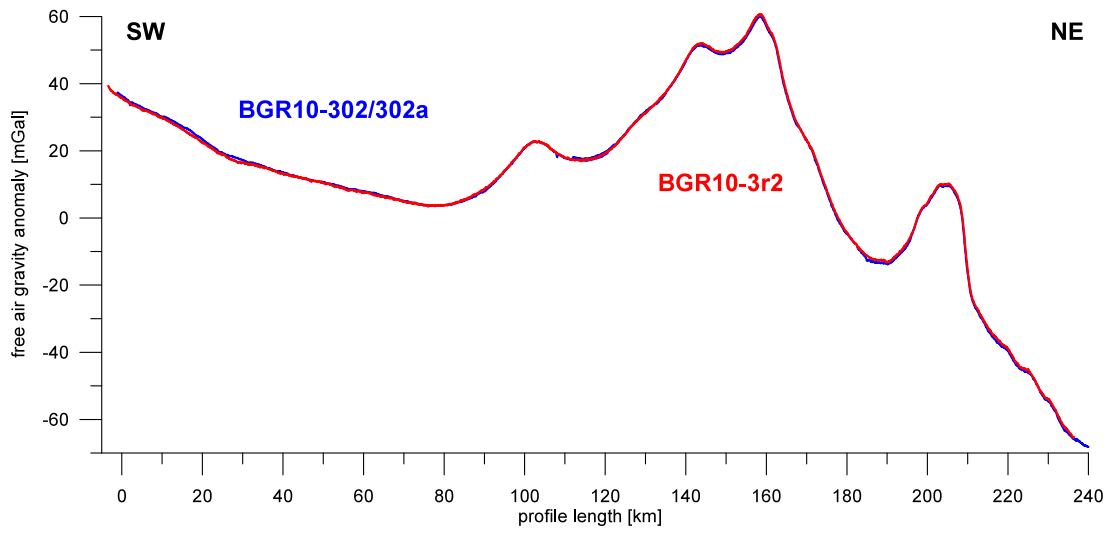


Fig. 7.6: Comparison of free-air gravity anomalies along profiles BGR10-302/302a and -3r2.

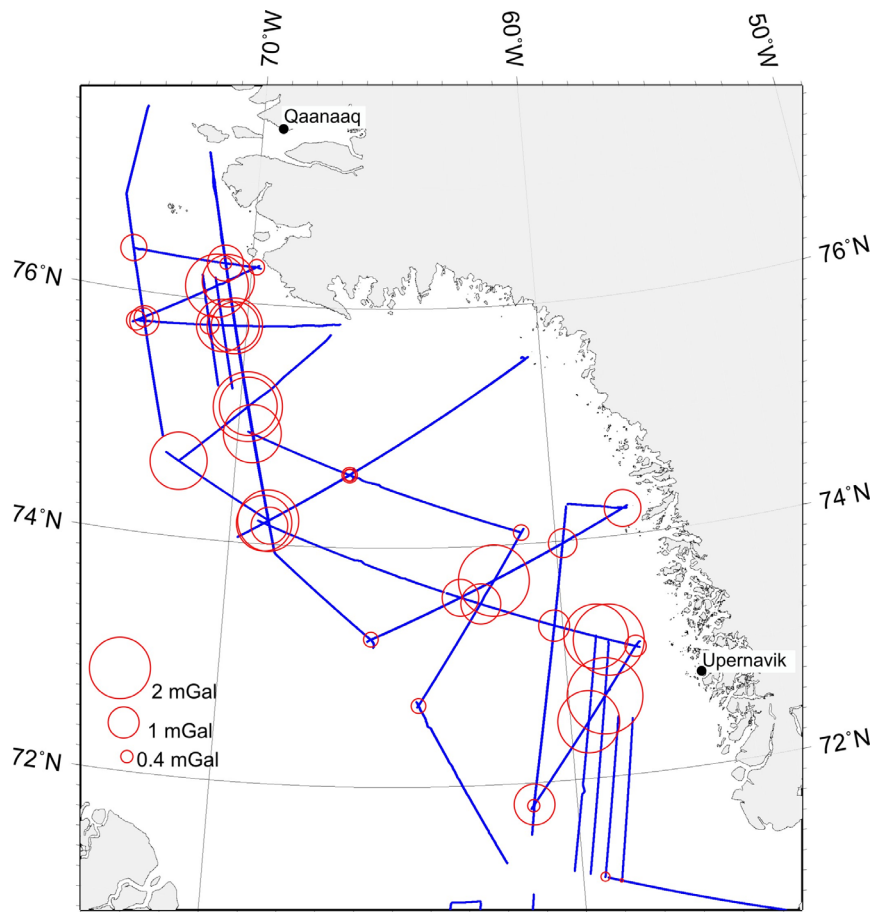


Fig. 7.7: Crossover errors (COE) of the KSS31 free-air gravity anomalies

7.5 Gravity data: description and preliminary results

7.5.1 Gravity database

Gravity measurements were carried out continuously during the cruise from Reykjavik to Bremerhaven along a total track length of more than 20,000 km. Thus gravity data along all 45 profiles with a total length of 7015 km were measured. In addition about 4200 km of the acquired data along transits and curves north of 64°N were usable. The distribution of the survey profiles can be seen in the track chart in Figure 2.2. Despite the coverage of the survey area is relatively sparse, a map of the free-air gravity anomalies was prepared. Figure 7.8 shows the map based on a 1 x 1 (arc-)minutes grid together with the survey tracks. The map is drawn up to a distance of 15 kilometres from the survey track.

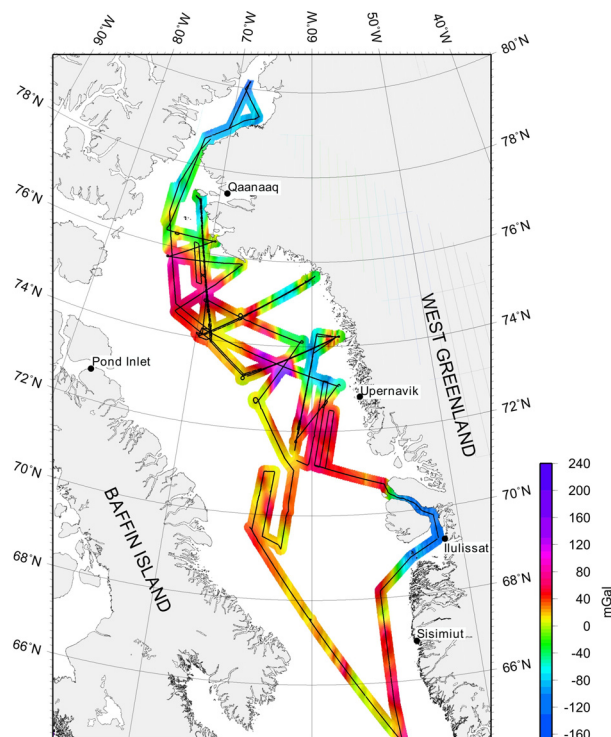


Fig. 7.8: Map of the free-air gravity anomalies in the survey area of cruise ARK-XXV/3. The map is drawn up to a distance of 15 kilometres from the tracks.

Global precise tracking coupled with dynamic orbit calculations provide an independent option to measure the height of the satellite above the ellipsoid. The difference between these two measurements is equal to the geoid height. So in marine areas the free-air anomaly can be calculated from the slope of the geoid. Closely spaced satellite altimeter profiles collected during the GEOSAT Geodetic Mission (~ 6 km) and the ERS 1 Geodetic phase (~ 8 km) were used by different groups to calculate grids of the free-air gravity anomalies.

Our dataset can serve as a reference for the comparison of two different satellite gravity data compilations. The first is the one from Sandwell and Smith (2005),

7 Gravimetry

version 18.1, referred to as SDW18.1. The second data set is from the DTU Space Centre, Copenhagen (Andersen et al., 2008) referred to as DNSC08. Andersen and colleagues (2008) implemented a new technique for the interpolation of the gravity field called adaptive interpolation. With adaptive interpolation the parameters for the covariance function have been determined empirically from the altimetry and subsequently interpolated to the position of interpolation. This demonstrated to be efficient in removing track-like structures in areas of high ocean variability as the variance is much better determined.

Subtracting the 1 x 1 minute grid of the SDW18.1 and DNSC08 data from the 1 x 1 minute grid of the shipboard data one obtains the maps of the differences shown in Figure 7.9.

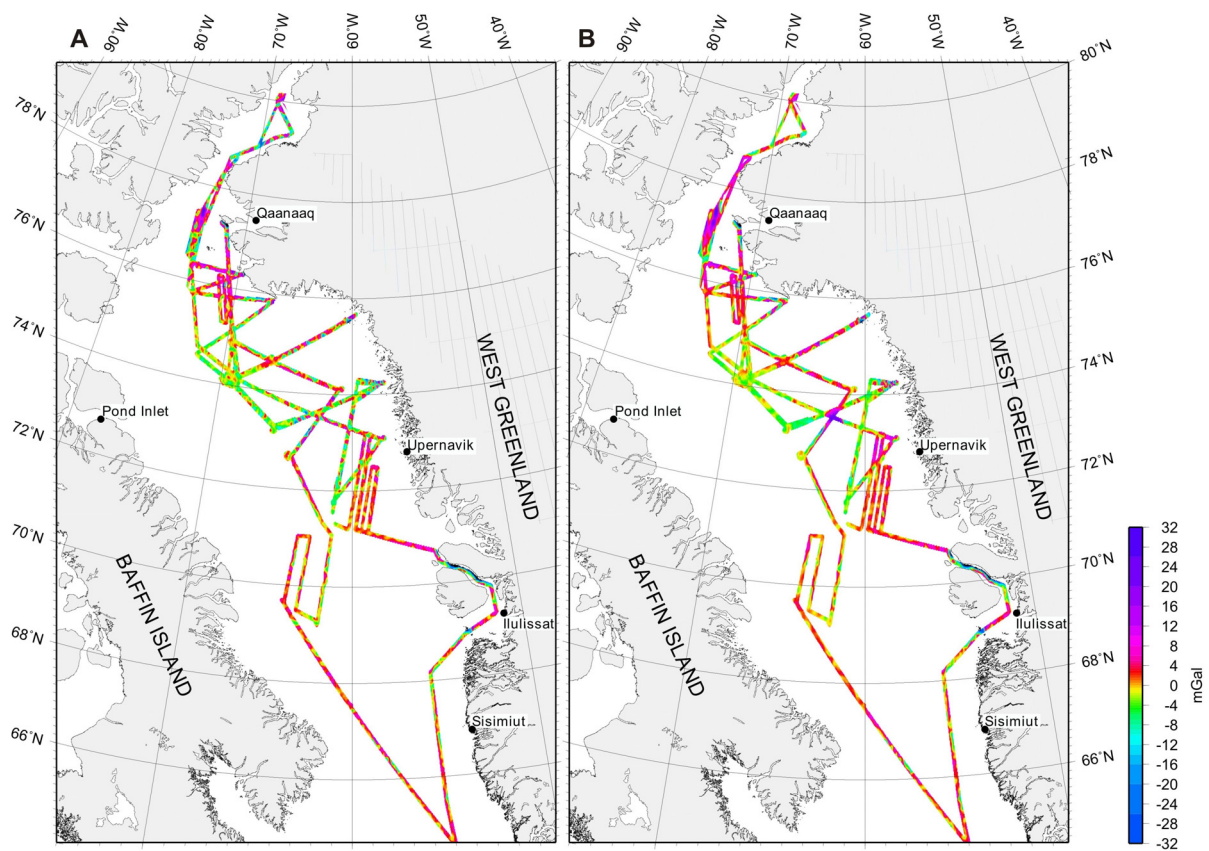


FIG. 7.9: Differences of the shipboard free-air gravity data and the gravity datasets derived from satellite altimetry (A: Sandwell and Smith (2005), version 18.1; B: Andersen et al. (2008), DNSC08). The maps are masked beyond a distance of 3 kilometres from the ARK-XXV/3 profiles.

The differences of both datasets range between +30 and -30 mGal, but the differences are below ± 10 mGal along most tracks. Higher positive differences are found in the Smith Sound and SW of Thule Airbase; higher negative differences north of Disko island. Generally a slight increase in the differences approaching the coast is noticeable.

Satellite gravity anomalies along the complete track were additionally calculated with bicubic interpolation out of the 1 x 1 minute grids and subtracted from the shipboard data (Fig. 7.10). The mean differences are comparable (SDW18.1: -0.20 mGal;

DNOSC08: 0.47 mGal). These values will change when the results of the final connection measurements will be available and the drift correction will have been applied (see chapter 7.3). The standard deviation is lower for the DNOSC08 data (4.66 mGal vs. 4.98 mGal). Considering the standard deviation as the main criteria, the above statistical results helped us to decide to use the DNOSC08 data set for further gravity map compilations in areas where no ARK-XXV/3 shipboard data were measured.

To illustrate the differences between the data sets in detail, Figure 7.11 shows exemplary a comparison along profiles BGR10-302/302a and -3r3. The wavelength range of satellite and shipboard anomalies is comparable in case of water depths greater than 1,000 m. However, especially along BGR10-3r3 the satellite data show oscillations with a wavelength of about 25 km and amplitudes of ± 3 to 5 mGal which do not correlate with anomalies in the shipboard data. We consider these differences to represent the error in the satellite data.

Moreover close to the coast anomalies of short wavelength are not resolved in the satellite data. This reflects the limited resolution of these datasets.

One can conclude that the free-air gravity anomalies derived from satellite altimetry are of great importance to get an overview of the gravity field in an oceanic area. For detailed investigations, however, shipboard gravity measurements are indispensable.

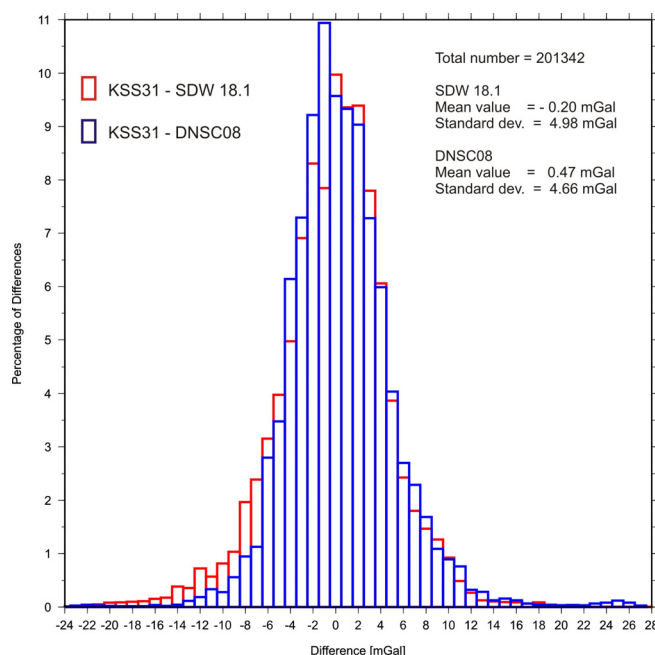


Fig. 7.10: Histogram of differences between shipboard KSS31 free-air gravity anomalies and the corresponding gravity datasets derived from satellite altimetry.

7.5.2 Gravity anomaly maps

Combined free-air gravity anomaly map

In order to get a more detailed idea of the gravity field in the survey area at first the shipboard gravity data from cruise MSM09/3 conducted in 2008 with *Maria S. Merian* were included for the compilation of the free-air gravity map shown in Figure 7.12. As a second stage also DNSC08 gravity data were included in areas with no shipboard data to get a complete overview of the gravity anomalies. The resulting free-air gravity anomaly map is shown in Figure 7.13. The anomalies range from -170 mGal in the Nares Strait to +240 mGal in the eastern Baffin Bay.

The oceanic crust in the Baffin Bay and the Labrador Sea in the south is characterized by free-air gravity anomalies from about -20 and to +15 mGal. In this area water depths of more than 2,000 m are reached. Higher gravity values can be correlated partly with topographic highs on the oceanic crust. The southern Baffin Bay shows similar anomalies. It is connected to its northern continuation by a narrow gateway. To the South it terminates at the topographic high of the Davis Strait. To the North the Baffin Bay narrows towards the entrance of the Nares Strait which is underlain by continental crust. This transition is marked by broad positive gravity anomalies.

Landward the gravity anomaly values increase considerably. The map reveals prominent positive anomalies parallel to the shelf break (up to +240 mGal) both on the western and the eastern side of Baffin Bay. In the Labrador region these maxima are rather symmetrically. North of the Davis Strait these anomalies are much broader offshore Greenland than offshore Baffin Island. Further north the positive anomalies are broader offshore Lancaster and Jones Sound than offshore NW-Greenland.

These anomalies are typical for rifted continental margins which are characterized by prominent free-air gravity anomalies elongated parallel to the ocean-continent transition. For example, these features could be observed along large portions of the Atlantic margins (Watts and Fairhead, 1999). Sleep and Fuyita (1997) demonstrated that a simplified ocean-continent transition (oceanic crust bordering directly on continental crust, both of uniform thickness and isostatically compensated) produces an asymmetric free-air anomaly located at this boundary with a high on the outer shelf and a low on the oceanic crustal edge.

Landward the gravity anomaly values decrease considerably. Prominent minima are reached southeast of Disko Island near the south- and the northwestern coast of the Cumberland Peninsula. Another less pronounced minimum on the Greenland side can be found northwest of Sisimiut. These areas with increased water depths to about 500 m correspond probably to Mesozoic sediment basins filled with thick sediments of relatively low density. The most extended minima with a length of 350 km and a width of 35 - 90 km reflects the Melville Bay Graben. South of Upernavik, however, the broad shelf is characterized by positive anomalies reflecting the widespread Palaeocene basalts. The Smith Sound and especially the Kane Basin show highly negative gravity anomalies.

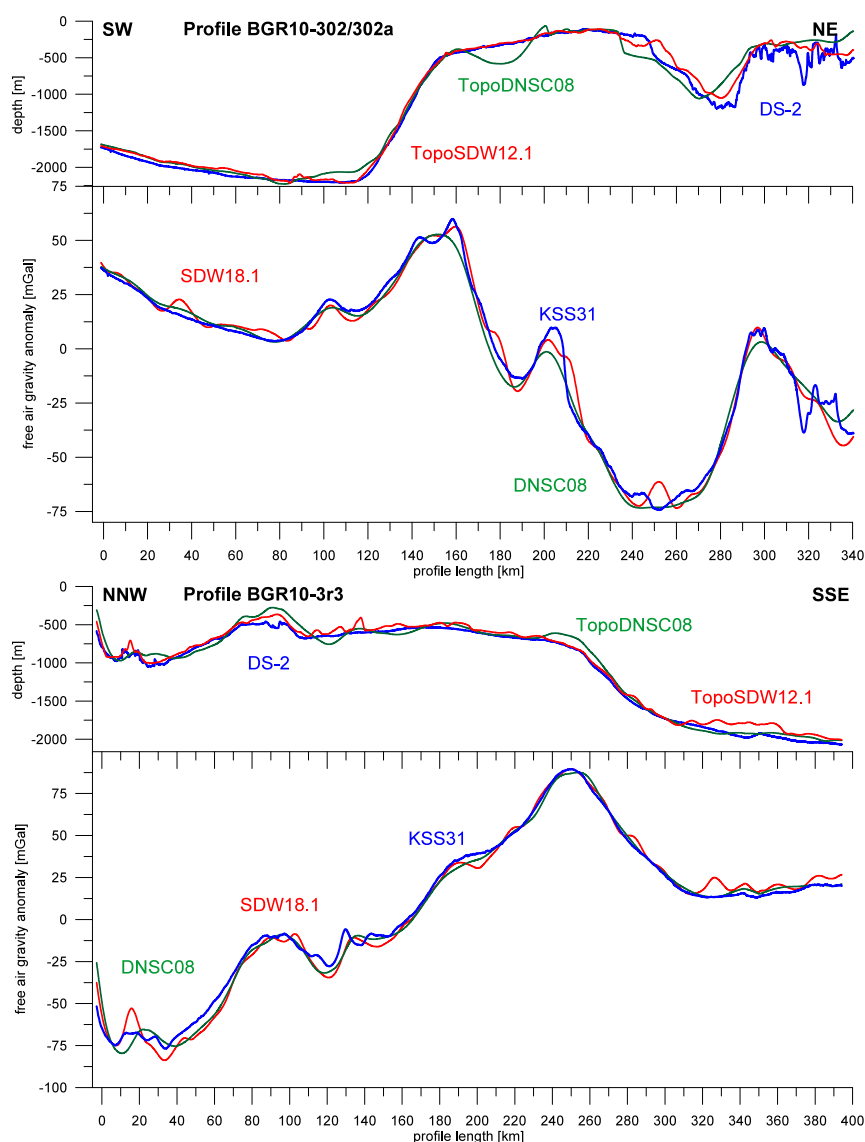


Fig. 7.11: Comparison of the ship-based KSS31M and satellite free-air gravity anomalies along profiles BGR10-302/302a (above) and BGR10-3r3 (below) together with the corresponding bathymetry measured with the Atlas Hydrosweep DS-2 multibeam system and from the global bathymetry of Sandwell and Smith (2005) and Andersen et al. (2008).

Figure 7.14 shows the detailed free-air gravity anomalies map of the survey area clarifying some further features. Starting in the North the Kane basin shows low gravity values (down to -170 mGal). This is surprising as the MCS results show that the sediment cover of the basin is fairly thin. The anomaly belongs to the Nares Strait Gravity Low and results from severe crustal thickening from continental collision during the Eureka Orogeny explaining the low values. Oakey and Stephenson (2008) calculated from gravity data a crustal thickness of 40 km in the Kane Basin area. Further south the negative anomaly in the Northwater Basin results from sediments with a thickness of up to 4 km. The positive, isolated, Carey Basin High anomaly (>60 mGal) is associated with significant Moho shallowing (Jackson and Reid, 1994). To the east the NW-SE running narrow negative gravity anomalies

7 Gravimetry

reflect the Carey and the Kap York basins. In Melville Bay the extended NW-SE striking gravity low (< -80 mGal) is related to the main depocentre of the Melville Bay Graben which should be deeper in its southern than its northern part. The graben is bounded to the east by the Melville Bay fault east of which Precambrian basement is exposed. On the west the basin is bounded by the Melville Bay Ridge to the west followed by the Kivioq Basin and the Kivioq Ridge (Whittaker et al., 1997). The southern end of the Kivioq ridge is marked by an extremely high gravity anomaly (240 mGal). Similar anomalies have been recorded in the outer part of the Labrador shelf, where they had been interpreted as mafic plugs that were intruded in the late Eocene and early Oligocene. MacLean et al. (1982) suggested that these mafic plugs were emplaced by mantle leakage along the Ungava transform fault along which they are aligned.

Southward the shelf is characterized by extended positive anomalies (50 – 80 mGal) reflecting the widespread Palaeocene flood basalts. The shelf offshore Baffin Island is very narrow. The gravity low running parallel to the coast off Baffin Island results from the Scott Graben (Skaarup et al., 2006). The deeper part of Baffin Bay, underlain by oceanic crust, is characterized by gravity anomalies between -30 and +30 mGal. The N-S running negative gravity anomaly at 64°W , correlating with a bathymetric low, could be interpreted as a transform fracture. The perpendicular running gravity low thus could be interpreted as marking the position of the extinct spreading axis in the Baffin Bay. The low could be followed uphill the continental slope into the Lancaster Sound marking the run of a failed rift arm.

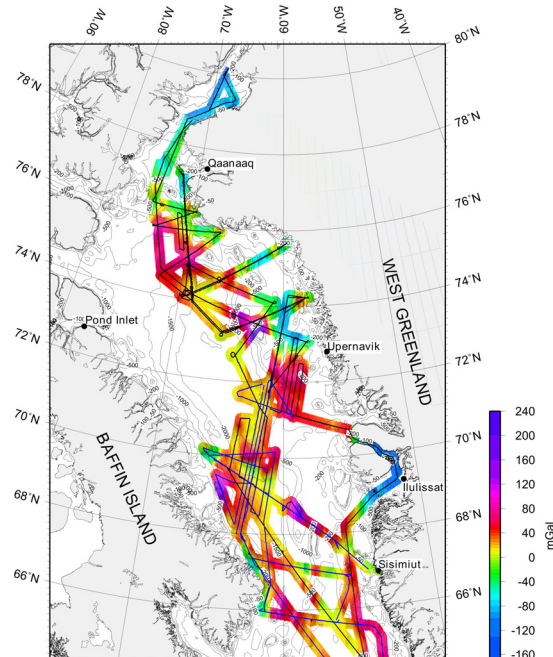


Fig. 7.12: Map of the free-air gravity anomalies. The underlying gravity grid was compiled by merging ARK-XXV/3 and MSM09/3 shipboard gravity observations. The map is drawn up to a distance of 15 kilometres from the tracks in a 1×1 (arc-)minutes grid and is underlain by the DNSC08 bathymetry (Andersen et al., 2008).

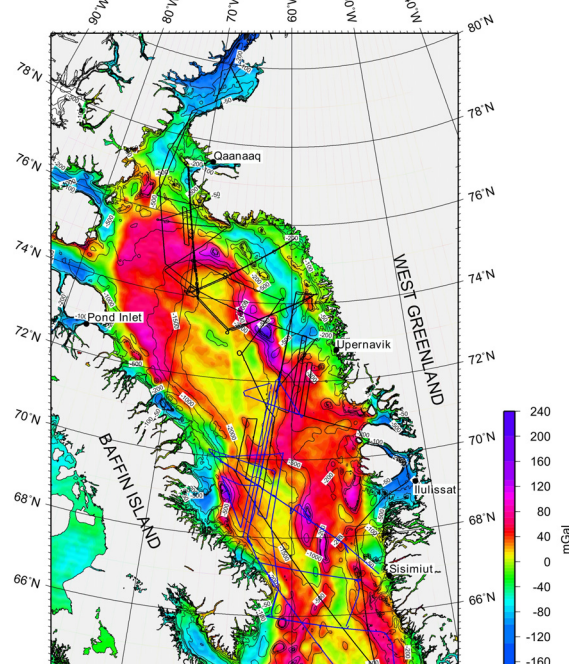


Fig. 7.13: Map of the free-air gravity anomalies. The underlying gravity grid was compiled by merging shipboard gravity observations and DNSC08 gravity data derived from satellite altimetry. The map is based on a 1 x 1 (arc-)minutes grid and is underlain by the DNSC08 bathymetry (Andersen et al., 2008).

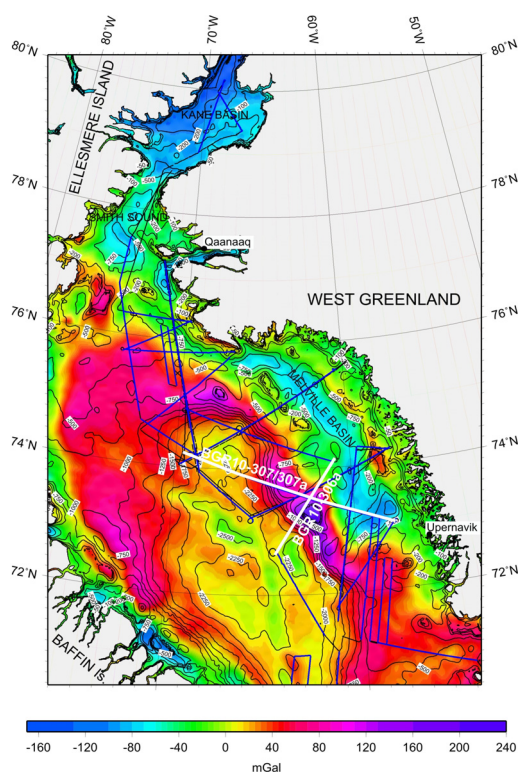


Fig. 7.14: Map of the free-air gravity anomalies of the ARK-XXV/3 survey area. The underlying gravity grid was compiled by merging shipboard gravity observations and DNSC08 gravity data derived from satellite altimetry. The map is based on a 1 x 1 (arc-) minutes grid and is underlain by the DNSC08 bathymetry (Andersen et al., 2008). The profiles modelled in chapter 8.5.4 are marked.

Bouguer gravity anomaly map

The underlying grid of gravity was compiled by merging ARK-XXV/3 and MSM09/3 gravity observations and DNSC08 gravity data derived from satellite altimetry. The water depth values were taken from the ship's echo sounding system and from the DNSC08 bathymetry data when no echo sounder data was available. The reduction density was 1.64 g/cm^3 and an infinite horizontal slab was assumed. A topographic reduction was not performed.

Figure 7.15 shows the map of the Bouguer gravity anomalies together with the bathymetry. On the oceanic crust the anomalies are positive (up to +220 mGal in the centre) with a clear North-South trending decrease of values towards the Davis Strait. But also towards the Smith Sound the gravity values decrease rapidly with decreasing water depth. The values decrease also landward rapidly. Low Bouguer gravity values (-100 mGal) were estimated for the area of the Mesozoic basins SW of Sisimiut, SE of Disko Island and the Melville Basin on the continental shelf. The lowest values (-160 mGal) are found in the northwestern part of the Kane Basin. Figure 7.16 shows the detailed Bouguer gravity anomalies map of the survey area.

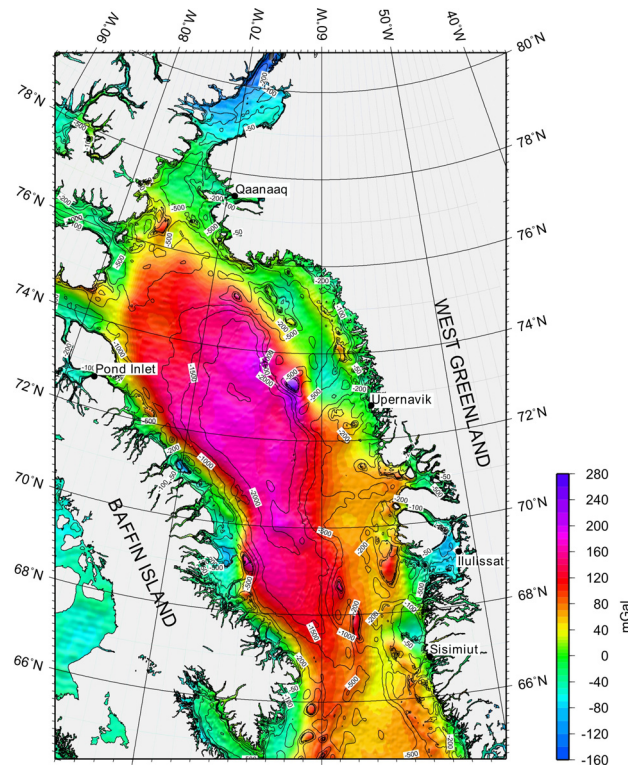


Fig. 7.15: Map of Bouguer gravity anomalies with no terrain corrections applied. The reduction density was 1.64 g/cm^3 . The map is underlain by the DNSC08 bathymetry (Andersen et al., 2008).

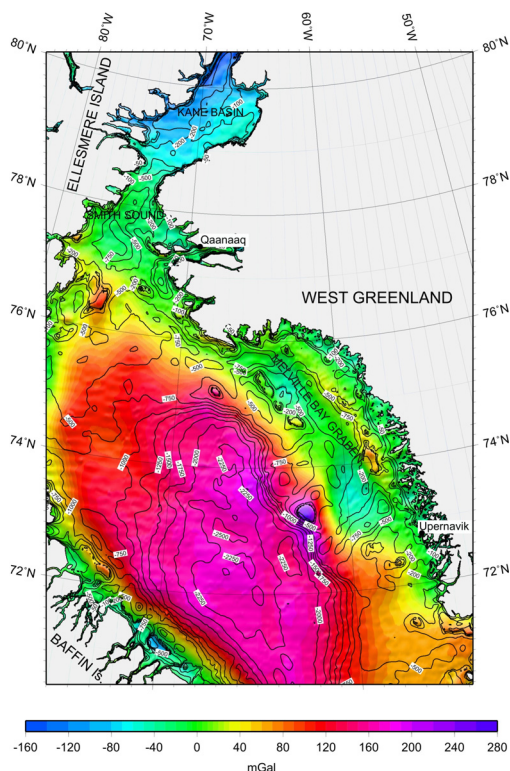


Fig. 7.16: Map of Bouguer gravity anomalies of the ARK-XXV/3 survey area with no terrain corrections applied. The reduction density was 1.64 g/cm^3 . The map is underlain by the DNSC08 bathymetry (Andersen et al., 2008).

7.5.3 Interpretation by forward modeling

2D forward modeling of the free-air gravity anomalies was carried out for selected profiles using the software GM-SYS (Northwest Geophysical Associates, Inc.). The corresponding results of the multi-channel seismic (MCS) data interpretation were taken into account. The interpretation of the MCS data was based on time-stacked data. These time sections yield valuable information about the upper sediment layers to the top of the basement. The depth of prominent horizons was calculated by using mean interval velocities. Furthermore, the velocities can be converted to density with density-velocity relations such as the extended Nafe and Drake relation (Ludwig et al., 1970). The 2D models represent first approaches to explain the observed free-air gravity and anomalies and form the basis of a comprehensive 3D density model which will be developed after the cruise.

LINE BGR10-306A

The profile BGR10-306a is about 200 km long and runs from the deep part of the Baffin Bay to the Kivioq basin. Figure 7.17 shows the resulting density model. The oceanic crust has a thickness of about 9 km with a nearly 4 km thick sediment cover. Towards the continental slope the oceanic crust thickens considerably. The broad positive gravity anomaly of more than 200 mGal is explained by thinned continental crust which is underlain by a 4 – 5 km thick and 60 km wide unit of high density

7 Gravimetry

material ($\rho=3.2 \text{ g/cm}^3$), which could be explained as a mafic intrusion as suggested by MacLean et al. (1982). However this unit does not cause significant magnetic anomalies. Northward the continental crust thickens rapidly to 28 km.

Line BGR10-307/-307a

The profile BGR10-307/-307a is nearly 400 km long and runs also from the deep part of the Baffin Bay to the Melville Bay Graben. It strikes nearly perpendicular to profile BGR10-306a which crosses at km 210. Figure 7.18 shows the resulting density model. The oceanic crust has a thickness of about 7 km with a 3.5 to 5 km thick sediment cover.

The top of the oceanic crust is rather rough. The transition to continental crust is smooth especially since thinned crust has to be assumed to explain the measured anomalies. The positive anomaly on the shelf results again from a higher density unit (mafic intrusion?) with a thickness of 5 – 6 km and a width of 60 km. Again, this unit does not cause significant magnetic anomalies. Northward the continental crust thickens remarkably to 27 km. At the eastern end of the Melville Bay basin the sediments thin out rapidly. However the basement should be overlain by a magnetic (basaltic?) layer since high magnetic anomalies were found.

The presented density models will change when further interpreted and depth-migrated MCS data become available. But it already provides right now some information concerning the thickness and density of the structural units of this part of the northeastern Baffin Bay.

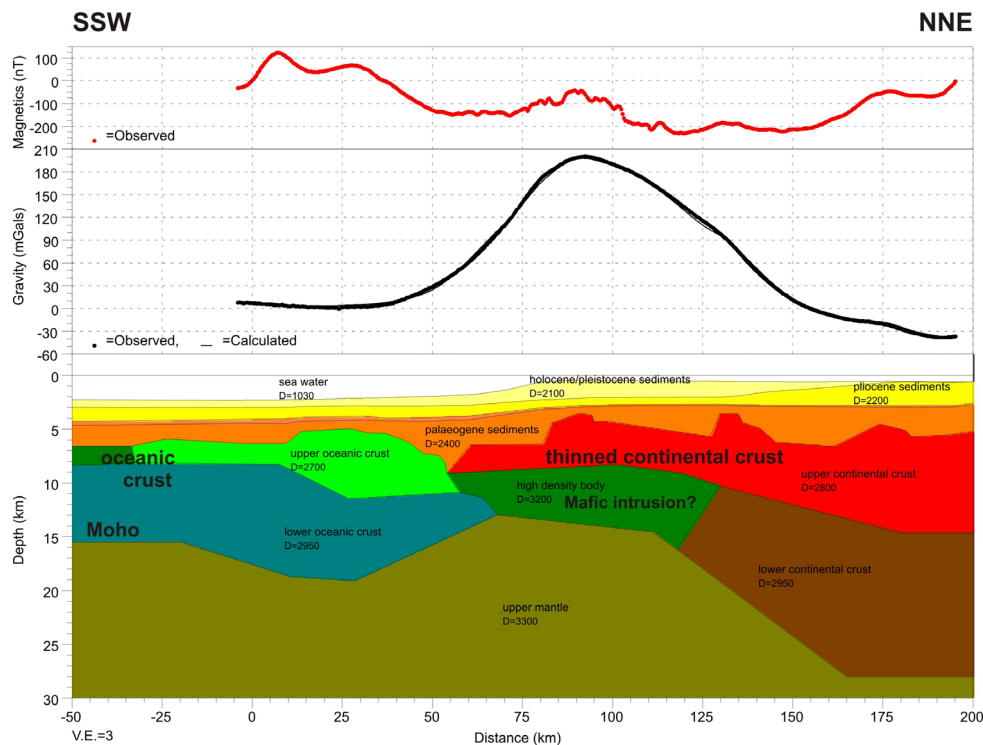


Fig. 7.17: 2D density model explaining the free-air gravity anomalies along BGR10-306a. Dotted lines: observed anomalies; Continuous line: calculated anomalies. Density values are given in kg/m^3 .

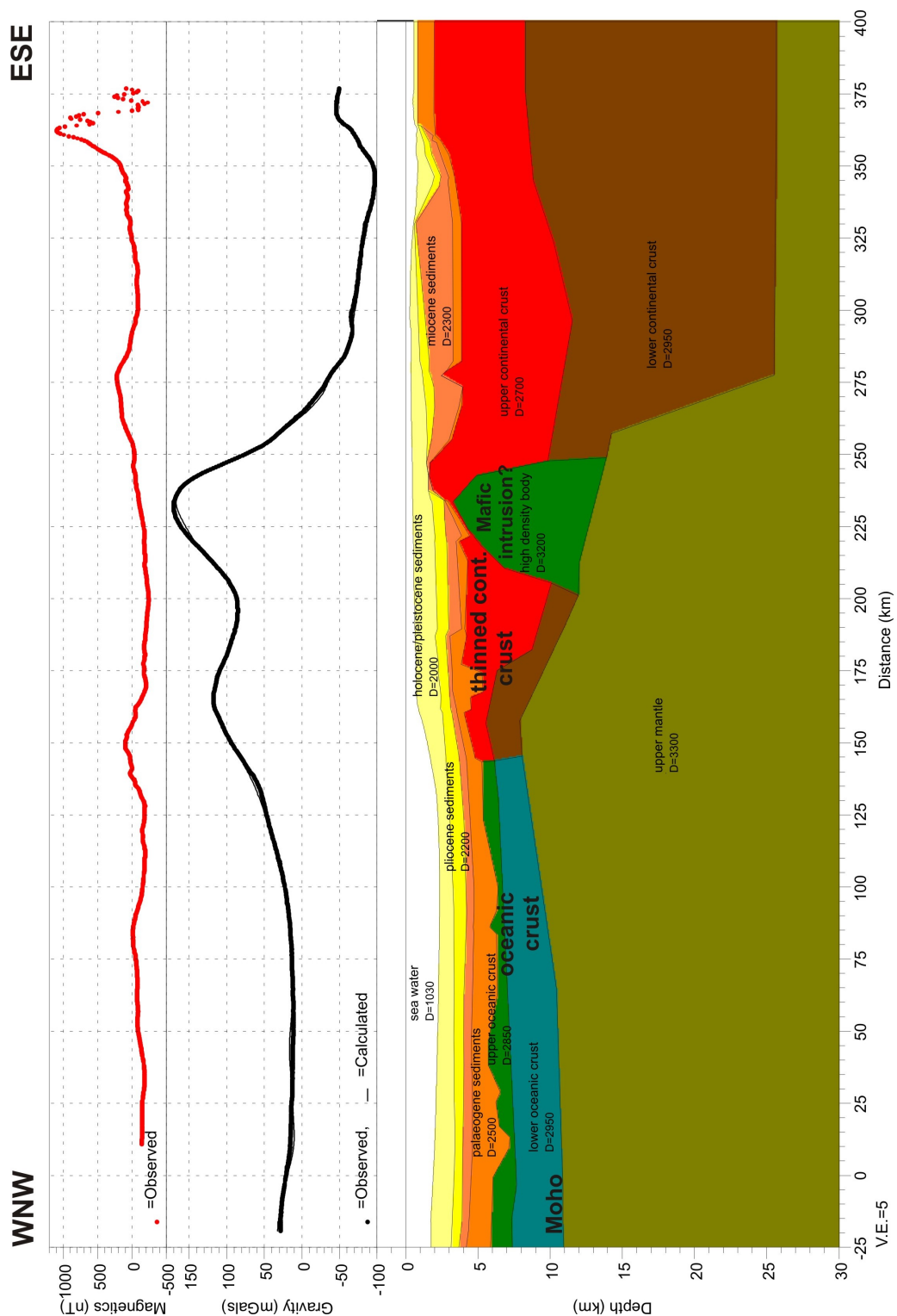


Fig. 7.18: 2D density model explaining the free-air gravity anomalies along BGR10-307/307a. Dotted lines: observed anomalies; Continuous line: calculated anomalies. Density values are given in kg/m³.

8. MAGNETICS

Bernd Schreckenberger, Hans-Otto Bargeloh, Ingo Heyde, Michael Zeibig
Bundesanstalt für Geowissenschaften und Rohstoffe
not on board: Detlef Damaske (BGR)

8.1 Marine magnetometer systems and operation

8.1.1 Towed magnetometer system

The towed magnetometer system consists of two different types of sensors (Fig. 8.1). Overhauser sensors measure the scalar absolute value of the total magnetic field while fluxgate magnetometers measure the magnetic field vector in its three components.

The SeaSpy™ Marine Gradiometer System manufactured by Marine Magnetics Corp. consists of two proton precession magnetometers, enhanced with the Overhauser effect. Two exactly equivalent magnetometers are towed 150 meters apart as a longitudinal array 750 meters astern of the ship (Fig. 8.1). Both sensors measure the total intensity of the magnetic field simultaneously. The difference between the two measurements is an approximation for the longitudinal gradient of the field in the direction of the profile line. Provided that the time variations are spatially homogeneous over the sensor spacing, the differences are free from temporal variations and their integration restores the variation-free total intensity or magnetic anomaly (apart from a constant value).

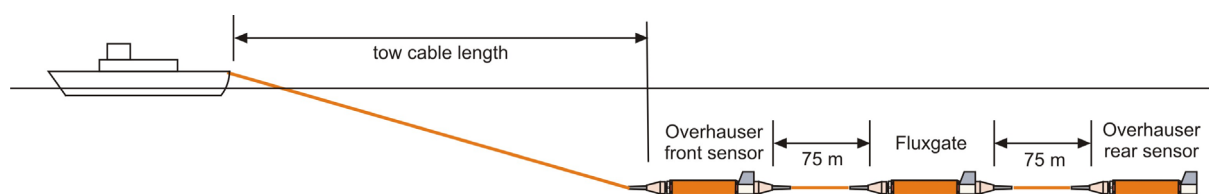


Fig. 8.1: Schematic sketch of the towed gradiometer system setup

A standard proton precession magnetometer uses a strong DC magnetic field to polarize itself before a reading can be taken. Overhauser sensors work similar to proton magnetometers with the exception that the excitation of the proton spin (polarization) is done by radio waves which excite the spin of the electrons in an organic fluid within the sensors. The electrons then transfer their spin to the protons in the fluid via a quantum mechanical process called Overhauser effect. Similar to every other proton magnetometer the relaxation frequency of the protons is a measure for the magnitude of the ambient magnetic field. The polarization power required is much smaller than that needed by normal proton magnetometer systems and the AC field may be left active while the sensor is producing a valid output signal.

This allows the sensor to cycle much faster and to produce more precise results than a standard proton magnetometer. As configured for this survey, the Overhauser sensors had a cycle time of one second. The sensors are specified with a noise level of $0.01 \text{ nT}/\sqrt{\text{Hz}}$, a resolution of 0.001 nT , and an absolute accuracy of 0.2 nT .

The fluxgate tow fish (Fig. 8.2) was designed by the BGR marine geophysics group. The fluxgate magnetometer and the electronics were built by MAGSON GmbH in Berlin and are installed into a standard SeaSPY tow fish housing. This assemblage uses the standard power supply and cables of the SeaSPY system and can easily be integrated into the towed magnetometer array. The system consists of i) a digital 3-axis MAGSON fluxgate magnetometer, ii) a two-axis tilt-meter, type 900H made by Applied Geomechanics Ltd., iii) a two-axis and single axis accelerometer, types ADXL203 and ADXL103 made by Analog Devices, iv) sensors for temperature, pressure, and humidity, and v) a data acquisition microprocessor built by MAGSON as well. Fluxgate and inclinometers are mounted on a common platform.



Fig. 8.2: Components inside the fluxgate magnetometer tow fish.

The MAGSON fluxgate uses the principle of vector-compensating all three ring-core-sensors by means of three independent Helmholtz-coils. The internal feedback circuit, using digitally controlled DC-currents fed into the Helmholtz-coils maintains precise nulling of the field inside the ring-core. Thus the amplitude of this current can be used as a signal to measure the vector components of the magnetic field. A factory calibration is required to provide offset, scale factor and non-orthogonality angle for each axis. All electronic components are integrated on the board of the data acquisition microprocessor. The MAGSON fluxgate sensor is specified with a noise level of $0.02 \text{ nT}/\sqrt{\text{Hz}}$, a resolution of 0.008 nT and a long term stability $< 10 \text{ nT}/\text{year}$.

Inside the tow fish a special platform is used to mount the fluxgate and both tilt-sensors. The first tilt-sensor by Applied Geomechanics (900H) measures pitch and roll angles by a conductive liquid in a half filled glass vial. The tilt angle is derived by the height of liquid covering five electrodes. This inclinometer covers an angular range of $\pm 25^\circ/\pm 40^\circ$ (first/second MAGSON tow fish) with an accuracy of about 0.01° of arc (noise level 0.005°). The second tilt-sensors are dual axis accelerometers by Analog Devices (ADXL203), measuring pitch and roll angles over a span of $\pm 50^\circ/\pm 20^\circ$ (first/second MAGSON tow fish) resolving 0.05° of arc (noise level 0.095°). A third accelerometer for the vertical axis (ADXL103) allows detecting an unintended upside down position of the tow fish.

The accuracy of the Applied Geomechanics sensor is significantly higher, but the calibration function is non-linear and temperature dependent. The Analog Devices sensor has a faster response (cross correlation results in 0.1 s difference), the calibration function is linear and almost temperature independent, but it suffers the noise level increased by factor 2. Both tilt meters measure not only the static

acceleration, which would provide the needed true roll and pitch angles. Instead, they measure also the dynamic acceleration due to the angular accelerations of the continuously moving tow fishes. This source of error can partly be reduced by filtering but remains a limiting factor of tilt estimation.

A high precision of angle measurement is necessary to rotate the field components measured in the sensors coordinate system of the moving fluxgate tow fish into the horizontal geomagnetic coordinate system. By Euler rotation it is possible to separate the vertical from the horizontal field vector components. The accuracy of the vector data is limited by the accuracy of the rotation angles. For example, a 0.01° tilt deviation may result in up to 10 nT component error in the survey area. Without any yaw angle estimation, the orientation of the horizontal field vector (i.e. the north and east component) remains unknown. A crude approximation might be the ship's course. Utilizing magnetic heading from the fluxgates themselves removes seafloor anomalies by default, however, a numerical yaw approximation has been introduced by Engels et al. (2008), demonstrating the advantages of vector component data analysis.

An embedded microprocessor with a flash disc is used to store all fluxgate and tilt-meter readings. The storage capacity of 1 GB is sufficient to allow for 11 days of continuous operation at a sampling rate of 10 Hz.

8.1.2 Onboard vector magnetometer

The onboard vector magnetometer consists of two orthogonal three-axis ring-core vector magnetometers systems installed in the ships crow nest one over the other in the direction of the ship's yaw axis. The sensors have a dynamic range of ± 100000 nT and a long-term stability of <10 nT/year. The data are recorded in the DShip data acquisition and management system. The data set also contains navigation data from the MINS inertial platform (ship's roll, pitch and heading angles).

8.1.3 Helicopter-borne magnetometer system

In one of the helicopters (D-HLSZ) of *Polarstern* the BGR aeromagnetic system was installed. It consists of a magnetometer bird that was towed on a cable about 30 m below the helicopter. The bird is equipped with a Scintrex CS-3 Cesium vapor magnetometer sensor head and an electronics module. In the helicopter a Pico Envirotec AGIS XP real time data acquisition and navigation system and a magnetometer processor MMS-4 was used to record the data and provide navigation information to the pilot via a Pilot Guidance Display (PGU). The System was equipped with a Novatel DL4-V3 dual frequency GPS receiver. The antenna was installed within the helicopter on the dashboard.

We also installed an experimental vector magnetometer system in the helicopter. This system was built by MAGSON GmbH in Berlin for BGR as an onboard system for research vessels. Because an equivalent system was already installed on *Polarstern* the BGR system could be used in the helicopter. It consists of two independent ring core fluxgate sensors, a data acquisition box and a GPS mouse. Unfortunately the sensors could not be installed outside of the cabin. Therefore, one

of them (Sensor 2) was fixed behind the pilot's seat and the other sensor (Sensor 1) in the cargo hold together with a Novatel SPAN IMU (Inertial Motion Unit) that provided roll, pitch and heading values (Fig. 8.3). Each sensor also contains a two-axis inclinometer and a regulated heating. The sensor temperatures proved to be fairly constant during the short flights and the heating was therefore not used.

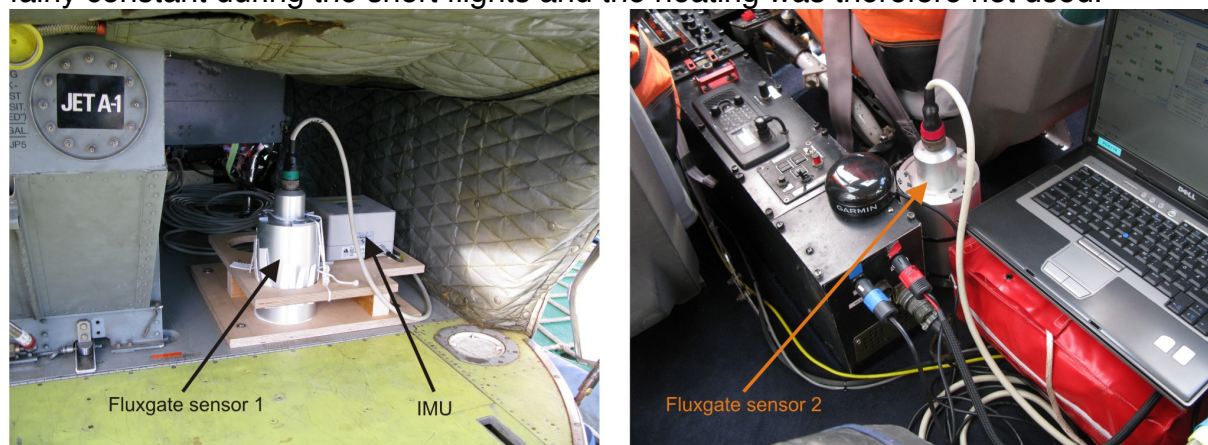


Fig. 8.3: Installation of an experimental fluxgate sensor system in the helicopter. Left: Fluxgate sensor 1 and Inertial Motion Unit (IMU) in the cargo hold. Right: Fluxgate sensor 2 in the cabin behind the pilot's seat.

8.2 Data acquisition

8.2.1 Towed magnetometer system

During the cruise the two Overhauser sensors S/N 13545 (front sensor) and S/N 13546 (rear sensor) and the vector tow fish with S/N 13143 were used for all deployments except of one line (BGR10-322) where S/N 13335 (front) and S/N 13140 (rear) and S/N 13142 as the vector sensor were used. Altogether we acquired 6835 km marine magnetic data on 40 profiles.

On lines BGR10-3M02A, -3M03, -3M04, -3M056, and -3M06 only one sensor (S/N 13546) was deployed because of severe sea ice conditions. On a few occasions we made the observation that the magnetometer array came in contact with ice floes. This did obviously not cause any damages except of the loss of some tow fish fins.

Two calibration loops were performed during the cruise. The first one was a simple circle on line BGR10-3M01 in the southern part of the survey area. The second calibration pattern was an 'eight-leaved' clover (Fig. 8.4) centered at $74^{\circ} 10.8'N / 68^{\circ} 55.6' W$. Each of the eight straight lines was surveyed in two directions. It took about four hours to sail the complete figure. We expect that it will be possible to use the calibration pattern to distinguish between the true gradients and the unavoidable offset between the sensors and to obtain some information about a possible influence of the vessel on the gradient values. The results (Fig. 8.5) show a clear azimuthal dependence of the gradient values at the center point that cannot be explained by natural gradients alone. Furthermore, it becomes obvious that the magnetic anomaly calculated from the vector components is offset from that of the scalar sensors by about 5 nT. This is a rather good value given that a cruise calibration has not yet

been performed and shows that a recent laboratory calibration was rather successful. Cruise calibrations of the vector components using calibration loops like this one usually reduce the difference between vector and scalar magnetometer total field values below 1 nT RMS error.

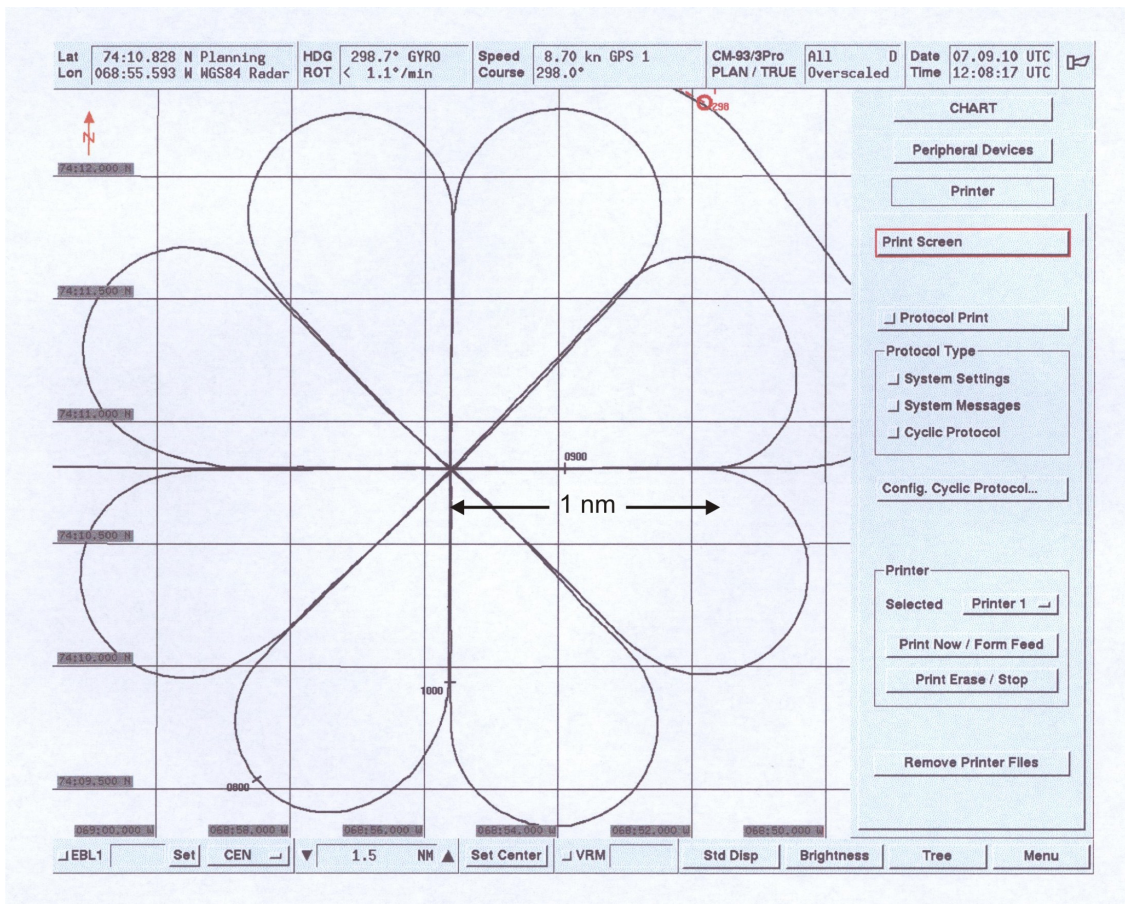


Fig. 8.4: Calibration figure sailed on September 07, 2010 (screen dump from the bridge's navigation terminal).

8.2.2 Onboard vector magnetometer

The data from the ships onboard vector magnetometers were retrieved from the DShip data base for the whole cruise together with positional data and timing information. One second records were generated that contain the total intensity, vector components, sensor temperature, orientation angles, position and time. Only two calibration loops were performed during the cruise. Because on almost all geophysical lines the towed magnetometer was deployed, which is expected to provide far more accurate magnetic field values than the onboard magnetometer, the onboard vector magnetometer data have not yet been processed.

Using the motion reference unit from the ship (MINS) it will later be attempted to compensate for the ships magnetic field by estimating the compensation matrix during turns. A comparison with the towed magnetometer shall test the accuracy limits of total magnetic field values for a shipborne fluxgate during post cruise

processing. It will also be attempted to apply methods that were used by e.g. Seama et al. (1993), Korenaga (1995), Parker and O'Brian (1997) and Engels et al. (2008) to utilize the vector components for the determination of magnetic strike directions.

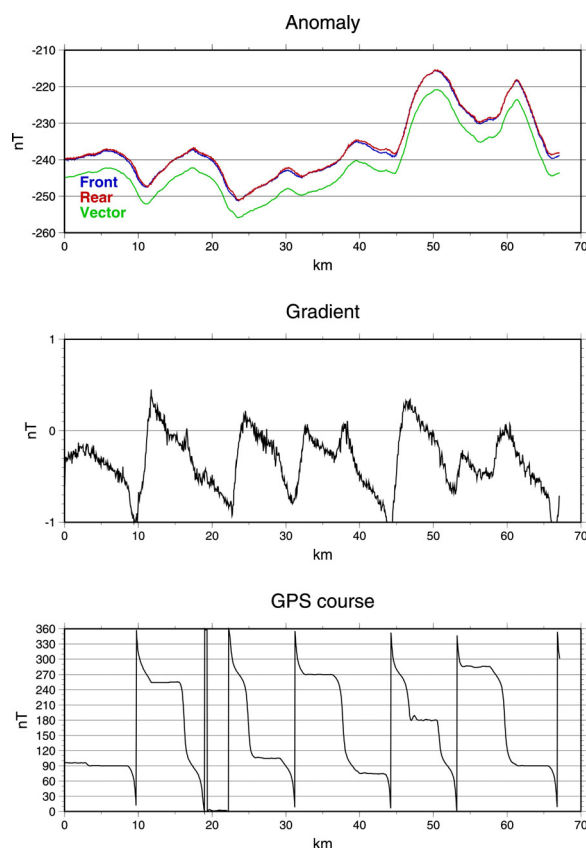


Fig. 8.5: Result of the calibration pattern (Fig. 8.4). Top: magnetic anomalies calculated from the front and rear scalar Overhauser sensors and from the vector magnetometer. Center: Gradient between both Overhauser sensors. Bottom: ship's course from GPS.

8.2.3 Helicopter-borne magnetometer system

Helicopter operations in the Canadian sector of the Baffin Bay could only be performed on a few days during the first part of the cruise because of often adverse weather conditions. Until August 25, when the decision was made to avoid Canadian waters, only six flights could be made. From September 1 onwards, flights in the Greenland part of the Baffin Bay were possible and another 34 flights were made until the end of flight operations. Therefore, 40 aeromagnetic survey flights (Tab. 8.1) with a length of 11,240 km on 119 (partly very short) lines were completed. It was intended to maintain a flight altitude of 300 feet (approx. 100 m) and a cruise speed of 90 knots (167 km/h) during survey flights. For several reasons the intended altitude could not be kept at all times. The mean of all altitude values of the helicopter on all lines is 108 m.

The planning of the lines was done using the Fugawi Global Navigator programme. Start and end coordinates of the planned lines were transferred to the PEIConvert

programme provided by Pico Envirotec where description files with strait lines in UTM coordinates were generated (special lines in their notation) that could be uploaded to the AGIS XP data acquisition and navigation system.

A similar procedure as mentioned for the onboard vector magnetometer in chapter 8.2.2 using the INS system in the helicopter will be tried after the cruise to evaluate the helicopter vector magnetic data.

Tab. 8.1: Date and time of aeromagnetic helicopter flights and associated data file names. On two flights (no 30 and 31) no usable data were acquired due to adverse weather conditions.

Flight number	Date	Start time	End time	Data file name
1	09.08.2010	18:40	19:45	B0080918.P37
2	10.08.2010	15:09	17:13	B0081015.P07
3	10.08.2010	19:51	21:19	B0081019.P52
4	14.08.2010	14:10	15:40	B0081414.P23
5	20.08.2010	18:26	20:54	B0082018.P51
6	20.08.2010	21:28	23:53	B0082021.P30, B0082022.P36, B0082023.P23
7	01.09.2010	9:55	11:50	B0090109.P56
8	04.09.2010	16:49	19:14	B0090417.P00
9	05.09.2010	9:11	11:37	B0090509.P18
10	05.09.2010	15:26	17:56	B0090515.P28, B0090515.P41
11	06.09.2010	14:22	16:56	B0090614.P27
12	07.09.2010	17:43	19:46	B0090717.P52
13	08.09.2010	10:11	12:27	B0090810.P14
14	08.09.2010	15:01	17:41	B0090815.P03
15	10.09.2010	9:51	11:42	B0091009.P53
16	10.09.2010	13:53	16:17	B0091013.P54
17	10.09.2010	18:15	20:38	B0091018.P15
18	14.09.2010	13:02	15:21	B0091413.P04
19	14.09.2010	18:12	20:28	B0091418.P18
20	15.09.2010	9:56	12:29	B0091510.P00
21	15.09.2010	13:08	15:36	B0091513.P10
22	15.09.2010	16:02	18:10	B0091516.P08
23	16.09.2010	9:20	11:58	B0091609.P23
24	16.09.2010	12:19	14:26	B0091612.P20
25	16.09.2010	14:51	17:20	B0091614.P57
26	17.09.2010	17:20	19:56	B0091717.P21
27	18.09.2010	9:29	11:59	B0091809.P37
28	18.09.2010	12:20	14:58	B0091812.P23
29	18.09.2010	15:44	18:20	B0091815.P56
30	20.09.2010	9:52	10:31	no data
31	20.09.2010	13:58	14:36	no data
32	21.09.2010	10:11	12:16	B0092110.B13
33	22.09.2010	10:04	12:29	B0092210.P09
34	22.09.2010	16:58	20:54	B0092218.P59
35	23.09.2010	10:37	13:04	B0092310.P39
36	23.09.2010	13:46	16:14	B0092313.P50, B0092315.P14
37	23.09.2010	16:53	19:25	B0092316.P58
38	24.09.2010	10:15	12:30	B0092410.P19
39	24.09.2010	13:04	14:19	B0092413.P05
40	01.10.2010	16:03	18:50	B0100116.P04, B0100117.P09

8.3 Data processing and calibration

8.3.1 Towed magnetometer system

The standard processing sequences for total field magnetic data includes a simple algorithm for cleaning erroneous data of one Overhauser sensor and the removal of the magnetic reference field (IGRF 2010). The resulting magnetic anomalies are stored using a 20 second sampling rate.

A programme package described by Eilers et al. (1994) and Roeser et al. (2002) was used to calculate the variation-free anomalies from the gradient. An alternative programme suite (Engels et al., 2008) was used on the first line (BGR10-3M01) only and for the second calibration loop. It gives similar results for the reconstruction of the residual total magnetic field anomalies and is also able to process and calibrate the vector data using constraints from the more accurate and stable Overhauser sensors. Processing of the vector data will be done after the cruise.

The philosophy of the second approach by Engels et al. (2008) is to pre-process raw data in the time domain in a comprehensive straight-forward and transparent way before the gradiometer anomaly reconstruction and further component analysis are performed. In the following the current status of the processing codes (version 8) is summarized briefly:

- Code READMAG reads all data formats from the individual sensors and the ship's GPS recordings. Gaps, erroneous data records and unphysical data exceeding certain thresholds are replaced by dummy values. From the GPS positions which are smoothed by a running mean, control parameters like way path kilometers, velocity, and azimuth are derived for each sample which is accepted as having reasonable values. The time delay of each sensor according to its position behind the vessel and the ship's velocity is taken into account. Clock shifts and drifts of the individual instruments are corrected.
- Code INTERMAG interpolates all data gaps marked by dummy values either linear or by cubic splines.
- Code IGRFMAG subtracts the ambient main field using IGRF model 2010.
- Code FILTMAG applies a band pass filter in the time domain in order to limit on wavelengths related to realistic anomalies originating from crustal sources.
- Code GRADMAG sums up total field differences between both Overhauser sensors.

From visual inspection, most of the lines acquired with the towed magnetometer system are only to a lesser amount disturbed by magnetic variations. Nevertheless, small disturbances occurred nearly every day and e.g. profiles BGR10-311, -313, and -320 (Fig. 8.6) proof that variations of up to 200 nT could be removed using the gradient method. Figure 8.7 shows all magnetic data acquired using the towed marine gradient magnetometer system.

8.3.2 Aeromagnetic data

Aeromagnetic data are stored on disk on the AGIS data acquisition system with a sampling rate of 10 Hz. They were reformatted to Geosoft XYZ files (Geosoft Oasis Montaj) using the propriety PEIView (Pico Envirotec) programme . Data processing was performed using the Geosoft Oasis Montaj programme suite. It included quality control, subdivision of the data files into single strait profiles and calculation of the IGRF reference field (IGRF 2010). Magnetic anomaly values were calculated for the whole survey using the IGRF total intensity values for one day (August 31, 2010) approximately in the middle of the survey. In order to display the data with the GMT programme s a second Geosoft data base was maintained with an reduced sampling

interval of 1 Hz. Unfortunately, we did not have a base station available and the magnetic profile map (wiggle traces) show high cross-over error values. We intend to obtain magnetic observatory data from the Canadian Arctic (e.g. Iqaluit and Resolute) and some coastal observatories of Greenland. Although no dedicated tie lines were flown, we tried to plan flights in a way that as many as possible crossings between ship and flight lines were generated to enable some kind of leveling in a later stage of data processing. Figure 8.8 shows the location of the magnetic flight lines and the anomalies as wiggle traces along the lines.

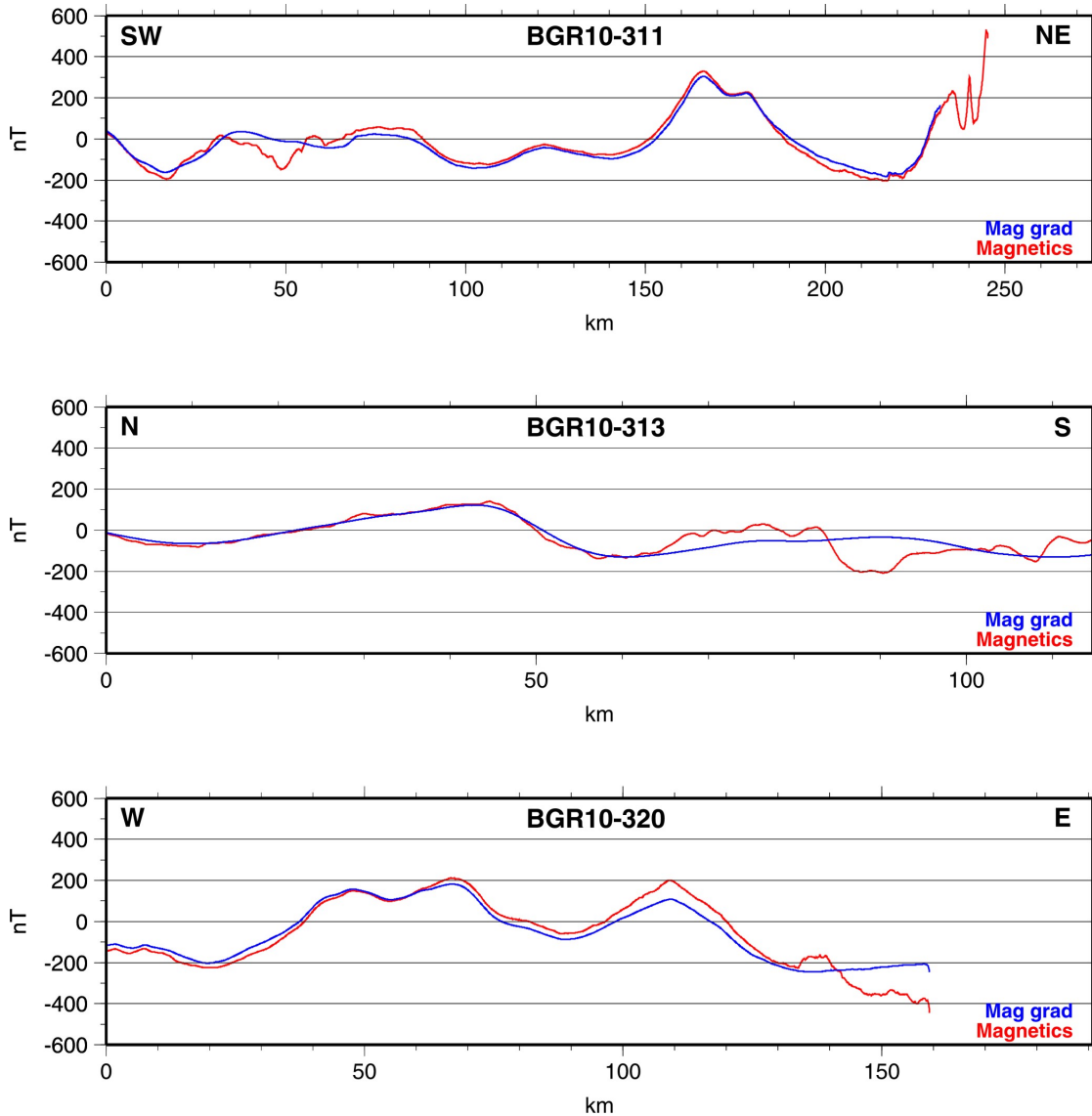


Fig. 8.6: Examples for the successful removal of magnetic variations from the magnetic records. Red curves denote the magnetic anomaly calculated from one sensor only, blue curves the anomaly reconstructed from the gradient. Please observe different distance scales used for the three panels. On line BGR10-311 (top) variations between 10 and 70 km were successfully removed. On line BGR10-313 (center) variations with an amplitude of 200 nT were present and on line BGR10-320 (bottom) a sudden onset of disturbances at 133 km was removed.

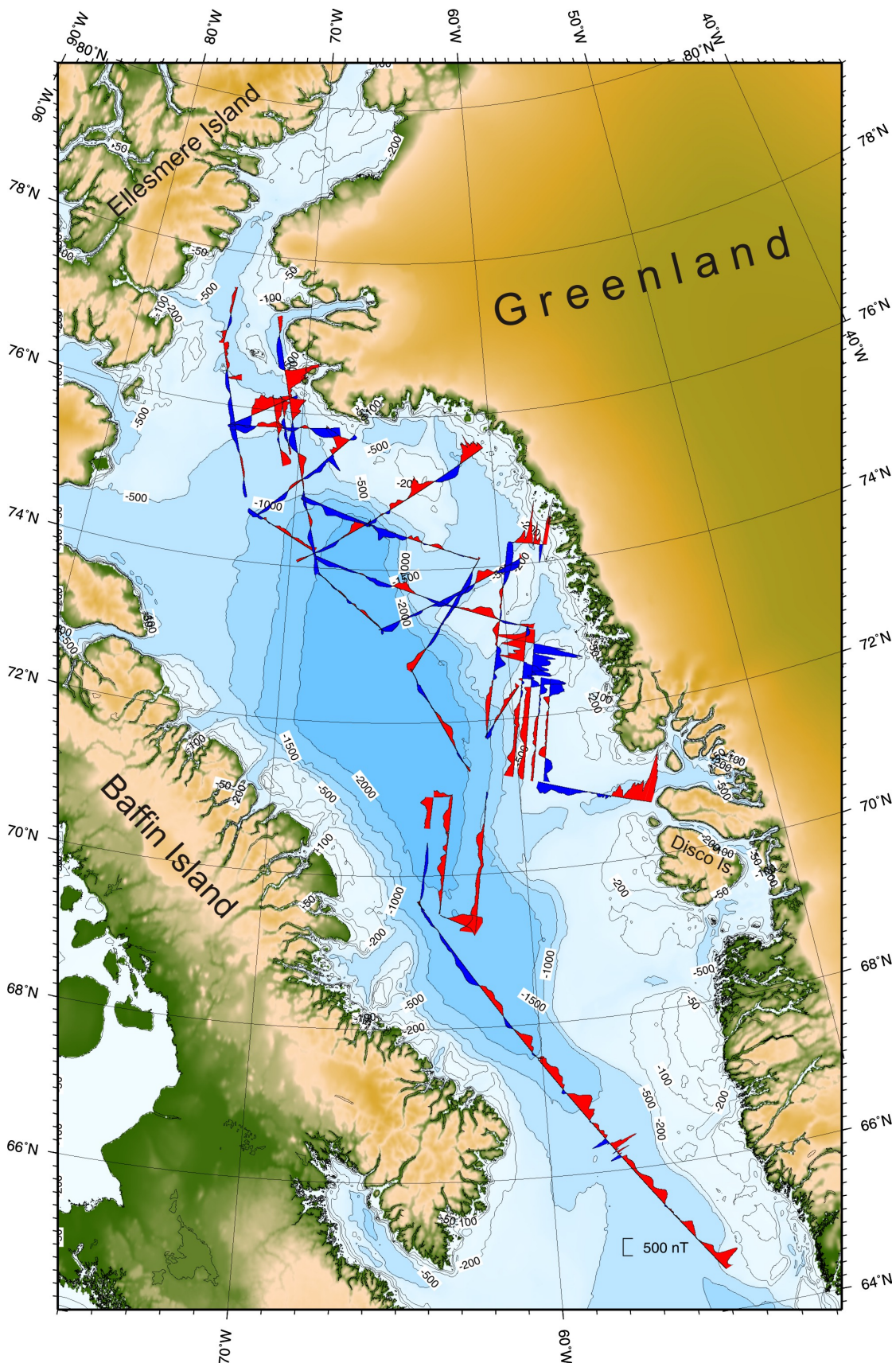


Fig. 8.7: Magnetic anomalies (red: positive; blue: negative) acquired with the marine gradient magnetometer system.

8.4 Preliminary results

Figure 8.9 shows all magnetic data that were acquired in the Baffin Bay, the Davis Strait region and the Kaine Basin. Two aeromagnetic lines southeast of Greenland and one long marine line across the western flank of the Reykjanes Ridge are discussed at the end of the chapter. For the purpose of interpretation we prefer to add the magnetic data from a former cruise to the Davis Strait and the southern Baffin Bay with *Maria S. Merian* in 2008 (Gohl et al., 2009) that were acquired by the same BGR marine magnetic group (Fig. 8.10).

Two main profile directions were chosen for the aeromagnetic survey that makes up the main part of the magnetic data. The first direction is oriented along the long seismic line BGR10-303a, -3r3, and -313 (346 degrees, see profile location map Fig. 2.2). The original intention was to survey the deep water parts of the Baffin Bay to decipher possible magnetic lineations of suspected oceanic crust. Due to the early end of the measurements in Canadian waters the profiles were extended into areas of suspected continental origin north of 75°N. The line separation was chosen to be between 6 and 8 nm.

The profiles north of 73°N and west of 65°W most probably cross a continental margin. South of 75°N/70°W weak magnetic lineations can be identified that strike in a WNW-ESE direction. Indications for at least two fracture zones can be observed. Some seismic lines (see chapter 15) also confirm the oceanic character of this part of the Baffin Bay. A detailed interpretation will become difficult because only a few wiggles (polarity intervals) are visible on the short oceanic parts of the profiles. To the North some strong negative anomalies may mark the continent/ocean boundary or the first continental features but they are not continuous as the gap at 70°W demonstrates. Even further north east of 70°W the landward end of the profiles is marked by a slightly curved E-W striking positive/negative (edge?) anomaly. West of 70°W positive amplitudes predominate while on the westernmost lines the amplitudes become smaller. In general, E-W striking structures predominate the magnetic residual field, in the suspected oceanic as well as in the continental areas. A detailed comparison with reflection and refraction seismic and gravimetric data will be necessary to decipher the structural elements of this part of the northern Baffin Bay.

A second subset of profiles between 71° and 73°N is oriented along seismic line BGR10-309 which is a prolongation of some MSM09/3 seismic and magnetic lines (Gohl et al., 2009). Just north of 72°N and west of 62°W weak linear anomalies are visible that resemble oceanic lineations. Again, the lines are too short to assign definitive magnetic chrons to single wiggles in this preliminary discussion.

The northern part of the margin segment between 62° and 65°W at 73°N is only covered by a few mostly SW-NE striking lines which nevertheless demonstrate that the shelf break that visually suggests the continent/ocean boundary shows no significant magnetic anomalies. The seismic interpretation (see chapter 15) of line BGR10-306a suggests that even the southernmost part of that line, despite of its location at greater water depth, may be underlain by a continental crustal block. This line also has an interesting aspect as it crosses an extremely high amplitude gravity anomaly. Figure 8.11 shows that the gravity anomaly is by no means related to a

magnetic anomaly. Some small wavelength anomalies around the gravity maximum at 100 km must be attributed to magnetic variations.

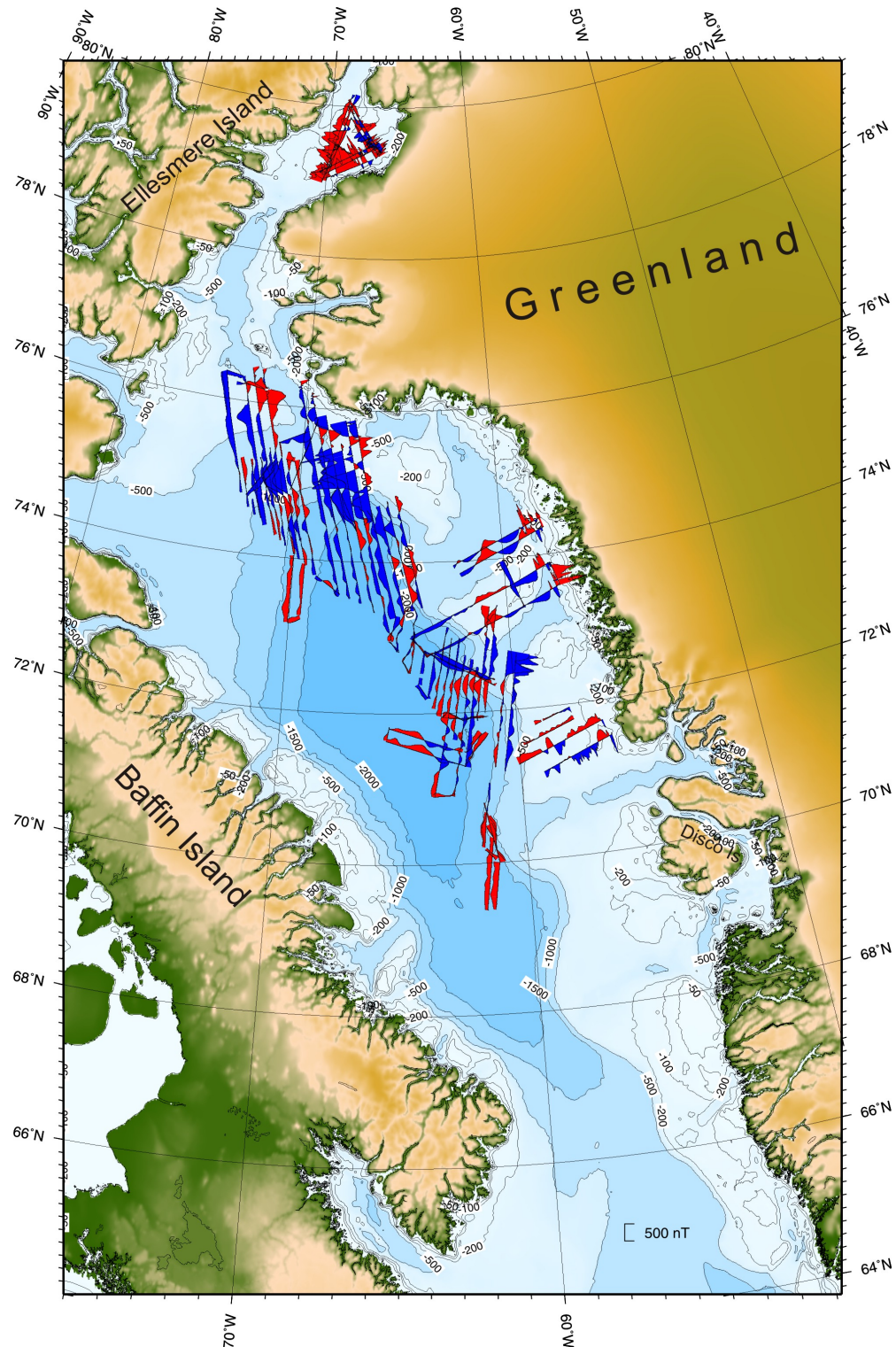


Fig. 8.8: Magnetic anomalies (red: positive; blue: negative) acquired during the aeromagnetic measurements (Cs-magnetometer in the tow bird)

The continental structures east of 63°W and north of 72.5°N show magnetic signatures with different strike directions. An E-W striking positive/negative anomaly just south of 73°N and east of 60°W has both, a short wavelength and a long wavelength character at rather high (up to 1,000 nT) amplitudes. This indicates the incidence of shallow highly magnetized rocks of probably volcanic origin. North of 73°N a N-S striking positive/negative amplitude pattern along the 60°W meridian is followed to the east by a curved negative edge anomaly. The easternmost parts of the SW-NE striking lines again show a high frequency anomaly pattern suggesting shallow magnetic source rocks near the coast. Between 71° and 72°N the amplitudes are moderate. The southernmost line in that area ends just north of Disko Island and shows extremely high amplitudes. Most probably these are related to the well known Disko Island basalt province.

Figure 8.12 shows a detailed view of three aeromagnetic flights in the Kane Basin. Because of severe ice conditions we did not deploy the towed magnetometer system. Instead, we surveyed the seismic ship track plus two additional lines parallel to the ship track. The parallel lines then contain information about the strike direction of the magnetic anomalies. The Kane Basin was already covered with an aeromagnetic survey in 1981/82 (Hood et al., 1985) and much more detailed in its southwestern part by a helicopter survey in 2001/2003 (Oakey and Damaske, 2004). The data in Figure 8.12 show similar structures as those of Hood et al., (1985) with a magnetically smooth region in the northern Kane Basin near the Kennedy Channel and higher amplitudes to the South. Short wavelength anomalies in the southeastern corner of our line pattern may be related to well known prominent anomalies from Inglefield Land. The data will be discussed in a later stage of the project in view of the newly acquired reflection seismic data.

Finally, two aeromagnetic and one marine magnetic test line (Fig. 8.13) shall be shown. They were surveyed during the transit back to Bremerhaven over the western flank of the Reykjanes Ridge. The data were acquired to enable a comparison between all five different magnetic methods (towed scalar gradient, towed vector, ship-borne vector, helicopter Cs scalar, and helicopter vector magnetometers). Unfortunately, the helicopter vector magnetometer did not work on the lines shown in Figure 8.13 for unknown reasons.

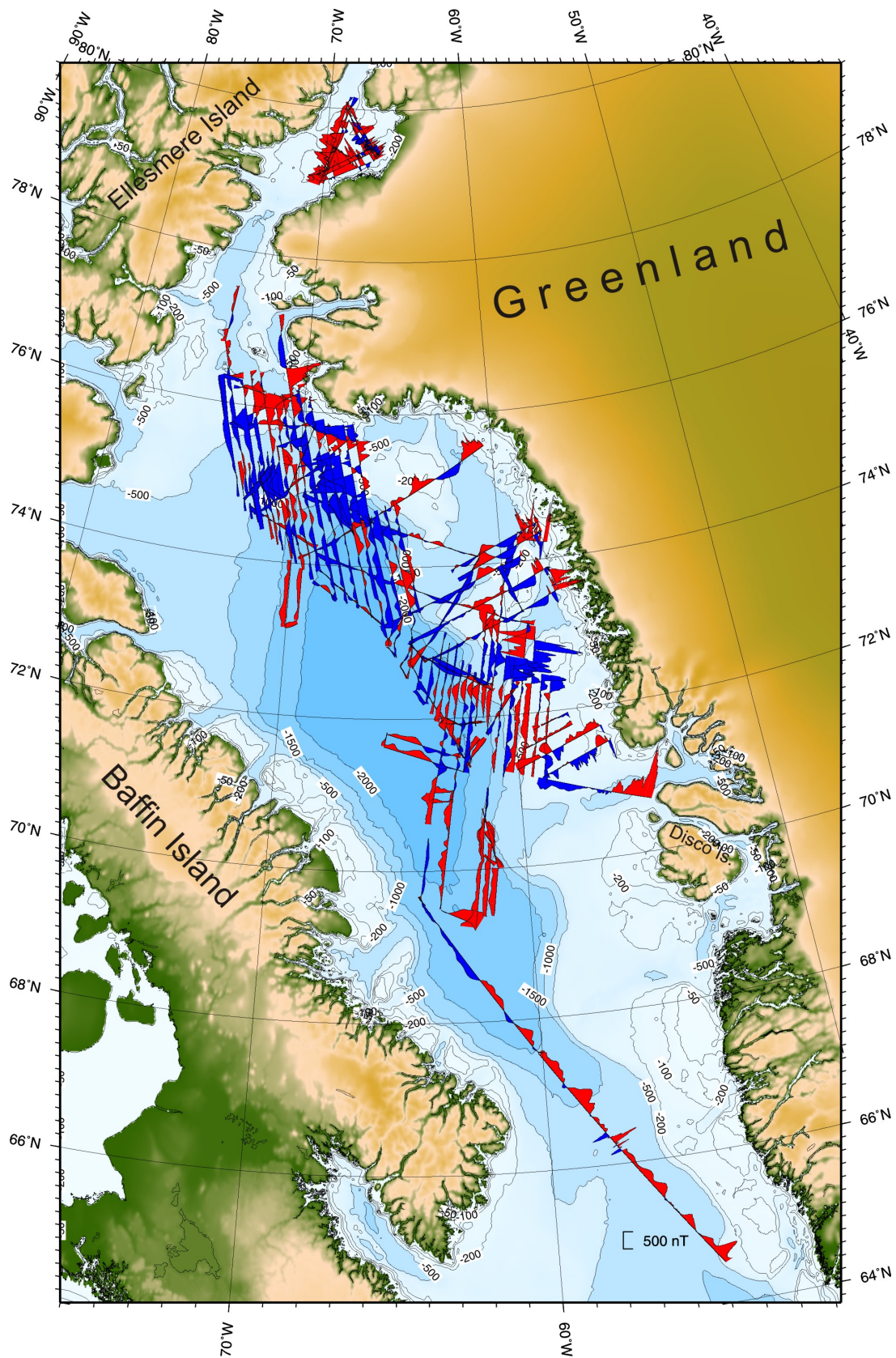


Fig. 8.9: Magnetic lines (shipborne and aeromagnetic) acquired during cruise ARK-XXV/3.

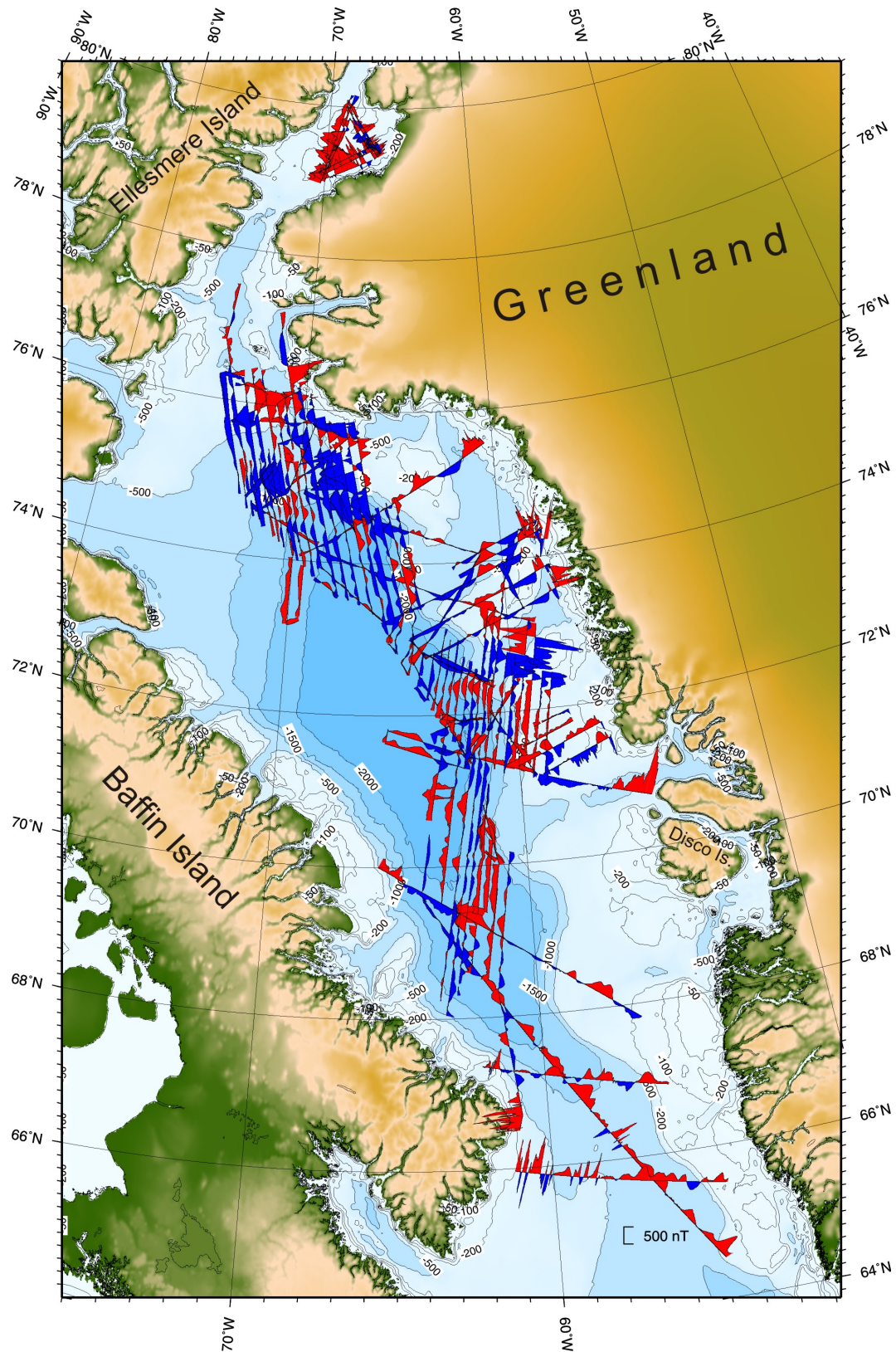


Fig. 8.10: Aeromagnetic and shipborne magnetic lines acquired during cruise ARK-XXV/3 and marine magnetic lines from cruise MSM09/3 (Gohl et al., 2009).

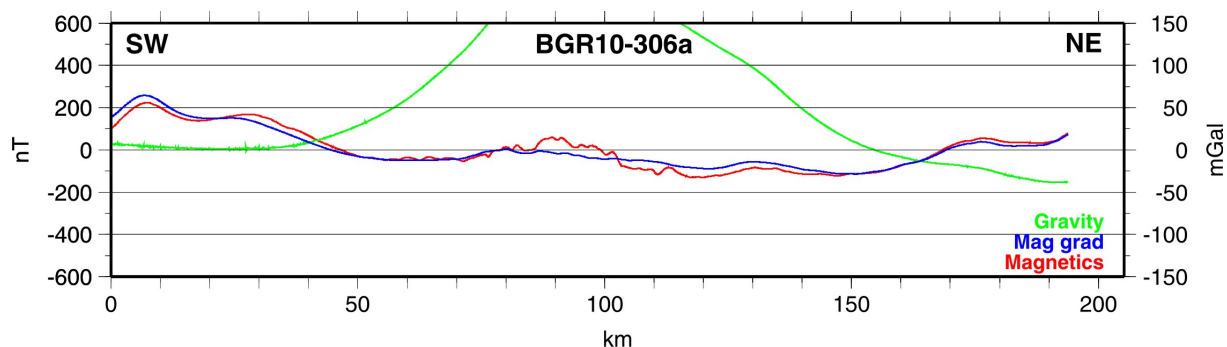


Fig. 8.11: Magnetic anomaly from one scalar sensor (red curve) and reconstructed from the gradient (blue curve) related to an extremely high gravity anomaly (green) on line BGR10-306a. The variation-free reconstructed curve (blue) shows that the gravity anomaly is not related to a magnetic anomaly

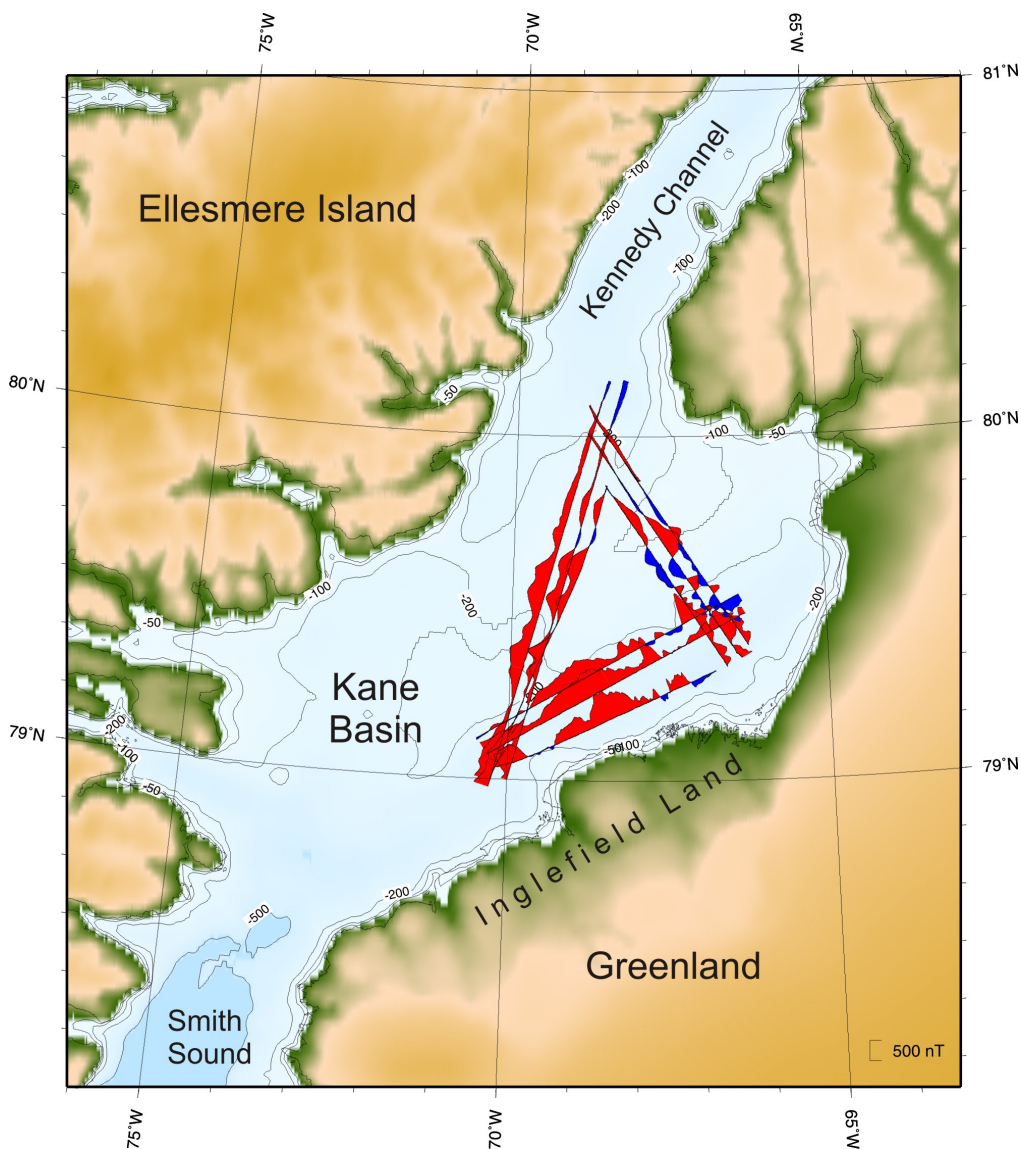


Fig. 8.12: Aeromagnetic lines acquired in the Kane Basin

8 Magnetics

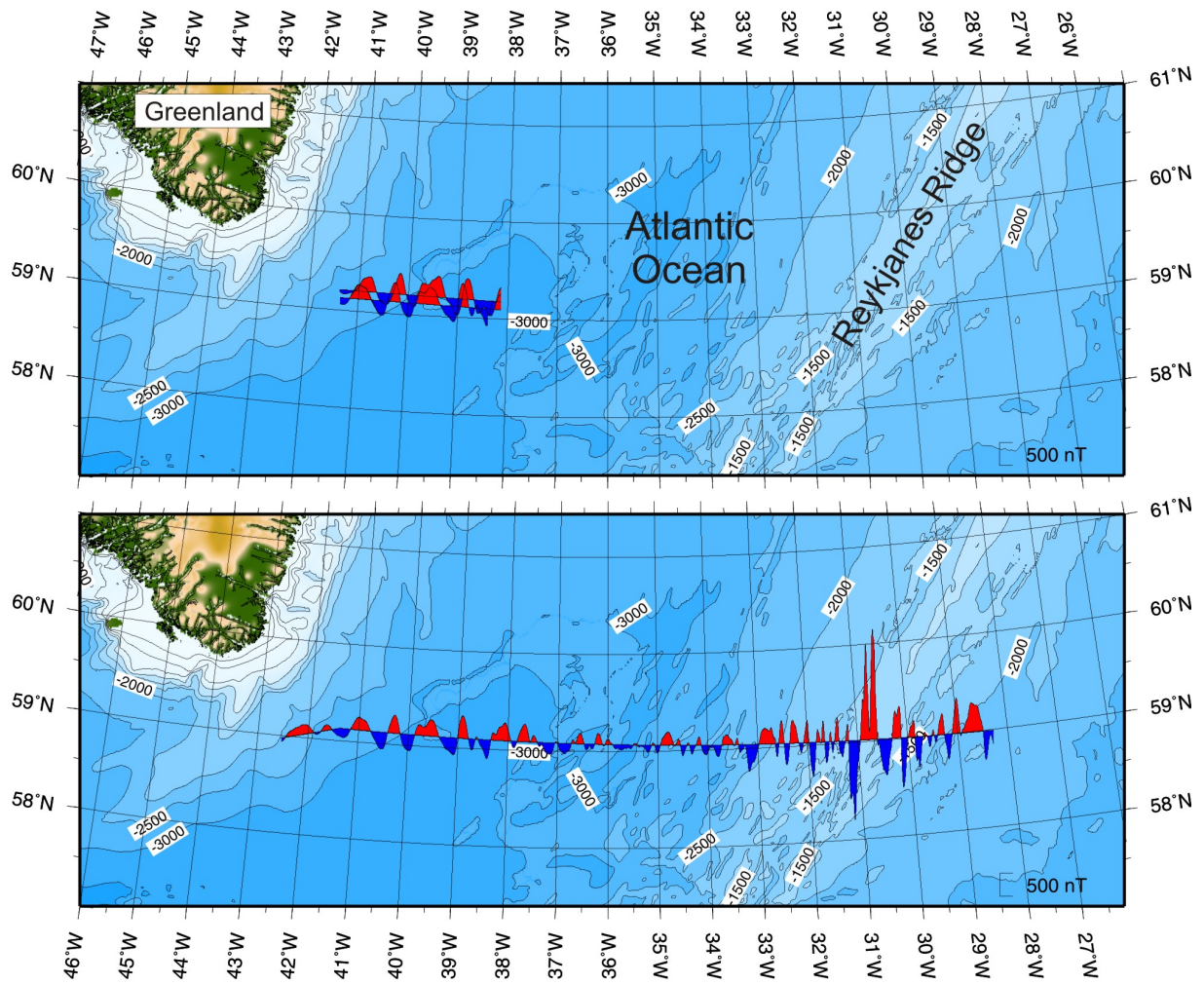


Fig. 8.13: Magnetic anomalies over the western flank of the Reykjanes ridge. Top: two parallel aeromagnetic lines. Bottom: marine magnetic line BGR10-3M14

9. SEISMICS

Jürgen Adam¹, Tabea Altenbernd¹, Kai Berglar¹, Thomas Behrens¹, Martin Block¹, Volkmar Damm¹, Axel Ehrhard¹, Jürgen Gossler², Anne Hegewald², Günter Kallaus¹, Edith Korger², Christine Läderach², Dirk Pitschmann¹, Michael Schnabel¹, Florian Schmid², Sonja Suckro

¹) Bundesanstalt für Geowissenschaften und Rohstoffe, Hannover

²) Alfred-Wegener-Institut, Bremerhaven

9.1 Methods

Three different types of seismic investigations were applied during the cruise in order to match the scientific tasks (Fig. 9.1). The imaging and identification of the sedimentary pattern and the uppermost crustal structure was realized with multi-channel seismics (MCS) (see chapter 9.4 and 9.5). For a better control on the seismic velocities, the MCS method was expanded by sonobuoy refraction measurements (see chapter 9.6). Finally, deep crustal information and imaging of the Moho depth was done with OBS refraction measurements (chapter 9.7).

Principles of marine seismic reflection and refraction surveying

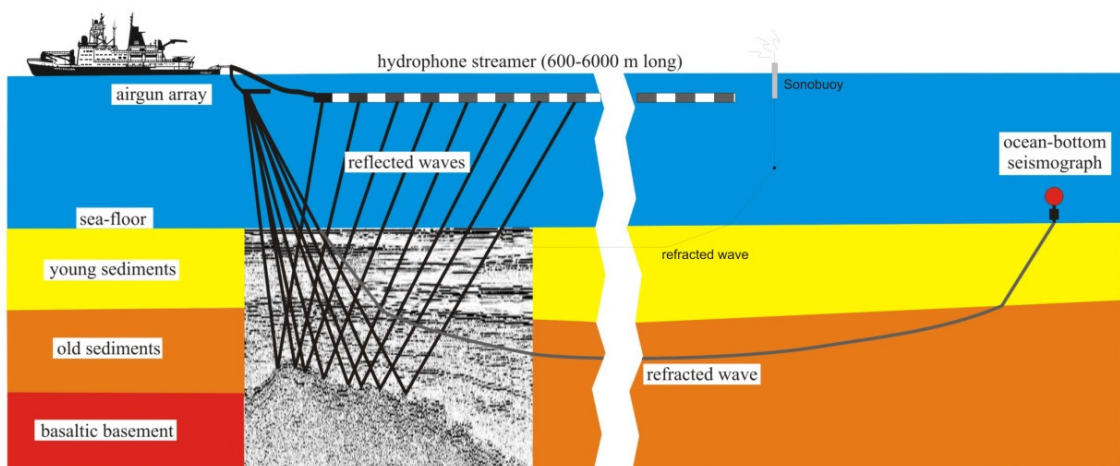


Fig. 9.1: Marine seismic methods: Multi-channel seismic (MCS) for recording of reflected waves, sonobuoy measurements for refracted waves, and ocean bottom seismometer (OBS) for wide angle seismics and refracted waves

9.2 Marine mammal observation to comply with environmental regulations

The Greenland Government required that seismic operations had to comply with the instructions from the Greenland National Environmental Research Institute (NERI)

and marine mammal observations need to be done during all seismic operations. The NERI recommendations of best practice for marine seismic operations refer to JNCC-standards (Joint Nature Conservation Committee – www.jncc.gov.uk/marine - for reference see: JNCC, 2004). The purpose of the JNCC guidelines is to minimize the risk of possible injury from seismic surveys to marine mammals including seals, whales, polar bears and walrus. There was one certified Marine Mammal Observers (MMO's) that was contracted through RPS Energy, UK to fulfill the obligations in mitigating for seismic operations in the Baffin Bay in Greenland waters during ARK-XXV/3. The role of the trained MMO was to advise on the use of the JNCC guidelines on all seismic activities and conduct pre-shooting searches for marine mammals before commencement of any seismic activity.

The specific mitigation measures adopted by the operator should be appropriate to minimize the risk of causing an offence and should implement the following best practice procedures. The roles of the Marine Mammal Observers were as follows:

- Conduct 30 minute pre-survey watches of a 500 m exclusion zone to ensure the clearance of marine mammals before commencement of ramp ups.
- To monitor ramp ups of seismic array for a minimum of 20 minutes but no greater than 40 minutes to ensure that marine mammals have the opportunity to leave the survey area and request a delay of a ramp up if a marine mammal is sighted within the exclusion zone.
- To advise the crew on the procedures set out in the JNCC guidelines and to provide advice to ensure that the survey programme is undertaken in accordance to the guidelines.
- To continue visual watches for marine mammals during all daylight hours and document any marine mammal sightings.
- To document and report all gun hours, observation hours, mitigation issues, marine mammal sightings, and compliance issues.

There was one certified Lead Marine Mammal Observer (MMO) who has completed the Protected Species Observer course and 6 onsite trained MMO's that performed the visual observations for this project. Originally, there were supposed to have been three Inuit marine mammal observers from Baffin Island to accompany the Lead MMO with observer duties. Due to the injunction from Canada, these three observers were not able to participate in the project. An on board training was held by the Lead MMO for the scientists who volunteered to be dedicated marine mammal observers for the project. The training consisted of the background in seismics with regard to environmental noise and potential impacts on marine life. JNCC regulations were explained in detail with flow charts describing the measures to be taken during ramp ups, survey and line changes. A section of the training was devoted to marine mammal biology and the characteristics of the most likely marine mammals in the area. Several guides books and handouts detailing whale and seal behaviour were available for reference on the bridge in the work place. MMOs worked all daylight hours on full watch during this reporting period. The number of daylight hours at the beginning of the project was 24 hour daylight and towards the beginning of October, daylight started to decrease to darkness for a total of 6 - 8 hours of darkness. The Lead marine mammal observer worked a maximum four hour shifts, with two hour

breaks for a total of 12 hours of watch per day. The other trained MMO's worked a two hour shift for a maximum of 12 hours a day. When there were periods of darkness, the watches would begin at civil dawn, which ranged from 07:30 - 08:30, and ended when the exclusion zone could no longer be effectively observed due to darkness between 23:00 - 01:30. These times were variable day to day due to cloud cover as well as our coordinate position. During ancillary watches, the Lead MMO observed on the bridge for two four hour shifts with a two hour break in between. The detailed final MMO report is attached in Appendix A.17.

9.3 Seismic equipment and survey setup

The survey area in the North Baffin Bay is characterized by high compacted sediments directly beneath the seafloor and unknown basement nature and above the sea surface unpredictable sea ice and ice berg conditions. The target was to ensure deep signal penetration in order to identify and map the basement structure. Owing to these preconditions we decided to use a hybrid streamer with a maximum length that can be handled by the BGR streamer winch. In order to be prepared for heavy ice conditions, the solid state sections were towed at the far end of the streamer. In the case of heavy sea ice, the streamer should be recovered and only the solid section would be kept in the water as they are considered to be less vulnerable regarding ice contact.

In general the streamer was towed in a depth of 12 and 18 m, respectively, for the enhancement of low frequencies and in order to avoid ice contact.

A powerful source of six 520 in³ G-Guns was fixed in a 2.5 x 6.5 m cage. This cage was towed close to the stern of the vessel (approx. 15 m behind the stern) in order to protect the guns and umbilicals from drifting icebergs and growlers.

The streamer consisted of 20 fluid sections (ALS, channel 1 – 240, near trace) and 5 solid state sections (SSAS, channel 241-300, far trace). No tail buoy was used, also because of the unpredictable ice conditions. The streamer winch was placed on the starboard side of the working deck and the streamer was fixed on the starboard side if no sea ice and less icebergs were along the seismic line. In case of increasing sea ice the streamer was towed from the stern of the vessel close to the airgun array on the starboard side (see Fig. 9.14 and 9.15).

In the Kane Basin, only the outer 750 m of the streamer that consisted of the solid state sections (SSAS) were deployed and towed midship at the stern of the vessel (Fig. 9.16) because of the heavy sea ice and iceberg density. In this setup no lead-in cable was used and the first channel was right beside the airgun array.

In order to fulfill the JNCC Guidelines for environmental protection, each line started with a ramp up (soft start) procedure. For a time period of 20 min a linear increase of the source volume was applied.

9.3.1 Seismic sources, triggering and timing

Airgun system

During the cruise the AWI G-Gun airgun cage was used. The dimensions of this cage are 6.5 x 2.5 x 1.5 m (l x w x h). The G-Gun cage consisted of six guns (Fig. 9.3 &

9.4). Each G-Gun had a volume of 520 in³, resulting in a total volume of 3,120 in³ (51.1 l). The towing depth was 10 m throughout the survey. During the MCS operations six G-Guns were used (total volume: 3120 in³ resp. 51,1l), and during the acquisition of the refraction lines all six and two additional G-Guns, with volumes of 520 in³ each were operated (resulting in a total maximum volume of 4160 in³ resp. 67,2 l). The working pressure was 2,142 psi (150 bar). During the measurements the G-Guns proved to be very reliable. Major maintenance was approximately every 48 h. Maintenance was restricted to line change periods in order to reduce down-time. The majority of the problems were due to broken air hoses and service of the G-guns.

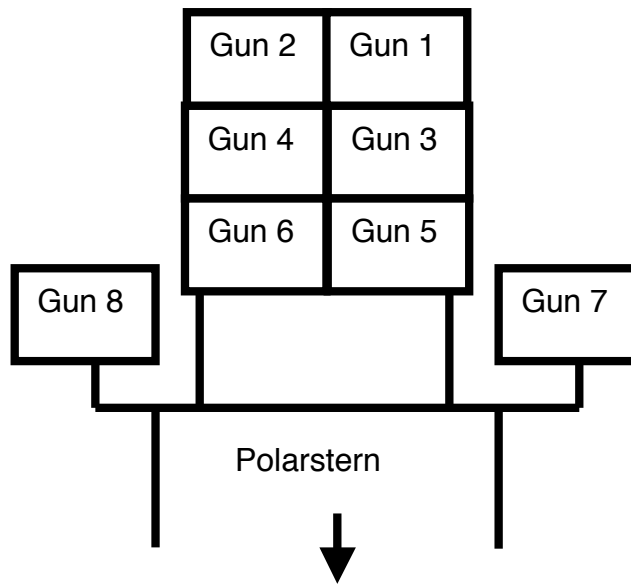


Fig. 9.3: Sketch of the G-Gun pattern with additional G-Guns on the port side and starboard side of the vessel

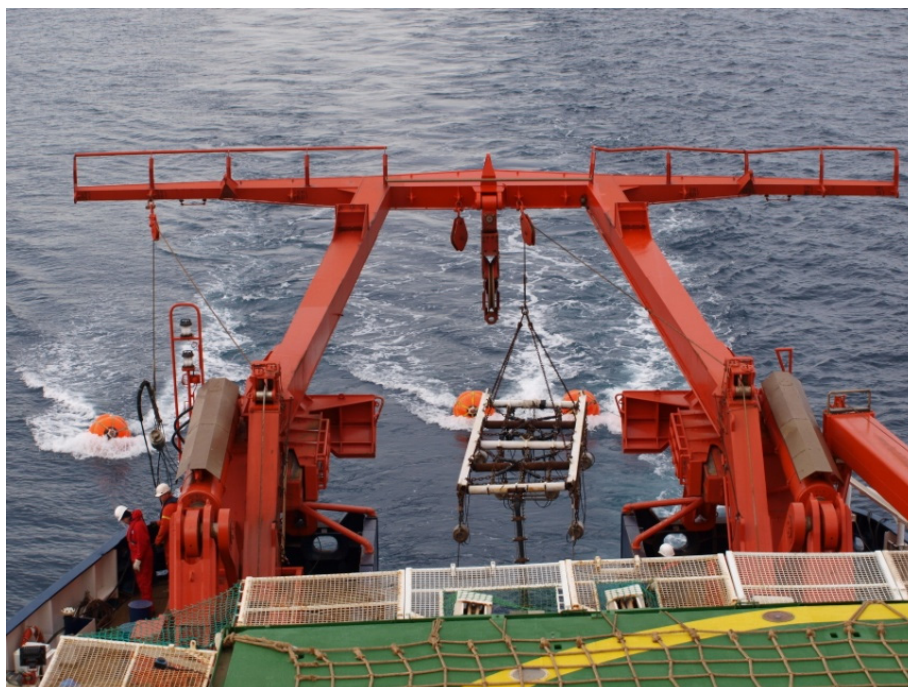


Fig. 9.4: The AWI G-Gun cage hanging from the A-Frame close before deployment. Note on the starboard side behind the vessel the buoy of one of the additional sources during refraction work

9.3.2 Multi-channel seismic reflection (MCS) recording system

BGR's SEAL seismic recording system and a digital cable with an active length of 3.750 m were used to record the seismic data. The bird controlling system (DigiCOURSE System 3) and the streamer control system are interfaced with the Master PC. The system start trigger is generated by the Master-PC. Here, the data for the external header, e.g. from the DigiCOURSE System 3, navigation system, GPS-clock, pressure, etc., are received and the external header is generated, stored and sent via an interface to the SEAL system and to the navigation system (Fig. 9.7). One OYO GEOSPACE GS642 thermal plotter for paper printouts of single trace plots was in use for quality control. The plotting parameters were 8 s record length and 25 traces per inch (TPI) for the single trace. An AGC with a 1,000 ms window length was applied to the data.

The DigiCOURSE System 3 was used to control the vertical streamer position (depth) and to measure the heading and temperature. DigiCOURSE System 3 is a hardware and software package that controls and collects data from a network of acoustic sensors and streamer positioning devices (Fig. 9.5). The system has online command, diagnostic, and performance-monitoring capability. System 3 employs a modular architecture which provides for a variety of configurations and levels of functionality. The minimum system equipment configuration includes two real-time processors: an Operator Interface (OI) and a Data Management Unit (DMU), a Line Interface Unit (LIU), and cable-mounted measuring devices: birds with compass. It is suggested to get the full equipped streaming device self buoyant. To produce more buoyancy we mounted at each bird position a floatation tube or instead that a

recovery system which has a self triggering mechanism at a depth of 50 m. We operated the cable at a depth of 12 m, and at a depth of 18 m.



Fig. 9.5: DigiCOURSE System 3 bird with compass

Streamer system

BGR's SEAL streamer consists of 25 seismic sections (20*ALS and 5*SSAS) with 300 channels (Fig. 9.6). It has a flexible architecture with redundant data transmission modes, i.e. data transmission may be reconfigured on line failure. Each channel has an individual 24 bit, Sigma Delta A/D converter. The active streamer sections have a diameter of 50 mm.

The SEAL recording system is capable to handle a maximum recording capacity of 2,000 channels (@ 12.5 m; 2 ms) per streamer, a maximum record length of 99 s, and a maximum number of 20,000 seismic channels and 60 AUX channels. The sampling rate may vary from 1/4 ms, 1/2 ms, 1 ms, 2 ms to 4 ms. During the cruise we sampled the data at 2 ms.

Up to 6 tape drives may be operated either simultaneously or in alternating modes. We operated two SDLT 320 and simultaneously two NAS systems during the cruise. Data format is 4byte - SEG-D revision 2, demultiplexed 32 bit IEEE, Code 8058.

In-water equipment

The seismic data are amplified, filtered, and analogue-digital converted within the SEAL streamer by using the following main modules installed in the streamer: 1 LCI, 1 DCXU, 4 LAUM, 1 TAPU, 1 AXCU and 1 HAU.

Survey ARK XXV/3													RU1		RU2 WB																																																											
3750m / 300 Channels													SHS		HAU		HESE		HESE		HESA																																																					
line No. BGR 10-302 to 315, 318 to 322													6m		50m		50m		10m		78 m																																																					
line No. BGR 10-316, 317 only with SSAS21- SSAS25 / 60 channels													1461		236		1435		2692		1389																																																					
RU3			RU4/R1			RU5			RU6/R2			RU7																																																														
ALS 1	ALS 2	ALS 3	ALS 4	ALS 5	LAUM	ALS 6	ALS 7	ALS 8	ALS 9	ALS 10	LAUM	ALS 11	ALS 12	ALS 13																																																												
1 - 12	13 - 24	25 - 36	37 - 48	49 - 60	1	61 - 72	73 - 84	85 - 96	97 - 108	109 - 120	2	121 - 132	133 - 144	145 - 156																																																												
7030	7029	8640	7027	8630	451	7026	7023	7024	7021	8633	557	7020	8628	8637																																																												
RU8/R3			RU9			RU10/R4			RU11/R5			RU12/R6																																																														
ALS 14	ALS 15	LAUM	ALS 16	ALS 17	ALS 18	ALS 19	ALS 20	LAUM	SSAS 21	SSAS 22	SSAS 23	SSAS 24	SSAS 25	TAPU																																																												
157 - 168	169 - 180	3	181 - 192	193 - 204	205 - 216	217 - 228	229 - 240	4	241 - 252	253 - 264	265 - 276	277 - 288	289 - 300																																																													
8617	8634	480	8636	7016	7012	7015	8638	1710	12075	12063	12076	12043	12080	186																																																												
<table border="1"> <tr> <td>TES</td> <td colspan="14">length over all (Stern - Tail TES): 3995m</td> </tr> <tr> <td>50m</td> <td colspan="14"></td> </tr> <tr> <td>1474</td> <td colspan="14"></td> </tr> </table>															TES	length over all (Stern - Tail TES): 3995m														50m															1474																													
TES	length over all (Stern - Tail TES): 3995m																																																																									
50m																																																																										
1474																																																																										
<table border="0"> <tr> <td>RU-No.</td><td>RU1</td><td>RU2</td><td>RU3</td><td>RU4</td><td>RU5</td><td>RU6</td><td>RU7</td><td>RU8</td><td>RU9</td><td>RU10</td><td>RU11</td><td>RU12</td><td colspan="2"></td></tr> <tr> <td>S/N</td><td>42461</td><td>36194</td><td>36878</td><td>37732</td><td>36273</td><td>36304</td><td>38125</td><td>38003</td><td>36003</td><td>36464</td><td>37927</td><td>42487</td><td colspan="2"></td></tr> <tr> <td></td><td></td><td></td><td></td><td>Recovery 1</td><td></td><td>Recovery 2</td><td></td><td>Recovery 3</td><td></td><td>Recovery 4</td><td>Recovery 5</td><td>Recovery 6</td><td colspan="2"></td></tr> <tr> <td>dist to stern</td><td></td><td>130m</td><td>280m</td><td>340m</td><td>490m</td><td>940m</td><td>1390m</td><td>1840m</td><td>2290m</td><td>2740m</td><td>3190m</td><td>3490m</td><td>3940m</td><td></td></tr> </table>															RU-No.	RU1	RU2	RU3	RU4	RU5	RU6	RU7	RU8	RU9	RU10	RU11	RU12			S/N	42461	36194	36878	37732	36273	36304	38125	38003	36003	36464	37927	42487							Recovery 1		Recovery 2		Recovery 3		Recovery 4	Recovery 5	Recovery 6			dist to stern		130m	280m	340m	490m	940m	1390m	1840m	2290m	2740m	3190m	3490m	3940m	
RU-No.	RU1	RU2	RU3	RU4	RU5	RU6	RU7	RU8	RU9	RU10	RU11	RU12																																																														
S/N	42461	36194	36878	37732	36273	36304	38125	38003	36003	36464	37927	42487																																																														
				Recovery 1		Recovery 2		Recovery 3		Recovery 4	Recovery 5	Recovery 6																																																														
dist to stern		130m	280m	340m	490m	940m	1390m	1840m	2290m	2740m	3190m	3490m	3940m																																																													
<table border="0"> <tr> <td>RU-No.</td><td>RU1</td><td>RU2</td><td>RU3</td><td colspan="11"></td></tr> <tr> <td>S/N</td><td>42461</td><td>36194</td><td>36878</td><td colspan="11">streamer on winch up to ALS20 at lines BGR10-316, -317</td></tr> <tr> <td></td><td>Recov 1</td><td>Recovery 2</td><td></td><td colspan="11"></td></tr> <tr> <td>dist to stern</td><td>159m</td><td>309m</td><td>609m</td><td colspan="11"></td></tr> </table>															RU-No.	RU1	RU2	RU3												S/N	42461	36194	36878	streamer on winch up to ALS20 at lines BGR10-316, -317												Recov 1	Recovery 2													dist to stern	159m	309m	609m											
RU-No.	RU1	RU2	RU3																																																																							
S/N	42461	36194	36878	streamer on winch up to ALS20 at lines BGR10-316, -317																																																																						
	Recov 1	Recovery 2																																																																								
dist to stern	159m	309m	609m																																																																							

Fig. 9.6: Streamer configuration used

ALS Acquisition Line Section

SSAS Solid State Acquisition Section

Both with a length of 150 m, an ALS/SSAS acquire data from 12 channels with an equal spacing of 12.5 m. Each channel receives data from a group of 16 hydrophones, with a capacity of 256 nF (@ 20°C), a sensitivity of 20 V/bar open circuit, and 17.4 V/bar, with electronics included.

HAU Head Auxiliary Unit

The HAU assures power supply for the TLFOI and measures the tensile strength value between the cable and the vessel. During cruise BGR10-3 the stress was about 0.9 t.

HESE Head Elastic Section Extension

LAUM Line Acquisition Unit, Marine

TAPU Tail Acquisition and Power Unit

Onboard equipment

AXCU	Auxiliary Channel Unit The AXCU box contains FDU2M (Field Digitizer Unit 2 Marine). It is used to convert analogue data coming from the airgun array and the waterbreak-section. 5 auxiliary channels (AUX) are recorded (max. 6): Aux1= WB (waterbreak), Aux2 - Aux5 were not used according the AWI-Gun-frame was not prepared for.
CM408XL	Control Module eXtra Large
DCXU	Deck Cable Cross Unit & Line Acquisition Unit, Cross line, Marine
LAUXM	The Deck Cable Unit, housing a Deck Cable Interface (DCI) and a Line
PWM2	PoWer Module generates a +175/-175 VDC voltage
PWMC	PoWer Module Controller
HCI	Human Computer Interface The HCI is the control unit for the operator. Script files can be saved to and/or loaded from another computer and an online help is available.

The QC software running on a 'SunBlade 150' workstation enables the control of the following functions and settings via a permanent graphic display:

- Operation and function control of the different units (PWMC, PRM, QC) with automatic central control unit acceptance tests
- Concise display of system activity
- Automatic log of observer report data
- Display of power status
- Acquisition sequence controlled by external shooting system
- On-line real-time signal graphic analyser
- Printout of all parameters

PRM	Processing Module The PRM is a processor software module that is used for transferring the data to and from the cartridge drive, the NAS-Servers, to the plotter and the SeaProQC system. It is installed on a separate 'SunBlade 2500' workstation.
-----	---

SeaProQC Sea Processing Quality Control

Continuous online seismic data quality control is performed using a SeaProQC workstation 'SunBlade 2500' connected directly to the PRM without slowing down the acquisition. Three main windows are used for quality control:

- The History display window with bar graphs shows a summary of errors and source attributes for the successive shots processed by the SeaProQC. It displays the attributes of the data from the previous shots.
- The Normal display window shows the latest incoming SEG-D shot record. The traces are displayed in the time/distance range with the noise of each trace on top of the display.
- The Single Trace window shows the data of one selected channel from the streamer. With each new shot the display is updated with the new acquired trace added to the window. Four single trace windows may be opened simultaneously.

Shot triggering for refraction

The shots for refraction lines BGR10-3r1 – BGR10-3r4 were triggered in time intervals of 60 seconds synchronized with GPS-Time over Meinberg GPS 170 interface card. The shot time interval representing an even distribution was generated on the Master PC with an interface card for triggering the airgun array via the SEAL408XL system and the Syntron GCS 90 shot trigger device.

The Master PC is running under Microsoft Windows XP and the Software is LabView Ver.8.6 from National Instruments.

Quality control

Quality control during acquisition comprised:

- Continuous control of the airgun pressure
- Observation of the hydrophone signals within the arrays and adjustment of the trigger delays for an optimum signal.
- Checking and recording the streamer depth and position (heading) every shot via the control screen of the DigiCOURSE System 3. These data are stored in the header and are written on the field tapes.
- Continuous checks whether all sections of the streamer are free of abnormal noise and give about the same signal amplitude. This was done for every shot via the QC Graphics display of the SeaProQC system.
- Continuous observation of the single resp. near trace records.

9.3.3 Sonobuoy instruments for wide-angle seismic data acquisition

Michael Schnabel, Axel Ehrhardt
Bundesanstalt für Geowissenschaften und Rohstoffe

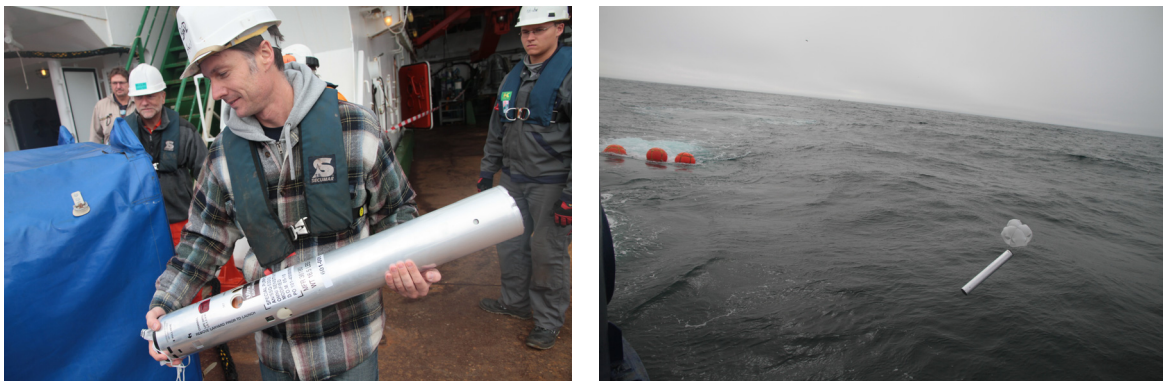


Fig 9.8: A sonobuoy before and directly after deployment from the ship

Marine sonobuoys (Fig. 9.8) were deployed to acquire wide angle reflection and refraction data to better determine the velocity structure of the sub-surface. Sonobuoys are recording the seismic energy released by the air guns and radio the information back to the seismic vessel. After entering the seawater, a salt water battery activates the sonobuoy. A surface unit (which contains the VHF-FM antenna) is inflated. After that, a cable pack pays out to a predefined length. At the lower end

of the cable, a hydrophone is situated. A hole is burned in the plastic material of the float after a predefined time and cause the system to scuttle.

We used sonobuoys manufactured by Ultra Electronics, Type AN/SSQ-53D(3). These instruments were modified to be suitable for the amplitude and frequency response of acoustic seismic refraction measurements. The frequency response was increased in the 5 - 60 Hz band of interest. Before deployment, the sonobuoy was programmed to the desired life time, hydrophone depth and radio frequency. The life time can be chosen between 0.5 and 8 hours, the hydrophone depth may be in a range of 30 to 300 m and the signals can be transmitted between 136.0 and 173.5 MHz.

On the rear side of *Polarstern's* funnel, a Yaggi antenna was installed. A radio-receiver (Yaesu VR-5000) was set up in front of the radio office. The signals were recorded on a METHUSALEM-MBS recorder (SEND GmbH, Hamburg).

9.3.4 Ocean-bottom seismometers (OBS) and landstations

The Alfred Wegener Institute (AWI) in Bremerhaven operates the German ocean bottom seismometer (OBS) instrument pool DEPAS consisting of 80 broad-band OBS of the type Longterm Ocean Bottom Seismometer for Tsunami and Earthquake Research (LOBSTER). On ARK-XXV/3 we employed 35 DEPAS OBS, five of them with brand-new 120 sec seismometers.

Each OBS is equipped with a Güralp 60 sec 3-component broad-band seismometer and a High Tech broad-band hydrophone. The AWI OBS (Fig. 9.9) is manufactured by Umwelt- und Meerestechnik GmbH (KUM) in Kiel, Germany. Major parts of the OBS are supplied from other manufacturers like Güralp Systems Ltd. (seismometer), SEND GmbH (recording unit) and High Tech Inc. (hydrophone).

The main goal of the LOBSTER design was to develop a compact OBS that can be easily assembled on board a vessel. A compact size helps to minimize noise signals from bottom water currents. Further developments of the LOBSTER system have been:

1. Simplified programming and data read-out procedures between subsequent deployments in refraction seismics.
2. An extended maximum operation interval of well above one year for seismicity and tsunami studies.
3. The use of broad-band sensors to register a wide frequency spectrum.
- 4.

The LOBSTER system consists of a titanium frame that holds 4 (+4) flotation units, one (or two) titanium pressure cylinders for the recording unit and the batteries, a 3-component 60 sec broad-band seismometer built-in in a titanium case, a broad-band hydrophone, a 24 bit recorder, an acoustic release unit, a flash and radio beacon, and an anchor weight (Fig. 9.9).

The heart of the LOBSTER system is a low power consuming (<0.65 W) SEND Geolon MCS 24 bit A/D converting and recording device providing three channels for the seismometer input signals and one for high impedance hydrophones. The

sampling rate can be adjusted in steps from 1-1,000 Hz. The pre-amplifier gain of each channel can be set individually to 1, 2, 4, 8, 16 and 32. All parameters can be set by the SENDCOM software using a connected laptop. During ARK-XXV/3 the sampling rate was set to 250 Hz on refraction lines and 100 Hz for the new test OBS. The gain of the hydrophone channel was set to 4 and 1 for the three seismometer channels, respectively. Additionally, the software offers test functionality to the sensor components prior to deployment. While on the seafloor, data is stored on a 20 GB harddisk that can be accessed via a 1 GB/min FireWire interface after recovery. Programming, GPS synchronization, and data retrieval can be performed while the recorder is located in its pressure housing which is connected via a GPD30 break-out box to an external GPS clock and a laptop computer (Fig. 9.10).

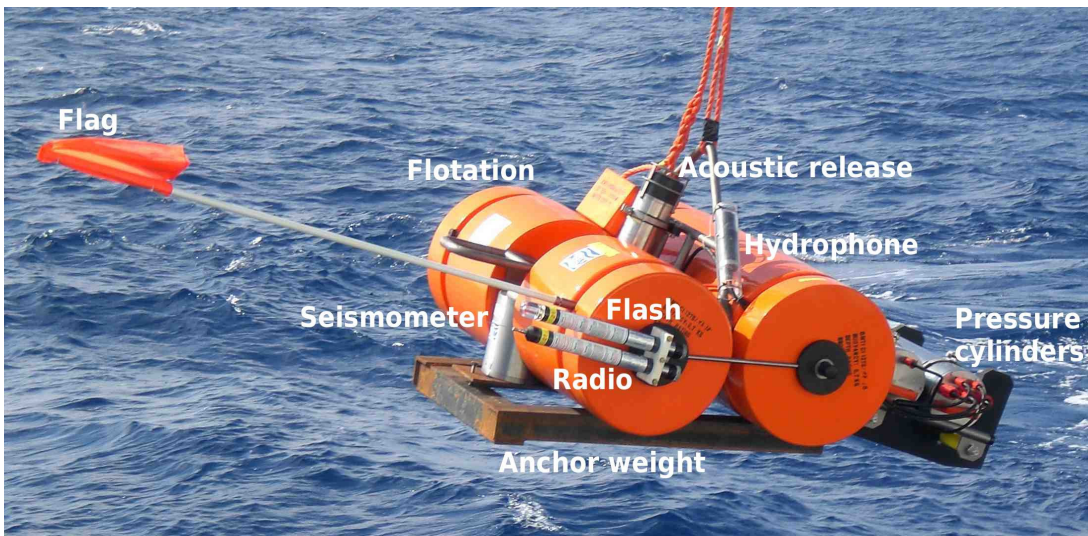


Fig. 9.9: The AWI Ocean bottom seismometer LOBSTER during deployment. The main instrument components are indicated.

Fig. 9.10: Connecting the LOBSTER via the yellow GPD30 box to an external GPS clock and a laptop computer to start or stop data acquisition and retrieval.



The GÜRALP CMG-40T 60 sec 3-component broad-band seismometer operates in a frequency range between 0.0167 Hz (=60 sec) and 50 Hz. Five new seismometers with an extended long-period range down to 120 sec have been tested during ARK-XXV/3. After settling on the seafloor it can be levelled horizontally in a range of $\pm 50^\circ$. First levelling and for long-term deployments subsequent levelling intervals can be set by software during parameter set-up. The MCS recorder then sends levelling pulses to the seismometer's gimbal system at the appropriate time. The High Tech HTI-04-PCA/ULF broad-band hydrophone operates in a frequency band between 0.01 Hz (=100 sec) and 8 kHz.

To recover the OBS, hydro-acoustic signals (12 kHz) are sent from the vessel to the KUM K/MT 562 acoustic release unit, which connects the anchor weight to the OBS frame. The release hook is opened remotely when needed. An automatic release can also be set as a fail-safe option. When the OBS has returned to the sea surface a Novatec ST-400A flash light and a Novatec RF-700A1 radio beacon are automatically switched on by pressure switches to allow easy location of the OBS in the water.

Before deployment correct operation of the sensors, radio beacon and the flash light were checked. After recovery, the OBS was cleaned with fresh water. Flag, radio beacon and flash light were removed. Recording was stopped and the internal clock of the recorder was synchronized again with the GPS signal. The data was then downloaded to an external computer and converted to MiniSEED continuous records of 24 hours. A shotfile was produced from the BGR UKOOA file to produce the 60 sec SEG-Y traces for the seismogram sections.

During ARK-XXV/3 a total of 91 OBS had been deployed and recovered successfully. Most OBS worked without major problems. A radio beacon and a flash light were lost during recovery, some flags were damaged. Some flashes started operating much later than the radio beacons, which made it hard to detect the OBS during night time. This was probably due to a delay of the pressure switch, which turns on radio beacon and flash light when they reach the surface. One OBS failed operation due to an external shock during deployment or when settling on the seafloor. Another OBS lost data because water could enter into the pressure housing and severely damage the recorder.

The onshore stations

The land stations are equipped with a RefTek 130 data logger sampling with 100 Hz, nine geophone chains with six geophones per chain recording the vertical component or alternatively with a GÜRALP CMG-3ESPC broadband seismometer recording three components (Fig. 9.11). We used one LifeLine 12 V sealed battery for a station with geophone chains and two batteries for stations equipped with a seismometer.

The data is recorded on two CompactFlash 2 GB memory cards inserted into the RefTek data logger. We installed the seismometer in a pit of about 40 cm depth in unconsolidated dry hillslope debris. The sensor was mounted on a wooden plate to guarantee a rigid base and covered with a plastic bucket with a stone on top to fix it (Fig. 9.12). Then the whole set up was covered with loose material from the pit to shield the sensor from temperature changes and wind noise.

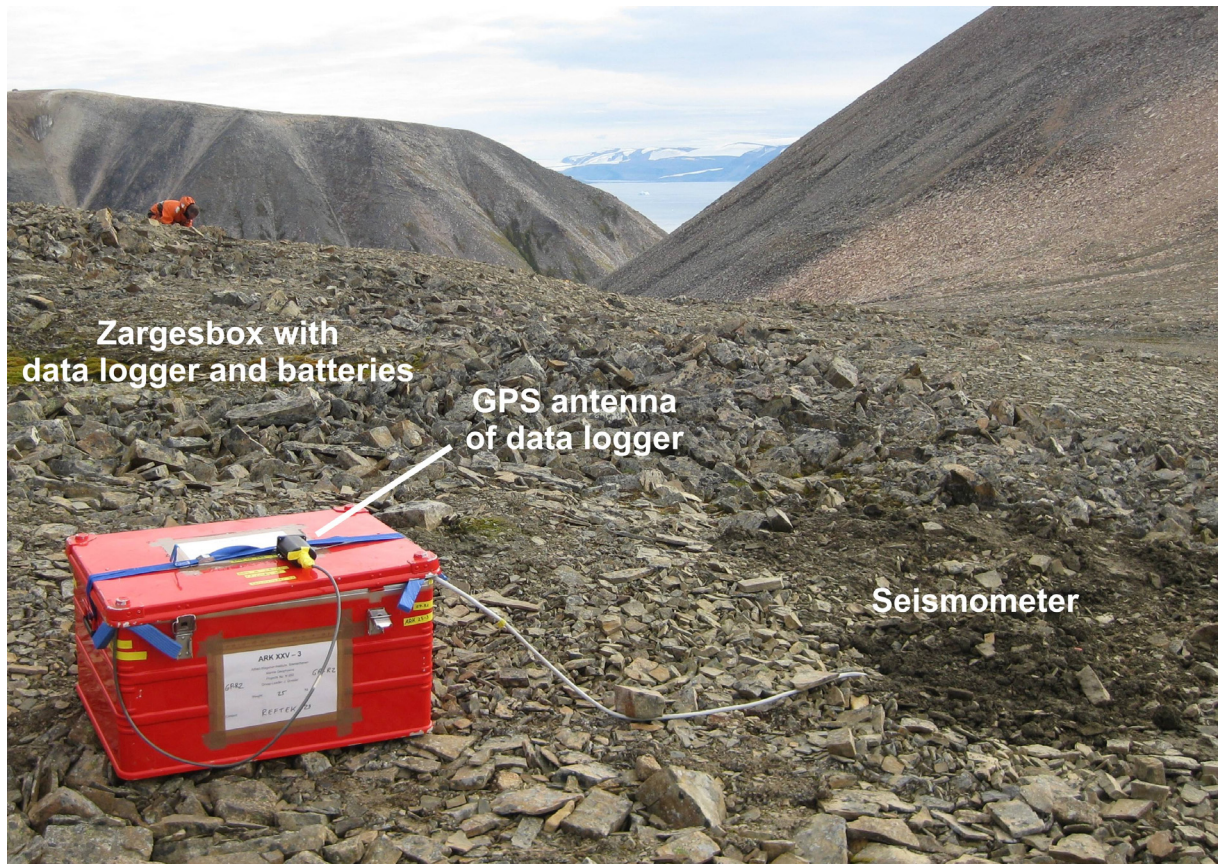


Fig. 9.11: Set up of land station 300stL2 equipped with a broadband seismometer



Fig. 9.12: Set up of the seismometer of land station 450stL2 on a wooden plate (left) and plastic bucket with stone to shield it from temperature changes and wind (right)

9.4 Processing of multi-channel reflection data

Seismic data processing was done using a Linux workstation with ProMAX™ 2D, Version 5000.0.1 licenses. The workstation (Fig. 9.13) has two Quadcore AMD CPUs, a RAM of 32 GB and a 170 GB system hard drive. The operating system is CentOS Linux 5.0. A raid disk array with 2 TB disk space is accessible from both workstations. Both workstations make use of the raid system for storage of seismic data, the database and job flows.

A raid system of 1.7 TB was connected to b3lx01 work station. This combination worked as a NAS system for data storage and easy data access.

Onboard processing was done for all acquired MCS data including the following steps: geometry setup, data and geometry input, prestack processing to enhance signal quality including multiple reduction, data stacking and Kirchhoff migration. The ProMAX™ processing flows for these steps are attached as Appendix A.5A to this cruise report.

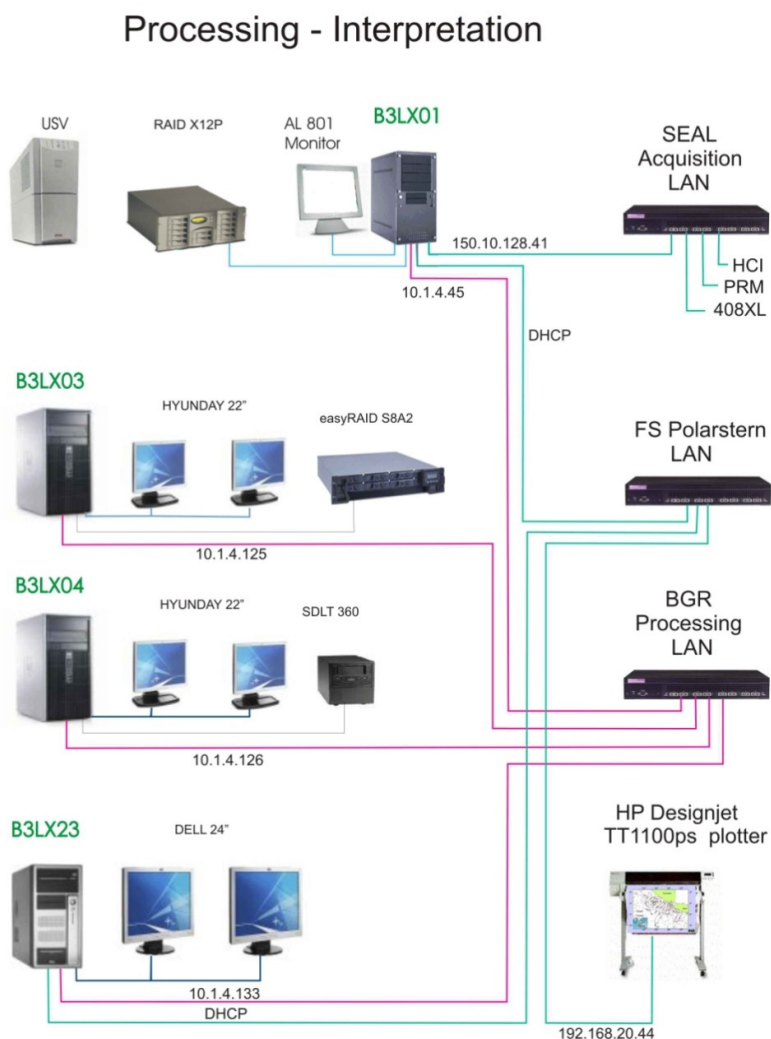


Fig. 9.13: Hardware setup scheme for seismic ProMAX processing. The link to the workstation for interpretation (b3lx23) is included at the bottom

Geometry setup

According to the ice conditions different streamer setups were used. For ice free conditions the streamer was towed on the starboard side of the vessel (Fig. 9.14). If the seismic line crossed ice fields with ice growlers the streamer was towed slightly offset to the center line of the vessel (Fig. 9.15). Two lines were recorded within the Kane Basin. Owing to the ice conditions in the Kane Basin only the 5 solid state sections were towed from the center line position (Fig. 9.16). The streamer was towed in different depths documented in the acquisition logs.

The geometry of the source and the receivers was set up in relation to the GPS antenna position. The active streamer length was set to 3.750 m with 300 channels for seismic lines within the Baffin Bay. In ProMAX the 2D Marine Geometry Spreadsheet was used. It includes the following steps which have to be carried out in the geometry setup sequence:

File. UKOAA Import:

The navigation data were transformed by the navigation group into rectangular UTM coordinates and saved in the format "STANDARD UKOAA 90 Marine 2D".

Setup:

All lines were acquired with 12.5 m nominal receiver spacing and 37.5 m nominal source station interval. The other parameters changed and are reported in the acquisition logs. All units are given in meters.

Sources:

The following columns in the spreadsheet have to be filled using the "Edit" option: "Source" and "Station", beginning with 1 and incrementing with 1. The streamer azimuth has to be calculated using "auto azimuth". The algorithm used for this by ProMAX is very crude. It is based only on the first and last source point, the calculated azimuth is assigned to all source positions. The column "Src Pattern" has to be filled with the number of the pattern defined in the next step. Shotpoint interval and error were checked by the QC tool.

Patterns:

The streamer and source patterns have to be defined according to the spreadsheet in Figures 9.14 to 9.16 and the configuration of the used sources.

Bin:

The binning consists of three steps:

1. Assign Midpoint.
2. Binning. Source station tie to CDP number: This is usually shot number 1. In some cases the shots were already recorded when the ramp up was applied and the vessel still turned. In these cases the first shot on the line was noted in

the acquisition logs and this shot should be entered as station tie to CDP number;

CDP Number tie to source station: 10000. This tie fulfils BGRs standard for CDP numbering: The first station with full coverage is tied approximately to CDP 10000. Distance between CDPs: 6.25. This implies a nominal CDP coverage of 50 (for 300 channels) in case of a shot increment of 37.5 m. Binning was done for CDP locations and receivers (channel number decrease in shot direction).

3. Finalize Database.

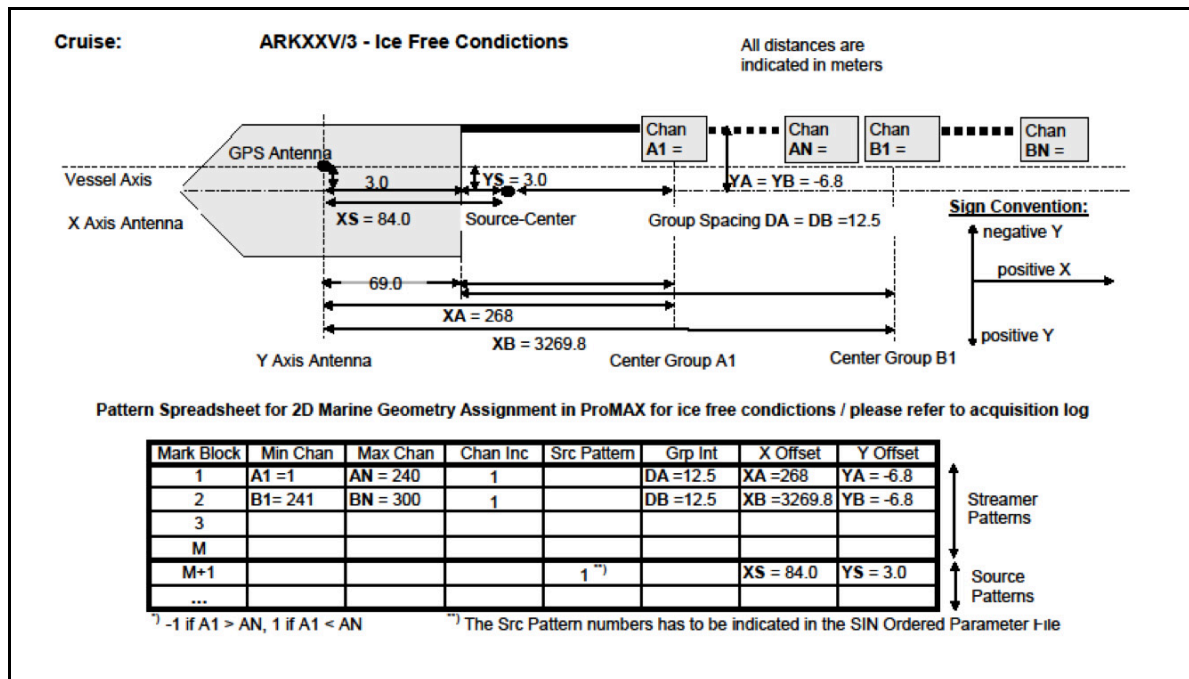


Fig. 9.14: Acquisition geometries for the seismic reflection lines including ProMAX spreadsheets for definition of streamer and source pattern for ice free conditions

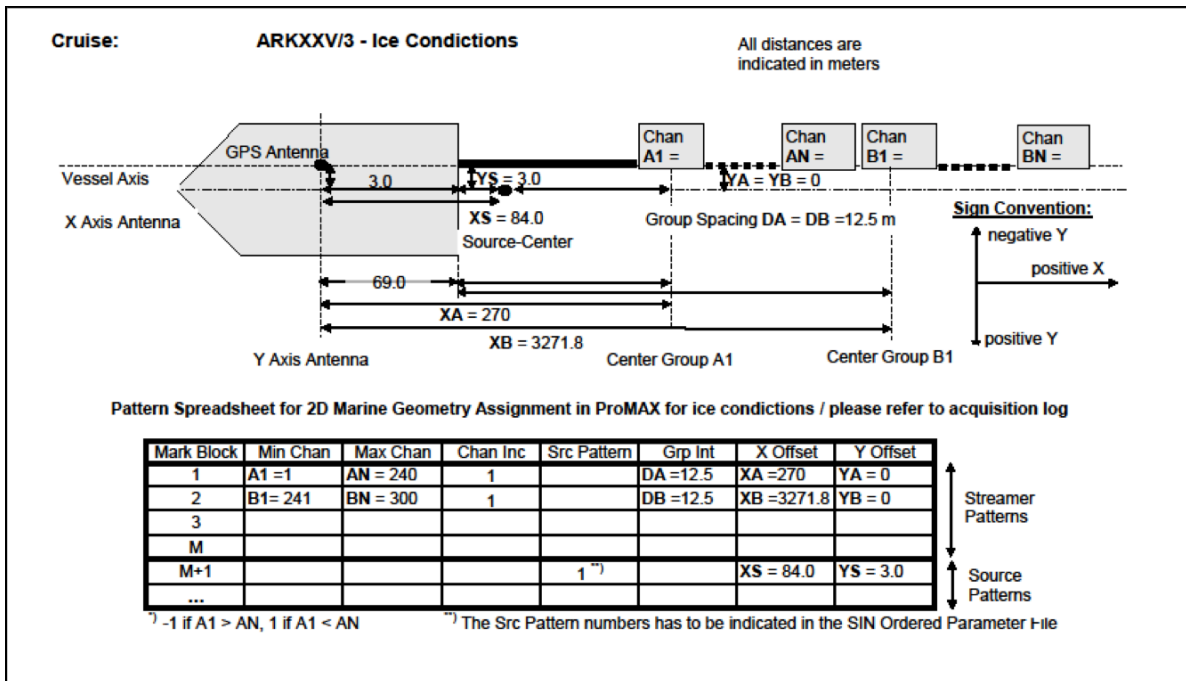


Fig. 9.15: Acquisition geometries for the seismic reflection lines including ProMAX spreadsheets for definition of streamer and source pattern for ice conditions.

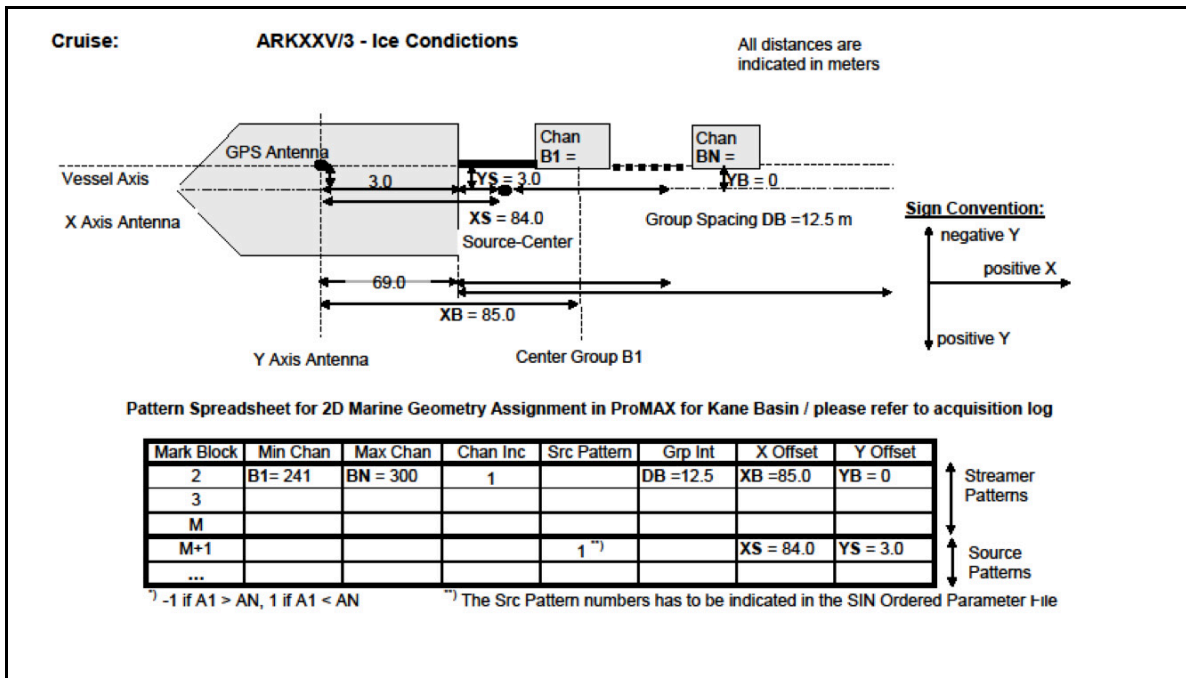


Fig. 9.16: Acquisition geometries for the seismic reflection lines including ProMAX spreadsheets for definition of streamer and source pattern for the Kane Basin.

TraceQC:

Quality control of the binning. Here two checks are undertaken:

- a) Checking the computed offsets with the offsets given in the streamer plan by comparing the values for the last hydrophone group (channel 300) and nearest hydrophone group (channel 1).
- b) Checking if the source and receiver locations (in UTM coordinates) are behind the vessel in relation to the sense of direction.

A further quality control was done by using the graphical display tools of the database application:

- c) CDP fold map (Database => View => Predefined => CDP fold map). X_COORD and Y_COORD – Axes; FOLD: Color coded and as histogram.
- d) CDP fold table (Database => View => Tabular => CDP): List of CDP Number, FOLD, X_COORD and Y_COORD.

SEG-D input from NAS and geometry application

Data were loaded from NAS hard drive using the ProMAX module SEG-D Input. The SEG-D Input module fails, if the path name to the segd files is too long. An acceptable work-around is to create a soft-link in the root directory to the segd-file directory.

The shot-ordered data consists of 300 data channels and 5 auxiliary channels sampled at 2 ms with a recording length of 13,000 ms. The auxiliary channels record data from the waterbreak hydrophone; the remaining 4 aux channels were void. With the “Display ensemble information” set to YES a summary of all imported shot is written to the log-file. This is helpful in case that there are problems during acquisition and the FFID does not resemble the correct shotpoint. In case that there are FFIDs duplicated on the records the data may be read in SOURCE order with the unwanted FFIDs excluded (e.g. 1-1249, 1251-2400).

Resampling (Resample/Desample)

The seismic data has been acquired at 2 ms sampling rate. To speed up the onboard processing, the data has been re-sampled to 4 ms applying a high-fidelity anti-alias filter.

SOD time correction (Header Statics)

The Sercel acquisition system starts registration 120 ms before triggering of the airguns occurs. This time delay has been verified on the auxiliary channel containing the signal from the waterbreak hydrophone at AUX CHAN -1 and on the direct water wave on the groups near to the source.

Geometry Apply (Inline Geometry Header Load)

With this ProMAX module, the geometry information from the database were written into the trace headers.

Finally, the *Trace Header Math* module inserted an entry for the line number header word.

The altered data was written to hard disk as new prestack data set (*Disk Data Output*).

Prestack processing (for detail of individual steps see Appendix A.5A)

Bad Trace Editing

The shot gathers were checked for bad traces. If present, these can be killed and thus been excluded from further processing. Anyway, the data recorded was of very good quality with no bad traces, which had to be deleted.

Bandpass Filter

After the examination of the interactive spectral analysis a zero phase Ormsby bandpass filter of 4-8-80-160 Hz was applied to the data.

Prestack Deconvolution

In order to reduce ringing within the dataset and to shorten the seismic wavelet, a single trace predictive deconvolution was applied. In general, the input ensemble can be a shot record, or a CDP or receiver gather. The deconvolution design gates were picked on CDP gathers.

One deconvolution design gate was specified for each location along the seismic section. The gate was picked within the uppermost part of the sediments, excluding the seafloor reflection which had to be adjusted according to the seafloor and subsurface morphology.

A single trace predictive deconvolution with an operator length of 170 to 220 ms and was applied with a prediction length of 32 ms. White noise level was 0.1. (For detail of usage see Appendix A.5A.)

Velocity analysis

Two different velocity analysis tools were applied for onboard processing. A) the classic velocity analysis with supergathers at a regular CDP interval. B) the new SeisSpace Java Constant Velocity Analysis tool using a java environment.

- A) Velocities were picked at regular intervals of 480 CDPs (equivalent to 3,000 m CDP spacing) along the lines. In case of large variations in seafloor topography and/or sub bottom structures the spacing was reduced to get an appropriate number of representative locations. Velocity analysis and QC were done in several steps.
- B) SeisSpace Java Constant Velocity Analysis tool:
 - 1. Picking of velocity analysis stations. The spacing between individual velocity stations was adjusted to the variations in seafloor morphology.
 - 2. Sorting into supergathers (each supergather was built out of 9 to 11 CDPs) and calculation of semblance values and CVS panels (*Velocity Analysis Precompute*).

3. Interactive *Velocity Analysis* using semblance velocity spectrum, animated reflection hyperbolas and constant velocity stack panels (CVS). (Fig. 9.21)
4. QC and smoothing the velocity field with *Velocity Viewer/Point Editor*.
5. Optional QC with *Volume Viewer* in interaction with *Velocity Analysis*. The *Volume Viewer* displays a poststack section with an overlay of the colour coded velocity field (RMS or interval velocity). Velocity stations and picks are shown on the section and could interact with the *Velocity Analysis*.

The various tools, namely to use QC during interactive velocity analysis, allow for careful estimation of stacking velocities. This was of special importance because of very high interval velocities right below the seafloor. The ProMAX velocity picking module included a semblance display with an interval velocity graph, a CDP supergather which could have NMO applied instantly, a series of constant velocity stack panels, and a dynamic stack panel (Fig. 9.17).

RMS stacking velocities were picked by examining the information of the semblance spectrum (left panel), supergather CDP (center, left), dynamic stack (center, right) and constant velocity stacks (right panel). For improving the signal to noise ratio, supergathers were formed by combining 11 adjacent CDP gathers, and these CDP gathers also made up the stack panels. Amplitudes were corrected roughly by using True Amplitude Recovery with manually given TAR velocity function (e.g. 0 - 1500, 9000 - 4000, 13000 - 6000).

To speed up the on screen velocity picking procedure, the velocity analysis displays were pre-computed. After velocity picking, RMS stacking velocities were viewed and QC'd on screen using the ProMAX velocity viewer module. This module was most useful for editing any unreasonable velocity picks and finally to smooth the velocity field for the further processing. Furthermore, the viewer module was used to compare the interval velocity field with a brute stack version of the line. Based on this QC subsequently the velocity field could be further adjusted during an additional velocity analysis. An example of the so estimated interval velocity field is shown in Figure 9.18.

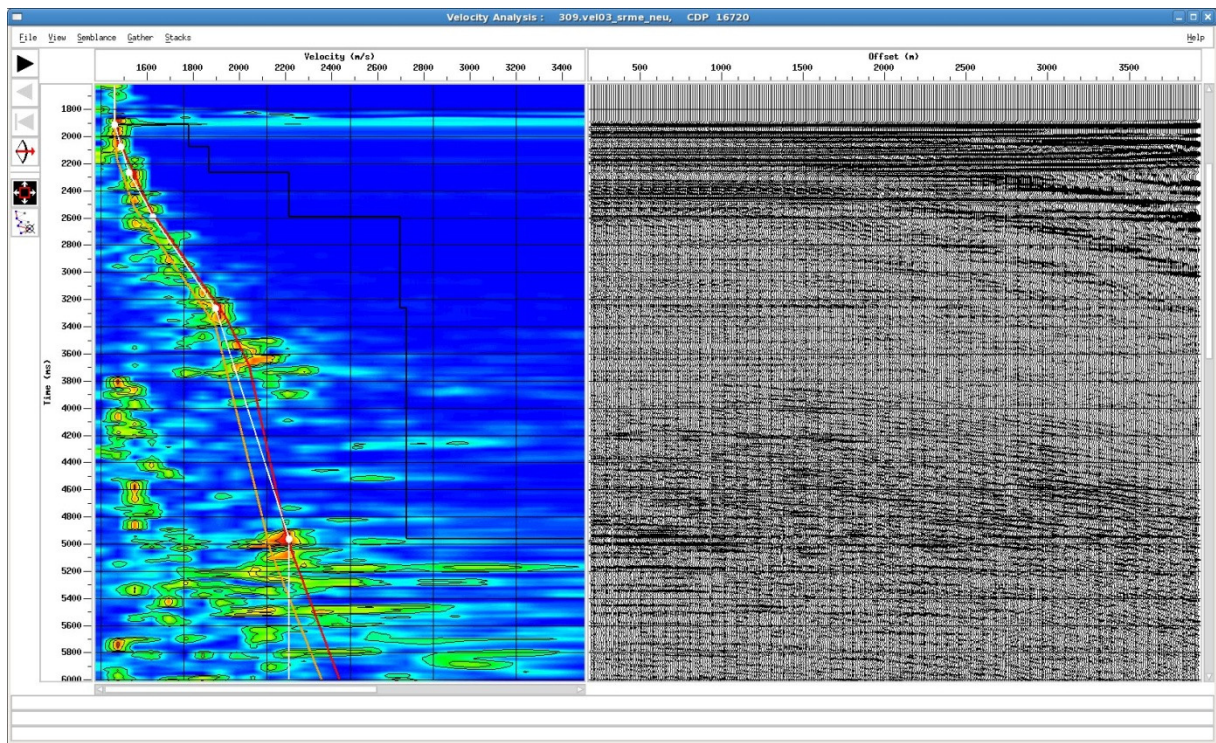


Fig. 9.17: Example of a velocity analysis done at a CDP supergather after applying srme multiple reduction. Note the prominent reflection at 5,000 ms, well below the seafloor multiple.

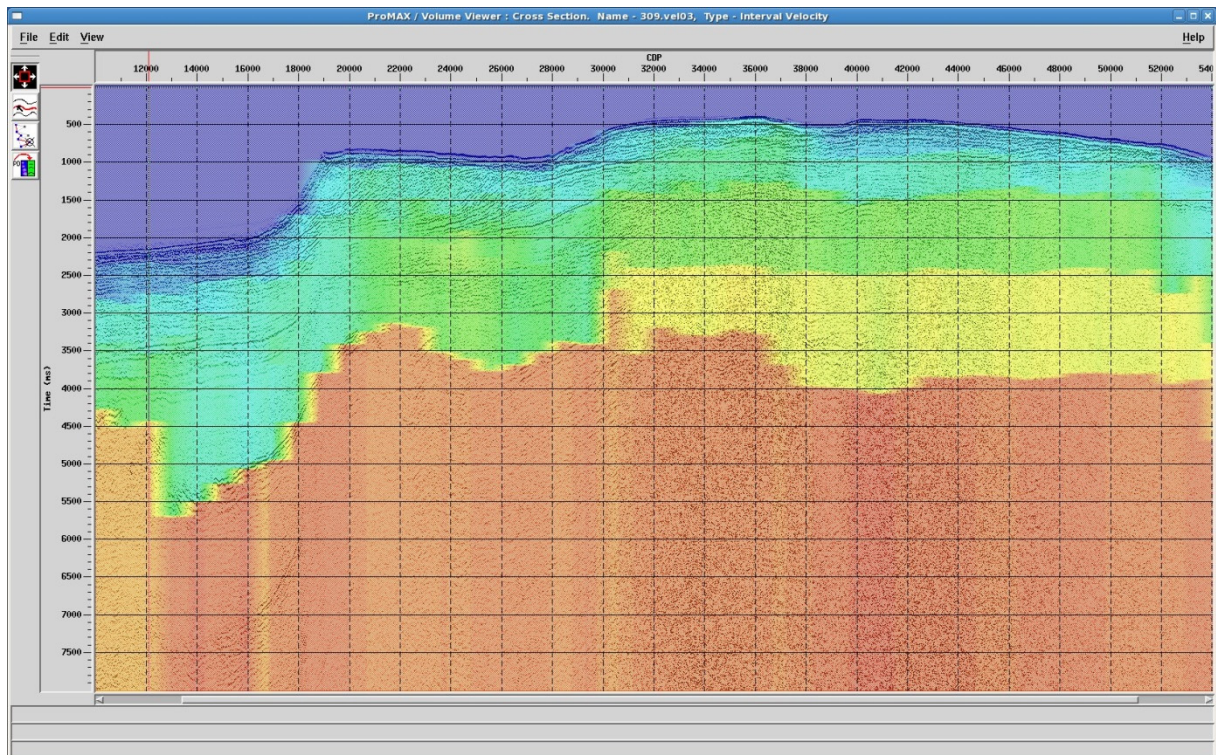


Fig. 9.18: Example of the interval velocity field based on the velocity analysis.

The Java Constant Velocity Analysis tool (Java CVS) uses the entire data set. This enables the user to analyse the velocities through the entire dataset and, thus, to pick along reflectors. The Java CVS tool consists of three windows. The first window switches between the stack of the entire data set and the velocity function (see Figures 9.19 and 9.20). The second window is subdivided into three frames. It uses a previously entered amount of traces (e.g. 200 traces) to calculate all CVS stack panels, the semblance results and the NMO corrections. The user can switch quickly through all velocities. After a reflector is imaged at a certain velocity the user can pick along the reflector. This tool allows having a good lateral velocity resolution (Fig. 9.21).

The Java CVS tool belongs to the new SeisSpace GUI that replaces the classic ProMAX GUI. SeisSpace needs to have an own reformatted data set, so the ProMAX data must be transformed (using the JavaSeis Create module). The Java CVS tool needs a lot of the computer memory to perform well. Our onboard machines with 32 GByte RAM performed not really well and we decided to increase the performance by using only 4,000 ms per trace and to resample the input data set for the velocity analysis with 8 ms. With these limitations we had an acceptable performance. Further details are documented in the online manual.



Fig. 9.19: Java CVS tool – The bottom window shows the stack of the entire section with all velocity picks. Note the lateral coherency of picks of a certain reflector. The blue lines indicate the cdp window that is active for doing the velocity analysis. The top window shows the semblance result of the selected time slice.

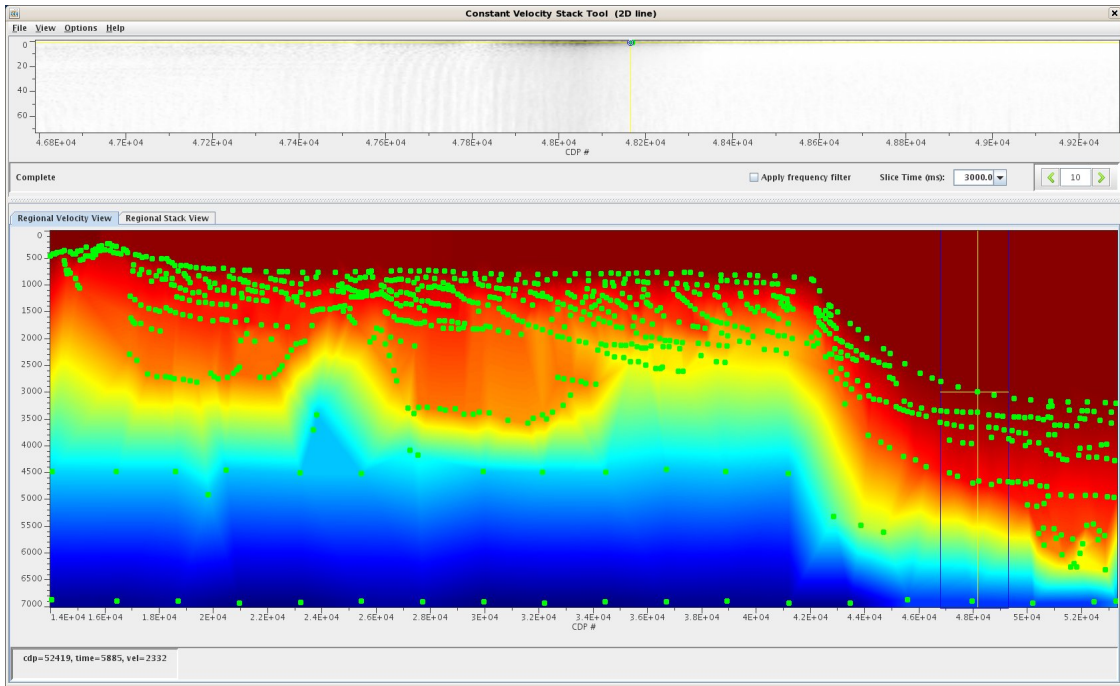


Fig. 9.20: Java CVS tool: The bottom window can switch between the stack view and the color coded velocity view. This view enables a good QC and unreasonable or conspicuous velocity picks can be quickly checked out.

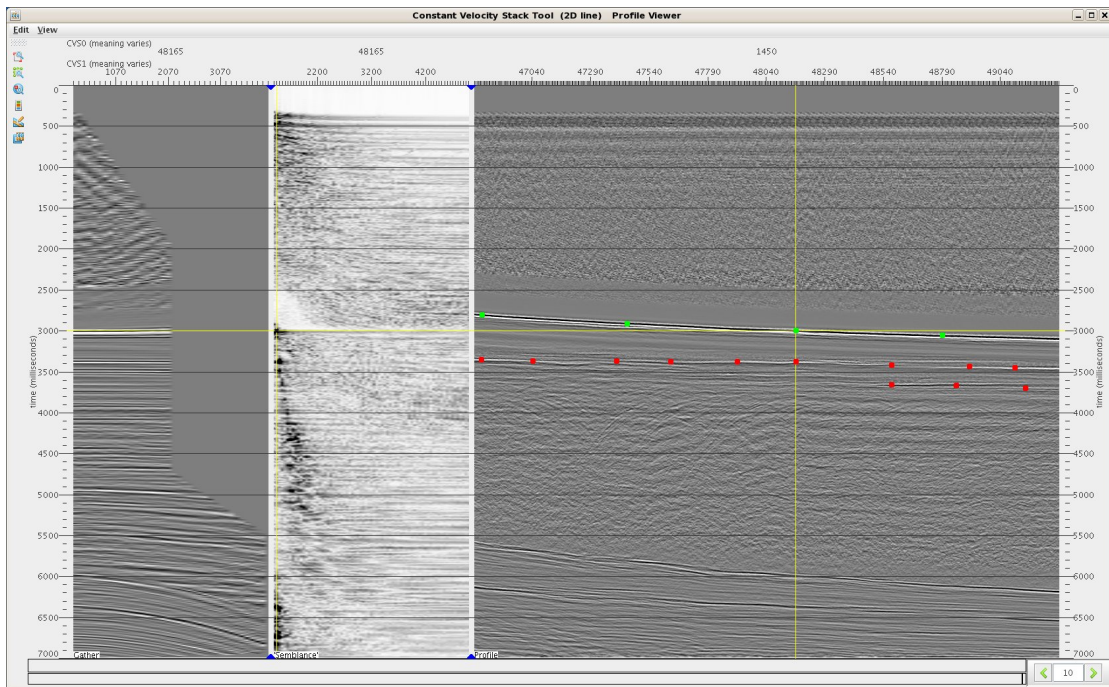


Fig. 9.21: Java CVS tool: This window is subdivided into three frames. The right hand frame shows this part of the entire dataset that is within the blue lines in Figs. 9.19 and 9.20. It shows altogether 200 traces with an increment of 5. Thus, the cdp window spans over a distance of 1,000 cdp's. The yellow cross shows the active position where to do a velocity pick. The center frame shows the semblance for the active cdp and the left hand frame shows the nmo animated cdp for the specific velocity.

Comparison between SeisSpace CVS and ProMAX Interactive Velocity Analysis:

The ProMAX Interactive Velocity Analysis (IVA) is very precise to elaborate a velocity depth function at a certain predefined CDP (or supergather). However, the lateral coherency of each picked event is not clear and the user is probably misled by noise, multiple energy or other artefacts.

The SeisSpace CVS tool has its strength by showing the lateral coherency of events at certain rms velocities and calculating a preliminary stack using the actual picked velocity function. Thus, it is easy to check if the picked velocities are reasonable or if events are caused by noise or artefacts.

Multiple suppression

The suppression or reduction of multiple energy was done mainly with *Surface Related Multiple Estimation (SRME)* techniques. The ProMAX implemented module is named *Surface-related wave equation multiple rejection (MASWEMR)*. It claims to be an improvement to the classic SRME technique, as synthetic shot gathers were modelled, using the picked seafloor reflection and the sound velocity within the water layer. In a second work flow a *Radon Velocity Filter* was applied on selected seismic lines.

Surface-related wave equation multiple rejection (ProMAX module MASWEMR)

On all lines Surface-Related Wave Equation Multiple Rejection (MASWEMR) was applied (see Figure 9.22). This process generates a synthetic shot for each receiver location. Time shifts and amplitude gains are applied to these shot-gathers to correct for the 2D structure of the sub-surface. Finally, the estimated multiples are shaped to the input data on a gate by gate and panel by panel basis. The workflow contains several steps:

- Horizon picking: pick water bottom on CDP-sorted brute stack.
- Extracting the amplitude of the water bottom by using Sequence Attribute Analysis.
- Create split spreads (SPLITZERO): the typical marine end-on spread with a nonzero near offset has to be transformed to a split spread. A zero offset trace is also extrapolated. The input has to be ungained data sorted by CDP:OFFSET.

MASWEMR: the output from SPLITZERO (sorted by SIN:OFFSET) serves as input for this tool. A top mute for the direct arrival has to be applied first.

Radon Velocity Filter

The *Radon Velocity Filter* was applied to CDP gathers after NMO correction. Since multiple reflections have an approximately parabolic moveout after NMO they can be imaged in the tau-P domain. The filter will reject all data within a certain velocity bandwidth around the picked velocities (-15%, +20%). The other data will be treated as multiple energy and re-transformed into x-t domain and subtracted from the input CDP gather. Because this technique models and subtracts multiple energy, the near offset traces should be attenuated in the same manner as far offsets. In general the Radon Velocity Filter works well. However, in areas with high velocity gradients the

Radon Velocity Filter produces high frequency noise, most likely because of the NMO stretch mute. Thus, the Radon Velocity Filter was applied only on selected lines (see Table 9.1).

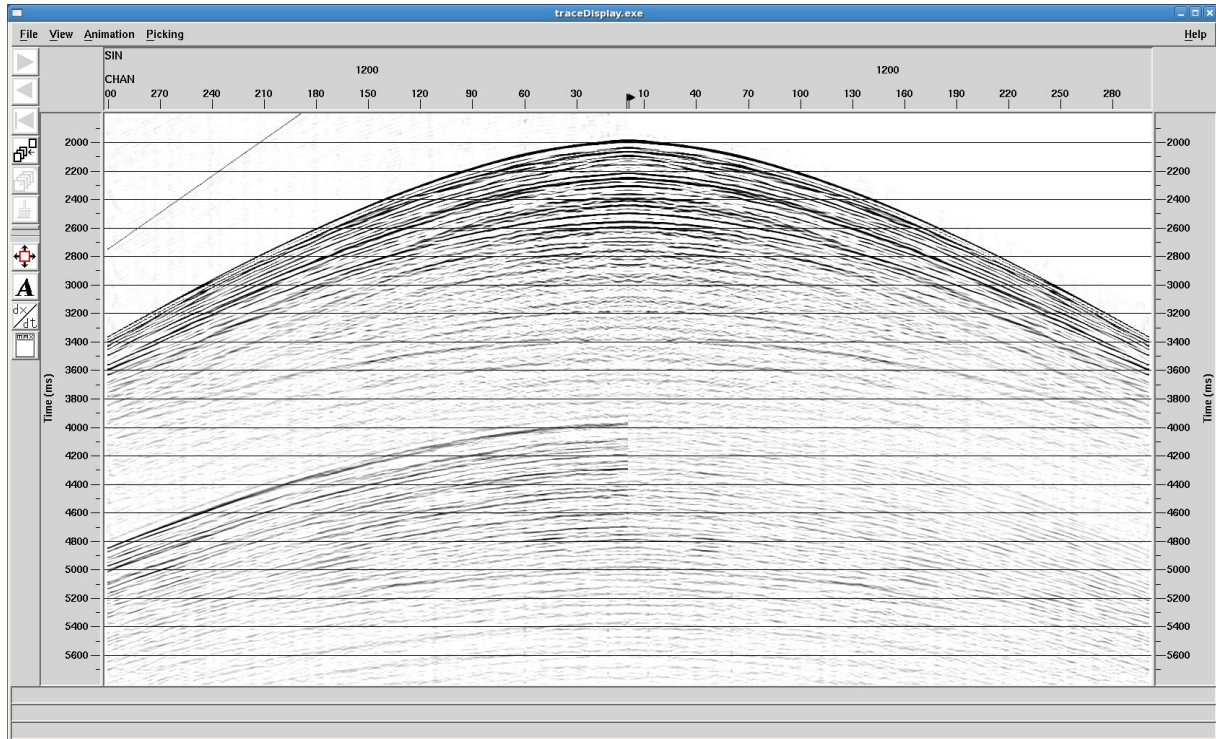


Fig. 9.22: Example from line BGR10-309, shot number 1200. The left hand side shows the raw data with multiple arrivals starting at 4,000 ms. The right hand side shows the same shot after application of MASWEMR.

Stacking

Before NMO correction of the CDP gathers a true amplitude recovery (TAR) has been applied using the smoothed RMS stacking velocity field to compensate for spherical divergence ($1/(time*vel^2)$). A radon velocity filter as described above was applied to suppress multiples on selected seismic lines prior to stacking. After stacking (mean stack) the traces in the CDP gathers, the stacked sections were written to disk.

Migration

All processed data are Kirchhoff time migrated. The migration velocities were calculated during the velocity analysis and had to be adjusted carefully sometimes. The stacking velocities (rms velocities) were scaled by about 90% for Kirchhoff migration. Migration aperture was set to 6,000 m, the maximum migration dip was 30°.

An example for signal enhancement by using the above described processing flows is shown in Figure 9.23.

Tab. 9.1: Summary of all MCS lines

MCS line parameter of the project ARK XXV/3												
Line No.	# of	first shot	Length				lat/lon		streamer	streamer	Kirchhoff	
	shots	on line	(km)	min cdp	max cdp	Δ cdp (m)	begin	lat/lon end	depth (m)	fixing	SRME	Migration
BGR10-302	3410	222	124	9686	29857	6.25	74° 39.927 N 66° 13.724 W	74° 03.265 N 69° 40.683 W	12	center	x	x
BGR10-302a	5510	32	204	9686	42742	6.25	75° 33.408 N 60° 24.886 W	74° 35.378 N 66° 28.307 W	12	star board, 490 center	x	x
BGR10-303a	7122	17:33h	267	9686	52905	6.25	74° 53.378 N 69° 30.603 W	77° 13.287 N 71° 56.615 W	18	star board	x	x
BGR10-305	4704		172	9686	37607	6.25	74° 06.069 N 61° 04.645 W	74° 37.243 N 66° 29.086 W	12	center	x	x
BGR10-305a	2960		107	8933	26536	6.25	74° 33.912 N 66° 15.788 W	74° 55.656 N 69° 40.163 W			x	x
BGR10-306	4686		172	9686	37660	6.25	71° 20.481 N 61° 58.144 W	72° 42.773 N 64° 18.837 W			x	x
BGR10-306a	5290	52	194	9686	41091	6.25	72° 39.980 N 64° 17.552 W	74° 07.529 N 60° 57.440 W	12	center	x	x
BGR10-307	5050	164	186	9686	39948	6.25	74° 11.573 N 69° 09.547 W	73° 37.638 N 63° 27.485 W	12	center	x	x
BGR10-307a	5105		187	9686	40090	6.25	73° 37.147 N 63° 22.614 W	73° 03.037 N 57° 50.361 W	12	center	x	x
BGR10-308	1723	170	63	8725	19160	6.25	73° 05.886 N 57° 48.260 W	72° 39.457 N 59° 01.301 W	12	center	x	x
BGR10-308a	3616	55	133	9414	31082	6.25	72° 43.341 N 58° 49.022 W	71° 46.952 N 61° 14.930 W	12	star board	x	x
BGR10-309	7662	140	285	9686	55698	6.25	71° 45.888 N 61° 10.234 W	74° 17.045 N 59° 35.537 W	12	star board	x	x
BGR10-110	1493		56	9686	18921	6.25	74° 18.082 N 59° 32.354 W	74° 13.127 N 57° 43.248 W	12	star board	x	x
BGR10-111	7425	138	274	8904	53305	6.25	74° 14.381 N 57° 42.333 W	73° 12.914 N 65° 44.009 W	12	star board	x	x
BGR10-112	3529	227	130	8612	29666	6.25	73° 10.024 N 65° 33.074 W	73° 56.794 N 68° 36.051 W	12	star board	x	x
BGR10-113	3098		115	9686	28148	6.25	73° 56.980 N 68° 36.163 W	74° 56.950 N 69° 33.918 W	12	star board	x	x
BGR10-114	6170	20:58h	228	9686	46610	6.25	74° 49.388 N 72° 23.909 W	76° 47.065 N 74° 49.834 W	18	star board	x	x
BGR10-115	2333	6180	83	9686	23412	6.25	76° 47.256 N 74° 49.774 W	77° 32.165 N 74° 32.185 W	18	star board	x	x
BGR10-116	2259	ca. 184	80	9924	22898	6.25	79° 21.296 N 66° 53.404 W	79° 58.266 N 68° 59.795 W	12	center, no lead-in	x	x
BGR10-117	3692	105	135	9867	31701	6.25	80° 09.613 N 68° 26.080 W	78° 59.453 N 70° 16.022 W	12	center, no lead-in	x	x
BGR10-118	537		20	9464	13009	6.25	76° 20.793 N 74° 16.191 W	76° 20.349 N 73° 30.116 W	18	star board	x	x
BGR10-318a	2757		104	9686	26645	6.25	76° 20.429 N 73° 36.604 W	76° 17.678 N 69° 40.470 W	18	star board	x	x
BGR10-319	3456	75	129	9686	30745	6.25	76° 19.006 N 69° 44.252 W	75° 44.070 N 73° 54.222 W	18	star board	x	x
BGR10-320	5177		191	9215	40204	6.25	75° 45.025 N 73° 47.039 W	75° 51.936 N 66° 47.418 W	18; 25	star board	x	x
BGR10-321	4991		184	9686	39626	6.25	75° 46.488 N 67° 06.247 W	74° 37.711 N 71° 48.319 W	18	star board	x	x
BGR10-322	4666	59	172			6.25	71° 09.586 N 59° 21.339 W	70° 41.190 N 54° 50.381 W	18 + several test depths	star board		

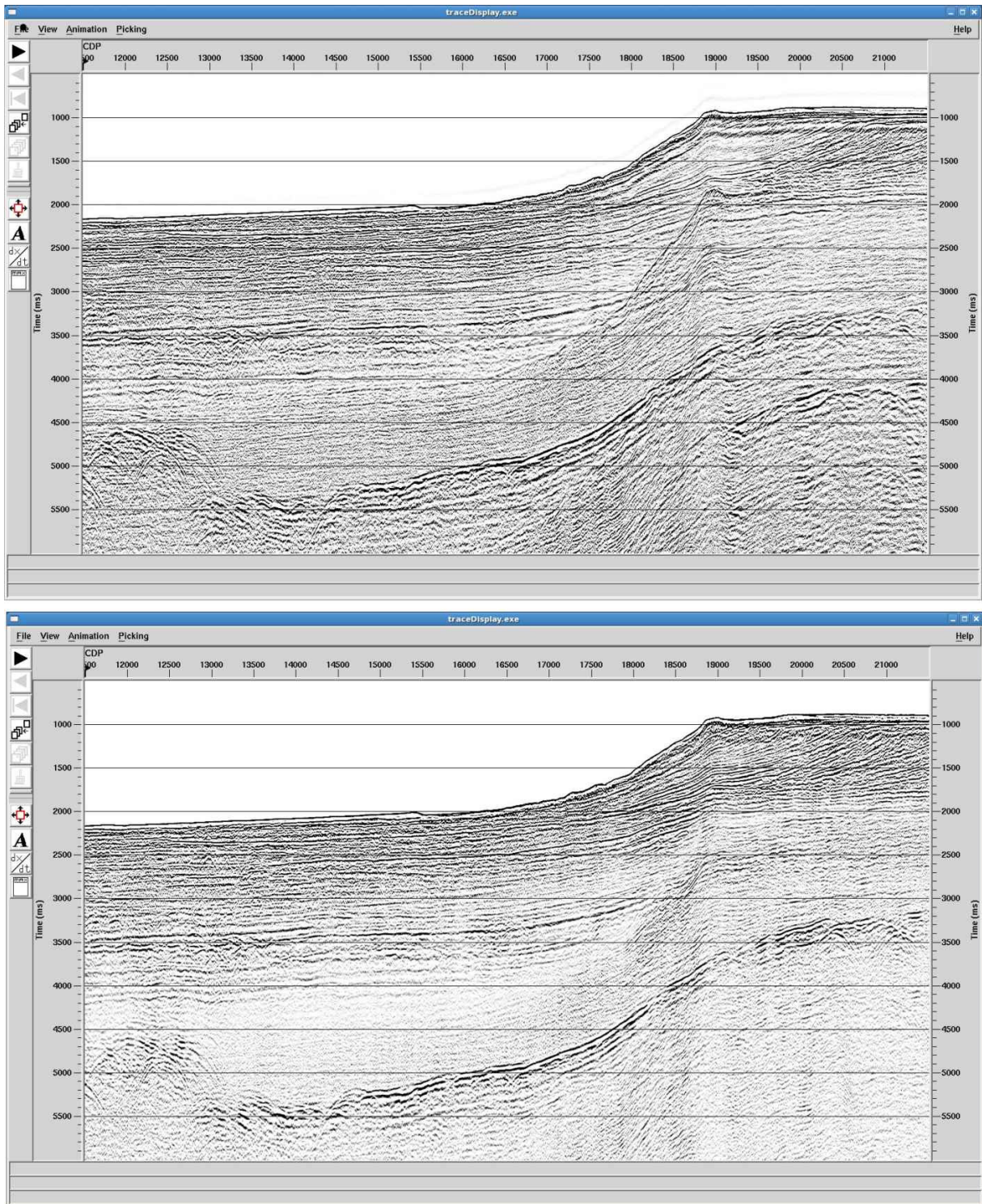


Fig. 9.23: Comparison between a raw stack section and the section after applying the above introduced processing sequence. Note the good imaging of crustal layers and high resolution of sedimentary layers.

9.5 Preliminary results of MCS data

The quality of the MCS data is good. The unusual seismic acquisition setup with the source array very close to the stern of the vessel and six guns in very close distance to each other reduced somehow the quality of the seismic signal. In addition the presence of another seismic vessel led to a contamination of the MCS data with the source energy of the other vessel. This interference downgraded the MCS data in distinct time periods.

9.5.1 Frequency spectrum and comparison to MCS data of the previous survey of 2008

The frequency spectrum of five shots with the AWI source array of line BGR10-309 recorded in a streamer depth of 12 m is displayed in Figure 9.24. The dominant frequency is around 28 - 30Hz. This part of the line was also shot in 2008 during the MSM09 *Maria S. Merian* Cruise. Line BGR08-304 covers the same area. Figure 9.25 displays the frequency spectrum of five shots with the BGR source array of line BGR08-304. The processed stacked and migrated seismic sections can be compared with Figure 9.26. The sediments are higher resolved within line BGR08-304. The low frequency seismic section of line BG10-309 does not provide additional information, especially deeper reflections. In contrast, the higher frequency seismic section of line BGR08-304 proves the same seismic penetration imaging of the deep reflections and in addition the higher resolved sedimentary pattern on top of the basement.

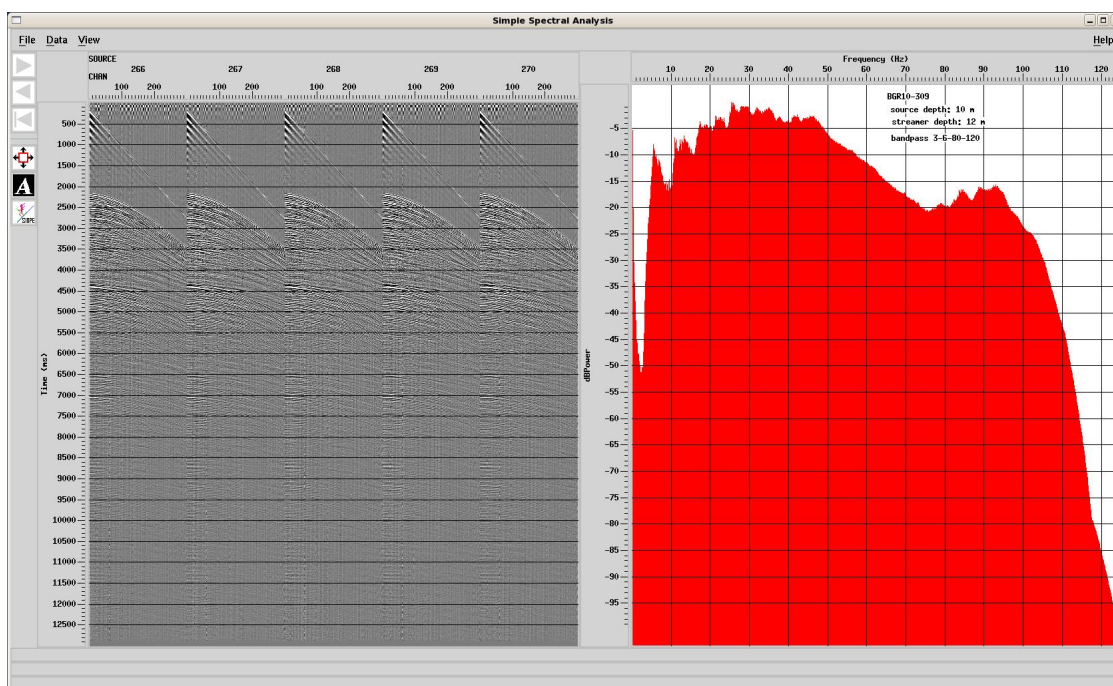


Fig. 9.24: Frequency spectrum of five shots of line BGR10-309 with the AWI source array. The dominant frequency is around 28-30Hz.

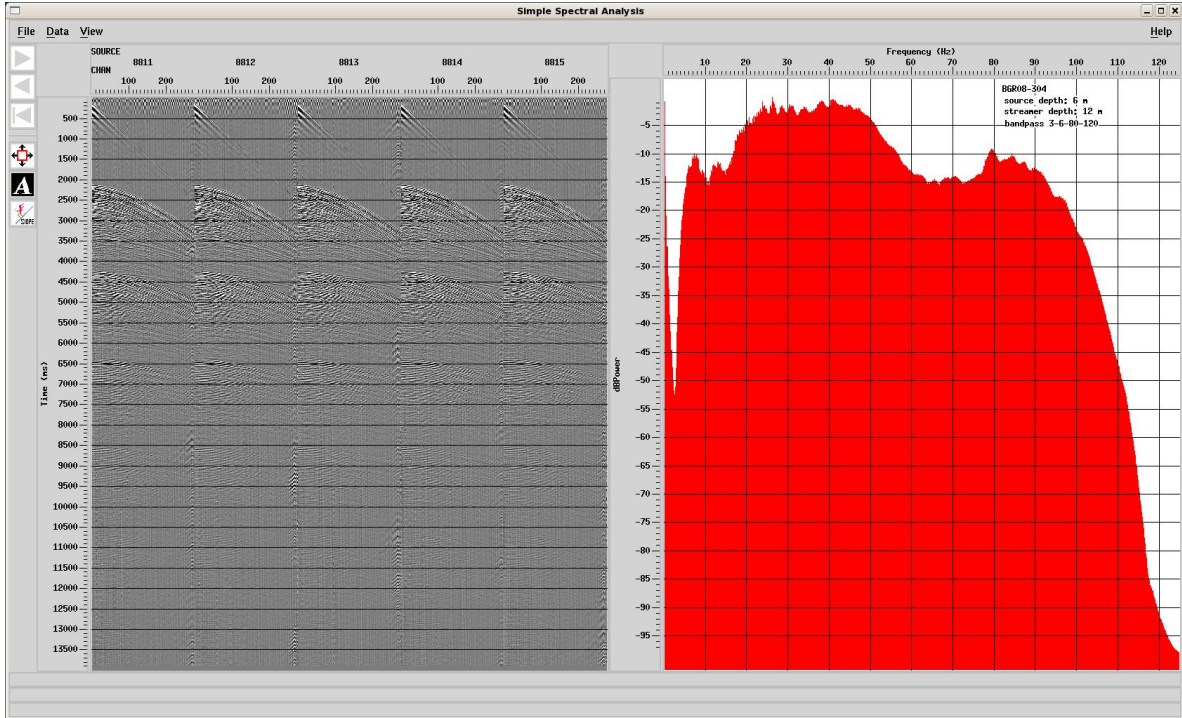


Fig. 9.25: Frequency spectrum of five shots of line BGR08-304 with the BGR source array. The dominant frequency is around 40-42Hz.

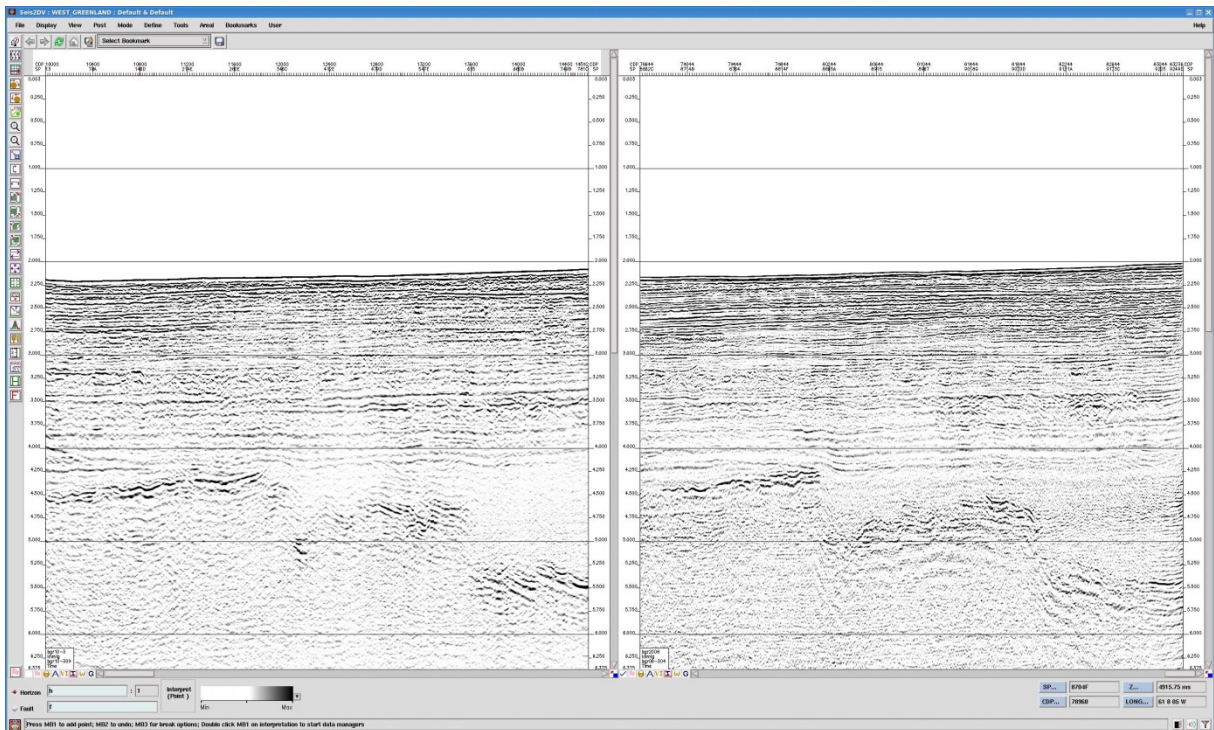


Fig. 9.26: Comparison of the migrated seismic sections of BGR10-309 on the left hand side and BGR08-304 on the right hand side.

9.5.2 The influence of the streamer towing depth on the seismic data

The streamer towing depth has a direct influence on the recorded frequency content of the seismic data. Frequencies with wavelength of $\lambda=4d$ (λ : wavelength and d : streamer depth) will be amplified, because of the negative reflection coefficient of the sea surface for upcoming waves.

On line BGR10-322 different streamer depths were tested in order to analyse the frequency content. The general depth was 18 m. This was altered for 200 shots to 25, 12 and 8 m. The amplified frequencies are as follows (with: $v_w=1450\text{m/s}$):

$$d_1=18\text{m} ; f_1=v_w/4d_1 \approx 20 \text{ Hz}$$

$$d_2=25\text{m} ; f_2=v_w/4d_2 \approx 15 \text{ Hz}$$

$$d_3=12\text{m} ; f_3=v_w/4d_3 \approx 30 \text{ Hz}$$

$$d_4= 8\text{m} ; f_4=v_w/4d_4 \approx 45 \text{ Hz}$$

Figure 9.27 shows the power spectra of five shots recorded at the depths d_1 to d_4 . There is a good correlation between the calculated amplified frequencies with the measured frequencies. The resulting shape of the power spectrum is also dependent on the frequency spectrum of the seismic source array. The chosen streamer depth is crucial to meet the scientific tasks for the seismic survey. The streamer depth of 25 m shows a significant drop of the high frequency energy. This will result in a limited resolution of thin sediment layers. The depths of 18 and 12 m show a good combination of high frequent energy and low frequent energy. With 12 m streamer depth a higher resolved seismic section should be possible to image, with 18 m the higher energy at low frequencies should enable to record deeper penetrated seismic energy.

9.5.3 Bias by another seismic vessel

Since another seismic vessel (*M/V Bergen Surveyor* of CGG Veritas) operated in the survey area some of our MCS data is biased by the shots of the *M/V Bergen Surveyor*. The shots coming from the *M/V Bergen Surveyor* are clearly visible as linear events within the shot records (see Figure 9.28). For the standard processing the noise did not significantly influence the preliminary result, however, it needs further investigation if it probably influences prestack processing techniques (e.g. radon transformation, srme, prestack migration). As the dip angle of the linear events depends on our position relative the *M/V Bergen Surveyor* a simple fk -dip filter is not suitable to suppress the bias.

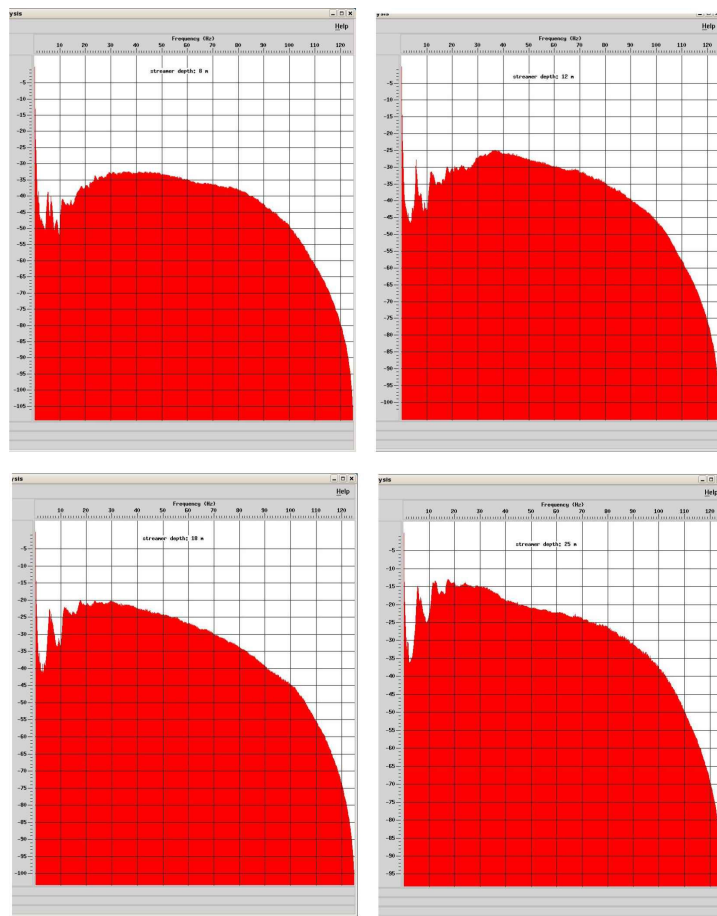


Fig. 9.27: Frequency power spectrum of 5 shots at different streamer towing depths. Upper left frame: Streamer depth of 8 m; Upper right frame: Streamer depth of 12 m; Lower left frame: Streamer depth of 18 m; Lower right frame: Streamer depth of 25 m.

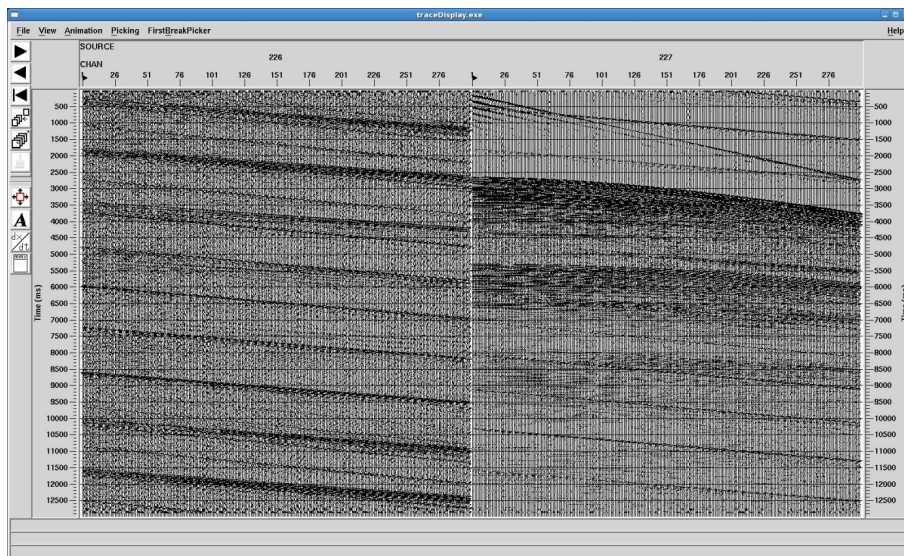


Fig. 9.28: Two records, without (left hand side) and with own shot (right hand side). Note the regular linear noise, coming from the M/V Bergen Surveyor.

9.6 Processing and preliminary results of wide-angle sonobuoy data

During ARK-XXV/3, 29 sonobuoys were deployed (see Appendix A.11 for details of each station). 26 stations recorded refracted seismic energy (see Figure 9.29 and Figure 9.30 for the spatial distribution of sonobuoys and recorded shots). Some stations stopped the transmission of signals within the first hour after deployment. A possible explanation is a collision of the buoy with floating ice.

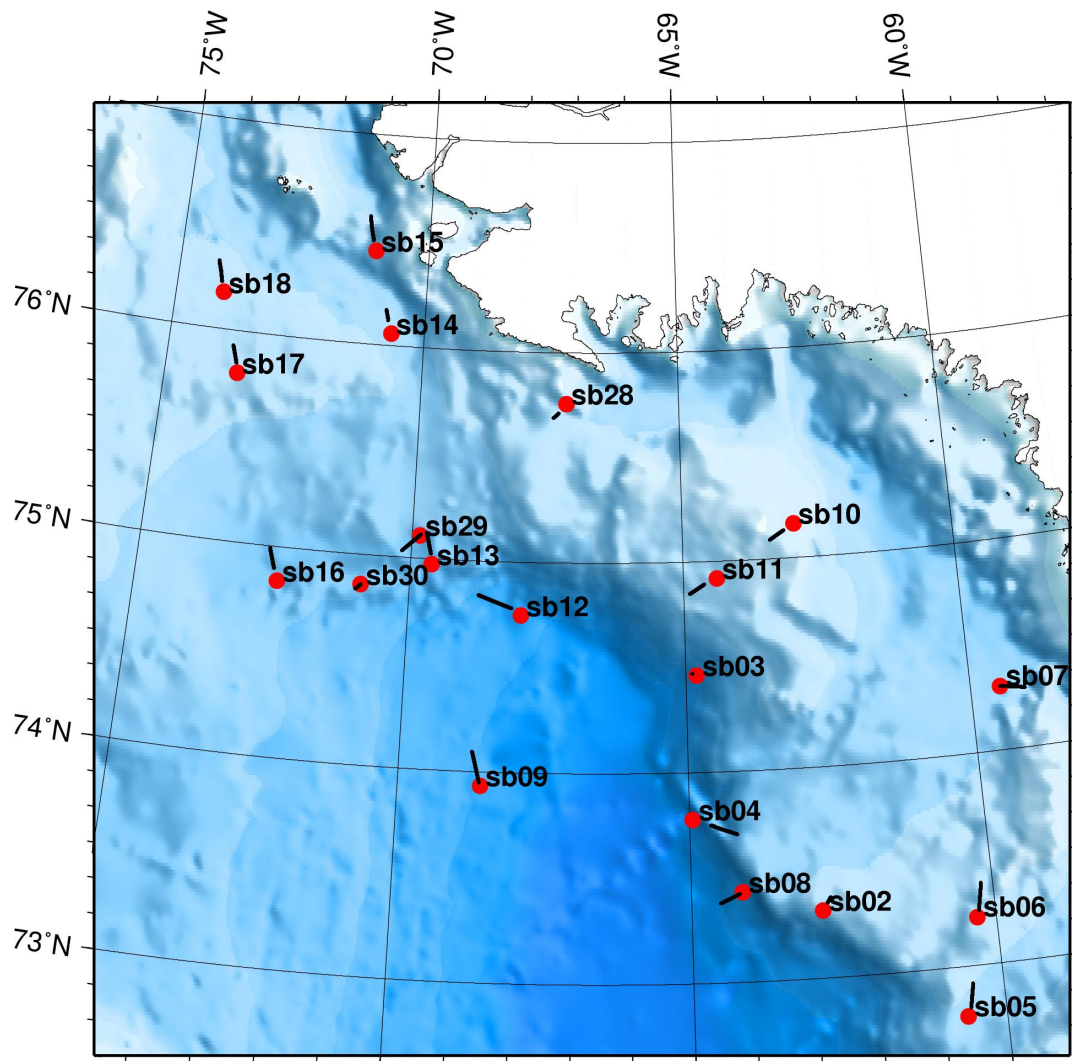


Fig. 9.29: Location map of the northern Baffin Bay. Red dots mark the positions of sonobuoys, black lines show the range of seismic shots with identified refracted arrivals at the station.

We deployed 16 sonobuoys with helicopter support at around 5 km behind the ship to avoid a collision of the buoy with the seismic streamer. In the Kane Basin, all sonobuoys were deployed directly from the ship because we used a short (600 m) streamer. Stations 29 and 30 were also deployed directly from the ship during BGR10-321. Both stations showed no problems due to the towed streamer.

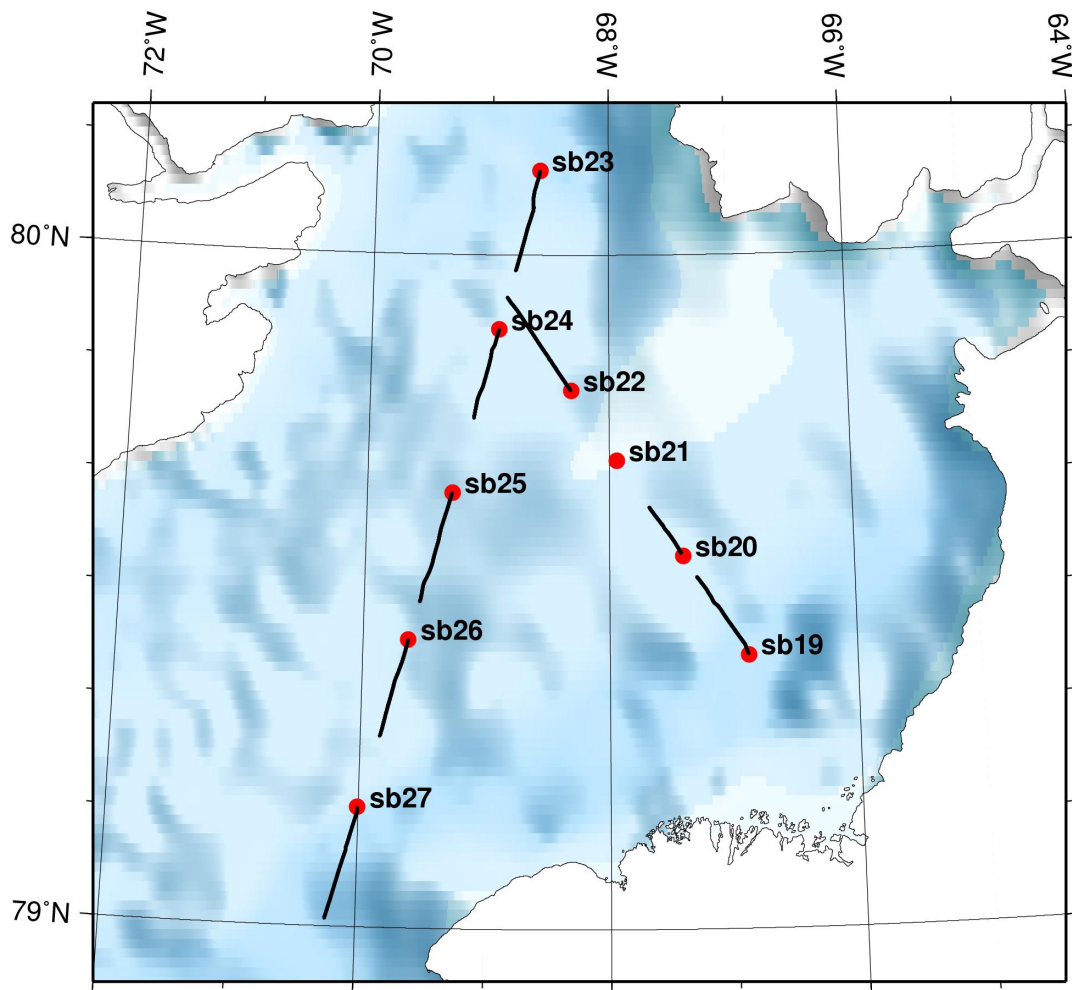


Fig. 9.30: Location map of the Kane Basin. Red dots mark the positions of sonobuoys, black lines show the range of seismic shots with identified refracted arrivals at the station.

The recorded data was converted to seg-y using the programme Send2X. Offsets for each shot to the sonobuoy were calculated with the assumption that the buoy stayed at the deployment position. During further processing, the drift of the station will be taken into account by analysing the arrival of the direct wave. To allow quality control, all stations were plotted with a reduced travel time and together with the bathymetry along the profile. An example of a seismic section is shown in Figure 9.31. At 1 sec zero offset two way travel time, the reflection hyperbola from the sea floor can be seen. The direct wave shows up as a straight line. Refracted waves arrive between 1.2 und 2.0 sec at offsets between 2 and 12 km.

Arrival times of refracted waves were picked at the seismic sections. Analysis of the slope of the travel time curves gave first information on the velocities of the different layers in the sub-surface. In a second step, we used REFLEXW to create a 1 D velocity depth model. The thickness and the velocity of each layer was adjusted manually until the measured travel times fitted to the calculated times based on the model. The result for SB 29 is shown in Figure 9.32. This information will help to make a depth migration of the MCS data more reliable. Furthermore, the velocity information will help to better interpret the sedimentary layers.

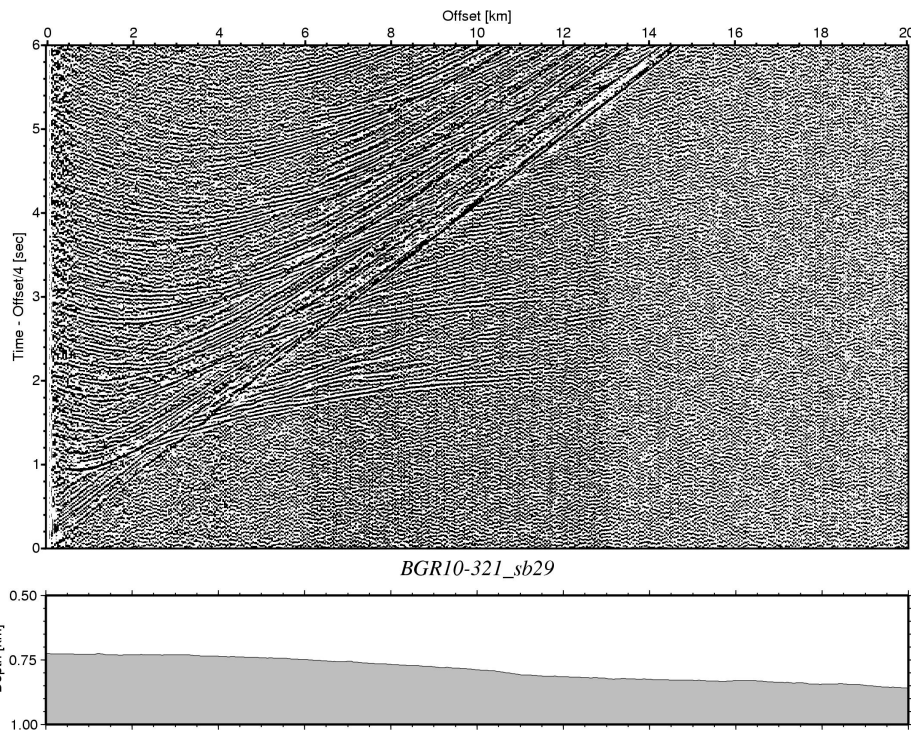


Fig. 9.31: Seismic section from Sonobuoy 29, located on profile BGR10-321. Refracted arrivals can be identified between 1.2 and 2.0 sec and up to offsets of 12 km. The lower panel shows the bathymetry along the profile.

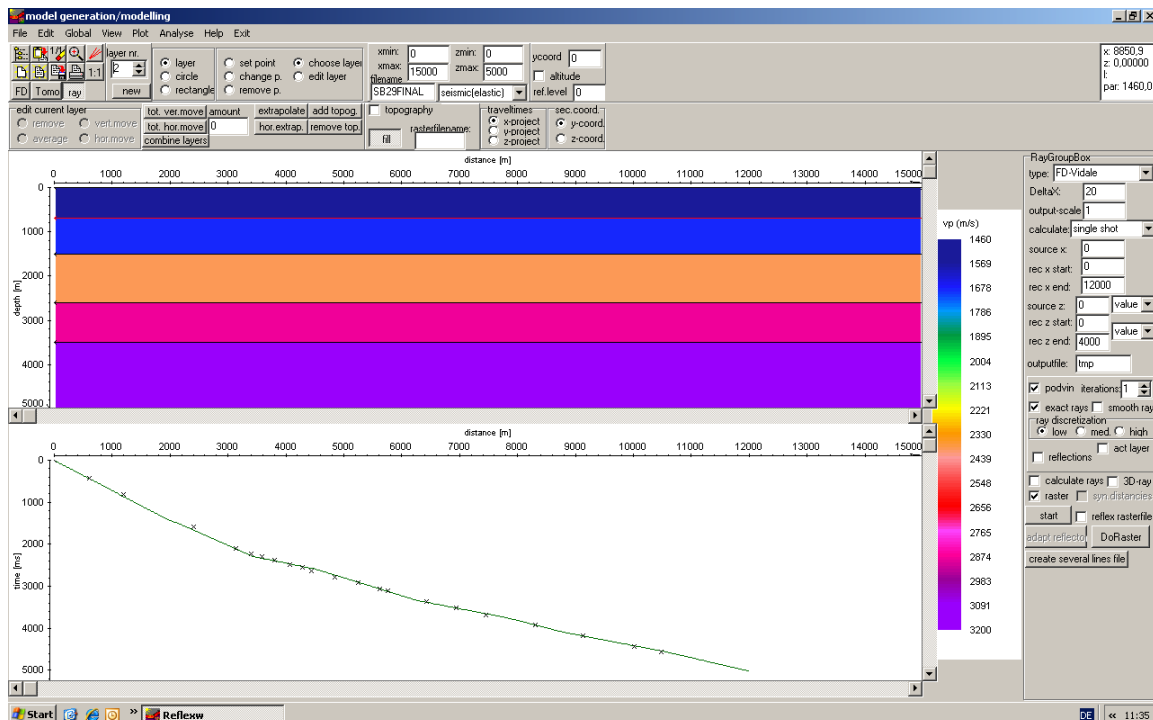


Fig. 9.32: Resulting velocity depth model for SB 29. The upper panel shows the velocity distribution with 4 sedimentary layers. The velocities range between 1700 and 3200 m/s. The lower box shows the picked travel times (black crosses) and the resulting travel times from the model (green line).

9.7 Processing of refraction/wide-angle OBS data and landstations

To detect possible problems with the OBS during the cruise, especially before a second deployment, the hydrophone and seismometer data was processed in the following steps:

- compilation of shot tables and the OBS deployment locations
- conversion from raw data to SEND2X intermediate data
- cutting and converting the intermediate data format into SEG-Y format according to the shot tables
- inserting shot offsets to the trace headers
- creating plots with the software ZP
- checking the continuous MiniSEED traces with PQL viewer
- data archiving

Shot tables, OBS deployment and recovery locations

Shot tables were compiled by the BGR team that was operating the air guns during the cruise. The files (bgr10-3r*.sp) contain the name of the profile, shot number, year, month, day, hour, minute, second, millisecond, latitude, longitude, and water depth in m. To archive the profiles in both the AWI and BGR database, each refraction seismic line has two names: AWI-20100200 = BGR10-3r2, AWI-20100300 = BGR-3R3, AWI-20100400 = BGR10-3r4, and AWI-20100450 = BGR10-3r1. Airgun maintenance loops during shooting were not deleted but numbered consecutively if a new shot file was started within the loop.

For further processing it has to be taken into account, that the BGR shot tables are not corrected for the offset between the air gun array and the reference point of the GPS positioning. The air gun array is 84 m behind the reference point of the vessel and not shifted to either side (see chapter 9.4).

The water depth in the BGR shot tables was extracted from the center beam of the hydrosweep system, which was operated by the bathymetry group.

Deployment and relocalization positions of the OBS were extracted from the *Polarstern* station book, which is kept by the bridge and logs all actions on deck. A table with deployment positions can be found in the appendices.

Conversion from raw data to MiniSEED and SEG-Y data

The data was directly downloaded from the recorder to a laptop computer via a FireWire interface connecting pressure housing and the computer. After downloading the raw data with the “mcs-copy” command from the SEND2X software package (from SEND GmbH), it had been converted into the intermediate SEND2X data format using “mcs-read”. The SEND2X format was then converted into continuous 24 hours MiniSEED data files to check if levelling and release operations were performed correctly, and to search for natural seismicity. After converting the UKOOA files into shotfiles, a SEG-Y file for each sensor component including the demultiplexed records of each airgun shot from the refraction line was produced using the “seg-ywrite” command from the SEND2X package. The software also linearly corrects for the drift of the OBS clock. Name convention of the SEG-Y files is as follows:

060744.H.00.00.2010.226.19.59.08.segy
060744.X.00.00.2010.226.19.59.08.segy
060744.Y.00.00.2010.226.19.59.08.segy
060744.Z.00.00.2010.226.19.59.08.segy

H indicates the hydrophone, X, Y the horizontal and Z the vertical component of the seismometer. Besides the recorder's serial number, year, Julian day and start time are included in the file name.

Writing shot offsets to the trace headers

The cut SEG-Y-files were transferred to a SUN workstation for further processing. A script was used to calculate the shot offsets from the shot table coordinates to the deployment position of each OBS. These lists were written to the trace headers with a Seismic Unix script and the resulting files 300st001_deploy_H.segy, where 300 is the profile number and 001 the station number. For further processing the data still needs to be re-localized. The offsets used here are only used for having a general idea of the data quality.

Creating plots with the software “zp”

The segy files with the offsets written to the trace headers were displayed with the interactive picking software "zp". The routine "zp1" reads in the SEG-Y data and creates the files "filename".head and "filename".tabl, the input files needed for the displaying part of the software. To view the data, a parameter file "zp.par" is needed in the same folder, used for the .head and .tabl files. The routine "zp2" plots the traces in an X-window and postscript plots can be created. For each station the hydrophone or Z-component plot was printed out for fast quality control. Within the zp-window the farthest offsets to both sides to which a refracted or reflected signal was detectable was noted.

Checking the continuous traces with PQL viewer

The levelling and release operations during an OBS deployment are very crucial for good data retrieval and a successful recovery of the instrument. The easiest way to proof these operations is to look at the continuous data stream. Another reason to obtain continuous data is to search the data for natural seismicity and marine mammal signals. We used continuous MiniSEED data and checked them by using the PQL viewer, a programme distributed with the PASSCAL earthquake analyzing software from USGS.

Data quality

Most of the 91 OBS deployed during ARK-XXV/3 operated fine and all four components showed data (Fig. 9.33). Two stations did not record any useful data due to a leakage in the pressure cylinder and a hard crash of the OBS during deployment or settling on the ocean floor, respectively. 21 stations had at least one seismometer component that did not work properly. One seismometer was damaged from the beginning. This was not recognized immediately, so it was deployed a second time.

9 Seismics

The five 120 sec prototype seismometers are not ready yet for routine work, they failed on 5 deployments completely, on 3 partly. Only one deployment was completely successful. At 3 stations a leakage of the seismometer connector is most likely the reason for a complete drop-out of the seismometers. In 7 cases one, in one case two seismometer components stuck due to a mechanical problem that is still not completely solved.

Some of the hydrophone records show some instability which results in strong long-period ringing or noise bursts of the signal. In most cases the OBS yielded very good data with long offsets up to 160 km on the first profiles (BGR10-3r2 / AWI-20100200 and BGR10-3r3 / AWI-20100300). The southernmost profiles (BGR10-3r1 / AWI-20100450 and BGR10-3r4 / AWI-20100400) had smaller offsets due to different geological regimes.

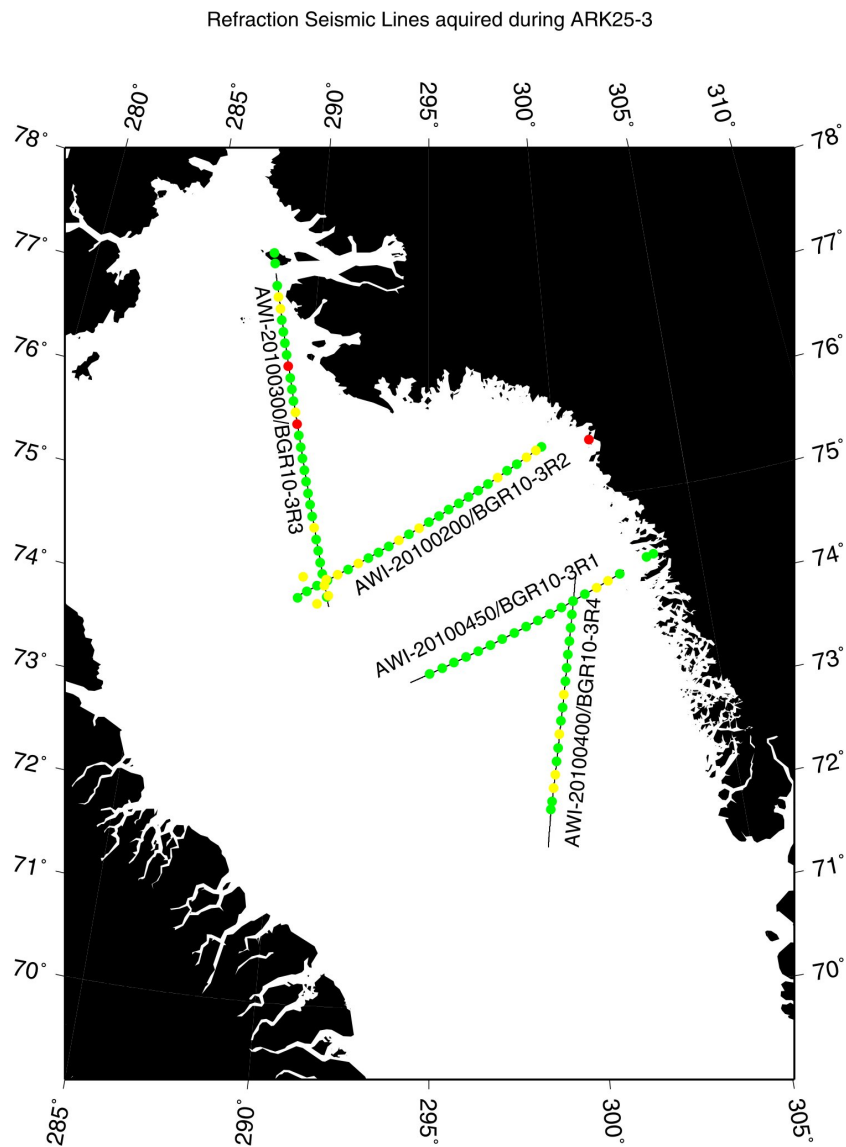


Fig. 9.33: OBS and land stations deployed during ARK-XXV/3. Green dots indicate perfect operation of the instrument, yellow dots indicate that at least one component of the seismometer failed, red dots indicate that no data was acquired.

9.8 Review of refraction/wide-angle OBS data

9.8.1 Profile BGR10-3r1 / AWI-20100450

Line AWI-20100450 / BGR10-3r1 crosses line AWI-20100400 / BGR10-3r4 at station 450st013. The E-W oriented profile covers most of the Greenland shelf area and will give an insight to the transition of continental to oceanic type crust.

17 OBS and 2 land stations were deployed on a 260 km long line. Only two OBS did not work in all seismometer components, all other stations operated well (Fig. 9.34). Offsets to which signals can be observed are around 50 km with 90 km in maximum. Two land stations were deployed with an offset of the profile line with a maximum of 2 km. Station 450stL1 was equipped with geophone chains and installed on an island with exposed bedrock 2 km north of the profile line, whereas station 450stL2 equipped with a broadband seismometer is located on a headland in the prolongation of the profile line.

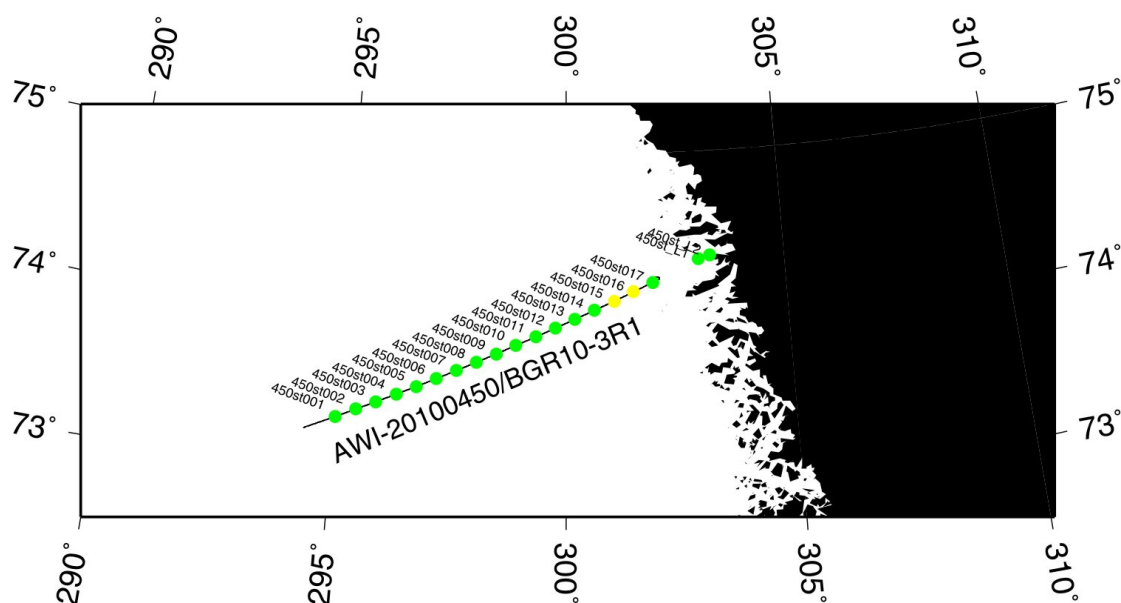


Fig. 9.34: OBS and land stations deployed on the line AWI-20100450/BGR10-3r1. Green dots indicate perfect operation of the instrument, yellow dots indicate that at least one component of the seismometer failed.

9.8.2 Profile BGR10-3r2 / AWI-20100200

On line AWI-20100200 / BGR10-3r2, 25 OBS were deployed on a 113 km long east-west transect with a land station set up on the Greenland coast (Fig. 9.35). The orientation was chosen to show the transition of continental to presumably oceanic crust in the Baffin Bay basin.

19 OBS out of 25 worked properly; six seismometers failed in at least one component.

Unfortunately, the land station did not record any data due to a problem in the parameter settings which could be solved afterwards. Due to a nature reserve area

which did not allow any deployment, the land station was located on an island with exposed bedrock about 20 km off the profile line.

Data quality is best on this profile, compared to the other three lines. Refracted and reflected signals can be traces to average offsets of 65 km with a 160 km maximum offset.

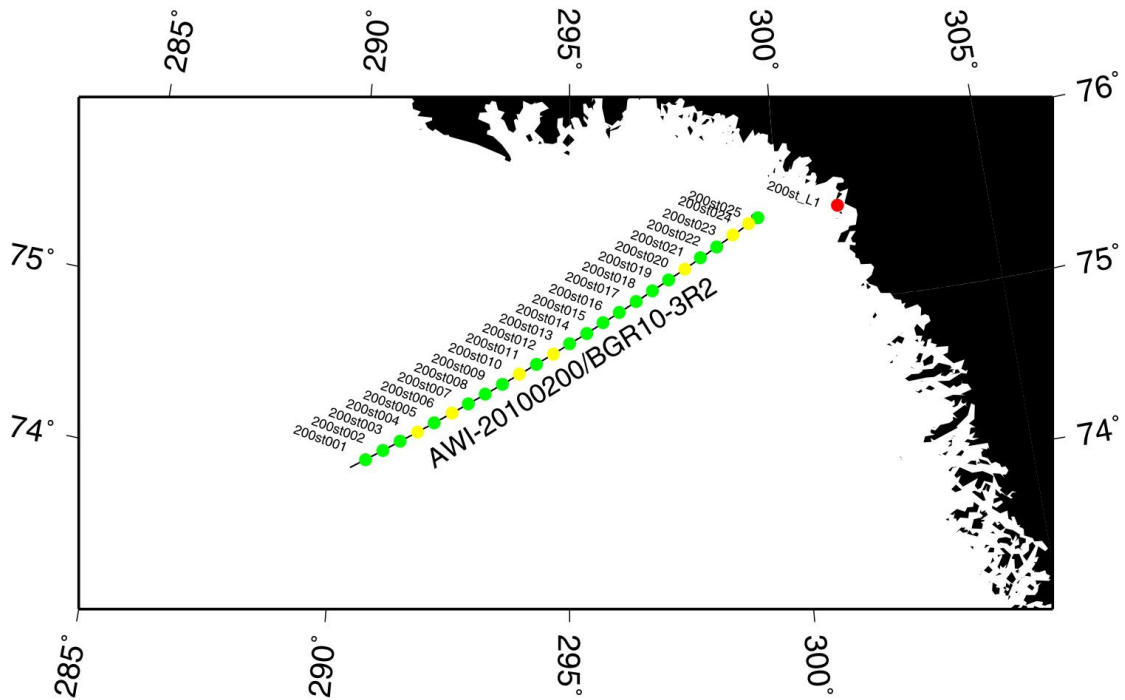


Fig. 9.35: OBS and land stations deployed on the line AWI-20100200/BGR10-3R2. Green dots indicate perfect operation of the instrument, yellow dots indicate that at least one component of the seismometer failed, red dot indicates that no data was acquired.

9.8.3 Profile BGR10-3r3 / AWI-20100300

Line AWI-20100300 / BGR10-3r3 with an extent of 374 km is the longest of the ARK-XXV/3 refraction seismic profiles. The north-south trending profile is covered by 28 OBS and three land stations (Fig. 9.36). This line should show the transition of proposed oceanic crust in the Baffin Bay Basin in the South to continental crust in the Nares Strait in the North.

Out of the 28 OBS, 21 stations fully operated, five failed in at least one seismometer component and two stations did not record any useful data. Refracted and reflected signals can be observed to offsets around 55 km on average. Maximum offsets of 180 km were obtained by station 300st002. Data examples are shown in Figure 9.37 and Figure 9.38.

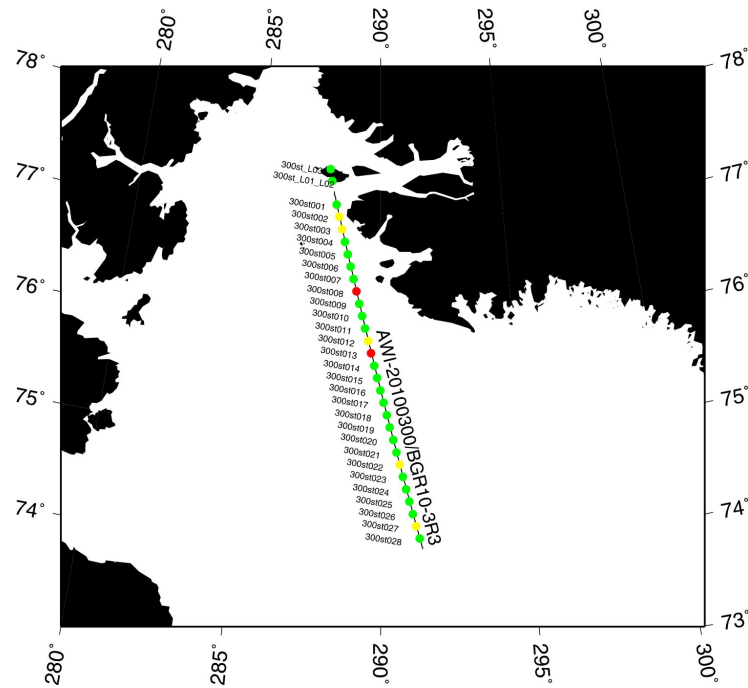


Fig. 9.36: OBS and land stations deployed on the line AWI-20100300/BGR10-3r3. Green dots indicate perfect operation of the instrument, yellow dots indicate that at least one component of the seismometer failed, red dots indicate that no data was acquired.

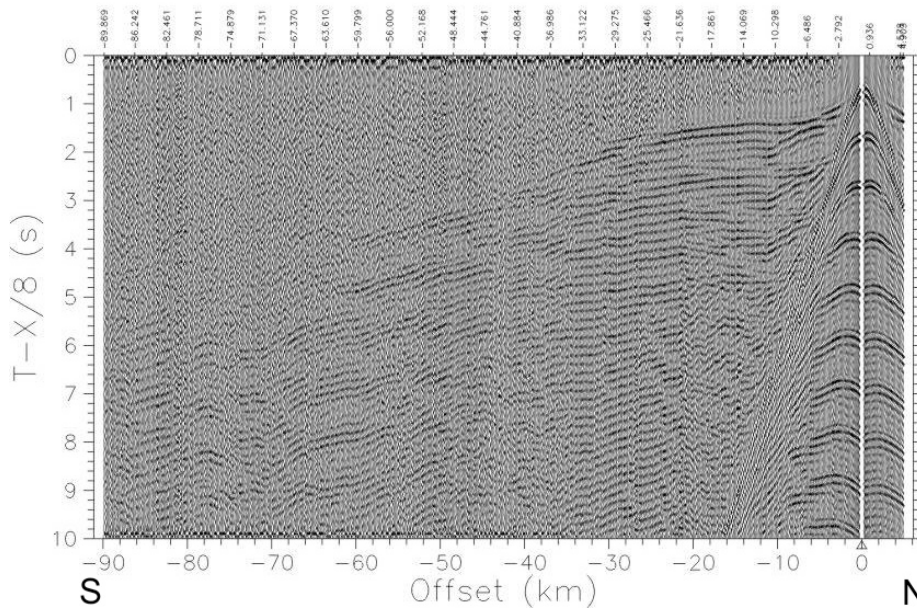


Fig. 9.37: Seismic record section of OBS 300st004 (hydrophone channel). The OBS was located on the continental shelf in the northern part of line AWI-20100300 / BGR10-3r3.

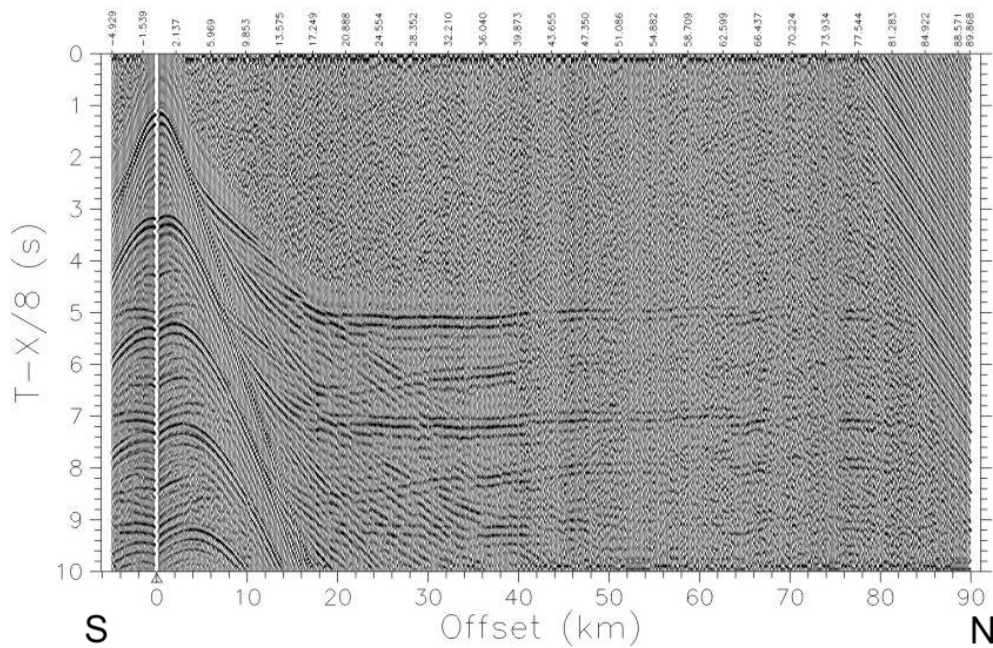


Fig. 9.38: Seismic record section of station 300st022 (hydrophone channel) on the southern part of line AWI-20100300 / BGR10-3r3. Clear lower crust or mantle refraction phases are visible.

The land stations were deployed on Northumberland Island in unconsolidated hillslope debris. The offsets from the profile line are less than 1 km. Two stations (300stL1, 300stL2) were installed at the southern part of the island and the third station (300stL3) was located on a steep cliff with debris coverage at the northern part of Northumberland Island. Station 300stL1 and 300stL3 were equipped with 9 geophone chains. Station 300stL2 was deployed nearby 300stL1 and equipped with a broadband seismometer. The small distance of about 100 m between 300stL1 and 300stL2 allows for a detailed comparison of the data recorded either by geophones or seismometer.

9.8.4 Profile BGR10-3r4 / AWI-20100400

Line AWI-20100400 / BGR10-3r1 (Fig. 9.39) is the continuation of AWI-20080500, which was acquired during a previous *Maria S. Merian* cruise in 2008. The old line indicates oceanic crust in the Baffin Bay Basin, but stops in some type of transitional crust before reaching crust of continental type. 17 OBS were deployed along 303 km to cover the transition to continental crust.

Four instruments failed in at least one component, while 13 worked completely. Offsets to which refracted and reflected signals can be observed are at 45 km on average, with a maximum of 120 km. Figure 9.40 shows a data example.

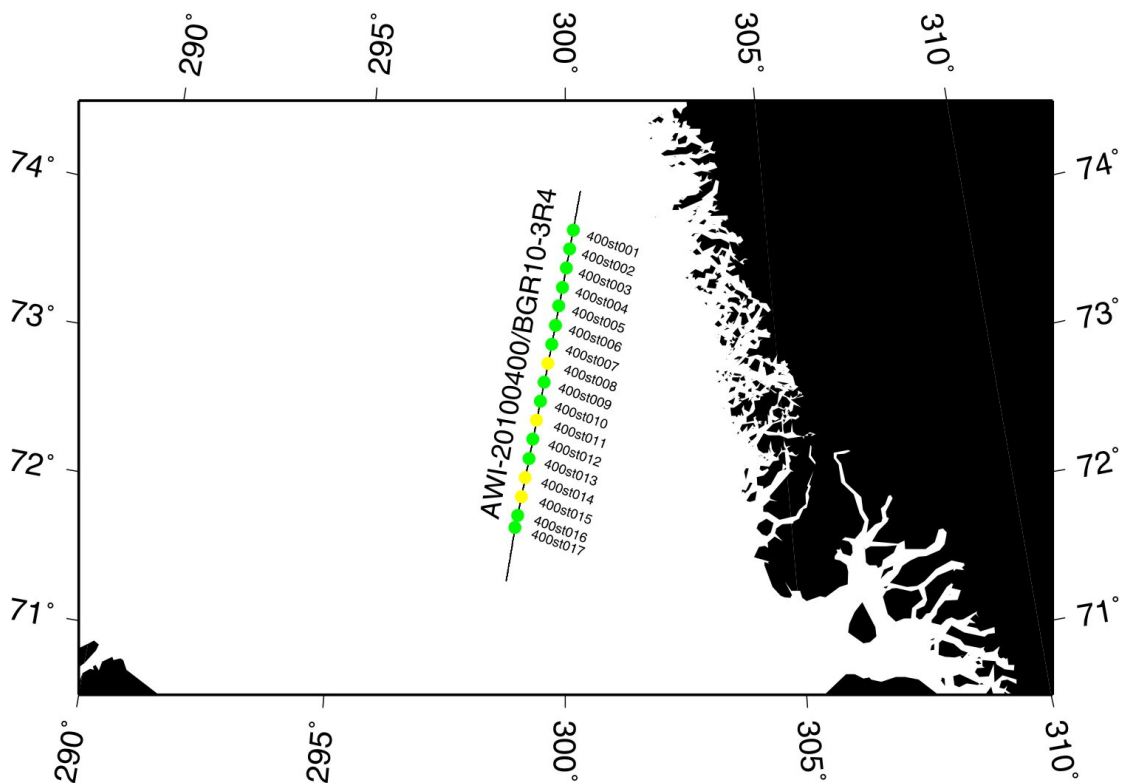


Fig. 9.39: OBS and land stations deployed on the line AWI-20100400/BGR10-3r4. Green dots indicate perfect operation of the instrument, yellow dots indicate that at least one component of the seismometer failed.

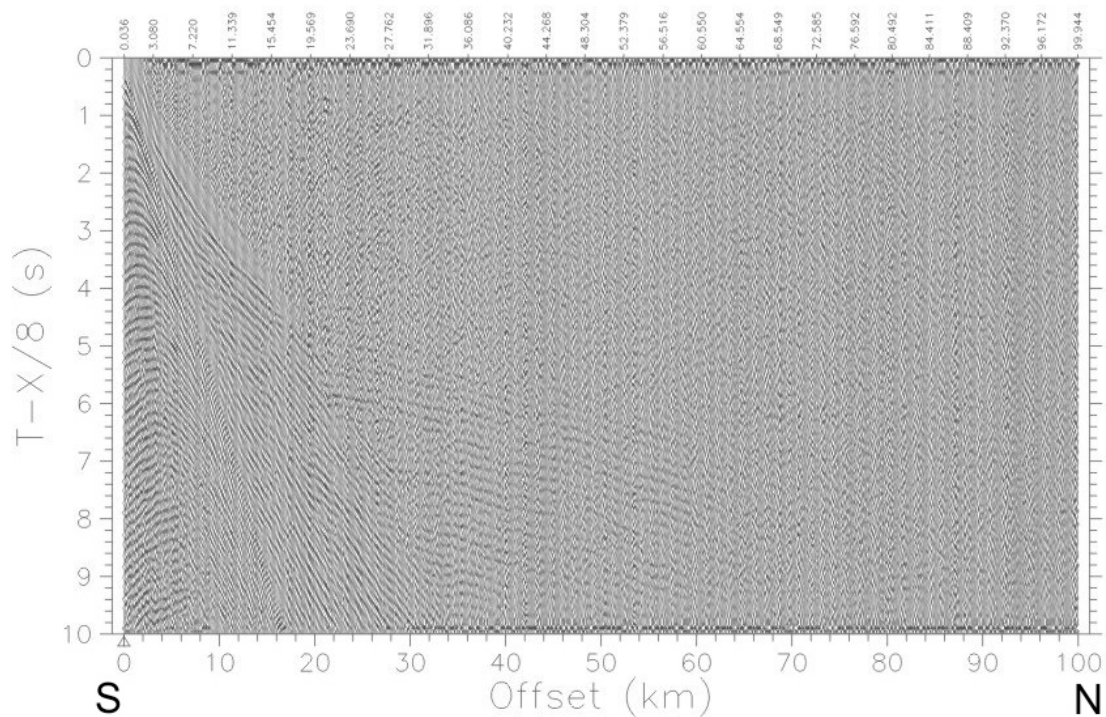


Fig. 9.40: Data example of the hydrophone component of OBS 400st006 from line AWI-20100400 / BGR10-3r4.

9.8.5 Long term test of new 120 sec seismometers

Five brand-new GÜRALP 120 sec prototype seismometers have been deployed for testing from 17-Aug-2010 until 06-Sep-2010 in the deep basin area of northern Baffin Bay (Fig. 9.41). Unfortunately, three of them failed totally, only two delivered data. To test the long-period behavior of such instruments, it is necessary to look for events that hold these very low frequencies. Normally, only strong teleseismic earthquakes provide such signals. During the operating period only a few teleseismic events occurred, the strongest was the 03-Oct-2010 16:35 UTC Christchurch (New Zealand) earthquake with magnitude 6.7. Unfortunately, this time interval was disturbed by seismic surveying of the industrial vessel M/V *Bergen Surveyor* close to the deployment area. This earthquake of all was far away to generate those long-period signals.

Besides this we were lucky to record a M=6.3 Aleutian Island event that occurred also on 03-Oct-2010 at 11:16 UTC (51.54°N; 175.88°W, 42 km depth). Nevertheless, this earthquake also did not provide 120 sec signals, it was good to compare the new instruments with the older ones which had been deployed on profile AWI-20100300 / BGR10-3r3 at the same time. Figure 9.42 shows the band-pass filtered vertical traces (Z) of this event of the test stations (st491, st493) and the southernmost profile stations 300st025-300st028. Especially, the traces of the closely spaced (1 nm) OBS st493 and st028 show almost no differences in their signals. This is a good result, but could not verify, if the new sensors have an enhanced long-period frequency characteristic in reality.

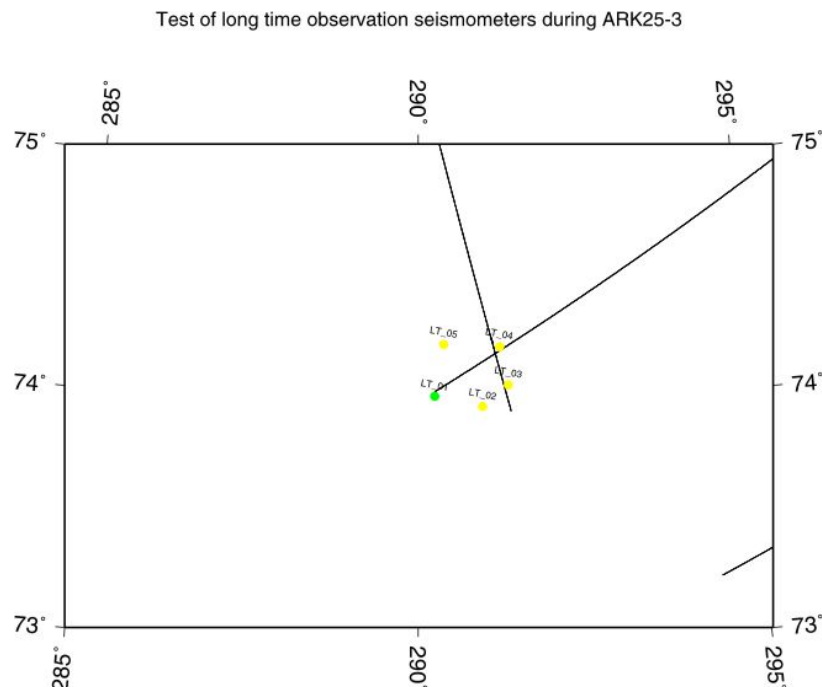


Fig. 9.41: Five OBS with new 120 sec prototype seismometers deployed on a test network in the deep sea area. Green dot indicates perfect operation of the instrument, yellow dots indicate that at least one component of the seismometer failed. Here, besides st491 (LT_01) only st493 (LT_03) provided useful data of Z and X components.

Data quality

The data of lines AWI-20100200 / BGR10-3r2 and AWI-20100300 / BGR10-3r3 show refracted and reflected signals with up to 160 km offsets, whereas on the lines AWI-20100400 / BGR10-3r4 and AWI-20100450 / BGR10-3r1 shorter offsets (by around 50 km) are more common. Weather conditions would even have favored good data quality on the last two lines. As this offset difference is not only observed in the seismometer components, but also in the hydrophone data, it does not seem to be a problem of bad coupling to the ground. The check of the continuous traces reveals a higher background noise during the last two lines which can be caused by motion of the nearby ice sheet of Greenland or by ground tremors in general. Also a stronger ground current can cause higher background noise. Interestingly the hydrophone shows longer ringing on the last two lines than before, when S signals are detected. This is characteristic of S-waves. Probably, the sediments in this region favor the conversion and propagation of S-waves that consume a major part of the energy.

Data archiving

The raw data, the intermediate data, as well as all data worked on, created plots, readme files, and tables are stored on external hard drives and will be transferred to the AWI and BGR servers after the cruise.

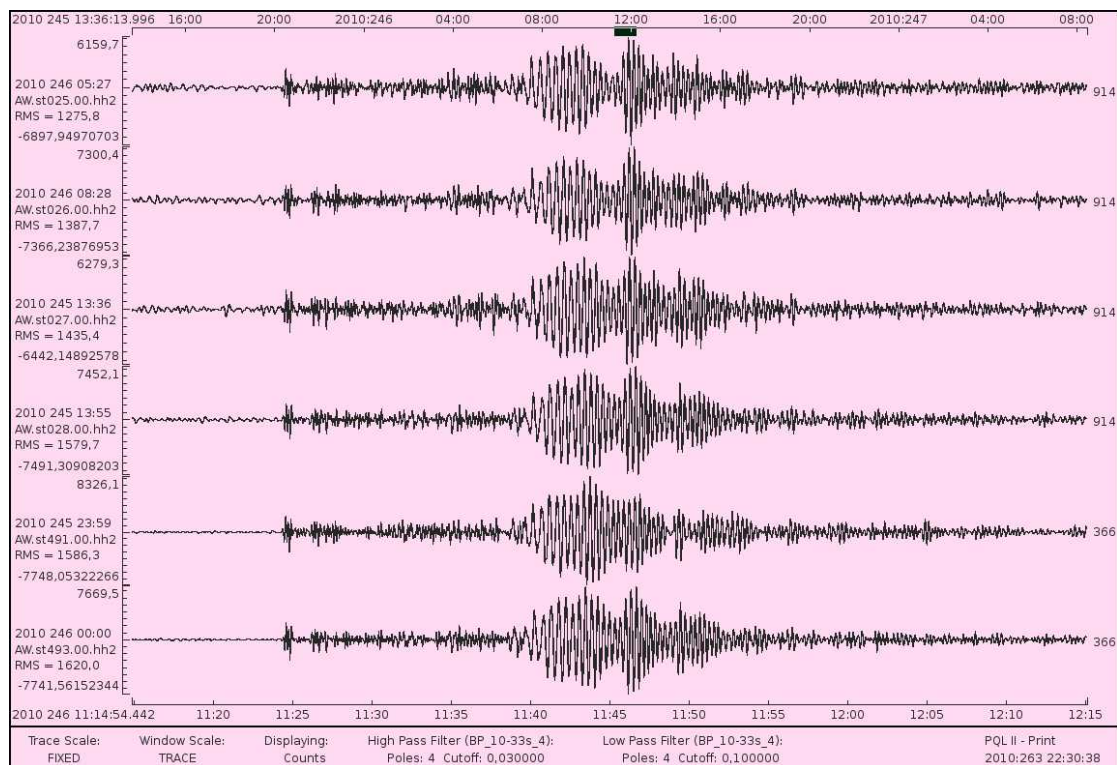


Fig. 9.42: Band-pass (10-33 sec) filtered seismograms (vertical components) of the $M=6.3$ Aleutian Island earthquake from 03-Oct-2010 11:16 UTC of test stations st491, st493 (bottom traces) and profile OBS 300st025-300st028. Traces presented with PQL viewer, time window 1 hour.

10. HEAT FLOW MEASUREMENTS

Ingo Heyde, Michael Zeibig
Bundesanstalt für Geowissenschaften und Rohstoffe

10.1 Method and instrument

Since tectonic processes in the oceans are primarily heat-driven, measurements of geothermal flux provide important boundary conditions for models that seek to explain how the ocean basins and their margins have evolved through time. Regional variations in the depth of the deep-sea floor are found to be linked closely to thermal processes. The knowledge of surface heat flow constrains mechanisms for subsidence and elevation arising from changes in heat balance. The heat flow through continental margins is also important because Paleo-temperatures and geothermal gradients affect the maturation of organic sequences. Basin modelling is based on sediment thicknesses and paleo-temperatures for assessment of the hydrocarbon genesis in sedimentary basins. As an additional tool, heat flow measurements might assist in restraining age estimates of the crust in the Northern Baffin Bay. Heat flow data spread over the area may help to identify the areal extent of oceanic floor or stretched continental crust, type of extension and sea-floor spreading.

However, the assumption that the sea floor cools solely by conduction is not always valid because heat flow in some areas shows such large variations over short distances that circulating fluids must play a major role in heat transfer. Venting of hot fluids on the crest of an oceanic ridge system is the most spectacular demonstration of this phenomenon.

It is possible to use shallow probes in the deep ocean because the seabed is generally in thermal equilibrium. On the continental slope and shelf, access to deep boreholes is essential since short-term variations in bottom water temperature and sediment movements disturb thermal gradients near the seabed so shallow coring does not yield values that reflect heat transfer at depth. If the bottom water temperature increases, the thermal gradient just below the sea floor is reduced and so heat flow decreases, and vice versa.

Equipment

BGR employs currently two different types of marine heat flow probes – a conventional probe, built after the so-called violin-bow concept and a second probe, specially designed for employment in hard ground situations. It was assumed that the sediments in the Northern Baffin Bay are characterized by rather hard top sediments (drop-stones, relatively coarse, ice-rafted debris), which excluded the use of the conventional type marine heat flow probe.

For this reason the BGR-“hard ground” heat flow probe (Figs. 10.1 and 10.2) turned out to be an indispensable instrument during this cruise. The “hard ground” heat flow probe features a 2.2 m long sensor rod made of steel with a diameter of 2 cm mounted along the long axis of a cage and held in position by a special mechanism to prevent bending during penetration of hard ground sediments. It contains 7 to 8 thermistors with a spacing of about 30 cm. The necessary force to press the sensor rod into the sediments is provided by a cylinder, which houses lead plates with a total weight of 600 kg and an electronic unit within a pressure vessel with a total weight of additional 144 kg. The purpose of the electronic unit housed in the pressure vessel is to control the data transfer and the measurements. All measured data are transferred via the ship’s coax cable in real time online to a laptop PC on board.

All measured data are recorded, stored, digitized and monitored by so-called “intelligent sensor modules” (ISM) installed in the pressure vessel. This technology relies on immediate digitization and downloads of measured values in the memory and enables us to improve the accuracy of measurement to $\sim 0.002\text{K}$. All recorded values are sent to an analogue-multiplexer and then to a 16bit-A/D-converter. The high accuracy and linearity during A/D-transformation is achieved by the application of the sigma delta method. To further improve the accuracy of the measurements, an arithmetic mean of 20 consecutive measurements per sensor is formed and then accepted as one single measured value.

All specific modules, which control the configuration, linearization and scaling data in the ISM-module, are stored in an EPROM. Storage and display of the measured data is done via a special computer code, stored on PC. A patent has been issued for this particular design.

Fig. 10.3 shows a typical heat flow measurement with the temperature graphs of 6 sensors from deployment to the seafloor until hoisting back through the water column. To achieve optimum thermistor calibration, the heat flow probe is stopped slightly above the seafloor on the down trip. A horizontal tilt meter (in the two perpendicular directions) in the recording device allows verifying when the probe stopped swinging. After a time period of typically less than 2 minutes, thermal stabilization within $\sim 0.001\text{K}$ is obtained at all thermistors. It is assumed that the thermistors measure identical seawater temperatures. Recalibration of all thermistors is achieved by using one thermistor as the master sensor, whose measured value is used to calibrate the data measured by the other thermistors.

Following this procedure, the probe is lowered with a velocity of 0.1 m/s, until penetration of the seafloor by the sensor rod is achieved. The tilt meter again gives information about the inclination of the probe. The thermal gradient in the sediments is measured continuously for a time period of typically 8 minutes. After this period, the frictional heat component caused by the penetration of the rod into the sediments has decayed to negligible values.

Thereafter, a constant electric current of about 1 A (@ 10 V) is sent through the heating wire (about 4 m long) for the measurement of the *in-situ* thermal conductivity (λ). The temperature increase in the metallic rod is inversely proportional to the *in-situ* thermal conductivity of the adjacent sediments. We have measured the linear T-increase after initial heat-up of the assemblage and will derive λ from this curve for all stations.

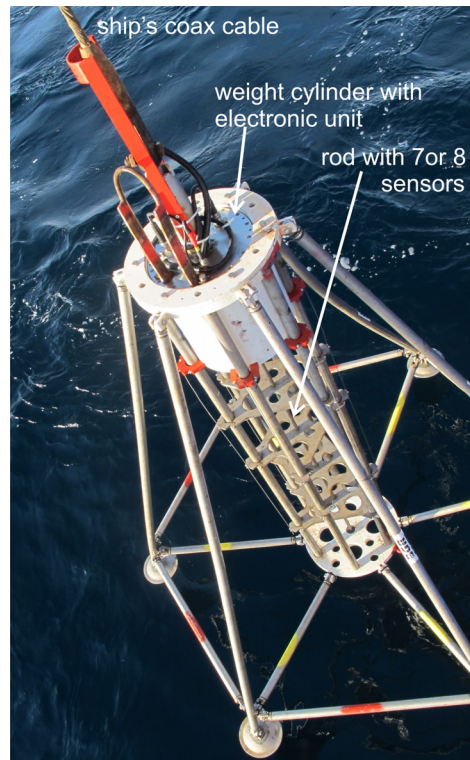


Fig. 10.1: BGR - hard ground heat flow probe

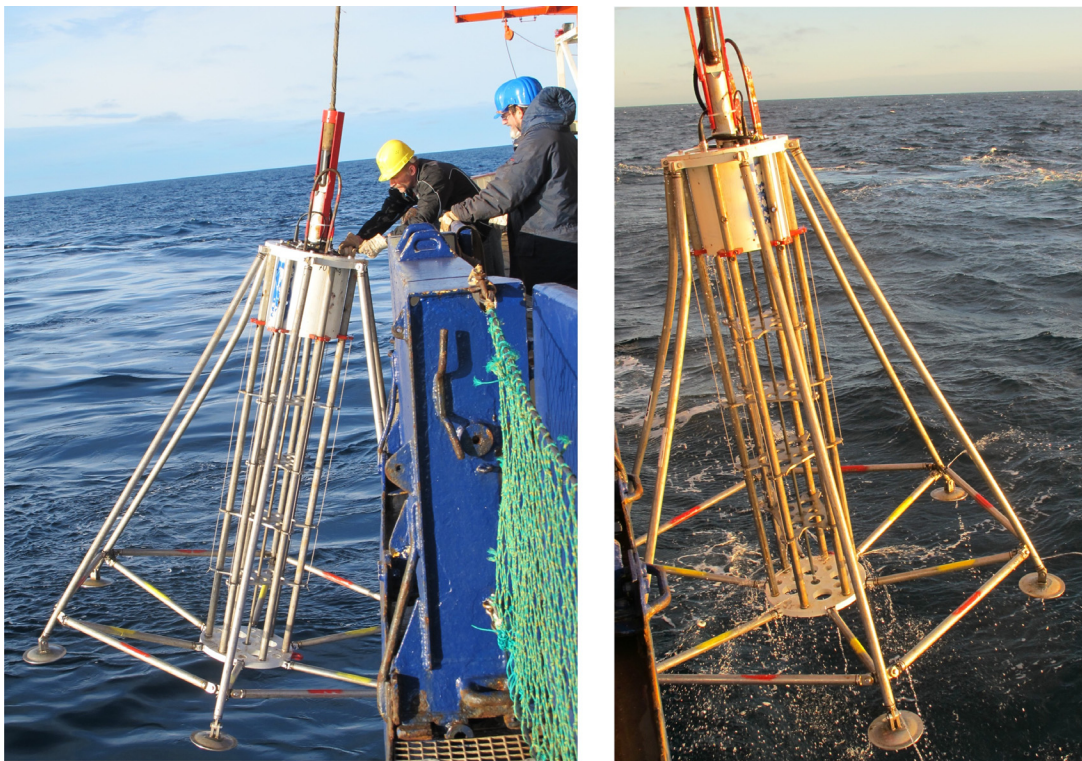


Fig. 10.2: BGR – hard ground probe prior deployment (left) and at the surface again before recovery (right). The cage with the supporting mechanism for the sensor rod can be seen clearly.

10.2 Station work and preliminary results

All heat flow measurements were conducted in areas where seismic lines give us information on the sediment thickness and a rough estimate on likely sedimentation rates. This way the true heat flow value, corrected for sedimentation effects, can be determined. The measurements were mostly combined with OBS station work and were thus conducted along all 4 refraction seismic lines. However the measurements were restricted to areas with water depths in excess of about 1440 m. Only two measurements in the Melville Basin were carried out with shallower water depths of 1150 m and 896 m.

Altogether at 32 stations heat flow measurements were conducted (Tab. A.12). Visual inspections after recovery showed that the probe penetrated at all stations the sediments till the maximum depth of 2.2 m. After 21 stations with a sensor rod with 7 thermistors another rod with 8 thermistors was used for the remaining stations. However both rods had one thermistor which failed to operate. Based on the stabilised ground temperature values at the different positions of the rod the temperature gradient was calculated by linear regression. Fig. 10.4 shows as example the temperature gradients at 3 stations.

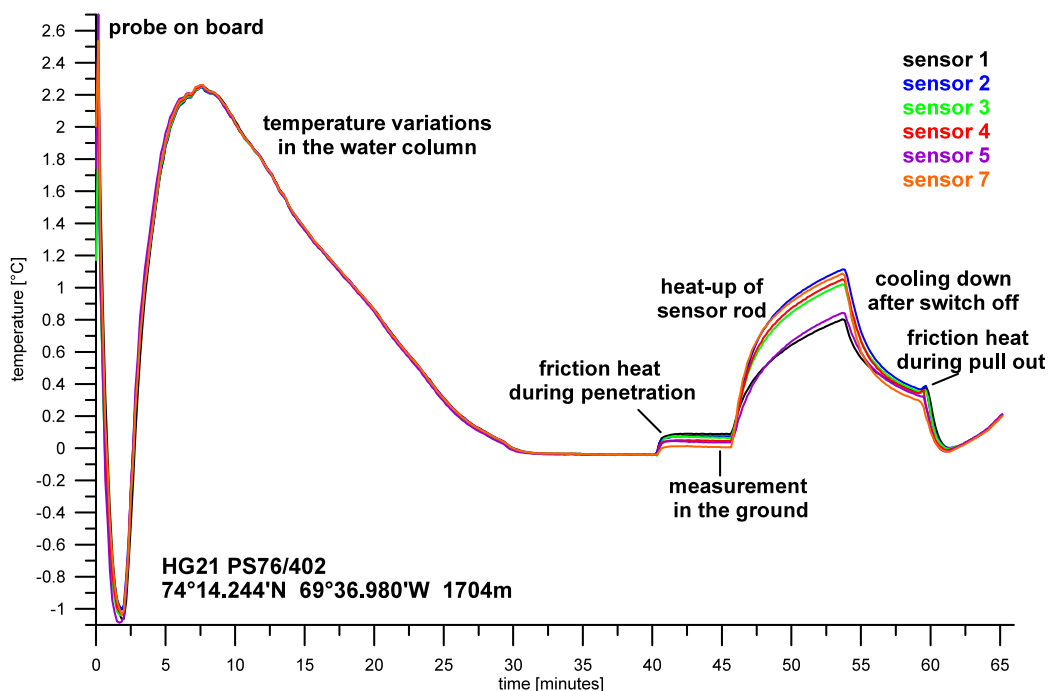


Fig. 10.3: Heat flow measurement HG21 with the temperature of the 6 working sensors from the deployment to the seafloor, penetration into the ground, heating and beginning hoisting back through the water column.

Fig. 10.5 shows a map of the stations with the measured temperature gradients. Gradients at 8 stations from the Global Heat Flow Data Base measured in the 70s are also shown. The present Data Base, compiled by Pollack et al. (1993), was a project initiated by the International Heat Flow Commission of the International Association of Seismology and Physics of the Earth's Interior (IASPEI).

10 Heat flow measurements

The temperature gradient in the Northern Baffin Bay is very homogeneous with values of about 60 to 70 mK/m in the deeper parts and lower values of 30 to 40 mK/m on the continental slope. However, oceanic crust underlying the Baffin Bay should be fairly young, since the most likely development occurred sometime during Paleocene/Eocene times. Therefore, we expected higher gradients resulting in high heat flow values. The derivation of the *in-situ* thermal conductivity of the adjacent sediments from the heat-up of the sensor rod will be calculated back in the labs. Thus also heat flow values will be determined only after the cruise. In combination with the results of the seismic measurements we expect to resolve the influence of high sedimentation rates which may reduce the heat flow.

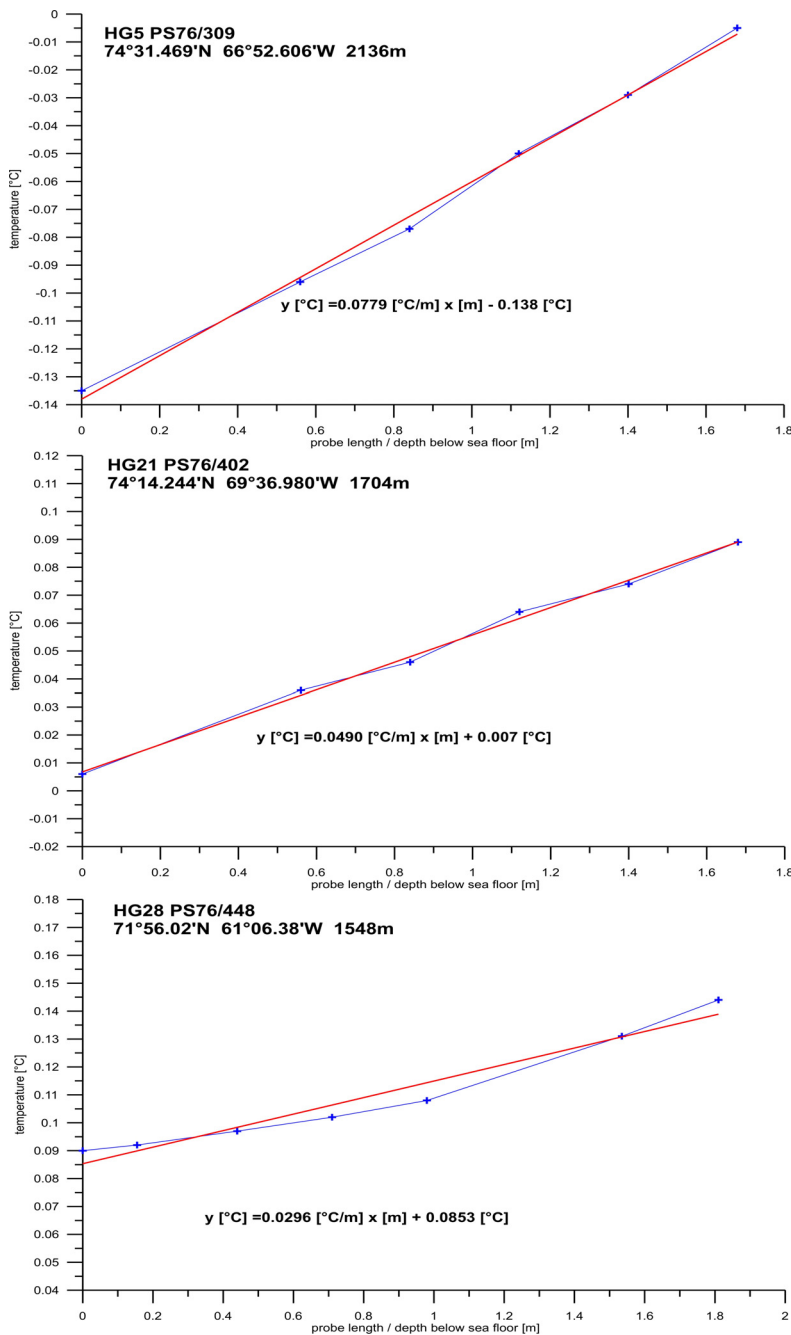


Fig. 10.4: Estimation of the temperature gradient by linear regression for 3 stations

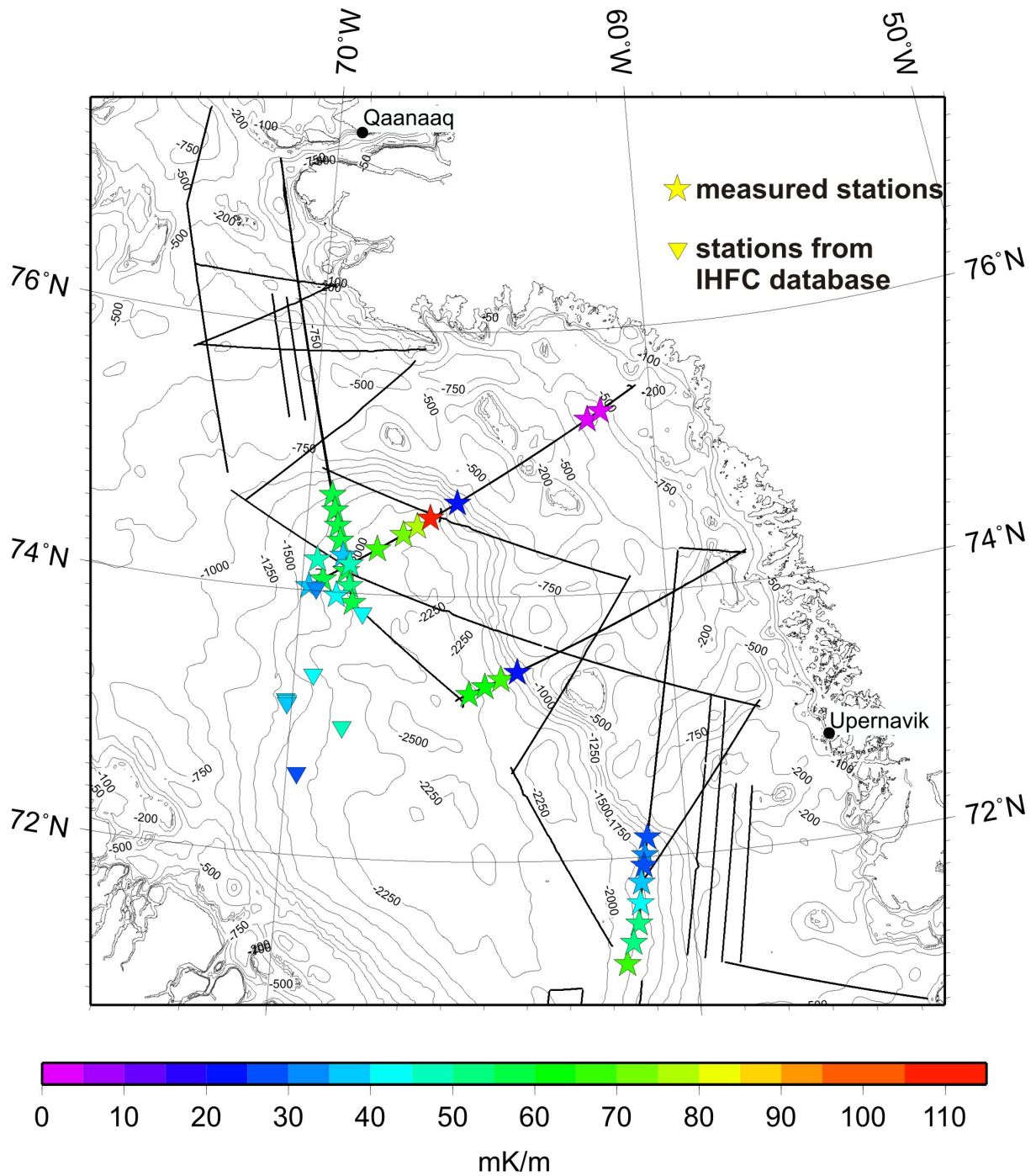


Fig. 10.5: Map of the stations with measured temperature gradients in mK/m. Additionally, the values at stations from the IHFC database (Pollack et al., 1993) are shown.

11. SEDIMENT CORING

Thomas Pletsch
Bundesanstalt für Geowissenschaften und Rohstoffe

Gravity cores were taken at 34 stations to make sediment samples available for gas geochemical and microbiologic analyses (Coring list – see Appendix A.13). For practical reasons, gravity core stations were selected along the same transects as the refraction seismic lines.

11.1 Instrumentation and procedures

A gravity corer with a 4.70 meter core barrel was used at all stations. The original setup of this device includes a nylon piston that is placed at the bottom of the core liner before the device is deployed. The piston is intended to avoid disturbance of the cored sediment surface and to separate the sediment entering the liner from the bottom from any sediment that would eventually enter the core barrel from the open top of the coring assembly. During our cruise, this original setup with the piston yielded unsatisfactory results: recovery was generally poor (1.4 meters on average) and there was sometimes more sediment on top of the piston than below it, indicating that the piston had blocked the intended intrusion of sediment from the bottom.

At station 290, we tested a core assembly where the piston was not loaded with water before deployment and had a better recovery (3.5 meters), but it was only after the complete removal of the piston and closing of the upper orifice of the coring weight with a wooden plug, from station 293 onward, that recovery picked up and remained at acceptable levels. Notably, there was rarely any sediment above the assumed sediment surface, marked by a prominent diatom-rich mud (see below).

To find the sediment surface within the open, sometimes incompletely filled liner, we used a flashlight. The position of the surface was simultaneously noted on the outer side of the liner. Although there may be more precise procedures to find this important marker, the flashlight method proved to be fast and relatively accurate. In most cases, the difference between the cutting position of the liner and the actual surface sediment (as indicated by the prominent diatom-rich mud, see above) was on the order of a few centimeters. Regarding potential posterior studies, it needs to be emphasised that we were unable to precisely locate the sediment-water interface within the core. For the purpose of our intended studies, however, such deviations are negligible.

The filled part of the liner was cut into one-meter sections using a commercial tube cutting tool and a clean masonry spatula. Before splitting the cut into one-meter core sections („sections“), they were stowed in a store at 4°C and sampled for gas and pore water analyses (see Chapter 12).

After the gas and pore water sampling was completed, sections were laterally opened using two sledge-mounted vibrational saws. The end caps were cut with a conventional cutting blade. When the liner and the end caps were separated, a simple, hand-held device with a thin stainless steel thread was used to separate the two halves of the section. The two halves were split by hitting the separated section on two wooden supports. Splitting was often incomplete and required the additional help of a masonry spatula. All masonry spatulas, the saw blades, the cutter and steel thread were surgically cleaned between the cutting processes.

The larger half of each section, where gas and pore water sampling had already been performed, was designated the WORKING HALF and immediately moved to the microbiology lab for further sampling. The smaller, intact half was designated the ARCHIVE HALF and was used for visual core description and smear-slide preparation (see below).

11.2 Core description

Core description follows the procedures outlined in several Ocean Drilling Program volumes (e.g. Shipboard Scientific Party, 2000; Fig. 11.1). Sediment composition and texture were estimated on the basis of c. 15 smear-slides that were taken from the test cores (stations 248 and 256). Time restrictions did not allow us to perform routine smear-slide analyses on each core taken subsequently, but a preliminary compositional estimate was given by comparison with the results from test cores. Sediment texture was estimated by probing the cut surface with a finger and chewing individual samples for sand and/or silt content. Sediment colour was determined by comparison of small sediment scrapings with the Munsell Chips of the USGS Rock Color Chart. Carbonate content was estimated using immersion of sediment scrapings with c. 10% HCl.

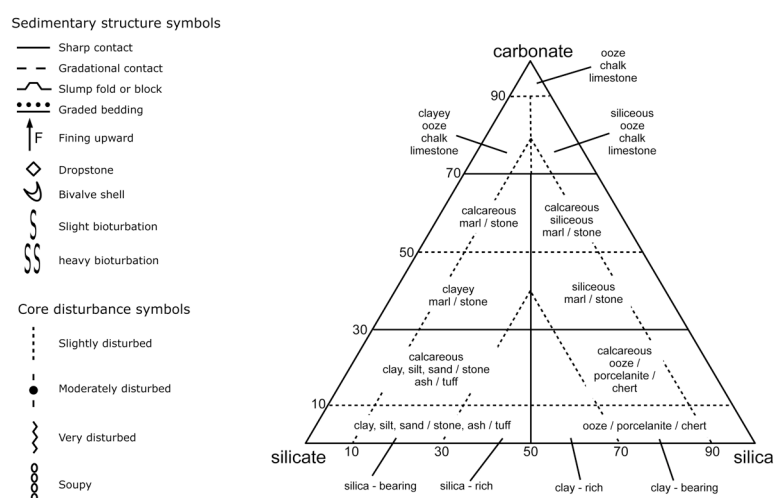


Fig. 11.1: Symbols used for visual core description (VCD) and sediment nomenclature applied.

Visual core descriptions (VCDs) were hand-written on A4-forms available as hard copies from the author upon request. Sediment nomenclature is mostly descriptive. Yet, genetic terms such as 'dropstone' and 'slump' were used as genetic terms, where deemed appropriate. By far the most common lithology recovered during this cruise was a mixture of clayey and abundant silty siliciclastic material. This material was described as silty mud to stress the abundance of the silt content.

12. GAS GEOCHEMISTRY

Thomas Pletsch
Bundesanstalt für Geowissenschaften und Rohstoffe

Objectives

To study the quantity, the chemical and the isotopic compositions of gases adsorbed to surface sediments on the bottom of the study area, we took samples from the gravity cores that were frozen for later laboratory analysis of adsorbed hydrocarbons (methane, ethane and propane) and other parameters (e.g. carbonate content, total organic carbon) These compositional data shall be interpreted in the context of the measured basin geometry and heat flow to be integrated into a model of hydrocarbon generation and migration. In addition we measured and sampled dissolved methane in the water column as a test for future expeditions. Due to restrictions regarding time and personnel, no analyses were performed on board.

12.1 Methods and material

Sampling positions were along the refraction seismic lines. Positions were screened and selected prior to gravity core deployment on the basis of Parasound data (see Chapter 6). Three types of samples were taken:

- Samples for adsorbed gas analyses
- Samples for free gas analyses
- Ocean water samples for dissolved methane analyses

Ten large samples (roughly the size of a fist) were taken for adsorbed gas analyses from the core catcher or from the cutting shoe, immediately after the core had been retrieved from the seafloor (Appendix A.14). In addition, 32 similarly-sized samples were taken after the core sections had been stored at +4° C for pore water extraction and subsequent splitting. The samples were placed in conventional polyethylene bags, refrigerated at -80° C and later stored at -20° C. Samples for analyses of the free gas within the sediment interstices analyses were taken using 5 ml syringes with cut-off tips, after the core sections had been stored at +4° C for pore water extraction and subsequent splitting. The samples were filled into 20 ml glass vials along with a known quantity of bactericide (Na-azide), vigorously agitated, and later stored at +4° C. Samples for analyses of the gases dissolved in deep ocean water were recovered with the water sampling flasks that are mounted on a rosette onto the device used for CTD measurements (see Chapter 5). These samples and the measurements done with a Franatech METS methane detector were used to test the equipment and procedures for future methane sampling of the water column and will be dealt with in more detail during their first routine deployments.

13. BIOGEOCHEMISTRY AND GEOMICROBIOLOGY

Friederike Gründger,
Bundesanstalt für Geowissenschaften und Rohstoffe
Camelia Algora
Helmholtz-Zentrum für Umweltforschung GmbH

Objectives

Together with echosounder and gas geochemical investigations in the water column, knowledge on the geochemistry and geomicrobiology of the northern Baffin Bay can support modelling and understanding of hydrocarbon generation. Geochemical characterisation of the sedimentary environments can help the identification of very low-intensity gaseous or oily hydrocarbon seepage as indicators of possible subsurface reservoirs. Microbiological investigations of the hydrocarbon degradation potential of the indigenous microbial communities by molecularbiological analysis (presence of special microbial groups known to thrive in rich hydrocarbon areas) together with the cultivation of such microorganisms (i.e. methanogens and sulphate reducers) in microcosms can give additional useful data to understand the hydrocarbon generation in the area.

Additionally, this study attempts to contribute to the understanding of one of the least known and potentially strangest ecosystems on earth which is the microbial biosphere of marine sediments. In fact, very little is known about the nature and activity of life in remote Arctic marine sediments. The phylogenetic and physiological diversity of marine Arctic sediment communities of the Baffin Bay is largely unknown. This is to our knowledge, the first microbiological study ever done in this area.

Previous studies on marine sediments have shown the presence of microbial representatives of several bacterial divisions suggesting a ubiquitous distribution. One of these ubiquitous bacterial divisions is *Chloroflexi* or Green Non Sulphur bacteria. The closest cultured microorganism from the great majority of the marine subsurface *Chloroflexi* is *Dehalococcoides spp.* No sub-seafloor representative from this group have been cultivated and isolated yet. Consequently, little is known with regard to their general properties of such a potentially environmentally importance in terms of being ubiquitous and in high numbers in the sub-seafloor group. In this study, attention is also focused on the presence and cultivation of this *Chloroflexi* group within the sediments of the Baffin Bay with a special attempt to its enrichment and further isolation. This is done based on the physiology of their closest relative: *Dehalococcoides spp.*, a specialist for the respiration of organo-halogenated compounds.

13.1 Methods and instruments

13.1.1 Biogeochemistry

Gas geochemical profiles along the cores

Retrieved sediment samples were placed in glass serum vials (50 ml of volume), suspended in 20 ml of anoxic 1M NaOH and vigorously vortexed. 100 μ l from the headspace from each serum vial was measured on board for methane concentration with a modified Gas Chromatograph (Shimadzu GC-14A/B). Later analysis involve CO₂ concentration profiles with depth and stable C- and H-isotope measurements to decipher the biological or thermogenic origin of methane in case this species is present.

Pore water samples for geochemical analysis along the cores

Pore water within the sediments was extracted by means of a rhizon (CSS-F 10 cm and 5 cm of porous length), with a tip diameter of 2.5 mm (Rhizosphere research products, Wageningen, NL) connected to a syringe where the pore water accumulated (see Fig. 13.1). The rhizons were kept inside the cores until syringes were filled and in any case for at least for 4 hours at 4° C.

Pore water samples needed a different treatment regarding further sulphide analysis or elemental composition. 0.5 ml Zinc-Acetate solution (consisting of 0.5 g zinc acetate in 50 ml MilliQ water and 50 μ l of acetic acid) per ml of pore-water was added in those vials meant for sulphide analysis and 10 μ l of nitric acid added per ml of pore-water in those pore-water meant for total elements analysis. Pore water samples were stored in plastic vials previously washed with 1% nitric acid and Milli-Q water. All samples were stored refrigerated at 4°C.

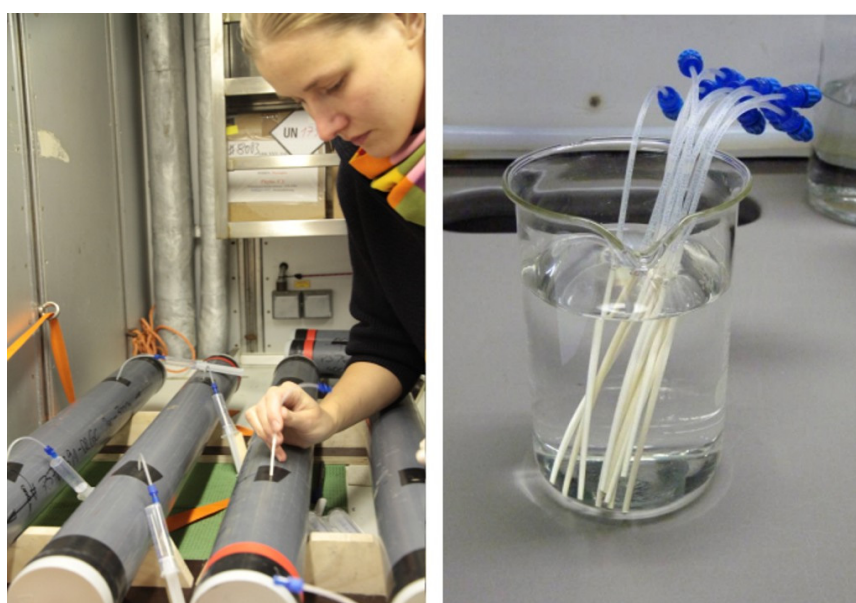


Fig.13.1: Pore water extraction in 1 m core sections by means of rhizon in 50 cm core intervals (left side); Rhizons moistened in MilliQ water prior to be used (right side)

13.1.2 Geomicrobiology

Microbiological samples for the qualitative and quantitative description of the microbial populations within the sediment and cultivation of specific microorganisms were taken from the uncontaminated centre of the sediment core immediately after the splicing in two halves. These samples were prepared for the subsequent laboratory analysis:

Numbers of living Bacteria and Archaea by CARD-FISH (Catalyzed Reporter Deposition-Fluorescence *In-situ* Hybridisation) by fluorescence microscopy.

For this purpose, 0.5 g of sediment from selected depths was placed in sterile 2ml-Eppendorf tubes and fixed in 1 ml of a cold 4% formaldehyde-PBS solution (phosphate buffered saline, 130 mmol Sodium chloride, 7 mmol di-Sodium hydrogen phosphate, 3 mmol Sodium di-hydrogen phosphate, sterile filtered 0.2 μm) for 2 hours at room temperature (20°C), washed twice with cold PBS using an Eppendorf centrifuge at 13,000 rpm for 10 min and finally stored at -20°C in 1 ml PBS-ethanol (1:1). All samples were frozen at -20°C until analysis in the shore-based laboratory.

Qualitative and quantitative description of microbial community inhabiting the sediments

Around 15 ml of sediment was sampled in duplicates with a cut sterile 2 ml/ 5 ml syringe and placed in Falcon screw capped vials. All samples were immediately frozen at -80°C until analyzed. Further analysis involves DNA extraction, quantification of specific Prokaryote groups with Q-PCR and clone libraries.

Sediment cultivation for an enrichment of specific groups of Prokaryotes

Two different approaches were used for the cultivation of Prokaryotes. For the study of Prokaryotes performing sulphate reduction, methane and carbon dioxide formation and consumption as well as biodegradation of different hydrocarbons, sediment cultures consist of sediment slurries in reduced minimal mineral medium hold in Hungate glass tubes. The cultivation of sediment for the biodegradation of halogenated organic compounds consisted of direct inoculation of sediment (10 - 20% of sediment) into reduced minimal mineral medium contained in glass serum vials. The culture was purged with $\text{N}_2:\text{CO}_2$ (0.8:0.2) immediately after the direct inoculation.

13.2 Processing of core material

The 1 m long gravity core sections were processed for subsequent geochemical analysis. This was done in short intervals along the core sections. Geochemical analysis consisted of gas and pore water analysis. Gas geochemical analysis aimed to obtain methane and CO_2 profiles with depth. Pore water geochemical analysis aimed for the elemental composition (especially Fe- and Mn- species and sulphate/sulphide concentration).

For the gas analysis, and to avoid degassing, holes (2 cm diameter) were drilled into the liner at intervals of 50 cm, starting at 25 cm below the sediment surface/top of the

core. Five ml of sediment was sampled with a cut 5 ml syringe. Holes were immediately sealed with tape after sample retrieval and stored in a climate room at 4° C. After this, pore water was extracted at the same intervals using rhizons (i.e. core solution samplers designed for sampling soluble components in undisturbed soil cores and sediments, see Fig. 13.1).

Pore water extracted with the rhizons was collected using a 10 ml syringe. Once cores were sampled for the geochemical analysis, they were split into two halves: for both processing and archive. An intact archive half was used to describe sedimentary structures and composition (see Chapter 12). The half for further processing was sampled for molecular biological studies of the quantitative and qualitative microbial community composition at same depth intervals as ones for the geochemical studies. Extra samples were taken in case of presence of diverse sediment layers. Some samples were partially fixed for FISH (Fluorescence *in-situ* hybridisation) microscopy studies. Additionally, sediment samples for later microbial cultivation were taken and stored at a temperature of 4°C in Schott bottles purged with a gas mixture of N₂:CO₂ (0.8:0.2).

Prior to sampling, the upper surface of the sediment was carefully removed to avoid contamination. All sediment samples were taken from the inner, intact and uncontaminated part of each working half.

14. ONSHORE ROCK SAMPLING

Thomas Pletsch, Kai Berglar, Tabea Altenbernd, Bundesanstalt für
Geowissenschaften und Rohstoffe
Michael Koch, Universität Jena

14.1 Objectives

Helicopter-supported onshore fieldwork was intended to collect samples for:

- thermochronologic techniques (apatite and zircon fission track and (U-Th-Sm)/He analyses)
- organic geochemistry and organic petrography of potential petroleum source rocks.

Both types of analyses will provide important clues to basin models that will form the basis of our planned numerical petroleum systems analysis for the northeastern margin of Baffin Bay and along the southeastern Nares Strait. The results of the two sampling programme mes are expected to contribute to regional numerical basin models that will be constrained by both offshore and onshore data. Usually, reflection seismics and the stratigraphy of adjacent drill holes provide the geometries and timing of deposition of the basin fill. However, the interpretation of major localised depositional and of erosional features, their onset, duration and rates, is commonly difficult without knowledge of the exhumation history of the basin shoulders. This history is documented in thermochronologic markers such as apatite and zircon fission tracks. Using the results of thermochronologic methods, we expect to contribute to a better understanding of the exhumation history of the northeastern margin of Baffin Bay and along the southeastern Nares Strait. Notably, we expect to decipher the relationship between the formation of the supposed Mesozoic to Palaeogene sedimentary basins and the source areas for the contemporary sedimentary infill. Organic geochemical/petrography results are important input parameters for modelling petroleum generation and migration, such as we intend to perform for the target area.

14.2 Methods and materials

Samples were taken for two types of analyses (see Figs. 2.2 and 14.1 for locations and Appendix A.15 for details):

Samples for thermochronologic methods were taken along two types of transect:

1. topographic transects within one structural unit, where systematic differences in fission track ages can be interpreted in terms of denudation/exhumation rates,
2. transects on a similar elevation to identify regional changes of denudation and exhumation.

In addition to that, sands from Holocene glacial outlets were sampled. Sampling positions were selected prior to individual sampling campaigns primarily on the basis of regional geological maps according to lithological criteria, i.e. the likelihood of finding appreciable quantities of apatite and/or zircon. Transport and sampling were done by the shipboard helicopters and with at least two geologically trained persons aboard which allowed for efficient use of the time windows mandated by the seismic operations and helicopter fuel and weather. Due to the lack of detailed topographic information of these remote areas, and to generally receding glaciers, individual sampling locations were ultimately selected on the spot.

Samples for organic geochemical / petrography methods were taken on an ad-hoc basis when the ship was in the range of appropriate geological units, e.g. the Silurian black shales of western Washington Land.

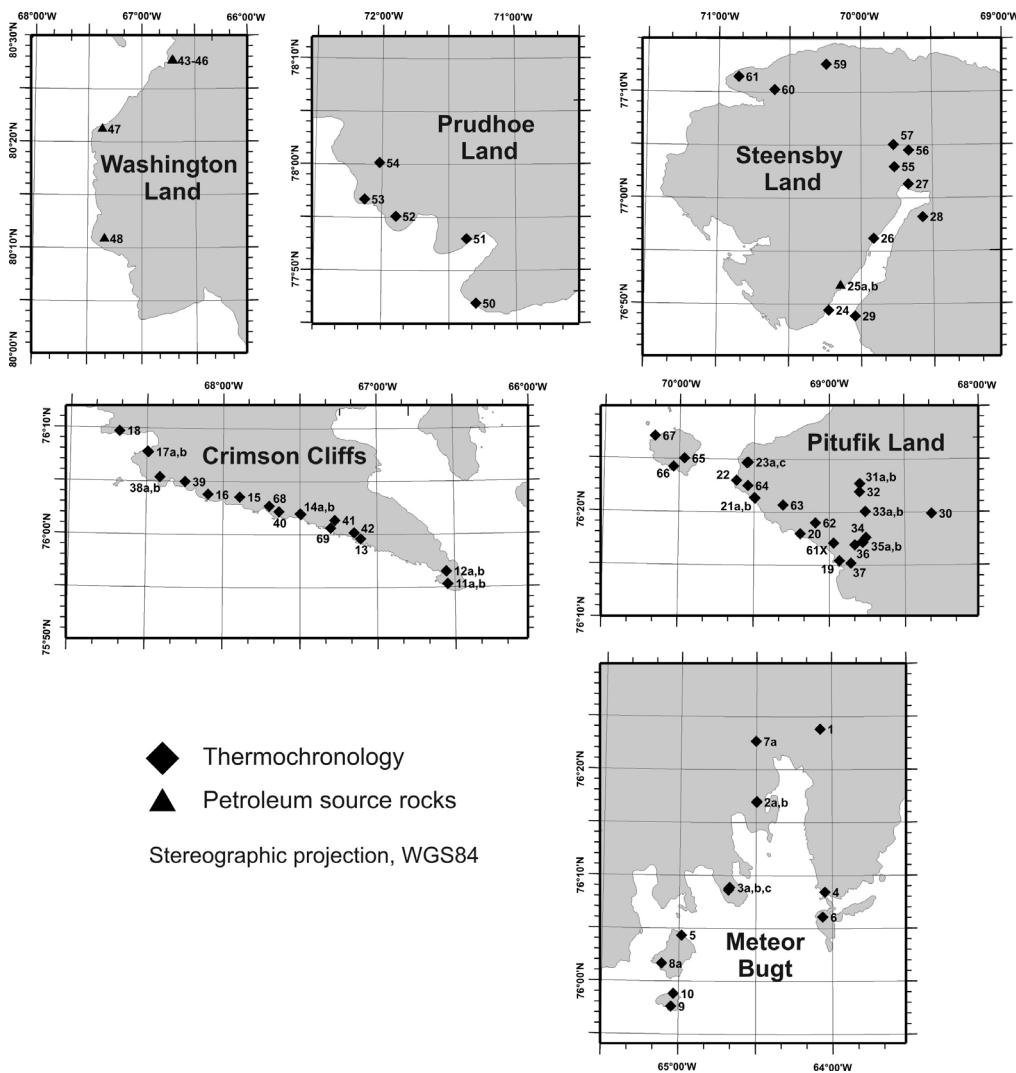


Fig. 14.1. Onshore sampling areas of cruise ARK-XXV/3.

15. JOINT INTERPRETATION OF KEY PROFILES AND DISCUSSION

Martin Block, Tabea Altenbernd, Kai Berglar, Volkmar Damm, Axel Ehrhardt,
Michael Schnabel
Bundesanstalt für Geowissenschaften und Rohstoffe

A comprehensive data set of multichannel reflection seismic (MCS) profiles with a total length of about 4,000 km have been acquired in the Greenland territorial waters of the central and northern Baffin Bay and the Kane Basin (Fig. 2.2). The MCS data set is spread out over the deep ocean basin, the Greenland continental margin and the adjacent shelf area. In the North of the Baffin Bay some of the profiles are covering the eastern Baffin Fan and the transition area to the Nares Strait. Two profiles with a total length of about 215 km were acquired further to the North in the Kane Basin. In the South the lines are tied to the MCS data acquired during cruise BGR08-3 (MSM09/3; Gohl et al., 2009) and in the North to the reflection seismic data from BGR cruise NARES01 (Neben et al., 2006) to integrate the new data with former surveys of BGR.

An initial onboard interpretation of the MCS data set was carried out to understand the plate tectonic history, the geology, and the structure of the margin as well as the adjacent shelf area. In particular, the aims were (1) to find an answer to the still debated question concerning the existence of oceanic crust in the Baffin Bay, (2) to distinguish the nature of the ocean-continent transition zone, and (3) to decipher the evolution of the sedimentary basins in this area.

GEOFRAME™ version 4.5 IESX, belonging to GeoQuest software products, was used as interpretation software. Seismic data was loaded from SEG-Y files. Both the common depth point (CDP) numbers and the shot point (SP) numbers were loaded from the trace headers. Navigation data were also provided in the SEG-Y trace headers. The projection used is UTM Zone 20, WGS84.

In this chapter a selection of profiles is presented as interpreted seismic sections and discussed.

15.1 Profile BGR10-306a

Line BGR10-306a crosses the Greenland slope North of about 73°N in an almost perpendicular direction and is running from SW to NE over the western shelf area. The interpreted 193 km long line is shown in Fig. 15.1. The profile is characterized by major basement blocks with sediment basins in between and a sedimentary cover of more than 1.9 s (TWT).

The highest basement blocks are located in the middle of the profile, one of them just below the shelf edge. In the SW an about 23 km wide basement block is present under the deep sea area near the foot of the slope. The top of the block is imaged by

a uniform reflector with high amplitudes and low frequencies and bounded to both sides by normal faults with large offsets.

The prominent reflector G4 is characterized by high amplitudes and relatively low frequencies and can be traced almost along the whole line. G4 onlaps on the highest basement blocks and is the top of the basin fill between the blocks. It is an erosional surface which is interpreted here as the breakup unconformity formed during the transition from rifting to drifting. The syn-rift sediments beneath G4 can be separated into two sequences, an early and late rift phase, after the seismic stratigraphy from Whittaker et al. (1997) and Harrison et al. (submitted). The early syn-rift succession was deposited in the Lower Cretaceous and the late syn-rift succession in Upper Cretaceous and Paleocene time. Both sequences could be well identified in the 2 s (TWT) deep syn-rift basin on the southwestern side of the line. The early syn-rift sequence is characterized by a divergent reflection pattern and bounded to the top by the folded unconformity G5.

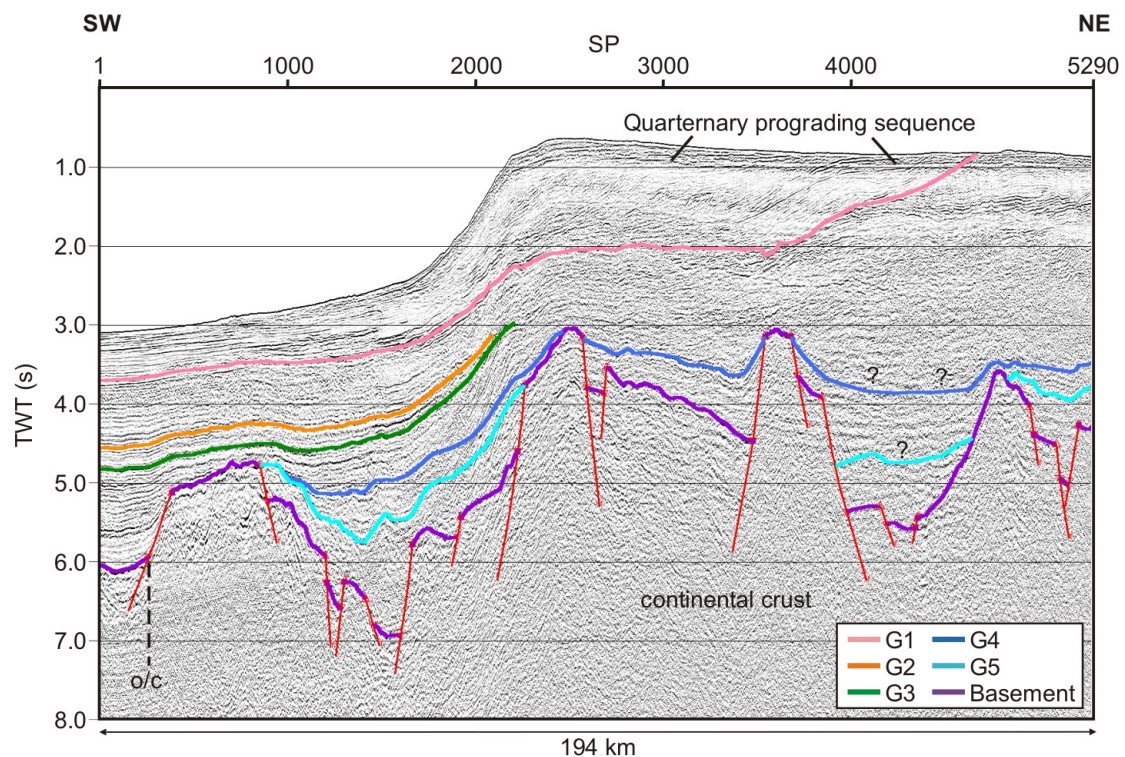


Fig. 15.1: Interpreted seismic line BGR10-306a showing the blockfaulted passive continental margin of Greenland, the breakup unconformity (G4), and the prominent Quarternary prograding sequence. See Fig. 2.2 for location.

A prominent sequence, bounded at its base by unconformity G1 and its top by the seafloor, extends from the deep sea to SP 4632 in the NE of the profile where the basal unconformity terminates at the seafloor. The sequence is characterized by a seaward prograding reflection pattern and is proposed to be of Quarternary age. Unconformity G1 could image the base of Pleistocene.

After a very preliminary correlation with ODP well 645, Reflector G2 could correspond to unconformity R1 (Srivastava et al., 1987) and therefore represents the base of Pliocene and reflector G3 could correspond to unconformity R2 which formed at the beginning of the middle Miocene. The reflectors G2 and G3 could not be recognized in the shelf area, probably masked by multiples.

The basement block beneath the deep sea area is classified here as a continental block due to its shape, the character of the top reflector, and the rift basin on its northeastern side. With respect to tie line BGR10-306, basement of oceanic nature is present at the southwestern end of the profile at about 6 s (TWT). Therefore the ocean-continent boundary can be placed here in a distance of 95 km from the shelf edge. The southwesternmost continental basement block and the breakup unconformity seaward of the shelf edge subsided considerably, probably due to cooling of the oceanic crust.

15.2 Profile BGR10-307/-307a

Profile BGR10-307 starts North of 74°N near the maritime boundary of Canada and Greenland from the lowermost Baffin-Fan and runs for 186 km to the SEE. The line traverses the deep water area of the Baffin Bay and ends just on the outermost Greenland shelf. After a small gap of about 3 km Profile BGR10-307a has been measured in the same direction and obliquely crosses the Greenland shelf for additional 187 km. The interpreted seismic lines are shown in Figures 15.2 and 15.3, respectively.

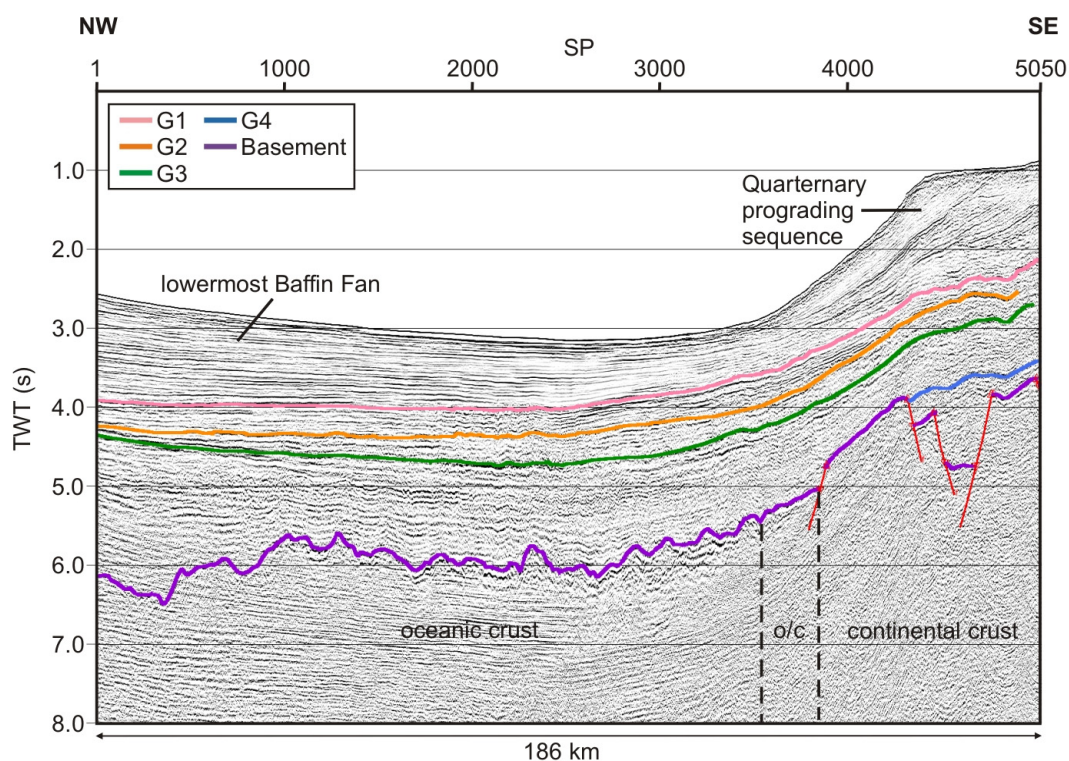


Fig. 15.2: Interpreted seismic line BGR10-307 showing the transition between the oceanic crust of the Baffin Bay and the continental crust of the Greenland Margin (o/c). See Fig. 2.2 for location.

Two different basement types are recognizable along line BGR10-307. In the deep sea area the basement could be identified easily by its high amplitude reflectors, the diffraction pattern, and the hummocky surface. These properties are typical for oceanic crust. The crust is lying in the range of 6.5 s (TWT) to 5.0 s (TWT). Under the slope and the outermost shelf block-faulted basement of continental nature is present, characterized by inclined plane reflection elements of high amplitudes and low frequencies which are separated by normal faults. The TWT to the rifted continental crust is in the range of about 5 s to 3.5 s. Along the profile the ocean-continent transition is defined quite well under the foot of the slope.

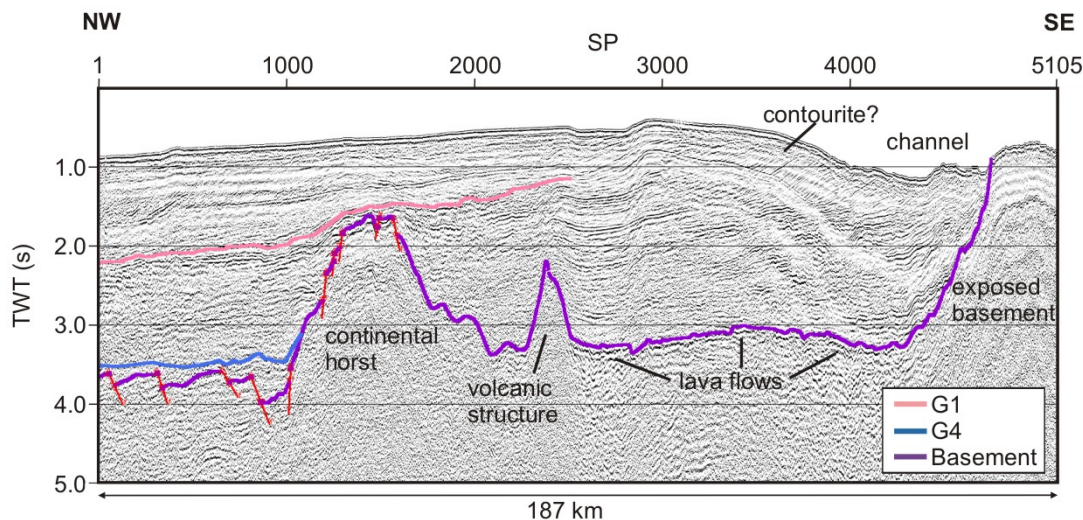


Fig. 15.3: Interpreted seismic line BGR10-307a showing the Tertiary flood basalts. See Fig. 2.2 for location.

In general, the thickness of the sediments deposited on the oceanic crust decreases from about 3.6 s (TWT) in the NWW to 2.4 s (TWT) at the ocean-continent transition due to the influence of the Baffin Fan which is a thick Eocene to Pleistocene sedimentary wedge located in the northwestern Baffin Bay (Harrison et al., submitted). The continental crust is covered by more than 2 s (TWT) thick sediments. The three regional reflectors G1, G2, and G3, which are discussed before under profile BGR10-306a, could be determined quite well along the line except under the shelf where the correlation is questionable. Under the shelf it was tried to correlate the breakup unconformity to get the boundary between syn-rift sediments and overlying Tertiary sequences. A seaward prograding sequence is present under the shelf and the slope.

The most prominent features along line BGR10-307a are two large basement highs and a volcanic structure in between. The anticlinal structure in the NW is about 1.8 s (TWT) high, about 40 km wide, and is buried by approximately by 1 s (TWT) thick sediments. Some normal faults on its NW flank and the character of its top reflector show that it is a continental horst. The other basement high is located in the SE at the end of the profile. There, the basement is outcropping at the seafloor. The high is associated with a positive magnetic anomaly but still it is not clear whether it is a

volcanic structure or a continental crustal block covered by thick lava flows. The high amplitude reflector connecting the large basement blocks at about 3 s (TWT) images the top of lava flows belonging to the submerged Paleocene Basalt Province described by Whittaker et al. (1997) and Storey et al. (1998). The flood basalt volcanism began in West Greenland between 60.9 and 61.3 Ma (Storey et al., 1998) and is associated with the beginning of seafloor spreading in the Baffin Bay. The depicted seavolcanic structure mount was formed by the same event. Probably Cretaceous rift basins are masked by the high reflective top of the flood basalts. The northern boundary of the flood basalt province is located at the southeastern flank of the buried continental horst, which is covered by lava flows. To the NW of the buried horst small scaled rifted continental crust exists in the range of 4.0 s to 3.6 s (TWT). Away from the basement highs the sediment cover is more than 2 s (TWT) thick. The maximum sediment thickness exceeds 3s (TWT) in the NW of the line, where the breakup unconformity continues from line BGR10-307 at around 3.5 s (TWT). Starting in the NW, unconformity G1 (base Pleistocene) was traced just over the buried volcanic structure. The other described reflectors on line BGR10-306 could not be identified on the onboard processed line due to strong multiples. The prograding sequence observed on line BGR10-307 continues on line BGR10-307a, but an outcropping of its basal unconformity could not be determined as on line BGR10-306a.

In the SE, the line crosses an about 38 km wide channel which is bounded by the outcropping high. The reflection pattern nearby could indicate current controlled sedimentation and subsequent erosion.

15.3 Profile BGR10-302/-302a

Line BGR10-302 runs for 123 km from the vicinity of the maritime boundary of Canada and Greenland somewhat North of 74°N to the NE and crosses profiles BGR10-307 and BGR10-313. The line ends shortly after the crossing point with BGR10-305a. Line BGR10-302a overlaps profile BGR10-302 for some kilometers and traverses the slope and the shelf of Greenland for 204 km, also in northeastern direction. The wide angle/refraction seismic traverse BGR10-3r2 was acquired during this cruise along both lines. The interpreted seismic lines are shown in Figures 15.4 and 15.5, respectively.

Line BGR10-302 covers the deep sea area from the lowermost Baffin Fan to the lowermost slope of Greenland. A 27 km wide and 1.7 s (TWT) high seamount is covered by sediments and is associated with a positive magnetic anomaly. The reflector imaging the basement in the SW of the seamount cannot easily be determined due to strong multiples. The hilly basement is located deeper than 5.5 s (TWT) and is assumed to be of oceanic nature also considering line BGR10-307. Northeast of the seamount the basement could be formed by lava flow series extruded during the formation of the seamount.

The sediments deposited on the oceanic crust during Tertiary time have an increasing thickness toward the Baffin Fan. They are approximately 2.7 s (TWT) thick at the southwestern foot of the seamount and 3.38 s (TWT) thick at the southwestern end of the profile. The Unconformities G1, G2 and G3, which are already described in

the foregoing pages, were determined by jump-correlation from line BGR10-306 on Line BGR10-312 and finally by correlation with line BGR10-313. G1 and G2 are interrupted by the seamount.

Line BGR10-302a is very complex due to the geology and plate tectonic events. Two large basement highs are crossed, one under the shelf edge and the other at the northeastern end of the line.

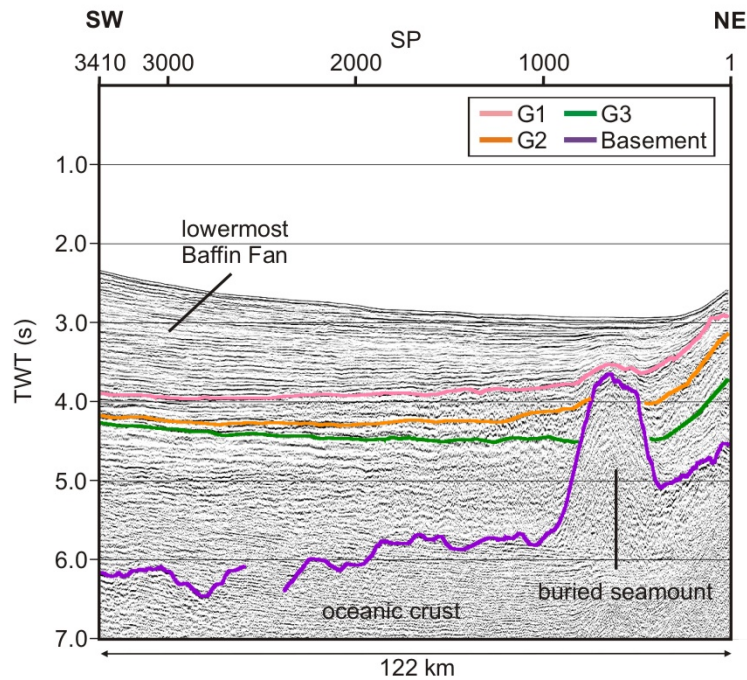


Fig. 15.4: Interpreted seismic line BGR10-302 showing the oceanic basement and a prominent buried seamount. See Fig. 2.2 for location.

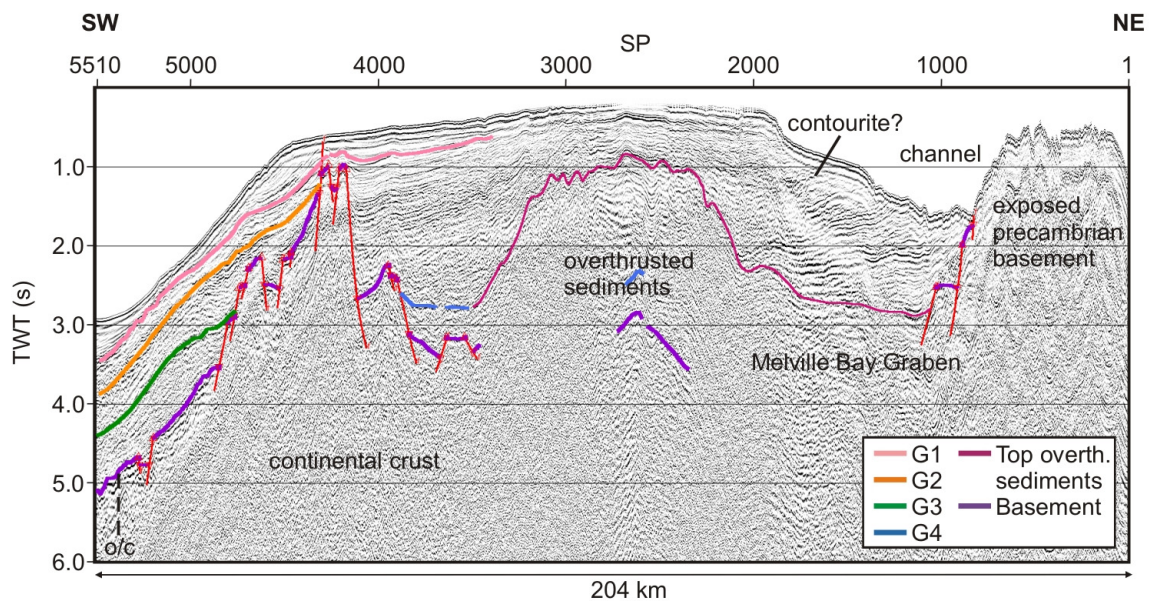


Fig. 15.5: Interpreted seismic line BGR10-302a showing that sediments from the Melville Bay Graben overthrust the western edge probably due to compression along the graben. See Fig. 2.2 for location.

The continental basement high under the shelf edge is about 50 km wide and intensively fractured by normal faults. The uppermost parts are covered by only 0.4 s (TWT) thick sediments. The other basement structure is exposed at the seafloor and has a rough surface. Precambrian rocks are outcropping there after Whittaker et al. (1997). Continental basement under the lower slope appears to be covered by lava flows probably extruded during the formation of the seamount on line BGR10-302. Therefore, the ocean continent transition is proposed to be located somewhere between the seamount on line BGR10-302 and the lowermost slope.

Two major sedimentary basins are present along line BGR10-302a. The Melville Bay Graben (Whittaker et al., 1997) is located in the NE of the line. After Whittaker et al. (1997) the graben is trending approximately NNW, is 30 - 90 km wide and is filled by at least 13,000 m of sediments. Along line BGR10-302a a reflection element was identified between 6 s and 7 s (TWT), but it is not clear whether it images the base of the graben or not. Other indications for the basement were not found on the onboard processed profile. The graben is bounded at the east by normal faults. The second basin is located east of the southwestern horst and is filled by sediments of more than 2.5 s (TWT) thickness. Due to multiples it was not possible to correlate the reflectors G2 and G3.

A 50 km wide domed structure in the middle of line BGR10-302a attracts attention. The structure is buried by less than 1 s (TWT) thick sediments only. Both flanks decline to nearly 3 s (TWT) without any indication of normal faulting. The top of the structure is intensively folded, and folding was also active at its northeastern flank. To the SW the structure has a chaotic internal reflection pattern, but in the other part internal folding of the layers and thrusting is recognizable. These properties and the character of the reflector forming its top and flanks show that it is not a basement structure. Probably it is an accretionary structure consisting mainly of overthrust sediments from the Melville Graben. Despite a questionable reflection element the basement is not recognizable under the structure. Probably the basement can be identified after further seismic processing and by the interpretation of the wide angle/refraction seismic data. After Oakey (2005) Greenland moved northward during the Eocene. Therefore it is proposed here that the folding and overthrusting was caused by compression along a left-lateral transform fault active during this movement of Greenland to the North. Consequently, the present top of the structure should be older than Oligocene. Minor folding is observed in the overlying sediments. An about 1.5 s (TWT) deep channel, which is bounded to the NE by the Precambrian basement high, cuts into the uppermost sedimentary sequence of the Melville Graben. The reflection pattern of this sequence could image current controlled sedimentation. The similarity to the erosion channel on line BGR10-307a is striking.

15.4 Profile BGR10-309

Profile BGR10-309 runs from the deep sea area South of 72°N for 285 km to the North crossing the slope of Greenland and traversing the shelf. Finally the line ends over the Melville Bay Graben. In the South the profile overlaps line BGR08-304 which was acquired during cruise MSM09/3 (Gohl et al., 2008). The location of line BGR10-

309 corresponds to the refraction/wide-angle reflection seismic line BGR10-3r4. The interpreted line BGR10-309 is shown in Figure 15.6.

In the southern half of line BGR10-309 a prominent basement reflector is located between 3 s and 5.5 s (TWT) under the deep sea area and the southern shelf which has indications for lava flows like smooth high amplitude reflectors and small scaled scarps probably imaging flow edges. Therefore the prominent reflector certainly images the top of the Paleocene Basalt Province (Whittaker et al., 1997). The lava flows were displaced by series of normal faults at two locations, one in the deep sea area and the other under the outer shelf. By the displacement half grabens developed over the flood basalts both with the normal faults to the South. The formation of half grabens indicates ongoing rifting after the flood basalt volcanism. Therefore the beginning of the drift phase and thus the oceanic crust of the Baffin Bay should be younger than the flood basalts. Another indicator for the different age between the flood basalts and the oceanic crust is the breakup unconformity (G4), which downlaps on the basement at the ocean-continent transition (Line BGR08-304) and which continues over the described half grabens. After Storey et al. (1998) the flood basalt volcanism was active between 61.3 Ma and 59.4 Ma. Consequently the onset of seafloor spreading in the Baffin Bay must be younger than ~60 Ma.

The reflector imaging the top of the Tertiary flood basalts can be correlated to the North with a gap of about 13 km in the middle of the line up to SP 5645. It can be assumed that the basaltic layer is masking rift grabens filled with Paleocene and Cretaceous sediments. Further to the North line BGR10-309 runs across the Melville Bay Graben. Due to multiples only some indications for intensive folding and thrusting are visible on the onboard processed seismic line probably caused by compression along a North-South trending transform fault which was active during the northward movement of Greenland.

An about 1 s (TWT) thick sequence characterized by a prograding reflection pattern is present under the outer shelf resting on unconformity G1 and bounded to the top by the seafloor.

In the northern half of the profile it is difficult to identify any reflector above the flood basalts and over the Melville Bay Graben due to multiples. Only just below the seafloor some weak indications for current controlled sedimentation are recognizable.

15.5 Profile BGR10-311

Profile BGR10-311 starts close to the maritime boundary of Canada and Greenland about 24 km North of 73°N and runs for 274 km to the NE over the deep ocean area, the slope of Greenland, and the Greenland shelf ending east of the Melville Bay Fault. The refraction/wide-angle reflection seismic line BGR10-3r1 was acquired along line BGR10-311 during this cruise. The interpreted seismic line is shown in Fig. 15.7.

The basement under the slope and shelf is block-faulted, and is typical for a passive continental margin. In the middle of the profile it was difficult to reliably identify the reflector imaging the basement. Under the southwestern part of the shelf the basement is located between 3.6 s and 4.3 s (TWT) and under the slope between 5 s and 6 s (TWT). In both areas the sedimentary cover is about 3 s (TWT) thick. At the

15 Joint interpretation of key profiles and discussion

eastern end of the line a horst forms the eastern margin of the Melville Bay Graben and continental crust is exposed at the seafloor. In the SW oceanic crust is present and the ocean-continent transition is located under the lowermost slope.

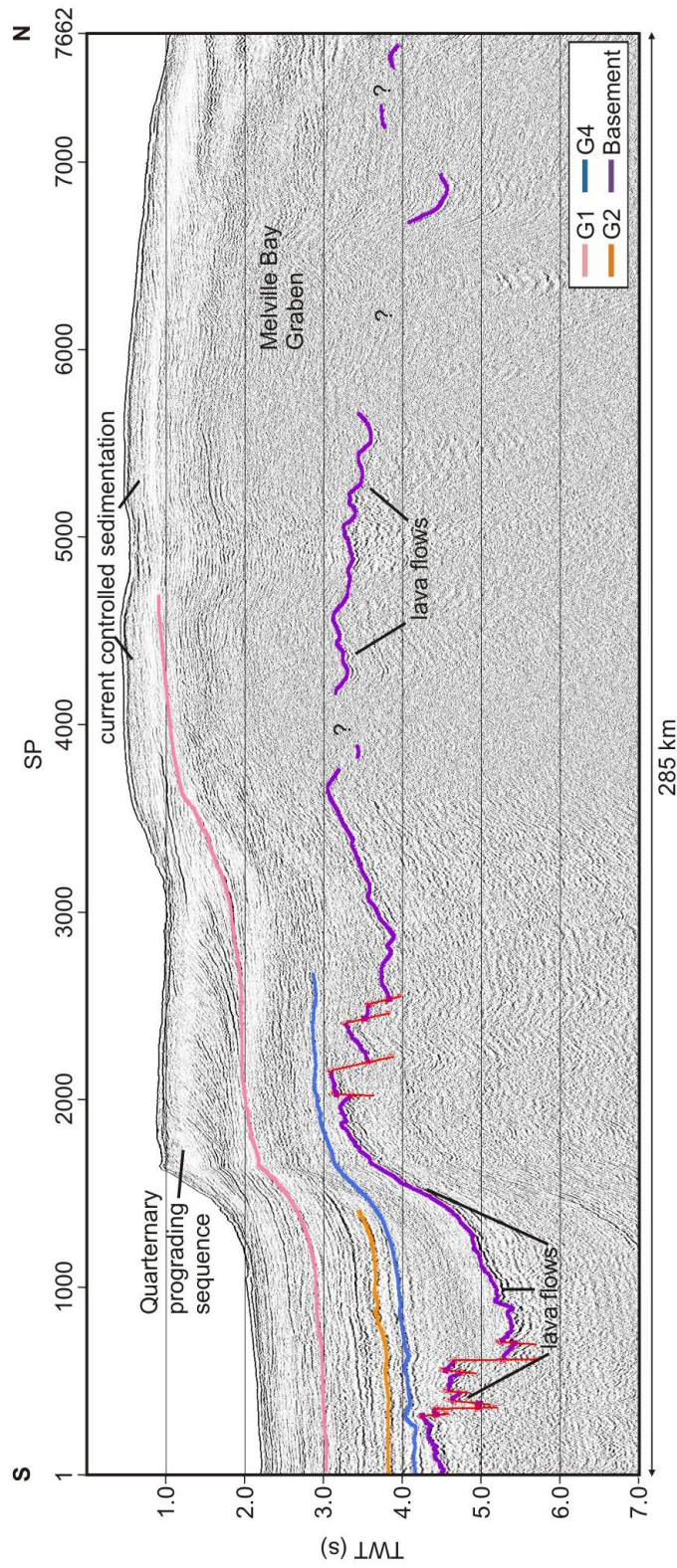


Fig. 15.6: Interpreted seismic line BGR10-309 crossing the Paleocene Basalt Province and the Melville Bay Graben and showing ongoing rifting after the flood basalt volcanism. G4 is the breakup unconformity. See Fig. 2.2 for location.

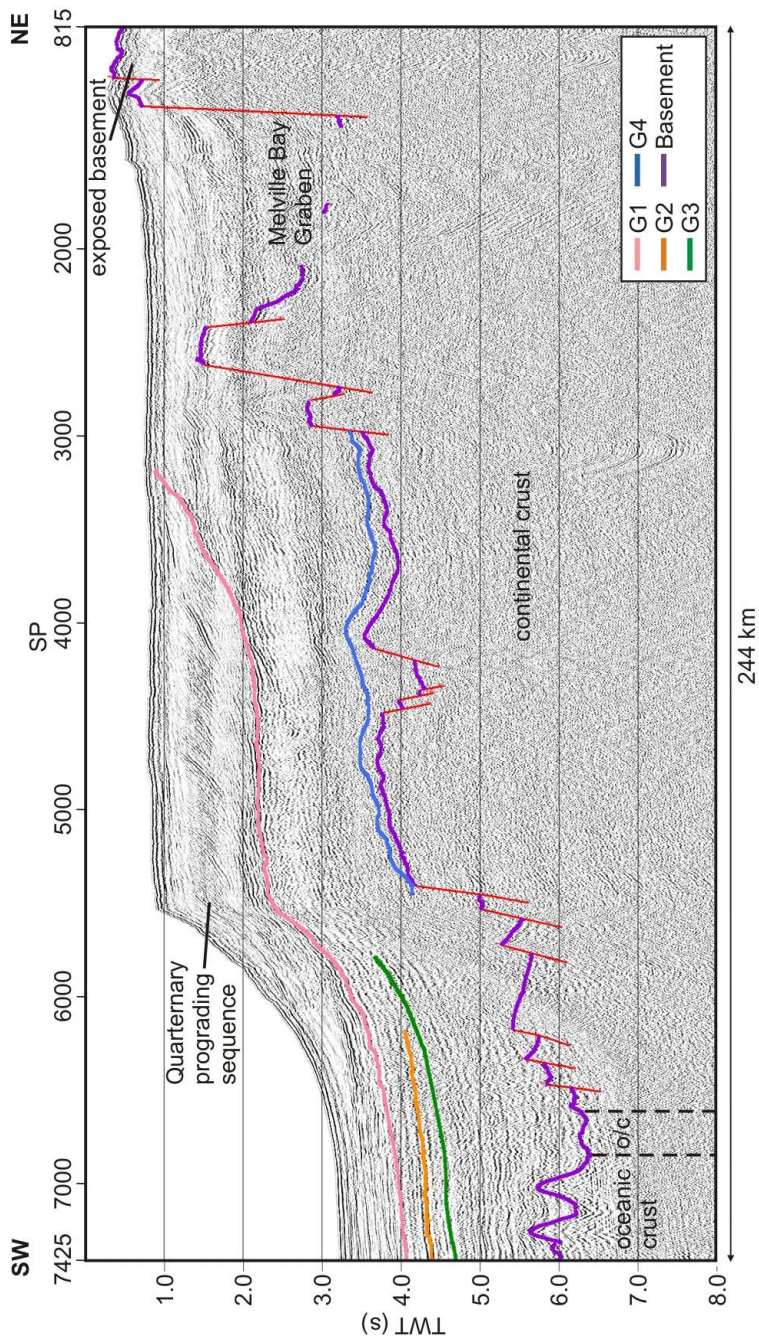


Fig. 15.7. Interpreted seismic line BGR10-311 crossing the ocean-continent transition, the blockfaulted continental crust and the Melville Bay Graben. See Fig. 2.2 for location.

The Melville Bay Graben is bounded to the west by a horst. The internal structure of the graben is indistinct on the seismic section due to the complex geology and the multiples. Also the basement could not be recognized, but it appears that the graben is filled by very thick sediments. Some folded reflection elements, deformed layering, and a folded layer at around 2 s (TWT) indicate that compression was active along the Melville Bay Graben. These properties of the Melville Bay Graben have already been observed along lines BGR10-309 and BGR10-302a and are discussed there. The folded layer could define the end of the compression in the Eocene.

A striking sequence with a prograding reflection pattern is located just below the outer shelf. The sequence is more than 1 s (TWT) thick, terminates at the seafloor about 120 km landward of the shelf edge, and is deposited in the Quarternary. The reflectors G2 and G3 could not be correlated under the shelf.

Results

- The MCS data show that oceanic crust is present in the deep water area of the Baffin Bay. Along some lines the ocean-continent transition could be identified.
- A breakup unconformity could be identified on some MCS lines formed during the transition from rifting to drifting. This unconformity defines the beginning of seafloor spreading in the Baffin Bay.
- A striking Quarternary sequence with prograding sedimentation is present just below the outer shelf.
- In the eastern Melville Bay a channel is crossed which is bounded to the east by the Melville Bay Fault and an exposed basement high. There are indications that a seismic unit probably formed by current controlled sedimentation is eroded along the channel.
- Compression was active in the Melville Bay Graben and sediments from the graben overthrust the western edge, probably caused by compression along a left-lateral transform fault active during the movement of Greenland to the North.
- Flood basalts of the Paleocene Basalt Province (Whittaker et al., 1997) were confirmed in the southern part of the area of investigation.
- The Tertiary flood basalts are older than the oceanic crust of the Baffin Bay.

16. CONCLUSIONS AND FUTURE WORK

Volkmar Damm

Bundesanstalt für Geowissenschaften und Rohstoffe

Due to the withdrawn Canadian research permission the operations during ARK-XXV/3 were restricted to Greenland territorial waters only. Therefore, parts of the objectives of the original working programme me could not be achieved. In particular, the acquisition of geophysical data along transects crossing the Canadian continental margin had to be cancelled. As a consequence there was no opportunity to tackle the problem of proving or disproving the existence of a plate boundary in northern Baffin Bay since some of the key areas for testing proposed plate kinematic models for the Paleocene-Eocene motion of Greenland relative to North America, in particular Lancaster Sound and Jones Sound could not be investigated.

It has to be the subject of a future project to acquire the necessary data for solving the still open questions.

Because of the synchronous operations of two seismic vessels (*R/V Polarstern* and *M/V Bergen Surveyor*) in the same survey area for most of the time operations had to be coordinated between the chief scientists of both parties. As a result of continuous negotiations the working plan had to be modified from time to time. Nevertheless, this could not prevent some interference of the seismic data.

All operations planned within the modified survey programme me were completed as per schedule and without any major technical problems or damages to any scientific equipment.

17. ACKNOWLEDGEMENTS

Volkmar Damm
Bundesanstalt für Geowissenschaften und Rohstoffe

After a 17 years break BGR Hannover was given the opportunity to use again *Polarstern* for a marine geoscientific research project in the polar regions. We experienced an excellent cooperation with the ship's master and crew, were perfectly assisted during our research operations and made use of an exemplary service. Many thanks go to Master Uwe Pahl and the whole crew of *Polarstern* for their support to complete our research programme me successfully and for making our stay onboard highly convenient and comfortable.

We would like to thank the crew of HeliService International for their assistance completing all airborne operations and the colleagues of the German Meteorological Service for continuously providing high resolution weather forecastings during the expedition.

We gratefully acknowledge the support of Prof. Karin Lochte, the AWI directorate and the cruise coordinator Dr. Eberhard Fahrbach in all issues of preparing and conducting our marine survey programme.

18. REFERENCES

- Andersen OB, Knudsen P, Berry P, Kenyon, S (2008). The DNSC08 ocean wide altimetry derived gravity field. Presented EGU-2008, Vienna, Austria, April, 2008.
- Chalmers JA, Pulvertaft TCR (2001). Development of the continental margins of the Labrador Sea: A review. In: RCL Wilson, RB Whitmarsh, B Taylor, N. Froitzheim (eds), Continental margins: a comparison of evidence from land and sea. Geol. Soc. London, Spec. Publ. 187: 77-105.
- Dawes PR (2009). Precambrian-Paleozoic geology of Smith Sound, Canada and Greenland: Key constraint to paleogeographic reconstructions of northern Laurentia and the North Atlantic region. *Terra Nova* 21, 1-13.
- Eilers G, Roeser HA, Kewitsch P (1994). Reduktion geomagnetischer Variationen durch ein Gradientenmagnetometer. BGR-Report 110.615, 1-73.
- Engels M, Barckhausen U, Gee JS (2008). A new towed vector magnetometer: Methods and results from a Central Pacific cruise. *Geophys. J. Int.*, 172, 115-129.
- Gohl K, Schreckenberger B, Funck T (2009). The expedition of the research vessel "Maria S. Merian" to the Davis Strait and Baffin Bay in 2008 (MSM09/3). Reports on Polar and Marine Research, 587, 99 pp., Alfred Wegener Institute for Polar and Marine Research, Bremerhaven, Germany.
- Harrison JC, Brent TA, Oakey GN (2010). Baffin Fan and its inverted rift system of Arctic eastern Canada: Stratigraphy, tectonics and petroleum resource potential. *GSL memoirs* 251, in print.
- Harrison JC (2006). In Search of the Wegener Fault: Re-Evaluation of Strike-Slip Displacements Along and Bordering Nares Strait. *Polarforschung*, 74, 129-160.
- Harrison JC, Brent TA, Oakey GN (2006). Overview of the bedrock geology of Nares Strait region, Arctic Canada and Greenland. GSC, Open File Report No. 5278.
- Hood P, Bower ME, Hardwick CD, Teskey DJ (1985). Direct geophysical evidence for displacement along Nares Strait (Canda-Greenland) from low-level aeromagnetic data: A progress report. *Current Research, Part A, Geol. Surv. Canada* 85-1A, 517-522.
- Jackson HR, Reid I (1994). Crustal thickness between the Greenland and Ellesmere Island margins determined from seismic refraction, *Ca. J. Earth Sci.*, 31, 1407-1418.
- JNCC (2004). Guidelines for minimizing acoustic disturbance to marine mammals from seismic surveys. www.jncc.gov.uk/marine, Joint Nature Conservation Committee, Aberdeen, 2004. 9 p.
- Keen CE, Barrett DL (1973). Structural Characteristics of some Sedimentary Basins in Northern Baffin Bay. *Geophys. J. Royal Astron. Soc.* 30; 253-271.
- Korenaga J (1995). Comprehensive analysis of marine magnetic vector anomalies. *J. Geophys. Res.*, 100 (B1), 365-378.
- Larsen HC, Saunders AD (1998). Tectonism and volcanism at the southeast Greenland rifted margin: A record of plume impact and later continental rupture. *Proc. ODP* 152, 503-533.

- Larsen LM, Heaman LM, Creaser RA, Duncan RA, Frei R, Hutchinson M (2009). Tectono-magmatic events during stretching and basin formation in the Labrador Sea and the Davis Strait: Evidence from Age and composition of Mesozoic to Palaeogene dyke swarms in West Greenland. *Journ. Geol. Soc.* 166, 999-1012
- Ludwig JW, Nafe JE, Drake CL (1970). Seismic refraction. in: AE Maxwell (Ed.), *The Sea*, Vol. 4, 53-84, Wiley, New York.
- MacLean B, Srivastava SP, Haworth RT (1982). Bedrock structures off Cumberland Sound, Baffin Island shelf: Core samples and geophysical data. In AF Embry and HR Balkwill (eds.), *Arctic geology and geophysics: Canadian Society of Petroleum Geologists Memoir* 8, 279-295.
- Morelli C (1974). The International Standardization Net 1971. *International Association of Geodesy Special Publication* 4, 194.
- Neben S, Damm V, Brent T, Tessensohn F (2006). New multi-channel seismic reflection data from Northwater Bay, Nares Strait: indications for pull-apart tectonics. *Polarforschung* 74/1-3, 77-96.
- Oakey GN, Stephenson R (2008). Crustal structure of the Innuitian region of Arctic Canada and Greenland from gravity modelling: implications for the Palaeogene Eurekan orogen. *Geophys. J. Int.*, 173, 1039-1063.
- Oakey GN, Chalmers J (2005). A new model for the Paleogene motion of Greenland relative to North America: A re-evaluation of the plate geometry of Baffin Bay. In: Chapter 4 of *Cenozoic evolution and lithosphere dynamics of the Baffin Bay - Nares Strait region of Arctic Canada and Greenland* (GN Oakey, ed.), Ph.D thesis, Free University of the Netherlands, Amsterdam, 64-91.
- Oakey GN (2005). *Cenozoic evolution and lithosphere dynamics of the Baffin Bay – Nares Strait region of Arctic Canada and Greenland*. PhD thesis, Dalhousie University, Wade Comp. Ltd., Halifax, 233 p.
- Oakey GN, Damaske D (2004). Continuity of basement structures and dyke swarms in the Kane Basin region of central Nares Strait constrained by aeromagnetic data. *Polarforschung*, 74 (1-3), 51-62.
- Parker RL, O'Brien MS (1997). Spectral analysis of vector magnetic field profiles. *J. Geophys. Res.*, 102 (B11), 24.815-24.824.
- Pollack HN, Hurter SJ, Johnson JR (1993). Heat flow from the earth's interior: Analysis of the global data set. *Reviews of Geophysics* 31(3), 267-280.
- Reid ID, Jackson HR (1997). Crustal structure of northern Baffin Bay: Seismic refraction results and tectonic implications. *J. Geophys. Res.* 102 (B1), 523-542.
- Roeser HA, Steiner C, Schreckenberger B, Block M (2002). Structural development of the Jurassic magnetic quiet zone off Morocco and identification of Middle Jurassic magnetic lineations. *Journal of Geophysical Research*, 107(B10), 2207.
- Sandwell DT, Smith WHF (2005). Retracking ERS-1 altimeter waveforms for optimal gravity field recovery. *Geophys. J. Int.*, 163, 79-89.
- Sandwell DT, Smith WHF (1997). Marine Gravity Anomaly from Geosat and ERS-1 Altimetry. *J. Geophys. Res.*, 102, pp. 10039-10054.
- Seama N, Nogi Y, Isezaki N (1993). A new method for precise determination of the position and strike of magnetic boundaries using vector data of the geomagnetic anomaly field. *Geophys. J. Int.*, 113, 155-164.

18 References

- Shipboard Scientific Party (2000). Explanatory notes. In: Plank T, Ludden JN, Escutia C, et al. (Eds): Proceedings of the Ocean Drilling Program, Initial Reports (College Station TX (Ocean Drilling Program)): 1–222 [Online].
- Skaarup N, Jackson HR, Oakey GN (2006). Margin segmentation of Baffin Bay/Davis Strait, eastern Canada, based on seismic reflection and potential field data. *Mar. Petr. Geol.*, 23, 127-144.
- Sleep NH, Fuyita K (1997). Principles of Geophysics. Blackwell Science, Malden, Mass..
- Srivastava SP, Arthur MA, Clement B., et al. (eds.), (1987). Proc. Init. Repts. (Pt. A), ODP, 105, College Station, TX (Ocean Drilling Program).
- Storey M, Duncan RA, Pedersen AK, Larsen LM, Larsen HC (1998). $^{40}\text{Ar}/^{39}\text{Ar}$ geochronology of the West Greenland Tertiary volcanic province. *Earth Planet. Sci. Lett.* 160, 569–586.
- Tessensohn F, von Gosen W, Piepjohn K, Saalman K, Mayr U (2008). Nares transform motion and Eureka compression along the northeast coast of Ellesmere island. In: *Geology of Northeast Ellesmere Island Adjacent to Kane Basin and Kennedy Channel, Nunavut*, U Mayr (ed.); Geological Survey of Canada, Bulletin 592, p 227-243.
- Tessensohn F, Jackson RH, Reid ID (2006). The Tectonic Evolution of Nares Strait: Implications of New Data. *Polarforschung* 74 (1-3), 191 – 198.
- Watts AB, Fairhead JD (1999). A process-oriented approach to modelling the gravity signature of continental margins. *Leading Edge*, 17, 258-263.
- Whittaker RC, Hamann NE, Pulvertaft TCR (1997). A new frontier province offshore Northwest Greenland: Structure, basin development, and petroleum potential of the Melville Bay area. *American Association of Petroleum Geologists Bulletin* 81, 978-998.

APPENDIX

- A.1 PARTICIPATING INSTITUTIONS**
- A.2 CRUISE PARTICIPANTS**
- A.3 SHIP'S CREW**
- A.4 STATION LIST**
- A.5 GEOPHYSICAL PROFILE LIST**
- A.5A EXEMPLARY PROCESSING WORK FLOW**
- A.6 OBS STATION LIST, PROFILE BGR10-3r1**
- A.7 OBS STATION LIST, PROFILE BGR10-3r2**
- A.8 OBS STATION LIST, PROFILE BGR10-3r3**
- A.9 OBS STATION LIST, PROFILE BGR10-3r4**
- A.10 LIST OF LAND STATIONS**
- A.11 SONOBUOY STATION LIST**
- A.12 HEAT FLOW STATION LIST**
- A.13 CORING STATION LIST**
- A.14 GAS GEOCHEMISTRY SAMPLING LIST**
- A.15 ONSHORE ROCK SAMPLING LIST**
- A.16 SUMMARY OF HELICOPTER OPERATIONS**
- A.17 WEEKLY MARINE MAMMAL OBSERVATION REPORTS**
- A.18 LIST OF FIGURES AND TABLES**

A.1 TEILNEHMENDE INSTITUTE / PARTICIPATING INSTITUTIONS

	Address
AWI	Stiftung Alfred-Wegener-Institut für Polar- und Meeresforschung in der Helmholtz-Gemeinschaft Am Handelshafen 12 27570 Bremerhaven Germany
BGR	Bundesanstalt für Geowissenschaften und Rohstoffe Stilleweg 2 30655 Hannover Germany
DWD	Deutscher Wetterdienst Geschäftsbereich Wettervorhersage Seeschiffahrtsberatung Bernhard Nocht Str. 76 20359 Hamburg Germany
GSC Atlantic	Geological Survey of Canada (Atlantic) Natural Resources Canada Earth Sciences Sector 1 Challenger Drive, Dartmouth, NS, B2Y 4A2 Canada
GSC Calgary	Geological Survey of Canada (Calgary) Natural Resources Canada 3303 – 33rd Street N.W. Calgary, Alberta T2L 2A7 Canada
HeliService	HeliService International GmbH Am Luneort 15 27572 Bremerhaven Germany
Laeisz	Reederei F. Laeisz (Bremerhaven) GmbH Brückenstrasse 25 27568 Bremerhaven Germany

A.1 Teilnehmende Institute / participating institutions

	Address
RPS Energy	Nelson House, Coombe Lane Axminster, Devon, EX 13 5 AX United Kingdom
UFZ	Helmholtz-Zentrum für Umweltforschung GmbH UFZ Permoserstr. 15 04318 Leipzig Germany
University Jena	Friedrich-Schiller-Universität Jena Burgweg 11 07749 Jena Germany

A.2 FAHRTTEILNEHMER / CRUISE PARTICIPANTS

Name/ Last name	Vorname/ First name	Institut/ Institute	Beruf/ Profession
Damm	Volkmar	BGR	Geophysicist, Chief Scientist
Adam	Jürgen	BGR	Technician
Algora	Camelia	UFZ	Biologist
Altenbernd	Tabea	BGR	Geoscientist
Bargeloh	Hans-Otto	BGR	Technician
Behrens	Thomas	BGR	Technician
Berglar	Kai	BGR	Geologist
Block	Martin	BGR	Geophysicist
Brauer	Jens	HeliService	Pilot / Mechanic
Brent	Thomas	GSC Calgary	Geologist
Buldt	Klaus	DWD	Meteorologist
Dufek	Tanja	AWI	Student, Geomatics
Ehrhardt	Axel	BGR	Geophysicist
Fossen	Drew	GSC Calgary	Student, Geosciences
Gossler	Jürgen	AWI	Geophysicist
Gründger	Friederike	BGR	Biologist
Hammrich	Klaus	HeliService	Pilot
Hegewald	Anne	AWI	Geophysicist
Heyde	Ingo	BGR	Geophysicist
Jauer	Christopher	GSC Atlantic	Geophysicist
Kallaus	Günter	BGR	Technician
Koch	Michael	University Jena	Student, Geology
Korger	Edith	AWI	Student, Geophysics
Läderach	Christine	AWI	Geophysicist
Möllendorf	Carsten	HeliService	Mechanic
Pitschmann	Dirk	BGR	Technician
Pletsch	Thomas	BGR	Geologist
Rentsch	Harald	DWD	Meteorologist
Rohardt	Ann-Kathrin	AWI	Student, Geodesy
Schmid	Florian	AWI	Student, Geosciences
Schmidt	Jörg	HeliService	Pilot
Schnabel	Michael	BGR	Geophysicist
Schrader	Uwe	BGR	Technician
Schreckenberger	Bernd	BGR	Geophysicist
Slabon	Patricia	AWI	Student, Geomatics
Steinbach	Volker	BGR	Geologist
Stelter	Sarah	RPS Energy	MMO
Suckro	Sonja	AWI	Geophysicist
Zeibig	Michael	BGR	Technician

A.3 SCHIFFSBESATZUNG / SHIP'S CREW

No.	Name	Rank
1.	Pahl, Uwe	Master
2.	Birnbaum, Tilo	1. Offc.
3.	Ziemann, Olaf	Ch. Eng.
4.	Hering, Igor	2. Offc.
5.	Janik, Michael	2. Offc.
6.	Reinstädler, Marco	2. Offc.
7.	Stüwe, Ursula	Doctor
8.	Koch, Georg	R. Offc.
9.	Kotnik, Herbert	2. Eng.
10.	Schnürch, Helmut	2. Eng.
11.	Westphal, Henning	2. Eng.
12.	Holtz, Hartmut	Elec. Eng.
13.	Dimmler, Werner	ELO
14.	Feiertag, Thomas	ELO
15.	Förb, Martin	ELO
16.	Nasis, Ilias	ELO
17.	Clasen, Burkhard	Boatsw.
18.	Neisner, Winfried	Carpenter
19.	Burzan, Gerd-Ekkehard	A.B.
20.	Hartwig-Labhan, Andreas	A.B.
21.	Kreis, Reinhard	A.B.
22.	Kretzschmar, Uwe	A.B.
23.	Moser, Siegfried	A.B.
24.	Schröder, Norbert	A.B.
25.	Schultz, Ottomar	A.B.
26.	Beth, Dethlef	Storek.
27.	Dinse, Horst	Mot-man
28.	Fritz, Günter	Mot-man
29.	Kliem, Peter	Mot-man
30.	Krösche, Eckard	Mot-man
31.	Watzel, Bernhard	Mot-man
32.	Fischer, Matthias	Cook
33.	Tupy, Mario	Cooksmate
34.	Völske, Thomas	Cooksmate
35.	Dinse, Petra	1. Stwdess
36.	Hennig, Christina	Stwdess/Nurse.
37.	Chen, Quan Lun	2. Steward
38.	Hischke, Peggy	2. Stwdess
39.	Möller, Wolfgang	2. Steward
40.	Streit, Christina	2. Stwdess
41.	Wartenberg, Irina	2. Stwdess
42.	Ruan, Hui Guang	Laundrym.

A.4 STATIONSLISTE / STATION LIST PS 76

Station	Date	Time	Position Lat	Position Lon	Depth [m]	Gear	Action	Comment
PS76/246-1	06.08.2010	13:12	64° 22.16' N	54° 43.53' W	613.5	Seismic reflection profile	profile start	Airgun im Wasser, Testbeginn
PS76/246-2	06.08.2010	13:48	64° 24.84' N	54° 47.66' W	414.3	Sonarboje	on ground/max depth	
PS76/246-1	06.08.2010	14:57	64° 29.97' N	54° 55.94' W	315.3	Seismic reflection profile	profile end	Testende
PS76/246-3	06.08.2010	15:29	64° 32.23' N	54° 59.58' W	324.9	Magnetic profile	on ground/max depth	auf 300m
PS76/246-3	06.08.2010	15:30	64° 32.30' N	54° 59.69' W	325.0	Magnetic profile	profile start	
PS76/246-3	06.08.2010	15:40	64° 32.99' N	55° 8.00' W	326.2	Magnetic profile	on ground/max depth	auf 850m
PS76/247-1	07.08.2010	16:01	67° 31.88' N	60° 7.17' W	1504.0	Magnetic Turn Circle	profile start	B.Schreckenberger
PS76/246-3	08.08.2010	10:34	69° 40.12' N	64° 11.33' W	1940.0	Magnetic profile	profile end	
PS76/248-1	08.08.2010	11:24	69° 41.66' N	64° 14.10' W	1929.0	Releaser Test	on ground/max depth	W 32.1 ; SLmax.: 1000m
PS76/248-2	08.08.2010	13:18	69° 41.59' N	64° 14.43' W	1926.0	CTD	on ground/max depth	1880 m, EL 31
PS76/248-3	08.08.2010	14:26	69° 41.58' N	64° 14.14' W	1928.0	Releaser Test	on ground/max depth	100 m, SE 32.1
PS76/248-4	08.08.2010	15:43	69° 41.49' N	64° 13.67' W	1930.0	Gravity corer	on ground/max depth	1890m, GE52.2
PS76/248-5	08.08.2010	16:48	69° 41.24' N	64° 13.14' W	1933.0	Releaser Test	on ground/max depth	SE 32.1 1000 m
PS76/248-6	08.08.2010	19:24	69° 39.14' N	64° 10.19' W	1936.0	Seismic reflection profile	on ground/max depth	300m ausgesteckt
PS76/249-1	08.08.2010	23:12	69° 34.32' N	63° 59.54' W	1915.0	Magnetic profile	on ground/max depth	800m ausgesteckt
PS76/249-1	08.08.2010	23:13	69° 34.44' N	63° 59.61' W	1916.0	Magnetic profile	profile start	Kurs 342 deg
PS76/249-1	08.08.2010	23:52	69° 38.60' N	64° 4.70' W	1950.0	Magnetic profile	profile end	
PS76/250-1	08.08.2010	23:52	69° 38.60' N	64° 4.70' W	1950.0	Magnetic profile	profile start	Kurs 008 deg
PS76/250-1	09.08.2010	05:29	70° 26.24' N	63° 44.22' W	2161.0	Magnetic profile	profile end	abgebrochen wegen Eislage
PS76/251-1	09.08.2010	09:39	70° 37.93' N	63° 38.44' W	2342.0	Magnetic profile	on ground/max depth	
PS76/251-1	09.08.2010	09:39	70° 37.93' N	63° 38.44' W	2342.0	Magnetic profile	profile start	
PS76/251-1	09.08.2010	13:07	71° 1.42' N	63° 28.77' W	2235.0	Magnetic profile	profile end	
PS76/252-1	09.08.2010	13:08	71° 1.54' N	63° 28.71' W	2235.0	Magnetic profile	alter course	88 Grad
PS76/252-1	09.08.2010	13:12	71° 1.80' N	63° 27.67' W	2237.0	Magnetic profile	profile start	
PS76/252-1	09.08.2010	15:17	71° 2.00' N	62° 42.55' W	2176.0	Magnetic profile	profile end	
PS76/253-1	09.08.2010	15:18	71° 1.99' N	62° 42.21' W	2175.0	Magnetic profile	alter course	188 Grad
PS76/253-1	09.08.2010	15:22	71° 1.67' N	62° 42.03' W	2170.0	Magnetic profile	profile start	
PS76/253-2	09.08.2010	18:39	70° 34.05' N	62° 54.01' W	2165.0	HeliMag	action	Profilbeginn
PS76/253-1	09.08.2010	18:46	70° 33.01' N	62° 54.46' W	2166.0	Magnetic profile	action	Unterbrechung des Profils

A.4 Stationsliste / station list PS 76

Station	Date	Time	Position Lat	Position Lon	Depth [m]	Gear	Action	Comment
PS76/253-1	09.08.2010	19:34	70° 33.22' N	62° 54.41' W	2167.0	Magnetic profile	action	weiter im Profil
PS76/253-2	09.08.2010	19:44	70° 31.86' N	62° 55.15' W	2164.0	HeliMag	action	Profil Ende
PS76/253-1	10.08.2010	04:05	69° 29.69' N	63° 20.82' W	2000.0	Magnetic profile	profile end	
PS76/254-1	10.08.2010	04:08	69° 29.24' N	63° 20.83' W	1999.0	Magnetic profile	profile start	
PS76/254-1	10.08.2010	07:03	69° 18.37' N	62° 14.48' W	1975.0	Magnetic profile	action	Kursaenderung auf 148
PS76/254-1	10.08.2010	07:50	69° 12.40' N	62° 4.78' W	1961.0	Magnetic profile	profile end	
PS76/255-1	10.08.2010	07:57	69° 12.30' N	62° 2.99' W	1960.0	Magnetic profile	profile start	
PS76/255-2	10.08.2010	15:09	70° 10.92' N	61° 37.83' W	1708.0	HeliMag	action	Profilanfang
PS76/255-2	10.08.2010	17:13	70° 29.29' N	61° 33.73' W	1561.0	HeliMag	action	Profil Ende
PS76/255-3	10.08.2010	19:51	70° 52.87' N	61° 24.28' W	1553.0	HeliMag	action	Profil Beginn
PS76/255-3	10.08.2010	21:16	71° 4.27' N	61° 19.43' W	1641.0	HeliMag	action	Profilende
PS76/255-1	10.08.2010	21:19	71° 4.54' N	61° 19.38' W	1645.0	Magnetic profile	profile end	
PS76/256-1	10.08.2010	23:29	71° 12.13' N	61° 38.08' W	1900.0	Heat Flow	on ground/max depth	W32.1 ; 1870m
PS76/256-2	11.08.2010	01:23	71° 12.13' N	61° 38.11' W	1904.0	Gravity corer	on ground/max depth	1860m, GE52.2
PS76/256-3	11.08.2010	04:10	71° 17.15' N	61° 50.03' W	2033.0	Seismic reflection profile	action	Beginn Walbeobachtung
PS76/256-3	11.08.2010	04:33	71° 18.23' N	61° 52.63' W	2053.0	Seismic reflection profile	on ground/max depth	Streamer mit 3900m ausgesetzt
PS76/256-4	11.08.2010	05:09	71° 20.51' N	61° 58.20' W	2098.0	Seismic reflection profile	action	erster Schuss
PS76/257-1	11.08.2010	05:10	71° 20.57' N	61° 58.35' W	2097.0	Seismic reflection profile	profile start	+PRM
PS76/257-1	11.08.2010	05:15	71° 20.89' N	61° 59.04' W	2107.0	Seismic reflection profile	action	Kursaenderung 332
PS76/257-1	12.08.2010	00:40	72° 42.78' N	64° 18.84' W	2312.0	Seismic reflection profile	profile end	
PS76/258-1	12.08.2010	00:51	72° 43.45' N	64° 20.56' W	2313.0	Seismic reflection profile	alter course	
PS76/258-1	12.08.2010	04:45	72° 39.92' N	64° 17.69' W	2312.0	Seismic reflection profile	action	Softstart / erster Schuss
PS76/258-2	12.08.2010	04:59	72° 40.79' N	64° 15.48' W	2310.0	Seismic reflection profile	profile start	
PS76/258-3	12.08.2010	15:05	73° 20.90' N	62° 46.09' W	458.4	HeliMag	on ground/max depth	Zielpunkterreicht, Sonde im Wasser
PS76/258-2	13.08.2010	02:48	74° 7.53' N	60° 57.43' W	625.3	Seismic reflection profile	profile end	Profil BGR 306A
PS76/259-1	13.08.2010	02:51	74° 7.72' N	60° 56.97' W	628.1	Seismic reflection profile	alter course	
PS76/259-1	13.08.2010	05:23	74° 6.06' N	61° 4.58' W	606.7	Seismic reflection profile	action	erster Schuss / Softstart

A.4 Stationsliste / station list PS 76

Station	Date	Time	Position Lat	Position Lon	Depth [m]	Gear	Action	Comment
PS76/259-2	13.08.2010	05:23	74° 6.06' N	61° 4.58' W	606.7	Seismic reflection profile	profile start	
PS76/259-3	13.08.2010	19:02	74° 27.80' N	64° 49.84' W	1568.0	Sonarboje	action	Abwurf durch Helicopter
PS76/259-2	14.08.2010	01:00	74° 37.26' N	66° 29.27' W	2176.0	Seismic reflection profile	profile end	
PS76/260-1	14.08.2010	01:12	74° 37.67' N	66° 32.36' W	2171.0	Seismic reflection profile	alter course	
PS76/260-1	14.08.2010	03:03	74° 39.92' N	66° 13.72' W	1948.0	Seismic reflection profile	action	Erster Schuss / Softstart
PS76/260-1	14.08.2010	03:58	74° 36.43' N	66° 21.03' W	2152.0	Seismic reflection profile	profile start	
PS76/260-2	14.08.2010	14:10	74° 11.05' N	68° 54.42' W	1985.0	HeliMag	action	Start Heliflug
PS76/260-2	14.08.2010	15:40	74° 7.24' N	69° 17.04' W	1876.0	HeliMag	on ground/max depth	Heli an Deck
PS76/261-1	14.08.2010	17:16	74° 3.22' N	69° 40.95' W	1734.0	Seismic reflection profile	profile end	
PS76/260-1	14.08.2010	17:16	74° 3.22' N	69° 40.95' W	1734.0	Seismic reflection profile	profile end	
PS76/261-2	14.08.2010	17:24	74° 2.99' N	69° 43.12' W	1744.0	Magnetic profile	profile end	
PS76/262-1	14.08.2010	21:01	74° 5.70' N	69° 26.34' W	1827.0	Ocean bottom seismometer	on ground/max depth	geslipt
PS76/263-1	14.08.2010	21:54	74° 9.37' N	69° 4.55' W	1939.0	Ocean bottom seismometer	on ground/max depth	
PS76/264-1	14.08.2010	22:42	74° 13.01' N	68° 42.84' W	2013.0	Ocean bottom seismometer	on ground/max depth	geslipt
PS76/265-1	14.08.2010	23:32	74° 16.68' N	68° 20.77' W	2063.0	Ocean bottom seismometer	on ground/max depth	geslipt
PS76/266-1	15.08.2010	00:33	74° 20.36' N	67° 58.83' W	2129.0	Ocean bottom seismometer	on ground/max depth	
PS76/267-1	15.08.2010	01:30	74° 24.07' N	67° 36.53' W	2157.0	Ocean bottom seismometer	on ground/max depth	
PS76/268-1	15.08.2010	02:24	74° 27.76' N	67° 14.65' W	2175.0	Ocean bottom seismometer	on ground/max depth	
PS76/269-1	15.08.2010	03:24	74° 31.43' N	66° 52.34' W	2198.0	Ocean bottom seismometer	on ground/max depth	
PS76/271-1	15.08.2010	05:02	74° 38.26' N	66° 10.64' W	1967.0	Ocean bottom seismometer	on ground/max depth	geslipt
PS76/272-1	15.08.2010	06:04	74° 42.43' N	65° 45.26' W	1213.0	Ocean bottom seismometer	on ground/max depth	geslipt
PS76/273-1	15.08.2010	06:57	74° 46.14' N	65° 22.61' W	539.6	Ocean bottom seismometer	on ground/max depth	geslipt
PS76/274-1	15.08.2010	07:52	74° 49.80' N	64° 59.84' W	414.3	Ocean bottom seismometer	on ground/max depth	geslipt

A.4 Stationsliste / station list PS 76

Station	Date	Time	Position Lat	Position Lon	Depth [m]	Gear	Action	Comment
PS76/275-1	15.08.2010	08:47	74° 53.51' N	64° 36.85' W	343.1	Ocean bottom seismometer	on ground/max depth	geslipt
PS76/276-1	15.08.2010	09:38	74° 57.23' N	64° 14.16' W	289.1	Ocean bottom seismometer	on ground/max depth	geslipt
PS76/277-1	15.08.2010	10:38	75° 0.90' N	63° 51.16' W	157.7	Gravity corer	on ground/max depth	GE52.2 , 160m
PS76/277-2	15.08.2010	10:53	75° 0.89' N	63° 51.13' W	157.6	Ocean bottom seismometer	on ground/max depth	geslipt
PS76/278-1	15.08.2010	11:45	75° 4.66' N	63° 28.08' W	129.5	Ocean bottom seismometer	on ground/max depth	geslipt
PS76/279-1	15.08.2010	12:40	75° 8.20' N	63° 5.11' W	152.0	Gravity corer	on ground/max depth	154 m, GE 52.2
PS76/279-2	15.08.2010	12:54	75° 8.23' N	63° 5.03' W	152.6	Ocean bottom seismometer	on ground/max depth	
PS76/280-1	15.08.2010	13:52	75° 11.93' N	62° 41.90' W	190.3	Gravity corer	on ground/max depth	190 m, GE 52.2
PS76/280-2	15.08.2010	14:06	75° 11.87' N	62° 41.83' W	188.8	Ocean bottom seismometer	on ground/max depth	
PS76/281-1	15.08.2010	14:58	75° 15.56' N	62° 18.22' W	593.7	Ocean bottom seismometer	on ground/max depth	
PS76/282-1	15.08.2010	16:04	75° 19.24' N	61° 55.17' W	924.4	Gravity corer	on ground/max depth	GE 52.2 908m
PS76/282-2	15.08.2010	16:27	75° 19.28' N	61° 55.17' W	923.8	Ocean bottom seismometer	on ground/max depth	geslipt
PS76/283-1	15.08.2010	17:18	75° 22.92' N	61° 31.35' W	1187.0	Ocean bottom seismometer	on ground/max depth	geslipt
PS76/284-1	15.08.2010	18:20	75° 26.65' N	61° 7.76' W	436.0	Gravity corer	on ground/max depth	GE 52.2 421m
PS76/284-2	15.08.2010	18:35	75° 26.65' N	61° 7.75' W	436.8	Ocean bottom seismometer	on ground/max depth	geslipt
PS76/285-1	15.08.2010	19:28	75° 30.34' N	60° 44.17' W	393.5	Ocean bottom seismometer	on ground/max depth	geslipt
PS76/286-1	15.08.2010	20:29	75° 33.97' N	60° 20.23' W	476.2	Gravity corer	on ground/max depth	453m, GE52.2
PS76/287-1	15.08.2010	21:13	75° 32.34' N	60° 30.52' W	471.9	Ocean bottom seismometer	on ground/max depth	geslipt
PS76/288-1	15.08.2010	22:07	75° 32.44' N	60° 38.27' W	451.7	Seismic refraction profile	action	1. Schuss, Beginn Softstart
PS76/288-2	15.08.2010	22:47	75° 32.46' N	60° 30.37' W	468.4	Seismic refraction profile	profile start	Verantw. Uwe Schrader
PS76/288-2	17.08.2010	09:10	74° 2.52' N	69° 45.12' W	1719.0	Seismic refraction profile	profile end	
PS76/290-1	17.08.2010	10:11	74° 1.35' N	69° 45.08' W	1721.0	Gravity corer	on ground/max depth	GE52.2 1680 m
PS76/291-1	17.08.2010	12:15	73° 58.70' N	69° 1.94' W	1966.0	Ocean bottom seismometer	on ground/max depth	
PS76/292-1	17.08.2010	13:49	74° 3.92' N	68° 38.41' W	2057.0	Gravity corer	on ground/max depth	2012 m, GE 52.2

A.4 Stationsliste / station list PS 76

Station	Date	Time	Position Lat	Position Lon	Depth [m]	Gear	Action	Comment
PS76/292-2	17.08.2010	14:26	74° 3.92' N	68° 38.53' W	2058.0	Ocean bottom seismometer	on ground/max depth	
PS76/293-1	17.08.2010	16:05	74° 13.50' N	68° 45.54' W	2001.0	Gravity corer	on ground/max depth	GE 52.2 1957m
PS76/293-2	17.08.2010	16:42	74° 13.52' N	68° 45.50' W	2002.0	Ocean bottom seismometer	on ground/max depth	geslipt
PS76/294-1	17.08.2010	18:37	74° 14.23' N	69° 36.55' W	1757.0	Gravity corer	on ground/max depth	GE52.2 1721m
PS76/294-2	17.08.2010	19:13	74° 14.24' N	69° 36.63' W	1759.0	Ocean bottom seismometer	on ground/max depth	geslipt
PS76/294-3	17.08.2010	21:34	74° 12.10' N	69° 15.57' W	1879.0	Seismic reflection profile	action	Walbeobachter auf Brueke
PS76/294-3	17.08.2010	21:49	74° 11.81' N	69° 12.05' W	1900.0	Seismic reflection profile	on ground/max depth	3900 m ausgesetzt
PS76/294-6	17.08.2010	21:58	74° 11.58' N	69° 9.61' W	1914.0	Seismic reflection profile	action	1. Schuss
PS76/294-5	17.08.2010	22:03	74° 11.47' N	69° 8.32' W	1920.0	Magnetic profile	profile start	
PS76/294-6	17.08.2010	22:15	74° 11.15' N	69° 5.15' W	1938.0	Seismic reflection profile	profile start	
PS76/294-5	17.08.2010	22:38	74° 10.52' N	68° 58.82' W	1972.0	Magnetic profile	profile end	
PS76/294-5	17.08.2010	23:16	74° 9.52' N	68° 48.42' W	2015.0	Magnetic profile	profile start	
PS76/294-7	18.08.2010	14:12	73° 45.27' N	64° 45.66' W	1742.0	Sonarboje	on ground/max depth	Boje ausgesetzt
PS76/294-6	18.08.2010	19:02	73° 37.63' N	63° 27.39' W	647.4	Seismic reflection profile	profile end	
PS76/294-6	18.08.2010	19:21	73° 37.14' N	63° 22.50' W	641.3	Seismic reflection profile	profile start	erster Schuss
PS76/294-6	19.08.2010	16:38	73° 3.01' N	57° 50.09' W	578.4	Seismic reflection profile	profile end	
PS76/294-5	19.08.2010	16:38	73° 3.01' N	57° 50.09' W	578.4	Magnetic profile	profile end	
PS76/295-1	19.08.2010	17:48	73° 5.89' N	57° 47.98' W	363.4	Seismic reflection profile	profile start	softstart
PS76/295-3	19.08.2010	18:30	73° 3.88' N	57° 56.85' W	500.9	Seismic reflection profile	profile start	Airgun/Streame r/ PRM
PS76/295-4	19.08.2010	18:42	73° 3.12' N	57° 58.89' W	569.5	Magnetic profile	profile start	
PS76/295-3	20.08.2010	01:00	72° 39.43' N	59° 1.36' W	184.8	Seismic reflection profile	profile end	
PS76/295-3	20.08.2010	02:10	72° 36.03' N	59° 10.23' W	199.6	Seismic reflection profile	alter course	
PS76/295-3	20.08.2010	05:18	72° 43.34' N	58° 49.20' W	175.9	Seismic reflection profile	action	Softstart
PS76/295-3	20.08.2010	05:31	72° 42.91' N	58° 52.20' W	180.1	Seismic reflection profile	profile start	

A.4 Stationsliste / station list PS 76

Station	Date	Time	Position Lat	Position Lon	Depth [m]	Gear	Action	Comment
PS76/295-4	20.08.2010	05:45	72° 42.06' N	58° 54.47' W	174.6	Magnetic profile	profile start	850m ausgesteckt
PS76/296-1	20.08.2010	20:21	71° 46.97' N	61° 14.89' W	1688.0	Seismic reflection profile	profile end	letzter Schuss
PS76/296-2	20.08.2010	22:02	71° 45.89' N	61° 10.24' W	1629.0	Seismic reflection profile	action	1.Schuss
PS76/296-3	20.08.2010	22:37	71° 48.55' N	61° 10.92' W	1635.0	Seismic reflection profile	profile start	Kurs 011 deg.
PS76/295-4	22.08.2010	05:57	74° 17.02' N	59° 35.56' W	783.6	Magnetic profile	profile end	
PS76/296-3	22.08.2010	05:57	74° 17.02' N	59° 35.56' W	783.6	Seismic reflection profile	profile end	
PS76/297-1	22.08.2010	06:15	74° 18.08' N	59° 32.35' W	800.2	Seismic reflection profile	profile start	
PS76/297-2	22.08.2010	06:15	74° 18.08' N	59° 32.35' W	800.2	Magnetic profile	profile start	
PS76/297-3	22.08.2010	06:27	74° 18.15' N	59° 28.91' W	809.1	Sonarboje	in the water	
PS76/297-1	22.08.2010	12:28	74° 13.13' N	57° 43.24' W	160.9	Seismic reflection profile	profile end	
PS76/297-2	22.08.2010	12:36	74° 12.97' N	57° 41.18' W	335.8	Magnetic profile	profile end	
PS76/298-1	22.08.2010	12:38	74° 12.89' N	57° 40.69' W	406.4	Seismic reflection profile	alter course	Line change, 246 Grad
PS76/298-2	22.08.2010	12:38	74° 12.89' N	57° 40.69' W	406.4	Magnetic profile	alter course	Line change, 246 Grad
PS76/298-1	22.08.2010	13:38	74° 14.38' N	57° 42.34' W	768.8	Seismic reflection profile	action	Softstart, 1. Schuss
PS76/298-1	22.08.2010	14:12	74° 13.28' N	57° 51.06' W	312.0	Seismic reflection profile	profile start	
PS76/298-2	22.08.2010	14:12	74° 13.28' N	57° 51.06' W	312.0	Magnetic profile	profile start	
PS76/298-1	23.08.2010	20:33	73° 12.95' N	65° 43.88' W	2402.0	Seismic reflection profile	profile end	
PS76/298-2	23.08.2010	20:33	73° 12.95' N	65° 43.88' W	2402.0	Magnetic profile	profile end	
PS76/298-2	23.08.2010	20:47	73° 12.16' N	65° 46.84' W	2404.0	Magnetic profile	alter course	310 deg
PS76/299-2	23.08.2010	22:17	73° 10.03' N	65° 33.06' W	2396.0	Seismic reflection profile	action	1. Schuss, Softstart
PS76/299-3	23.08.2010	23:13	73° 14.00' N	65° 37.59' W	2394.0	Seismic reflection profile	profile start	Kurs 310 deg
PS76/299-4	23.08.2010	23:13	73° 14.00' N	65° 37.59' W	2394.0	Magnetic profile	profile start	
PS76/299-3	24.08.2010	12:36	73° 55.26' N	68° 32.62' W	2087.0	Seismic reflection profile	profile end	
PS76/299-4	24.08.2010	12:36	73° 55.26' N	68° 32.62' W	2087.0	Magnetic profile	profile end	
PS76/300-1	24.08.2010	12:42	73° 55.63' N	68° 33.68' W	2080.0	Seismic reflection profile	alter course	346 Grad

A.4 Stationsliste / station list PS 76

Station	Date	Time	Position Lat	Position Lon	Depth [m]	Gear	Action	Comment
PS76/300-2	24.08.2010	12:42	73° 55.63' N	68° 33.68' W	2080.0	Magnetic profile	alter course	346 Grad
PS76/300-1	24.08.2010	12:58	73° 56.72' N	68° 36.00' W	2068.0	Seismic reflection profile	profile start	
PS76/300-2	24.08.2010	12:58	73° 56.72' N	68° 36.00' W	2068.0	Magnetic profile	profile start	
PS76/300-1	25.08.2010	01:56	74° 56.98' N	69° 33.94' W	999.8	Seismic reflection profile	profile end	
PS76/300-2	25.08.2010	01:56	74° 56.98' N	69° 33.94' W	999.8	Magnetic profile	profile end	
PS76/302-1	25.08.2010	11:14	74° 5.28' N	69° 26.71' W	1820.7	Ocean bottom seismometer	information	aufgetaucht
PS76/302-1	25.08.2010	11:30	74° 5.43' N	69° 26.02' W	1824.8	Ocean bottom seismometer	on deck	
PS76/302-2	25.08.2010	12:24	74° 5.40' N	69° 26.21' W	1823.8	Heat Flow	on ground/max depth	1797 m, GE 52.1
PS76/303-1	25.08.2010	15:06	74° 9.45' N	69° 4.69' W	1933.1	Ocean bottom seismometer	action	aufgetaucht
PS76/303-1	25.08.2010	15:30	74° 9.22' N	69° 4.71' W	1933.5	Ocean bottom seismometer	on deck	
PS76/304-1	25.08.2010	17:22	74° 12.81' N	68° 42.33' W	2009.2	Ocean bottom seismometer	action	aufgetaucht
PS76/304-1	25.08.2010	17:41	74° 12.78' N	68° 42.47' W	2007.5	Ocean bottom seismometer	on deck	
PS76/305-1	25.08.2010	19:32	74° 16.51' N	68° 20.85' W	2055.7	Ocean bottom seismometer	action	aufgetaucht
PS76/305-1	25.08.2010	19:58	74° 16.67' N	68° 20.28' W	2058.0	Ocean bottom seismometer	on deck	
PS76/306-1	25.08.2010	21:44	74° 20.29' N	67° 59.02' W	2121.7	Ocean bottom seismometer	at surface	aufgetaucht
PS76/306-1	25.08.2010	21:53	74° 20.42' N	67° 58.56' W	2096.0	Ocean bottom seismometer	on deck	
PS76/306-2	25.08.2010	22:50	74° 20.47' N	67° 58.63' W	2121.9	Heat Flow	on ground/max depth	GE52.1 2089 m
PS76/307-1	26.08.2010	01:41	74° 24.12' N	67° 36.14' W	2153.0	Ocean bottom seismometer	action	aufgetaucht
PS76/307-1	26.08.2010	02:00	74° 24.16' N	67° 36.69' W	2150.8	Ocean bottom seismometer	on deck	
PS76/308-1	26.08.2010	03:59	74° 27.54' N	67° 14.54' W	2171.7	Ocean bottom seismometer	action	aufgetaucht
PS76/308-1	26.08.2010	04:25	74° 27.64' N	67° 15.51' W	2170.0	Ocean bottom seismometer	on deck	
PS76/308-2	26.08.2010	05:20	74° 27.56' N	67° 15.54' W	2170.7	Heat Flow	on ground/max depth	GE 52.1 2140m
PS76/309-1	26.08.2010	08:13	74° 31.52' N	66° 52.33' W	2190.6	Ocean bottom seismometer	at surface	aufgetaucht

A.4 Stationsliste / station list PS 76

Station	Date	Time	Position Lat	Position Lon	Depth [m]	Gear	Action	Comment
PS76/309-1	26.08.2010	08:23	74° 31.44' N	66° 52.79' W	2190.0	Ocean bottom seismometer	on deck	
PS76/309-2	26.08.2010	09:18	74° 31.49' N	66° 52.52' W	2190.1	Heat Flow	on ground/max depth	GE52.1 21 m
PS76/310-1	26.08.2010	12:04	74° 35.27' N	66° 30.21' W	2188.3	Ocean bottom seismometer	action	aufgetaucht
PS76/310-1	26.08.2010	12:17	74° 35.28' N	66° 31.03' W	2187.9	Ocean bottom seismometer	on deck	
PS76/310-2	26.08.2010	13:18	74° 35.33' N	66° 31.03' W	2187.0	Heat Flow	on ground/max depth	2152 m, GE 52.1
PS76/311-1	26.08.2010	16:10	74° 38.85' N	66° 7.76' W	1856.0	Ocean bottom seismometer	at surface	aufgetaucht
PS76/311-1	26.08.2010	16:21	74° 38.77' N	66° 8.13' W	1871.0	Ocean bottom seismometer	on deck	
PS76/312-1	26.08.2010	17:50	74° 42.37' N	65° 44.91' W	1203.5	Ocean bottom seismometer	at surface	
PS76/312-1	26.08.2010	18:05	74° 42.40' N	65° 45.50' W	1212.8	Ocean bottom seismometer	on deck	
PS76/312-2	26.08.2010	18:52	74° 42.44' N	65° 45.28' W	1207.5	Heat Flow	on ground/max depth	GE52.1 1193m
PS76/313-1	26.08.2010	20:56	74° 46.06' N	65° 22.84' W	541.4	Ocean bottom seismometer	at surface	aufgetaucht
PS76/313-1	26.08.2010	21:10	74° 46.00' N	65° 23.36' W	551.4	Ocean bottom seismometer	on deck	
PS76/314-1	26.08.2010	22:17	74° 49.88' N	65° 0.18' W	413.5	Ocean bottom seismometer	at surface	aufgetaucht
PS76/314-1	26.08.2010	22:23	74° 49.77' N	65° 0.10' W	415.4	Ocean bottom seismometer	on deck	
PS76/315-1	26.08.2010	23:31	74° 53.47' N	64° 36.81' W	340.9	Ocean bottom seismometer	at surface	
PS76/315-1	26.08.2010	23:40	74° 53.47' N	64° 37.28' W	341.6	Ocean bottom seismometer	on deck	
PS76/316-1	27.08.2010	00:48	74° 57.32' N	64° 14.24' W	287.1	Ocean bottom seismometer	at surface	aufgetaucht, Hydrofon an Deck
PS76/316-1	27.08.2010	01:03	74° 57.19' N	64° 14.59' W	284.1	Ocean bottom seismometer	on deck	
PS76/317-1	27.08.2010	02:16	75° 0.86' N	63° 51.03' W	157.2	Ocean bottom seismometer	at surface	Hydrophon an Deck, aufgetaucht
PS76/317-1	27.08.2010	02:26	75° 0.84' N	63° 51.33' W	157.7	Ocean bottom seismometer	on deck	
PS76/318-1	27.08.2010	03:30	75° 4.57' N	63° 28.14' W	132.5	Ocean bottom seismometer	at surface	Hydrophon an Deck, aufgetaucht
PS76/318-1	27.08.2010	03:42	75° 4.68' N	63° 28.27' W	132.7	Ocean bottom seismometer	on deck	

A.4 Stationsliste / station list PS 76

Station	Date	Time	Position Lat	Position Lon	Depth [m]	Gear	Action	Comment
PS76/319-1	27.08.2010	04:45	75° 8.11' N	63° 5.38' W	153.4	Ocean bottom seismometer	at surface	
PS76/319-1	27.08.2010	05:00	75° 8.19' N	63° 5.14' W	154.4	Ocean bottom seismometer	on deck	
PS76/320-1	27.08.2010	05:57	75° 11.77' N	62° 41.83' W	191.1	Ocean bottom seismometer	at surface	
PS76/320-1	27.08.2010	06:12	75° 11.86' N	62° 41.87' W	190.5	Ocean bottom seismometer	on deck	
PS76/321-1	27.08.2010	07:17	75° 15.46' N	62° 18.20' W	590.2	Ocean bottom seismometer	at surface	
PS76/321-1	27.08.2010	07:27	75° 15.53' N	62° 18.41' W	590.4	Ocean bottom seismometer	on deck	
PS76/322-1	27.08.2010	08:44	75° 19.25' N	61° 54.75' W	917.7	Ocean bottom seismometer	at surface	aufgetaucht
PS76/322-1	27.08.2010	08:55	75° 19.29' N	61° 55.15' W	920.2	Ocean bottom seismometer	on deck	
PS76/322-2	27.08.2010	09:48	75° 19.20' N	61° 55.42' W	923.5	Heat Flow	on ground/max depth	GE52.1 ; 916 m
PS76/323-1	27.08.2010	11:55	75° 22.87' N	61° 29.99' W	1171.7	Ocean bottom seismometer	at surface	aufgetaucht
PS76/323-1	27.08.2010	12:11	75° 22.93' N	61° 31.45' W	1178.0	Ocean bottom seismometer	on deck	
PS76/323-2	27.08.2010	12:53	75° 22.82' N	61° 31.59' W	1179.3	CTD/rosette water sampler	on ground/max depth	1151 m, EL 31
PS76/323-3	27.08.2010	14:01	75° 22.82' N	61° 31.59' W	1179.7	Heat Flow	on ground/max depth	1170 m, GE 52.1
PS76/324-1	27.08.2010	16:10	75° 26.54' N	61° 7.44' W	436.6	Ocean bottom seismometer	at surface	
PS76/324-1	27.08.2010	16:33	75° 26.67' N	61° 8.44' W	439.5	Ocean bottom seismometer	on deck	
PS76/325-1	27.08.2010	17:38	75° 30.30' N	60° 44.15' W	395.6	Ocean bottom seismometer	at surface	
PS76/325-1	27.08.2010	17:48	75° 30.32' N	60° 44.21' W	390.8	Ocean bottom seismometer	on deck	
PS76/326-1	27.08.2010	18:43	75° 32.31' N	60° 30.30' W	448.4	Ocean bottom seismometer	at surface	
PS76/326-1	27.08.2010	18:54	75° 32.41' N	60° 30.77' W	429.0	Ocean bottom seismometer	on deck	
PS76/327-1	28.08.2010	01:11	75° 35.87' N	60° 8.07' W	470.1	Seismic reflection profile	profile start	Streamer komplett draussen
PS76/327-3	28.08.2010	02:09	75° 33.41' N	60° 24.90' W	869.4	Seismic reflection profile	profile start	Softstart
PS76/327-4	28.08.2010	02:09	75° 33.41' N	60° 24.90' W	869.4	Magnetic profile	profile start	

A.4 Stationsliste / station list PS 76

Station	Date	Time	Position Lat	Position Lon	Depth [m]	Gear	Action	Comment
PS76/327-3	29.08.2010	01:06	74° 35.39' N	66° 28.23' W	2193.0	Seismic reflection profile	profile end	
PS76/327-4	29.08.2010	01:06	74° 35.39' N	66° 28.23' W	2193.0	Magnetic profile	profile end	
PS76/328-1	29.08.2010	01:08	74° 35.31' N	66° 28.74' W	2193.0	Seismic reflection profile	alter course	Kanonengestell aus dem Wasser
PS76/328-1	29.08.2010	02:35	74° 33.91' N	66° 15.78' W	2177.0	Seismic reflection profile	action	Softstart
PS76/328-1	29.08.2010	03:24	74° 36.52' N	66° 21.41' W	2155.0	Seismic reflection profile	profile start	
PS76/328-2	29.08.2010	03:24	74° 36.52' N	66° 21.41' W	2155.0	Magnetic profile	profile start	
PS76/328-1	29.08.2010	14:53	74° 55.61' N	69° 39.70' W	1044.0	Seismic reflection profile	profile end	
PS76/328-2	29.08.2010	14:53	74° 55.61' N	69° 39.70' W	1044.0	Magnetic profile	profile end	
PS76/329-2	29.08.2010	14:54	74° 55.64' N	69° 39.98' W	1042.0	Magnetic profile	alter course	346 Grad
PS76/329-1	29.08.2010	17:15	74° 53.38' N	69° 30.61' W	1154.0	Seismic reflection profile	action	Softstart
PS76/329-1	29.08.2010	17:33	74° 54.80' N	69° 31.87' W	1098.0	Seismic reflection profile	profile start	
PS76/329-1	29.08.2010	17:33	74° 54.80' N	69° 31.87' W	1098.0	Seismic reflection profile	profile start	
PS76/330-1	30.08.2010	22:55	77° 13.23' N	71° 56.36' W	790.5	Seismic reflection profile	profile end	
PS76/329-2	30.08.2010	22:56	77° 13.29' N	71° 56.63' W	780.5	Magnetic profile	profile end	
PS76/331-1	31.08.2010	03:19	77° 6.29' N	71° 48.67' W	857.2	Ocean bottom seismometer	on ground/max depth	
PS76/332-1	31.08.2010	04:25	76° 59.51' N	71° 41.52' W	1048.0	Ocean bottom seismometer	on ground/max depth	abgetaucht
PS76/333-1	31.08.2010	05:31	76° 52.70' N	71° 33.40' W	936.8	Ocean bottom seismometer	on ground/max depth	ausgeloest
PS76/334-1	31.08.2010	06:34	76° 45.93' N	71° 25.89' W	776.8	Ocean bottom seismometer	on ground/max depth	ausgeloest
PS76/335-1	31.08.2010	07:36	76° 39.12' N	71° 18.51' W	661.5	Ocean bottom seismometer	on ground/max depth	ausgeloest
PS76/336-1	31.08.2010	08:37	76° 32.34' N	71° 11.00' W	490.6	Ocean bottom seismometer	on ground/max depth	ausgeloest
PS76/337-1	31.08.2010	09:33	76° 25.59' N	71° 3.74' W	537.1	Ocean bottom seismometer	on ground/max depth	geslipt
PS76/338-1	31.08.2010	10:29	76° 18.80' N	70° 56.46' W	641.5	Ocean bottom seismometer	on ground/max depth	geslipt
PS76/339-1	31.08.2010	11:30	76° 11.97' N	70° 49.21' W	648.6	Ocean bottom seismometer	on ground/max depth	geslipt

A.4 Stationsliste / station list PS 76

Station	Date	Time	Position Lat	Position Lon	Depth [m]	Gear	Action	Comment
PS76/340-1	31.08.2010	12:28	76° 5.22' N	70° 42.12' W	609.2	Ocean bottom seismometer	on ground/max depth	
PS76/341-1	31.08.2010	13:31	75° 58.45' N	70° 35.07' W	599.3	Ocean bottom seismometer	on ground/max depth	
PS76/342-1	31.08.2010	14:32	75° 51.65' N	70° 27.70' W	571.9	Ocean bottom seismometer	on ground/max depth	
PS76/343-1	31.08.2010	15:33	75° 44.91' N	70° 21.02' W	534.4	Ocean bottom seismometer	on ground/max depth	
PS76/344-1	31.08.2010	16:33	75° 38.05' N	70° 14.13' W	544.9	Ocean bottom seismometer	on ground/max depth	ausgeloest
PS76/345-1	31.08.2010	17:33	75° 31.29' N	70° 7.35' W	578.3	Ocean bottom seismometer	on ground/max depth	geslipt
PS76/346-1	31.08.2010	18:33	75° 24.51' N	70° 0.52' W	636.9	Ocean bottom seismometer	on ground/max depth	geslipt
PS76/347-1	31.08.2010	19:36	75° 17.75' N	69° 53.76' W	675.1	Ocean bottom seismometer	on ground/max depth	geslipt
PS76/348-1	31.08.2010	20:39	75° 10.96' N	69° 47.01' W	701.8	Ocean bottom seismometer	on ground/max depth	geslipt
PS76/349-1	31.08.2010	21:39	75° 4.14' N	69° 40.36' W	769.5	Ocean bottom seismometer	on ground/max depth	geslipt
PS76/350-1	31.08.2010	22:41	74° 57.36' N	69° 33.65' W	975.1	Ocean bottom seismometer	on ground/max depth	geslipt
PS76/351-1	31.08.2010	23:44	74° 50.54' N	69° 27.09' W	1292.0	Ocean bottom seismometer	on ground/max depth	geslipt
PS76/352-1	01.09.2010	01:27	74° 43.83' N	69° 20.44' W	1564.0	Heat Flow	on ground/max depth	1535 m, GE 52.1
PS76/352-2	01.09.2010	02:19	74° 43.84' N	69° 20.42' W	1563.0	Ocean bottom seismometer	on ground/max depth	
PS76/353-1	01.09.2010	04:12	74° 37.05' N	69° 14.06' W	1716.0	Heat Flow	on ground/max depth	GE52.1 1680m
PS76/353-2	01.09.2010	05:07	74° 37.03' N	69° 14.04' W	1716.0	Ocean bottom seismometer	on ground/max depth	geslipt
PS76/354-1	01.09.2010	06:53	74° 30.23' N	69° 7.57' W	1793.0	Heat Flow	on ground/max depth	GE52.1 1747m
PS76/354-2	01.09.2010	07:49	74° 30.21' N	69° 7.55' W	1792.0	Ocean bottom seismometer	on ground/max depth	geslipt
PS76/355-1	01.09.2010	09:36	74° 23.46' N	69° 1.19' W	1863.0	Heat Flow	on ground/max depth	GE52.1 ; 1815 m
PS76/355-2	01.09.2010	10:30	74° 23.46' N	69° 1.24' W	1863.0	Ocean bottom seismometer	on ground/max depth	geslipt
PS76/356-1	01.09.2010	12:21	74° 16.70' N	68° 54.82' W	1948.0	Heat Flow	on ground/max depth	1910 m, GE 52.1
PS76/356-2	01.09.2010	13:17	74° 16.68' N	68° 54.94' W	1947.0	Ocean bottom seismometer	on ground/max depth	
PS76/357-1	01.09.2010	15:13	74° 9.89' N	68° 48.62' W	2012.0	Heat Flow	on ground/max depth	1977 m, GE 52.1

A.4 Stationsliste / station list PS 76

Station	Date	Time	Position Lat	Position Lon	Depth [m]	Gear	Action	Comment
PS76/357-2	01.09.2010	16:09	74° 9.91' N	68° 48.55' W	2011.0	Ocean bottom seismometer	on ground/max depth	geslipt
PS76/358-1	01.09.2010	17:18	74° 3.15' N	68° 42.18' W	2040.0	Ocean bottom seismometer	on ground/max depth	geslipt
PS76/359-1	01.09.2010	18:53	73° 57.52' N	68° 36.62' W	2066.0	Seismic refraction profile	profile start	Softstart
PS76/359-1	01.09.2010	22:54	74° 16.47' N	68° 54.06' W	1952.0	Seismic refraction profile	profile end	
PS76/359-1	01.09.2010	23:03	74° 17.18' N	68° 54.74' W	1947.0	Seismic refraction profile	on deck	Kannonengeste II Stb, Grund : Reperatur
PS76/359-1	01.09.2010	23:03	74° 17.18' N	68° 54.74' W	1947.0	Seismic refraction profile	on deck	Kannonengeste II Mitte, Grund Reperatur
PS76/359-1	02.09.2010	01:04	74° 14.74' N	68° 51.26' W	1974.0	Seismic refraction profile	action	Airgung Softstart
PS76/359-1	02.09.2010	01:27	74° 16.48' N	68° 54.08' W	1953.0	Seismic refraction profile	profile start	
PS76/359-1	03.09.2010	12:05	77° 13.36' N	71° 55.97' W	787.0	Seismic refraction profile	profile end	
PS76/361-1	03.09.2010	13:53	77° 5.77' N	71° 47.34' W	922.8	Gravity corer	on ground/max depth	900 m, GE 52.2
PS76/361-2	03.09.2010	15:22	77° 6.31' N	71° 47.98' W	860.8	Ocean bottom seismometer	on ground/max depth	aufgetaucht
PS76/361-2	03.09.2010	15:36	77° 6.32' N	71° 48.97' W	847.5	Ocean bottom seismometer	on deck	
PS76/362-1	03.09.2010	16:59	76° 59.71' N	71° 41.85' W	1048.0	Ocean bottom seismometer	action	aufgetacht
PS76/362-1	03.09.2010	17:08	76° 59.64' N	71° 42.03' W	1053.0	Ocean bottom seismometer	on deck	
PS76/363-1	03.09.2010	18:21	76° 52.76' N	71° 33.52' W	931.6	Ocean bottom seismometer	at surface	
PS76/363-1	03.09.2010	18:48	76° 52.88' N	71° 34.05' W	937.8	Ocean bottom seismometer	on deck	
PS76/363-2	03.09.2010	19:13	76° 52.92' N	71° 34.01' W	939.1	Gravity corer	on ground/max depth	GE52.2 917m
PS76/364-1	03.09.2010	20:55	76° 46.01' N	71° 25.82' W	778.7	Ocean bottom seismometer	at surface	aufgetaucht
PS76/364-1	03.09.2010	21:09	76° 46.01' N	71° 26.37' W	778.1	Ocean bottom seismometer	on deck	
PS76/365-1	03.09.2010	22:24	76° 39.14' N	71° 18.57' W	662.0	Ocean bottom seismometer	at surface	aufgetaucht
PS76/365-1	03.09.2010	22:31	76° 39.09' N	71° 18.64' W	662.0	Ocean bottom seismometer	on deck	
PS76/365-2	03.09.2010	22:49	76° 39.04' N	71° 18.79' W	658.0	Gravity corer	on ground/max depth	GE52.2 ; 645 m

A.4 Stationsliste / station list PS 76

Station	Date	Time	Position Lat	Position Lon	Depth [m]	Gear	Action	Comment
PS76/366-1	04.09.2010	00:15	76° 32.37' N	71° 10.59' W	494.2	Ocean bottom seismometer	on ground/max depth	aufgetaucht, Hydrophon an Deck
PS76/366-1	04.09.2010	00:32	76° 32.33' N	71° 11.02' W	490.7	Ocean bottom seismometer	on deck	
PS76/367-1	04.09.2010	01:37	76° 25.60' N	71° 3.84' W	537.3	Ocean bottom seismometer	on ground/max depth	aufgetaucht, Hydrophon an Deck
PS76/367-1	04.09.2010	01:51	76° 25.46' N	71° 3.66' W	541.8	Ocean bottom seismometer	on deck	
PS76/367-2	04.09.2010	02:18	76° 26.84' N	71° 4.84' W	498.4	Gravity corer	on ground/max depth	485 m, GE 52.2
PS76/368-1	04.09.2010	03:42	76° 18.70' N	70° 56.40' W	649.5	Ocean bottom seismometer	on ground/max depth	aufgetaucht, Hydrophon an Deck
PS76/368-1	04.09.2010	03:55	76° 18.64' N	70° 57.07' W	662.8	Ocean bottom seismometer	on deck	
PS76/369-1	04.09.2010	05:05	76° 11.93' N	70° 48.61' W	648.4	Ocean bottom seismometer	at surface	
PS76/369-1	04.09.2010	05:31	76° 11.89' N	70° 48.31' W	650.0	Ocean bottom seismometer	on deck	
PS76/369-2	04.09.2010	05:48	76° 11.94' N	70° 48.07' W	651.5	Gravity corer	on ground/max depth	GE52.2 630 m
PS76/370-1	04.09.2010	07:09	76° 5.18' N	70° 40.96' W	613.4	Ocean bottom seismometer	at surface	
PS76/370-1	04.09.2010	07:25	76° 5.13' N	70° 41.02' W	610.2	Ocean bottom seismometer	on deck	
PS76/371-1	04.09.2010	08:26	75° 58.35' N	70° 34.48' W	597.4	Ocean bottom seismometer	at surface	
PS76/371-1	04.09.2010	08:36	75° 58.30' N	70° 34.91' W	599.0	Ocean bottom seismometer	on deck	
PS76/371-2	04.09.2010	08:55	75° 58.24' N	70° 34.86' W	597.9	Gravity corer	on ground/max depth	GE52.2 ; 580m
PS76/372-1	04.09.2010	10:14	75° 51.59' N	70° 27.54' W	572.7	Ocean bottom seismometer	at surface	
PS76/372-1	04.09.2010	10:19	75° 51.56' N	70° 27.80' W	569.3	Ocean bottom seismometer	on deck	
PS76/373-1	04.09.2010	11:24	75° 44.83' N	70° 20.78' W	536.5	Ocean bottom seismometer	at surface	
PS76/373-1	04.09.2010	11:32	75° 44.82' N	70° 21.09' W	537.5	Ocean bottom seismometer	on deck	
PS76/373-2	04.09.2010	11:50	75° 44.74' N	70° 21.27' W	535.9	Gravity corer	on ground/max depth	GE52.2 ; 517 m
PS76/374-1	04.09.2010	13:07	75° 37.89' N	70° 13.57' W	544.7	Ocean bottom seismometer	on ground/max depth	aufgetaucht, Hydrophon an Deck
PS76/374-1	04.09.2010	13:20	75° 38.03' N	70° 14.15' W	545.9	Ocean bottom seismometer	on deck	
PS76/375-1	04.09.2010	14:25	75° 31.15' N	70° 6.88' W	579.4	Ocean bottom seismometer	on ground/max depth	aufgetaucht, Hydrophon an Deck

A.4 Stationsliste / station list PS 76

Station	Date	Time	Position Lat	Position Lon	Depth [m]	Gear	Action	Comment
PS76/375-1	04.09.2010	14:39	75° 31.25' N	70° 7.54' W	577.7	Ocean bottom seismometer	on deck	
PS76/376-1	04.09.2010	15:45	75° 26.60' N	70° 28.29' W	615.3	Magnetic profile	profile start	
PS76/377-1	04.09.2010	20:47	76° 10.62' N	71° 13.72' W	604.3	Magnetic profile	profile end	
PS76/377-1	04.09.2010	20:50	76° 11.06' N	71° 14.19' W	608.5	Magnetic profile	alter course	
PS76/377-1	04.09.2010	21:44	76° 12.12' N	71° 42.22' W	545.5	Magnetic profile	profile start	Ende Kursaenderung
PS76/378-1	05.09.2010	04:02	75° 17.58' N	70° 47.33' W	621.5	Magnetic profile	profile end	
PS76/379-1	05.09.2010	04:07	75° 16.95' N	70° 46.12' W	626.1	Magnetic profile	profile start	B. Schreckenberger / Transit
PS76/379-1	05.09.2010	04:54	75° 15.63' N	70° 18.70' W	651.9	Magnetic profile	profile end	
PS76/380-1	05.09.2010	04:57	75° 15.97' N	70° 17.86' W	651.6	Magnetic profile	profile start	B. Schreckenberger
PS76/380-1	05.09.2010	06:24	75° 28.37' N	70° 30.03' W	609.2	Magnetic profile	profile end	
PS76/381-1	05.09.2010	06:28	75° 28.91' N	70° 30.56' W	605.7	Magnetic profile	action	Beginn Einholen
PS76/382-1	05.09.2010	08:06	75° 24.46' N	70° 0.33' W	633.6	Ocean bottom seismometer	at surface	
PS76/382-1	05.09.2010	08:16	75° 24.53' N	70° 0.58' W	636.3	Ocean bottom seismometer	on deck	
PS76/383-1	05.09.2010	09:24	75° 17.71' N	69° 53.42' W	675.2	Ocean bottom seismometer	at surface	aufgetaucht
PS76/383-1	05.09.2010	09:36	75° 17.70' N	69° 53.72' W	673.3	Ocean bottom seismometer	on deck	
PS76/383-2	05.09.2010	09:59	75° 17.69' N	69° 53.75' W	673.9	Gravity corer	on ground/max depth	GE52.2 ; 658 m
PS76/384-1	05.09.2010	11:23	75° 11.02' N	69° 46.94' W	701.3	Ocean bottom seismometer	at surface	
PS76/384-1	05.09.2010	11:30	75° 10.93' N	69° 47.09' W	701.7	Ocean bottom seismometer	on deck	
PS76/385-1	05.09.2010	12:50	75° 4.05' N	69° 40.25' W	770.0	Ocean bottom seismometer	on ground/max depth	aufgetaucht, Hydrophon an Deck
PS76/385-1	05.09.2010	12:55	75° 4.08' N	69° 40.29' W	769.5	Ocean bottom seismometer	on deck	
PS76/386-1	05.09.2010	14:10	74° 57.40' N	69° 33.57' W	972.5	Ocean bottom seismometer	on ground/max depth	aufgetaucht, Hydrophon an Deck
PS76/386-1	05.09.2010	14:22	74° 57.25' N	69° 33.71' W	980.9	Ocean bottom seismometer	on deck	
PS76/387-1	05.09.2010	15:44	74° 50.57' N	69° 26.84' W	1293.0	Ocean bottom seismometer	on ground/max depth	aufgetaucht, Hydrophon an Deck
PS76/387-1	05.09.2010	15:56	74° 50.41' N	69° 27.12' W	1299.0	Ocean bottom seismometer	on deck	
PS76/387-2	05.09.2010	16:22	74° 50.42' N	69° 27.18' W	1300.0	Gravity corer	on ground/max depth	GE52.2 1266m

A.4 Stationsliste / station list PS 76

Station	Date	Time	Position Lat	Position Lon	Depth [m]	Gear	Action	Comment
PS76/388-1	05.09.2010	18:08	74° 43.83' N	69° 20.16' W	1564.0	Ocean bottom seismometer	at surface	
PS76/388-1	05.09.2010	18:18	74° 43.81' N	69° 20.18' W	1564.0	Ocean bottom seismometer	on deck	
PS76/389-1	05.09.2010	19:51	74° 36.87' N	69° 13.79' W	1720.0	Ocean bottom seismometer	at surface	
PS76/389-1	05.09.2010	20:03	74° 37.05' N	69° 13.73' W	1716.0	Ocean bottom seismometer	on deck	
PS76/389-2	05.09.2010	20:31	74° 37.05' N	69° 13.75' W	1716.0	Gravity corer	on ground/max depth	GE52.2 ; 1674 m
PS76/390-1	05.09.2010	22:31	74° 30.13' N	69° 7.47' W	1792.0	Ocean bottom seismometer	at surface	aufgetaucht
PS76/390-1	05.09.2010	22:41	74° 30.19' N	69° 7.35' W	1794.0	Ocean bottom seismometer	on deck	
PS76/391-1	06.09.2010	00:16	74° 23.43' N	69° 1.08' W	1864.0	Ocean bottom seismometer	on ground/max depth	aufgetaucht
PS76/391-1	06.09.2010	00:25	74° 23.35' N	69° 1.23' W	1865.0	Ocean bottom seismometer	on deck	
PS76/391-2	06.09.2010	00:57	74° 23.36' N	69° 1.22' W	1864.0	Gravity corer	on ground/max depth	1821 m, GE 52.2
PS76/392-1	06.09.2010	03:05	74° 16.67' N	68° 54.70' W	1951.0	Ocean bottom seismometer	on ground/max depth	aufgetaucht
PS76/392-1	06.09.2010	03:10	74° 16.69' N	68° 54.57' W	1951.0	Ocean bottom seismometer	on deck	
PS76/393-1	06.09.2010	04:26	74° 13.35' N	68° 46.09' W	2004.0	Ocean bottom seismometer	at surface	
PS76/393-1	06.09.2010	04:50	74° 13.50' N	68° 45.78' W	2002.0	Ocean bottom seismometer	on deck	
PS76/394-1	06.09.2010	05:52	74° 13.03' N	68° 42.86' W	2013.0	Heat Flow	on ground/max depth	GE52.1 1980m
PS76/395-1	06.09.2010	08:06	74° 9.82' N	68° 46.58' W	2020.0	Ocean bottom seismometer	at surface	
PS76/395-1	06.09.2010	08:21	74° 9.90' N	68° 48.24' W	2014.0	Ocean bottom seismometer	on deck	
PS76/396-1	06.09.2010	09:39	74° 3.85' N	68° 38.01' W	2058.0	Ocean bottom seismometer	at surface	
PS76/396-1	06.09.2010	09:53	74° 3.95' N	68° 37.94' W	2057.0	Ocean bottom seismometer	on deck	
PS76/397-1	06.09.2010	10:44	74° 3.02' N	68° 42.02' W	2040.0	Ocean bottom seismometer	at surface	aufgetaucht
PS76/397-1	06.09.2010	10:55	74° 3.23' N	68° 42.00' W	2040.0	Ocean bottom seismometer	on deck	
PS76/397-2	06.09.2010	11:55	74° 3.14' N	68° 42.09' W	2041.0	Heat Flow	on ground/max depth	GE52.1 ; 2003 m
PS76/398-1	06.09.2010	14:52	73° 55.78' N	68° 35.12' W	2076.0	Heat Flow	on ground/max depth	2040 m, GE 52.1

A.4 Stationsliste / station list PS 76

Station	Date	Time	Position Lat	Position Lon	Depth [m]	Gear	Action	Comment
PS76/399-1	06.09.2010	17:46	73° 58.45' N	69° 0.16' W	1974.0	Ocean bottom seismometer	at surface	
PS76/399-1	06.09.2010	18:00	73° 58.66' N	69° 1.94' W	1964.0	Ocean bottom seismometer	on deck	
PS76/399-2	06.09.2010	19:01	73° 58.71' N	69° 1.73' W	1964.0	Heat Flow	on ground/max depth	GE 52.1 1929m
PS76/400-1	06.09.2010	22:00	74° 1.30' N	69° 43.86' W	1726.0	Ocean bottom seismometer	at surface	aufgetaucht
PS76/400-1	06.09.2010	22:10	74° 1.28' N	69° 44.69' W	1721.0	Ocean bottom seismometer	on deck	
PS76/401-1	06.09.2010	23:18	74° 1.98' N	69° 47.89' W	1708.0	CTD	on ground/max depth	EL31 ; 1657 m
PS76/401-2	07.09.2010	00:49	74° 1.99' N	69° 47.94' W	1708.0	Heat Flow	on ground/max depth	1678 m, GE 52.1
PS76/402-1	07.09.2010	04:08	74° 14.27' N	69° 36.99' W	1758.0	Ocean bottom seismometer	on deck	
PS76/402-2	07.09.2010	05:00	74° 14.21' N	69° 37.30' W	1755.0	Heat Flow	on ground/max depth	GE 52.1 1724m
PS76/403-1	07.09.2010	06:10	74° 13.76' N	69° 32.38' W	1780.0	Magnetic profile	in the water	komplett
PS76/403-2	07.09.2010	07:17	74° 10.79' N	68° 59.40' W	1966.0	Magnetic profile	profile start	Kalibrierungs-Drehkreis
PS76/403-2	07.09.2010	07:30	74° 10.78' N	68° 52.17' W	1995.0	Magnetic profile	alter course	
PS76/403-2	07.09.2010	07:42	74° 11.56' N	68° 53.06' W	1989.0	Magnetic profile	alter course	
PS76/403-2	07.09.2010	07:55	74° 10.15' N	68° 58.06' W	1974.0	Magnetic profile	alter course	
PS76/403-2	07.09.2010	08:07	74° 9.83' N	68° 55.61' W	1982.0	Magnetic profile	alter course	auf 360 deg
PS76/403-2	07.09.2010	08:21	74° 11.97' N	68° 55.60' W	1975.0	Magnetic profile	alter course	
PS76/403-2	07.09.2010	08:32	74° 11.47' N	68° 58.09' W	1966.0	Magnetic profile	alter course	auf 135 deg
PS76/403-2	07.09.2010	08:45	74° 10.04' N	68° 52.80' W	1998.0	Magnetic profile	alter course	
PS76/403-2	07.09.2010	08:56	74° 10.82' N	68° 51.76' W	1996.0	Magnetic profile	alter course	auf 270 deg
PS76/403-2	07.09.2010	09:10	74° 10.82' N	68° 59.32' W	1967.0	Magnetic profile	alter course	
PS76/403-2	07.09.2010	09:23	74° 10.17' N	68° 57.85' W	1975.0	Magnetic profile	alter course	auf 045 deg
PS76/403-2	07.09.2010	09:36	74° 11.59' N	68° 52.75' W	1989.0	Magnetic profile	alter course	
PS76/403-2	07.09.2010	09:48	74° 11.70' N	68° 55.63' W	1975.0	Magnetic profile	alter course	auf 180 deg
PS76/403-2	07.09.2010	10:01	74° 9.78' N	68° 55.66' W	1984.0	Magnetic profile	alter course	
PS76/403-2	07.09.2010	10:13	74° 10.15' N	68° 53.17' W	1994.0	Magnetic profile	alter course	auf 315 deg
PS76/403-2	07.09.2010	10:27	74° 11.64' N	68° 58.60' W	1963.0	Magnetic profile	alter course	
PS76/403-2	07.09.2010	10:39	74° 10.79' N	68° 58.98' W	1967.0	Magnetic profile	alter course	auf 090 deg
PS76/403-3	07.09.2010	10:50	74° 10.79' N	68° 52.76' W	1992.0	Magnetic profile	profile start	
PS76/403-2	07.09.2010	10:50	74° 10.79' N	68° 52.76' W	1992.0	Magnetic profile	profile end	

A.4 Stationsliste / station list PS 76

Station	Date	Time	Position Lat	Position Lon	Depth [m]	Gear	Action	Comment
PS76/403-3	07.09.2010	17:59	74° 41.64' N	72° 14.95' W	985.7	Magnetic profile	profile end	
PS76/404-1	07.09.2010	18:02	74° 41.88' N	72° 15.25' W	977.8	Magnetic profile	profile end	Beginn Hieven
PS76/404-2	07.09.2010	18:19	74° 42.48' N	72° 15.99' W	961.8	Seismic reflection profile	in the water	Th.Behrens/Beginn Aussetzen Streamer
PS76/404-3	07.09.2010	20:31	74° 49.37' N	72° 23.88' W	906.4	Seismic reflection profile	action	Ramp up, 1.Schuss
PS76/404-4	07.09.2010	20:31	74° 49.37' N	72° 23.88' W	906.4	Seismic reflection profile	profile start	Kurs 343 deg
PS76/404-1	07.09.2010	20:48	74° 50.67' N	72° 25.44' W	895.1	Magnetic profile	profile start	Kurs 343 deg
PS76/405-1	08.09.2010	22:14	76° 47.07' N	74° 49.83' W	489.5	Seismic reflection profile	alter course	auf 005 deg
PS76/405-2	08.09.2010	22:14	76° 47.07' N	74° 49.83' W	489.5	Seismic reflection profile	profile start	Kurs 005 deg, Line BGR10-315
PS76/405-3	08.09.2010	22:14	76° 47.07' N	74° 49.83' W	489.5	Magnetic profile	profile start	Kurs 005 deg
PS76/405-2	09.09.2010	08:00	77° 32.19' N	74° 32.14' W	708.1	Seismic reflection profile	profile end	letzter Schuss
PS76/405-3	09.09.2010	08:00	77° 32.19' N	74° 32.14' W	708.1	Magnetic profile	profile end	
PS76/406-2	09.09.2010	08:12	77° 33.12' N	74° 30.52' W	681.5	Seismic reflection profile	on deck	
PS76/406-3	09.09.2010	08:28	77° 34.22' N	74° 28.66' W	533.5	Magnetic profile	on deck	
PS76/406-4	09.09.2010	10:35	77° 39.62' N	74° 18.29' W	296.1	Seismic reflection profile	on deck	
PS76/407-1	10.09.2010	07:26	79° 21.17' N	66° 54.46' W	558.0	Seismic reflection profile	action	Softstart
PS76/407-1	10.09.2010	07:56	79° 22.58' N	66° 44.81' W	470.8	Seismic reflection profile	profile start	
PS76/407-1	10.09.2010	16:54	79° 58.27' N	68° 59.81' W	200.4	Seismic reflection profile	profile end	
PS76/408-1	10.09.2010	19:12	80° 9.59' N	68° 26.05' W	326.9	Seismic reflection profile	action	Softstart
PS76/408-1	10.09.2010	19:37	80° 9.08' N	68° 32.89' W	306.1	Seismic reflection profile	profile start	
PS76/409-1	11.09.2010	10:35	78° 59.45' N	70° 16.03' W	334.7	Seismic reflection profile	profile end	letzterr Schuss
PS76/409-2	11.09.2010	10:42	78° 58.97' N	70° 16.92' W	334.3	Seismic reflection profile	on deck	
PS76/409-3	11.09.2010	11:19	78° 57.88' N	70° 27.97' W	342.0	Seismic reflection profile	on deck	
PS76/410-1	12.09.2010	06:59	76° 32.98' N	74° 27.98' W	584.8	Seismic reflection profile	in the water	Th. Behrens/Beginn Aussetzen Streamer

A.4 Stationsliste / station list PS 76

Station	Date	Time	Position Lat	Position Lon	Depth [m]	Gear	Action	Comment
PS76/410-2	12.09.2010	09:25	76° 21.18' N	74° 37.73' W	478.4	Seismic reflection profile	action	Start Ramp up, 1.Schuss
PS76/410-3	12.09.2010	09:44	76° 20.94' N	74° 31.52' W	479.8	Magnetic profile	profile start	
PS76/410-4	12.09.2010	12:43	76° 20.35' N	73° 30.10' W	618.9	Seismic reflection profile	profile end	Airgun stopp
PS76/410-3	12.09.2010	13:32	76° 18.31' N	73° 24.16' W	588.7	Magnetic profile	profile end	3 Magnetometer, komplett an Deck
PS76/410-4	12.09.2010	13:55	76° 18.08' N	73° 29.61' W	574.7	Seismic reflection profile	action	Streamer komplett im Wasser
PS76/410-4	12.09.2010	14:28	76° 18.16' N	73° 38.79' W	551.4	Seismic reflection profile	action	Kanonengestell im Wasser
PS76/410-4	12.09.2010	14:30	76° 18.16' N	73° 39.49' W	552.3	Seismic reflection profile	action	Airgin softstart
PS76/410-4	12.09.2010	15:30	76° 20.43' N	73° 36.59' W	586.1	Seismic reflection profile	profile start	
PS76/411-1	13.09.2010	02:57	76° 17.72' N	69° 41.10' W	187.5	Seismic reflection profile	alter course	240 Grad, Airgun stopp
PS76/410-4	13.09.2010	02:57	76° 17.72' N	69° 41.10' W	187.5	Seismic reflection profile	profile end	
PS76/411-1	13.09.2010	04:11	76° 18.29' N	69° 49.60' W	217.7	Seismic reflection profile	profile start	
PS76/411-2	13.09.2010	06:24	76° 12.96' N	70° 28.41' W	668.8	Magnetic profile	profile start	
PS76/411-1	13.09.2010	18:17	75° 44.07' N	73° 54.23' W	402.2	Seismic reflection profile	profile end	
PS76/411-2	13.09.2010	18:17	75° 44.07' N	73° 54.23' W	402.2	Magnetic profile	profile end	
PS76/411-1	13.09.2010	18:17	75° 44.07' N	73° 54.23' W	402.2	Seismic reflection profile	alter course	Drehkreis
PS76/411-2	13.09.2010	18:17	75° 44.07' N	73° 54.23' W	402.2	Magnetic profile	alter course	Drehkreis
PS76/412-2	13.09.2010	20:05	75° 45.02' N	73° 47.14' W	404.4	Seismic reflection profile	profile start	Kurs 086 deg, Line BGR10-321, Th. Behrens
PS76/412-3	13.09.2010	20:05	75° 45.02' N	73° 47.14' W	404.4	Magnetic profile	profile start	Kurs 086 deg, B.Schreckenberger
PS76/412-3	14.09.2010	13:56	75° 50.72' N	67° 59.62' W	279.5	Magnetic profile	profile end	
PS76/412-2	14.09.2010	17:39	75° 51.93' N	66° 47.51' W	94.2	Seismic reflection profile	profile end	
PS76/413-1	14.09.2010	19:34	75° 46.48' N	67° 6.26' W	357.0	Seismic reflection profile	profile start	Softstart
PS76/413-2	14.09.2010	19:57	75° 45.03' N	67° 10.85' W	357.5	Magnetic profile	profile start	
PS76/414-1	15.09.2010	16:22	74° 37.67' N	71° 48.47' W	1129.0	Seismic reflection profile	profile end	

A.4 Stationsliste / station list PS 76

Station	Date	Time	Position Lat	Position Lon	Depth [m]	Gear	Action	Comment
PS76/413-2	15.09.2010	16:22	74° 37.67' N	71° 48.47' W	1129.0	Magnetic profile	profile end	
PS76/415-1	16.09.2010	10:38	73° 15.83' N	65° 23.58' W	2378.0	Heat Flow	on ground/max depth	Ge52.1 ; 2340 m
PS76/416-1	16.09.2010	13:53	73° 19.18' N	64° 58.27' W	2301.0	Heat Flow	on ground/max depth	2260 m, GE 52.1
PS76/416-2	16.09.2010	15:02	73° 19.15' N	64° 58.30' W	2301.0	Ocean bottom seismometer	on ground/max depth	
PS76/417-1	16.09.2010	16:52	73° 22.50' N	64° 32.74' W	2063.0	Heat Flow	on ground/max depth	GE52.1 2025m
PS76/417-2	16.09.2010	17:50	73° 22.48' N	64° 32.74' W	2062.0	Ocean bottom seismometer	on ground/max depth	abgetaucht
PS76/418-1	16.09.2010	19:44	73° 25.75' N	64° 6.76' W	1515.0	Heat Flow	on ground/max depth	GE52.1 1500m
PS76/418-2	16.09.2010	20:30	73° 25.77' N	64° 7.35' W	1516.0	Ocean bottom seismometer	on ground/max depth	geslipt
PS76/419-1	16.09.2010	21:44	73° 29.06' N	63° 41.84' W	643.1	Ocean bottom seismometer	on ground/max depth	geslipt
PS76/420-1	16.09.2010	22:48	73° 32.33' N	63° 16.19' W	597.7	Ocean bottom seismometer	on ground/max depth	geslipt
PS76/421-1	16.09.2010	23:52	73° 35.65' N	62° 50.38' W	567.4	Ocean bottom seismometer	on ground/max depth	geslipt
PS76/422-1	17.09.2010	00:56	73° 38.98' N	62° 24.59' W	578.6	Ocean bottom seismometer	on ground/max depth	
PS76/423-1	17.09.2010	02:00	73° 42.29' N	61° 58.70' W	594.7	Ocean bottom seismometer	on ground/max depth	
PS76/424-1	17.09.2010	03:03	73° 45.61' N	61° 32.76' W	577.1	Ocean bottom seismometer	on ground/max depth	
PS76/425-1	17.09.2010	04:09	73° 48.98' N	61° 6.91' W	444.9	Ocean bottom seismometer	on ground/max depth	abgetaucht
PS76/426-1	17.09.2010	05:15	73° 52.21' N	60° 40.37' W	551.4	Ocean bottom seismometer	on ground/max depth	abgetaucht
PS76/427-1	17.09.2010	06:17	73° 55.50' N	60° 14.33' W	555.3	Ocean bottom seismometer	on ground/max depth	abgetaucht
PS76/428-1	17.09.2010	07:21	73° 58.83' N	59° 47.83' W	512.6	Ocean bottom seismometer	on ground/max depth	abgetaucht
PS76/429-1	17.09.2010	08:20	74° 2.09' N	59° 21.49' W	367.9	Ocean bottom seismometer	on ground/max depth	geslipt
PS76/430-1	17.09.2010	09:22	74° 5.36' N	58° 54.84' W	227.5	Ocean bottom seismometer	on ground/max depth	geslipt
PS76/431-1	17.09.2010	10:21	74° 8.62' N	58° 28.28' W	138.9	Ocean bottom seismometer	on ground/max depth	geslipt
PS76/432-1	17.09.2010	11:22	74° 11.95' N	58° 1.51' W	598.2	Ocean bottom seismometer	on ground/max depth	geslipt
PS76/433-1	17.09.2010	15:08	73° 50.94' N	59° 53.33' W	438.4	Ocean bottom seismometer	on ground/max depth	

A.4 Stationsliste / station list PS 76

Station	Date	Time	Position Lat	Position Lon	Depth [m]	Gear	Action	Comment
PS76/434-1	17.09.2010	17:45	73° 43.08' N	59° 58.55' W	372.9	Ocean bottom seismometer	on ground/max depth	abgetaucht
PS76/435-1	17.09.2010	18:49	73° 35.17' N	60° 3.77' W	328.4	Ocean bottom seismometer	on ground/max depth	abgetaucht
PS76/436-1	17.09.2010	19:44	73° 27.41' N	60° 8.94' W	339.9	Ocean bottom seismometer	on ground/max depth	abgetaucht
PS76/437-1	17.09.2010	20:44	73° 19.53' N	60° 14.01' W	367.9	Ocean bottom seismometer	on ground/max depth	geslipt
PS76/438-1	17.09.2010	21:42	73° 11.65' N	60° 19.08' W	309.4	Ocean bottom seismometer	on ground/max depth	geslipt
PS76/439-1	17.09.2010	22:41	73° 3.80' N	60° 24.06' W	328.6	Ocean bottom seismometer	on ground/max depth	geslipt
PS76/440-1	17.09.2010	23:42	72° 55.95' N	60° 29.24' W	410.8	Ocean bottom seismometer	on ground/max depth	geslipt
PS76/441-1	18.09.2010	01:38	72° 48.11' N	60° 34.59' W	701.9	Ocean bottom seismometer	on ground/max depth	
PS76/442-1	18.09.2010	02:38	72° 40.23' N	60° 39.27' W	719.2	Ocean bottom seismometer	on ground/max depth	
PS76/443-1	18.09.2010	03:38	72° 32.36' N	60° 44.24' W	672.8	Ocean bottom seismometer	on ground/max depth	
PS76/444-1	18.09.2010	04:38	72° 24.50' N	60° 48.96' W	644.5	Ocean bottom seismometer	on ground/max depth	abgetaucht
PS76/445-1	18.09.2010	05:38	72° 16.63' N	60° 53.83' W	877.1	Ocean bottom seismometer	on ground/max depth	abgetaucht
PS76/446-1	18.09.2010	07:24	72° 8.79' N	60° 58.66' W	1488.0	Heat Flow	on ground/max depth	GE52.1 1470 m
PS76/446-2	18.09.2010	08:11	72° 8.79' N	60° 58.71' W	1488.0	Ocean bottom seismometer	on ground/max depth	geslipt
PS76/447-1	18.09.2010	09:57	72° 0.93' N	61° 3.40' W	1549.0	Heat Flow	on ground/max depth	GE52.1 ; 1525m
PS76/447-2	18.09.2010	10:47	72° 0.93' N	61° 3.45' W	1550.0	Ocean bottom seismometer	on ground/max depth	geslipt
PS76/448-1	18.09.2010	12:11	71° 56.01' N	61° 6.37' W	1595.0	Heat Flow	on ground/max depth	1568 m, GE 52.1
PS76/448-2	18.09.2010	12:59	71° 56.00' N	61° 6.52' W	1597.0	Ocean bottom seismometer	on ground/max depth	
PS76/449-1	18.09.2010	15:22	71° 33.10' N	61° 16.87' W	1727.0	Seismic refraction profile	profile start	Kanonengestell und Stb. Kanone im Wasser
PS76/449-2	18.09.2010	15:32	71° 33.93' N	61° 16.62' W	1725.0	Seismic refraction profile	profile start	
PS76/449-2	19.09.2010	23:55	74° 14.77' N	59° 36.95' W	740.2	Seismic refraction profile	profile end	letzter Schuss
PS76/450-1	20.09.2010	00:08	74° 15.75' N	59° 36.24' W	748.3	Seismic refraction profile	on deck	Kanonengestell komplett

A.4 Stationsliste / station list PS 76

Station	Date	Time	Position Lat	Position Lon	Depth [m]	Gear	Action	Comment
PS76/451-1	20.09.2010	02:25	74° 13.67' N	58° 10.45' W	321.4	Seismic refraction profile	in the water	Kanonengestell , Stb. Kanone
PS76/451-1	20.09.2010	02:34	74° 13.74' N	58° 7.14' W	666.8	Seismic refraction profile	action	Bb. Kanone im Wasser
PS76/451-2	20.09.2010	03:30	74° 13.03' N	57° 53.43' W	242.4	Seismic refraction profile	profile start	
PS76/452-1	21.09.2010	08:08	73° 13.98' N	65° 37.97' W	2395.0	Seismic refraction profile	hoisting	Th. Behrens
PS76/451-2	21.09.2010	08:08	73° 13.98' N	65° 37.97' W	2395.0	Seismic refraction profile	profile end	letzter Schuss
PS76/453-1	21.09.2010	10:56	73° 19.11' N	64° 58.43' W	2302.0	Ocean bottom seismometer	at surface	aufgetaucht
PS76/453-1	21.09.2010	11:07	73° 19.36' N	64° 58.11' W	2299.0	Ocean bottom seismometer	on deck	
PS76/453-2	21.09.2010	11:17	73° 19.37' N	64° 58.11' W	2300.0	Gravity corer	on ground/max depth	GE52.2 ; 2244 m
PS76/454-1	21.09.2010	14:15	73° 22.49' N	64° 32.88' W	2065.0	Ocean bottom seismometer	action	aufgetaucht
PS76/454-1	21.09.2010	14:27	73° 22.52' N	64° 32.63' W	2060.0	Ocean bottom seismometer	on deck	
PS76/455-1	21.09.2010	15:58	73° 25.67' N	64° 7.70' W	1540.0	Ocean bottom seismometer	action	aufgetaucht
PS76/455-1	21.09.2010	16:10	73° 25.75' N	64° 7.75' W	1532.0	Ocean bottom seismometer	on deck	
PS76/456-1	21.09.2010	16:49	73° 25.00' N	64° 5.98' W	1526.0	Gravity corer	on ground/max depth	GE52.2 1490m
PS76/457-1	21.09.2010	18:30	73° 29.08' N	63° 41.76' W	642.1	Ocean bottom seismometer	at surface	aufgetaucht
PS76/457-1	21.09.2010	18:42	73° 29.02' N	63° 42.05' W	644.1	Ocean bottom seismometer	on deck	
PS76/458-1	21.09.2010	19:52	73° 32.20' N	63° 16.25' W	597.0	Ocean bottom seismometer	at surface	aufgetaucht
PS76/458-1	21.09.2010	20:06	73° 32.33' N	63° 16.19' W	597.1	Ocean bottom seismometer	on deck	
PS76/459-1	21.09.2010	20:29	73° 31.98' N	63° 16.10' W	592.8	Gravity corer	on ground/max depth	Ge52.2 ; 575m
PS76/460-1	21.09.2010	21:57	73° 35.58' N	62° 50.52' W	564.8	Ocean bottom seismometer	at surface	aufgetaucht
PS76/460-1	21.09.2010	22:02	73° 35.55' N	62° 50.23' W	563.8	Ocean bottom seismometer	on deck	
PS76/461-1	21.09.2010	23:12	73° 39.01' N	62° 24.59' W	576.1	Ocean bottom seismometer	at surface	aufgetaucht
PS76/461-1	21.09.2010	23:19	73° 38.90' N	62° 24.54' W	574.5	Ocean bottom seismometer	on deck	
PS76/461-2	21.09.2010	23:36	73° 38.91' N	62° 24.61' W	575.1	Gravity corer	on ground/max depth	GE52.2, 560m

A.4 Stationsliste / station list PS 76

Station	Date	Time	Position Lat	Position Lon	Depth [m]	Gear	Action	Comment
PS76/462-1	22.09.2010	01:01	73° 42.21' N	61° 58.59' W	595.7	Ocean bottom seismometer	action	aufgetaucht
PS76/462-1	22.09.2010	01:13	73° 42.21' N	61° 58.83' W	597.3	Ocean bottom seismometer	on deck	
PS76/463-1	22.09.2010	02:24	73° 45.44' N	61° 33.11' W	574.8	Ocean bottom seismometer	action	aufgetaucht
PS76/463-1	22.09.2010	02:35	73° 45.52' N	61° 32.81' W	576.6	Ocean bottom seismometer	on deck	
PS76/464-1	22.09.2010	03:04	73° 46.01' N	61° 28.16' W	570.1	Gravity corer	on ground/max depth	GE52.2, 556m
PS76/465-1	22.09.2010	04:38	73° 49.01' N	61° 7.23' W	534.6	Ocean bottom seismometer	at surface	aufgetaucht
PS76/465-1	22.09.2010	04:45	73° 48.99' N	61° 6.84' W	536.8	Ocean bottom seismometer	on deck	
PS76/466-1	22.09.2010	05:53	73° 52.26' N	60° 40.39' W	551.4	Ocean bottom seismometer	at surface	aufgetaucht
PS76/466-1	22.09.2010	06:08	73° 52.21' N	60° 40.54' W	550.0	Ocean bottom seismometer	on deck	
PS76/466-2	22.09.2010	06:25	73° 52.22' N	60° 40.46' W	550.9	Gravity corer	on ground/max depth	GE52.2, 535m
PS76/467-1	22.09.2010	07:48	73° 55.53' N	60° 14.04' W	554.5	Ocean bottom seismometer	at surface	aufgetaucht
PS76/467-1	22.09.2010	08:01	73° 55.58' N	60° 14.17' W	556.0	Ocean bottom seismometer	on deck	
PS76/468-1	22.09.2010	09:08	73° 58.84' N	59° 48.02' W	515.7	Ocean bottom seismometer	at surface	aufgetaucht
PS76/468-1	22.09.2010	09:13	73° 58.78' N	59° 47.85' W	512.1	Ocean bottom seismometer	on deck	
PS76/468-2	22.09.2010	09:28	73° 58.80' N	59° 47.75' W	511.4	Gravity corer	on ground/max depth	Ge52.2 ; 500 m
PS76/469-1	22.09.2010	10:46	74° 2.05' N	59° 21.44' W	369.1	Ocean bottom seismometer	at surface	aufgetaucht
PS76/469-1	22.09.2010	10:53	74° 2.10' N	59° 21.13' W	367.6	Ocean bottom seismometer	on deck	
PS76/470-1	22.09.2010	11:57	74° 5.35' N	58° 55.03' W	225.6	Ocean bottom seismometer	at surface	aufgetaucht
PS76/470-1	22.09.2010	12:07	74° 5.34' N	58° 54.83' W	227.4	Ocean bottom seismometer	on deck	
PS76/471-1	22.09.2010	12:43	74° 6.01' N	58° 48.05' W	222.8	Gravity corer	on ground/max depth	207 m, GE 52.2
PS76/472-1	22.09.2010	14:07	74° 8.59' N	58° 28.44' W	137.5	Ocean bottom seismometer	action	Hydrophon an Deck, aufgetaucht
PS76/472-1	22.09.2010	14:21	74° 8.67' N	58° 28.11' W	156.6	Ocean bottom seismometer	on deck	
PS76/473-1	22.09.2010	15:32	74° 12.01' N	58° 1.60' W	595.5	Ocean bottom seismometer	action	aufgetaucht

A.4 Stationsliste / station list PS 76

Station	Date	Time	Position Lat	Position Lon	Depth [m]	Gear	Action	Comment
PS76/473-1	22.09.2010	15:40	74° 11.89' N	58° 1.85' W	594.0	Ocean bottom seismometer	on deck	
PS76/473-2	22.09.2010	16:02	74° 11.94' N	58° 1.53' W	599.4	Gravity corer	on ground/max depth	GE52.2 590m
PS76/474-1	22.09.2010	20:09	73° 50.92' N	59° 53.43' W	437.3	Ocean bottom seismometer	at surface	aufgetaucht
PS76/474-1	22.09.2010	20:15	73° 50.90' N	59° 53.19' W	439.2	Ocean bottom seismometer	on deck	
PS76/475-1	22.09.2010	21:21	73° 43.08' N	59° 58.58' W	372.0	Ocean bottom seismometer	at surface	aufgataucht
PS76/475-1	22.09.2010	21:30	73° 43.06' N	59° 58.25' W	374.5	Ocean bottom seismometer	on deck	
PS76/476-1	22.09.2010	22:34	73° 35.16' N	60° 3.73' W	329.3	Ocean bottom seismometer	at surface	aufgetaucht
PS76/476-1	22.09.2010	22:41	73° 35.21' N	60° 3.62' W	327.0	Ocean bottom seismometer	on deck	
PS76/477-1	22.09.2010	23:45	73° 27.37' N	60° 8.98' W	340.1	Ocean bottom seismometer	at surface	aufgetaucht
PS76/477-1	22.09.2010	23:51	73° 27.39' N	60° 8.84' W	340.1	Ocean bottom seismometer	on deck	
PS76/478-1	23.09.2010	00:56	73° 19.53' N	60° 14.01' W	368.1	Ocean bottom seismometer	action	Hydrophon an Deck, aufgetaucht
PS76/478-1	23.09.2010	01:11	73° 19.33' N	60° 14.00' W	360.4	Ocean bottom seismometer	on deck	
PS76/479-1	23.09.2010	02:15	73° 11.61' N	60° 19.75' W	307.3	Ocean bottom seismometer	action	Hydrofon an Deck, aufgetaucht
PS76/479-1	23.09.2010	02:26	73° 11.57' N	60° 19.38' W	309.4	Ocean bottom seismometer	on deck	
PS76/480-1	23.09.2010	02:47	73° 11.98' N	60° 17.97' W	308.7	Gravity corer	on ground/max depth	301 m, GE 52.2
PS76/481-1	23.09.2010	04:12	73° 3.64' N	60° 23.80' W	324.9	Ocean bottom seismometer	at surface	
PS76/481-1	23.09.2010	04:26	73° 3.74' N	60° 24.38' W	326.6	Ocean bottom seismometer	on deck	
PS76/482-1	23.09.2010	05:35	72° 55.80' N	60° 29.13' W	412.8	Ocean bottom seismometer	at surface	aufgetaucht
PS76/482-1	23.09.2010	05:47	72° 55.89' N	60° 29.10' W	414.0	Ocean bottom seismometer	on deck	
PS76/483-1	23.09.2010	07:00	72° 47.79' N	60° 34.35' W	707.6	Ocean bottom seismometer	at surface	aufgetaucht
PS76/483-1	23.09.2010	07:15	72° 47.90' N	60° 34.39' W	707.8	Ocean bottom seismometer	on deck	
PS76/484-1	23.09.2010	08:27	72° 40.14' N	60° 39.29' W	722.1	Ocean bottom seismometer	at surface	aufgetaucht

A.4 Stationsliste / station list PS 76

Station	Date	Time	Position Lat	Position Lon	Depth [m]	Gear	Action	Comment
PS76/484-1	23.09.2010	08:32	72° 40.17' N	60° 39.14' W	718.4	Ocean bottom seismometer	on deck	
PS76/484-2	23.09.2010	08:52	72° 40.17' N	60° 39.21' W	719.1	Gravity corer	on ground/max depth	GE52.2 ; 704m
PS76/485-1	23.09.2010	10:19	72° 32.27' N	60° 44.28' W	670.8	Ocean bottom seismometer	at surface	aufgetaucht
PS76/485-1	23.09.2010	10:23	72° 32.33' N	60° 44.15' W	671.5	Ocean bottom seismometer	on deck	
PS76/486-1	23.09.2010	11:51	72° 24.43' N	60° 49.07' W	643.0	Ocean bottom seismometer	at surface	aufgetaucht
PS76/486-1	23.09.2010	11:58	72° 24.49' N	60° 48.92' W	643.7	Ocean bottom seismometer	on deck	
PS76/486-2	23.09.2010	12:18	72° 24.51' N	60° 48.85' W	644.8	Gravity corer	on ground/max depth	630 m, GE 52.2
PS76/487-1	23.09.2010	14:00	72° 16.62' N	60° 53.50' W	875.0	Ocean bottom seismometer	action	aufgetaucht
PS76/487-1	23.09.2010	14:12	72° 16.66' N	60° 54.01' W	876.5	Ocean bottom seismometer	on deck	
PS76/488-1	23.09.2010	15:52	72° 8.73' N	60° 59.29' W	1497.0	Ocean bottom seismometer	action	aufgetaucht
PS76/488-1	23.09.2010	16:05	72° 8.82' N	60° 58.73' W	1492.0	Ocean bottom seismometer	on deck	
PS76/488-2	23.09.2010	16:38	72° 8.80' N	60° 58.86' W	1493.0	Gravity corer	on ground/max depth	GE52.2 1460m
PS76/489-1	23.09.2010	18:40	72° 0.80' N	61° 3.66' W	1554.0	Ocean bottom seismometer	at surface	aufgetaucht
PS76/489-1	23.09.2010	18:54	72° 0.83' N	61° 3.52' W	1551.0	Ocean bottom seismometer	on deck	
PS76/490-1	23.09.2010	20:00	71° 55.93' N	61° 6.46' W	1597.0	Ocean bottom seismometer	at surface	aufgetaucht
PS76/490-1	23.09.2010	20:05	71° 56.01' N	61° 6.23' W	1591.0	Ocean bottom seismometer	on deck	
PS76/491-1	23.09.2010	21:47	71° 48.54' N	61° 10.94' W	1629.4	CTD/rosette water sampler	on ground/max depth	EL31; 1593 m
PS76/491-1	23.09.2010	22:14	71° 48.52' N	61° 10.95' W	1629.9	CTD/rosette water sampler	on deck	
PS76/491-2	23.09.2010	23:00	71° 48.53' N	61° 10.88' W	1634.0	Heat Flow	on ground/max depth	GE52.1 ; 1608 m
PS76/492-1	24.09.2010	01:32	71° 39.12' N	61° 14.80' W	1696.0	Heat Flow	on ground/max depth	1676 m, GE 52.1
PS76/493-1	24.09.2010	03:55	71° 30.08' N	61° 18.51' W	1737.0	Heat Flow	on ground/max depth	1711 m, GE 52.1
PS76/494-1	24.09.2010	06:25	71° 21.58' N	61° 27.71' W	1831.0	Heat Flow	on ground/max depth	GE52.1 1797m
PS76/496-1	24.09.2010	10:12	71° 13.96' N	60° 13.83' W	760.5	Magnetic profile	profile start	Kurs: 010 deg
PS76/497-1	24.09.2010	22:15	73° 11.14' N	59° 3.49' W	690.7	Magnetic profile	profile start	B.Schreckenberger, Kurs105 deg

A.4 Stationsliste / station list PS 76

Station	Date	Time	Position Lat	Position Lon	Depth [m]	Gear	Action	Comment
PS76/496-1	24.09.2010	22:15	73° 11.14' N	59° 3.49' W	690.7	Magnetic profile	profile end	
PS76/498-1	24.09.2010	22:58	73° 9.41' N	58° 40.99' W	823.5	Magnetic profile	profile start	B.Schreckenberger, Kurs: 190 deg
PS76/499-1	25.09.2010	11:00	71° 11.77' N	59° 48.85' W	493.0	Magnetic profile	profile start	Kurs: 108 deg
PS76/500-1	25.09.2010	11:46	71° 9.41' N	59° 26.56' W	366.3	Magnetic profile	profile start	B.Schreckenberger, Kurs: 010 deg
PS76/501-1	25.09.2010	20:00	72° 30.07' N	58° 38.95' W	250.1	Magnetic profile	alter course	B.Schreckenberger
PS76/502-1	25.09.2010	20:43	72° 28.47' N	58° 15.83' W	212.6	Magnetic profile	profile start	Kurs: B.Schreckenberger
PS76/502-1	26.09.2010	04:48	71° 8.26' N	59° 0.30' W	369.5	Magnetic profile	profile end	
PS76/503-1	26.09.2010	05:08	71° 8.12' N	59° 5.19' W	370.2	Magnetic profile	on deck	komplett
PS76/504-1	26.09.2010	08:31	71° 9.81' N	59° 23.73' W	362.9	Seismic reflection profile	on ground/max depth	Streamer komplett ausgelegt
PS76/504-2	26.09.2010	08:40	71° 9.61' N	59° 21.57' W	360.0	Seismic reflection profile	action	Beginn rump up,, 1.Schuss
PS76/505-1	26.09.2010	08:55	71° 9.28' N	59° 18.07' W	353.2	Seismic reflection profile	profile start	BGR 10-322
PS76/504-3	26.09.2010	09:16	71° 8.77' N	59° 13.17' W	364.0	Magnetic profile	profile start	850 m ausgelegt
PS76/504-3	27.09.2010	04:07	70° 41.19' N	54° 50.37' W	397.7	Magnetic profile	profile end	
PS76/505-1	27.09.2010	04:07	70° 41.19' N	54° 50.37' W	397.7	Seismic reflection profile	profile end	
PS76/506-1	27.09.2010	04:27	70° 40.15' N	54° 48.31' W	415.8	Seismic reflection profile	hoisting	Streamer
PS76/506-2	27.09.2010	06:48	70° 34.14' N	54° 41.56' W	481.9	Magnetic profile	on deck	drei Sonden
PS76/506-1	27.09.2010	08:16	70° 29.29' N	54° 36.99' W	424.1	Seismic reflection profile	on deck	
PS76/507-1	01.10.2010	10:55	58° 58.14' N	42° 34.06' W	2058.0	Magnetic profile	in the water	Verantw.: B.Schreckenberger
PS76/507-1	01.10.2010	11:20	58° 58.64' N	42° 30.29' W	2097.0	Magnetic profile	profile start	
PS76/507-1	03.10.2010	08:21	58° 59.32' N	28° 15.00' W	2165.0	Magnetic profile	profile end	
PS76/507-1	03.10.2010	08:44	58° 59.28' N	28° 10.66' W	2179.0	Magnetic profile	on deck	

A.5 GEOPHYSICAL PROFILE LIST

line number	shot point start/end	date	time UTC	latitude	longitude	course	S=seis. reflect. OBS=seis. Refr. M=magnetics G=gravity B=bathymetrie P=Parasound	length (km)
BGR10-3M01		06.08.10	15:28	64° 32.180 N	54° 59.502 W		M,G,B,P	
		08.08.10	10:30	69° 39.814 N	64° 10.535 W	329°		692.79 km
BGR10-3M02		08.08.10	23:02	69° 33.176 N	63° 59.045 W		M,G,B,P	
		09.08.10	05:24	70° 25.999 N	63° 44.560 W	5°		98.24 km
BGR10-3M02A		09.08.10	09:31	70° 37.061 N	63° 38.345 W		M,G,B,P	
		09.08.10	13:07	71° 01.414 N	63° 28.767 W	7°		45.47 km
BGR10-3M03		09.08.10	13:14	71° 01.821 N	63° 26.966 W		M,G,B,P	
		09.08.10	15:18	71° 01.979 N	62° 42.234 W	89°		26.92 km
BGR10-3M04		09.08.10	15:23	71° 01.574 N	62° 42.125 W		M,G,B,P	
		10.08.10	04:04	69° 29.844 N	63° 20.776 W	188°		171.56 km
BGR10-3M05		10.08.10	04:12	69° 28.994 N	63° 19.369 W		M,G,B,P	
		10.08.10	07:50	69° 12.404 N	62° 04.785 W	122°		57.59 km
BGR10-3M06		10.08.10	08:12	69° 14.307 N	62° 03.090 W		M,G,B,P	
		10.08.10	21:15	71° 04.146 N	61° 19.479 W	7°		205.22 km
BGR10-306	1	11.08.10	05:08:43	71° 20.481 N	61° 58.144 W		S,M,G,B,P	
	4686	12.08.10	00:40:07	72° 42.773 N	64° 18.837 W	333°		172.25 km
BGR10-306a	1	12.08.10	04:46:09	72° 39.980 N	64° 17.552 W		S,M,G,B,P	
	5290	13.08.10	02:48:16	74° 07.529 N	60° 57.440 W	32°		193.57 km
BGR10-305	1	13.08.10	05:23:29	74° 06.069 N	61° 04.645 W		S,M,G,B,P	
	4704	14.08.10	00:59:21	74° 37.243 N	66° 29.086 W	292°		171.86 km
BGR10-302	1	14.08.10	03:03:01	74° 39.927 N	66° 13.724 W		S,M,G,B,P	
	3410	14.08.10	17:15:19	74° 03.265 N	69° 40.683 W	238°		123.59 km
BGR10-3r2	1	15.08.10	22:07:00	75° 32.439 N	60° 38.250 W		OBS,G,B,P	
	2103	17.08.10	09:09:00	74° 02.566 N	69° 44.851 W	242°		312.87 km
BGR10-307	1	17.08.10	21:58:26	74° 11.573 N	69° 09.547 W		S,M,G,B,P	
	5050	18.08.10	19:01:53	73° 37.638 N	63° 27.485 W	107°		186.36 km
BGR10-307a	1	18.08.10	19:20:59	73° 37.147 N	63° 22.614 W		S,M,G,B,P	
	5105	19.08.10	16:37:07	73° 03.037 N	57° 50.361 W	107°		187.31 km
BGR10-308	1	19.08.10	17:49:15	73° 05.886 N	57° 48.260 W		S,M,G,B,P	

A.5 Geophysical profile list

	1723	20.08.10	00:59:44	72° 39.457 N	59° 01.301 W	227°		63.09 km
BGR10-308a	1	20.08.10	05:17:23	72° 43.341 N	58° 49.022 W		S,M,G,B,P	
	3616	20.08.10	20:21:18	71° 46.952 N	61° 14.930 W	219°		132.96 km
BGR10-309	1	20.08.10	22:02:00	71° 45.888 N	61° 10.234 W		S,M,G,B,P	
	7662	22.08.10	05:57:21	74° 17.045 N	59° 35.537 W	10°		284.51 km
BGR10-310	1	22.08.10	06:15:00	74° 18.082 N	59° 32.354 W		S,M,G,B,P	
	1493	22.08.10	12:28:06	74° 13.127 N	57° 43.248 W	99°		55.56 km
BGR10-311	1	22.08.10	13:38:00	74° 14.381 N	57° 42.333 W		S,M,G,B,P	
	7425	23.08.10	20:33:53	73° 12.914 N	65° 44.009 W	249°		274.33 km
BGR10-312	1	23.08.10	22:17:00	73° 10.024 N	65° 33.074 W		S,M,G,B,P	
	3529	24.08.10	12:59:01	73° 56.794 N	68° 36.051 W	314°		129.19 km
BGR10-313	1	24.08.10	13:01:27	73° 56.980 N	68° 36.163 W		S,M,G,B,P	
	3098	25.08.10	01:55:43	74° 56.950 N	69° 33.918 W	346°		114.68 km
BGR10-302a	1	28.08.10	02:09:16	75° 33.408 N	60° 24.886 W		S,M,G,B,P	
	5510	29.08.10	01:06:34	74° 35.378 N	66° 28.307 W	241°		203.80 km
BGR10-305a	1	29.08.10	02:35:00	74° 33.912 N	66° 15.788 W		S,M,G,B,P	
	2960	29.08.10	14:54:57	74° 55.656 N	69° 40.163 W	294°		107.38 km
BGR10-303a	1	29.08.10	17:15:00	74° 53.378 N	69° 30.603 W		S,M,G,B,P	
	7122	30.08.10	22:56:19	77° 13.287 N	71° 56.615 W	347°		267.08 km
BGR10-3r3	1	01.09.10	18:53:00	73° 57.517 N	68° 36.613 W		OBS,G,B,P	
	242	01.09.10	22:54:00	74° 16.463 N	68° 54.059 W	346°		36.18 km
BGR10-3r3a	1	02.09.10	01:04:00	74° 14.741 N	68° 51.250 W		OBS,G,B,P	
	2102	03.09.10	12:05:00	77° 13.355 N	71° 55.968 W	347°		341.19 km
BGR10-3M07		04.09.10	15:47	75° 26.866 N	70° 28.616 W		M,G,B,P	
		04.09.10	20:58	76° 11.727 N	71° 17.413 W	345°		85.96 km
BGR10-3M08		04.09.10	21:45	76° 11.980 N	71° 42.145 W		M,G,B,P	
		05.09.10	04:03	75° 17.441 N	70° 47.199 W	166°		104.04 km
BGR10-3M07a		05.09.10	04:58	75° 16.098 N	70° 17.958 W		M,G,B,P	
		05.09.10	06:51	75° 30.755 N	70° 31.144 W	347°		27.83 km
BGR10-3Kali		07.09.10	07:17			div	M,G,B,P	
		07.09.10	11:00					
BGR10-3M09		07.09.10	11:09	74° 12.378 N	68° 52.244 W		M,G,B,P	
		07.09.10	18:00	74° 41.782 N	72° 15.161 W	300°		114.47 km
BGR10-314	1	07.09.10	20:31:32	74° 49.388 N	72° 23.909 W		S,M,G,B,P	
	6170	08.09.10	22:14:06	76° 47.065 N	74° 49.834 W	344°		227.71 km

A.5 Geophysical profile list

BGR10-315	6180	08.09.10	22:16:36	76° 47.256 N	74° 49.774 W		S,M,G,B,P	
	8513	09.09.10	07:59:53	77° 32.165 N	74° 32.185 W	5°		83.47 km
BGR10-316	1	10.09.10	07:29:00	79° 21.296 N	66° 53.404 W		S,G,B,P	
	2259	10.09.10	16:54:13	79° 58.266 N	68° 59.795 W	330°		80.30 km
BGR10-317	1	10.09.10	19:12:30	80° 09.613 N	68° 26.080 W		S,G,B,P	
	3692	11.09.10	10:35:00	78° 59.453 N	70° 16.022 W	197°		135.02 km
BGR10-318	1	12.09.10	10:29:00	76° 20.793 N	74° 16.191 W		S,M,G,B,P	
	537	12.09.10	12:43:04	76° 20.349 N	73° 30.116 W	92°		20.16 km
BGR10-318a	1	12.09.10	15:30:00	76° 20.429 N	73° 36.604 W		S,G,B,P	
	2757	13.09.10	02:59:13	76° 17.678 N	69° 40.470 W	91°		103.53 km
BGR10-319	1	13.09.10	03:53:16	76° 19.006 N	69° 44.252 W		S,M,G,B,P	
	3456	13.09.10	18:17:00	75° 44.070 N	73° 54.222 W	242°		129.10 km
BGR10-320	1	13.09.10	20:05:30	75° 45.025 N	73° 47.039 W		S,M,G,B,P	
	5177	14.09.10	17:39:28	75° 51.936 N	66° 47.418 W	83°		190.82 km
BGR10-321	1	14.09.10	19:34:00	75° 46.488 N	67° 06.247 W		S,M,G,B,P	
	4991	15.09.10	16:21:23	74° 37.711 N	71° 48.319 W	229°		184.34 km
BGR10-3r4	1	18.09.10	15:32:00	71° 33.926 N	61° 16.620 W		OBS,G,B	
	1944	19.09.10	23:55:00	74° 14.767 N	59° 36.955 W	10°		302.69 km
BGR10-3r1	1	20.09.10	02:45:00	74° 13.792 N	58° 03.558 W		OBS,G,B	
	1764	21.09.10	08:08:00	73° 13.987 N	65° 37.951 W	249°		260.18 km
BGR10-3M10		24.09.10	10:15	71° 14.347 N	60° 13.278 W		M,G,B,P	
		24.09.10	22:15	73° 11.133 N	59° 03.468 W	10°		219.82 km
BGR10-3M11		24.09.10	23:10	73° 07.570 N	58° 43.262 W		M,G,B,P	
		25.09.10	11:00	71° 11.782 N	59° 48.799 W	190°		217.59 km
BGR10-3M12		25.09.10	11:49	71° 09.787 N	59° 26.076 W		M,G,B,P	
		25.09.10	19:58	72° 29.805 N	58° 39.485 W	10°		150.59 km
BGR10-3M13		25.09.10	20:45	72° 28.172 N	58° 15.802 W		M,G,B,P	
		26.09.10	04:44	71° 08.926 N	58° 59.945 W	190°		148.94 km
BGR10-322	1	26.09.10	08:41:00	71° 09.586 N	59° 21.339 W		S,M,G,B,P	
	4666	27.09.10	04:07:12	70° 41.190 N	54° 50.381 W	106°		172.16 km
BGR10-3M14		01.10.10	11:11	58° 58.458 N	42° 31.665 W		M,G,B,P	
		03.10.10	08:15	58° 59.344 N	28° 16.593 W	84°		814.35 km

A.5A EXEMPLARY PROCESSING WORK FLOW

The exemplary processing work flow shows detailed processing parameters from the point of prestack multiple suppression. Input data for this workflow are geometry applied raw data. Exemplary mcs line is BGR10-307. Other lines may differ.

=====

Create Splitspreads:

```
*** Disk Data Input ***
Select dataset = 307.geom
Propagate input file history = Yes
Trace read option = Sort
Interactive Data Access? = No
Select primary trace header entry = CDP bin number
Select secondary trace header entry = Absolute value
of offset
Select tertiary trace header entry = No trace header
entry selected
Sort order list for dataset = */
Presort in memory or on disk? = Memory
Read the data multiple times? = No
Process trace headers only? = No
Override input data's sample interval? = No
```

```
*** Bandpass Filter ***
TYPE of filter = Single Filter
Type of filter specification = Ormsby bandpass
PHASE of filter = Minimum
Percent additive noise factor = 1.0
Domain for filter application = Frequency
Percent zero padding for FFT's = 25.0
Apply a notch filter? = No
Ormsby filter frequency values = 3-6-80-120
Re-apply trace mute after filter? = Yes
```

```
*** Create Split Spreads ***
Min near offset for extrapolation = 255.0
Distance between traces = 60.0
Limit created side of split spread? = Yes
Max offset on created side = 1000.0
Width of edge taper = 250.0
Max feathering = 100.0
Get NMO velocities from database? = Yes
Select Velocity file = 307.vel01
Max offset to model = 1000.0
Number of P-values = 7
Min P-value to model = -20.0
Max P-value to model = 10.0
Damping for Radon solution = 0.03
Verbose listing? = No
```

```
*** Disk Data Output ***
Output Dataset Filename = 307.splitspreads
New, or Existing, File? = New
Record length to output = 0.0
Trace sample format = 16 bit
Skip primary disk storage? = No
```

Apply SRME:

```
*** Disk Data Input ***
Select dataset = 307.splitspreads
Propagate input file history = Yes
Trace read option = Sort
Interactive Data Access? = No
```

```
Select primary trace header entry = Source index
number (internal)*
Select secondary trace header entry = Signed source-
receiver offset
Select tertiary trace header entry = No trace header
entry selected
Sort order list for dataset = */
Presort in memory or on disk? = Memory
Read the data multiple times? = No
Process trace headers only? = No
Override input data's sample interval? = No
```

```
*** Parallel Begin ***
Enter host name(s) for parallel execution = b3lx04,
b3lx04, b3lx04, b3lx04
Unit of data distribution/collection = Ensemble
Data distribution/collection policy = Round-robin
```

```
*** Trace Muting ***
Re-apply previous mutes = No
Mute time reference = Time 0
TYPE of mute = Top
Starting ramp = 30.0
EXTRAPOLATE mute times? = Yes
Get mute file from the DATABASE? = Yes
SELECT mute parameter file = mute_splitspreads
```

```
*** Surface-Related Wave Eq Mult Rej ***
= ----- Earth Model Parameters -----
```

```
-----
Number of horizons = 1
Get amplitudes from database? = Yes
Select horizon file 1 = seafloor4srme
Select amplitude file 1 = Hor 1 RMS Amplitude
00:50:44 28-Aug-10
Polarity of horizon 1 = Pos
Is horizon 1 the water bottom? = Yes
Water velocity = 1465.0
= ----- Output Parameters -----
```

```
--
Type of output = Estimate and Remove Multiples
Output spikes at gate times? = No
Discard prep traces? = Yes
SELECT water bottom time trace header entry = Water
bottom time at mid-point
= ----- Convolution Parameters -----
```

```
-----
Distance between traces = 12.5
Max convolution distance = 3930.0
Convolution method = Window
= ----- Shaping Parameters -----
```

```
---
Shaping method = Least-squares filter with lag
Filter gate spacing = 1.0
Filter design gate length = 1000
Filter design gate skew = 0.25
Filter length = 200
Max expected time shift = 30
Percent white noise = 0.1
Use panels in shaping? = No
```

*** Parallel End ***

*** Disk Data Output ***

Output Dataset Filename = 307.srme
 New, or Existing, File? = New
 Record length to output = 0.0
 Trace sample format = 16 bit
 Skip primary disk storage? = No

Deconvolution, Radon Velocity Filter, NMO and Stack:

*** Disk Data Input ***

Select dataset = 307.srme
 Propagate input file history = Yes
 Trace read option = Sort
 Interactive Data Access? = No
 Select primary trace header entry = CDP bin number
 Select secondary trace header entry = Absolute value
 of offset
 Select tertiary trace header entry = No trace header
 entry selected
 Sort order list for dataset = */
 Presort in memory or on disk? = Memory
 Read the data multiple times? = No
 Process trace headers only? = No
 Override input data's sample interval? = No

*** Parallel Begin ***

Enter host name(s) for parallel execution = b3lx04,
 b3lx04, b3lx04, b3lx04
 Unit of data distribution/collection = Ensemble
 Data distribution/collection policy = Round-robin

*** Bandpass Filter ***

TYPE of filter = Single Filter
 Type of filter specification = Ormsby bandpass
 PHASE of filter = Zero
 Domain for filter application = Frequency
 Percent zero padding for FFT's = 25.0
 Apply a notch filter? = No
 Ormsby filter frequency values = 3-6-80-120
 Re-apply trace mute after filter? = Yes

*** Spiking/Predictive Decon ***

TYPE of deconvolution = Minimum phase predictive
 Decon operator length(s) = 170
 Operator prediction distance(s) = 32
 Is prediction distance water relative? = No
 Apply prediction filter correction? = No
 Apply user specified taper? = No
 Operator 'white noise' level(s) = 0.1
 Window rejection factor = 2.0
 Time gate reference = Time 0
 Get decon gates from the DATABASE? = Yes
 SELECT decon gate parameter file = deco02
 Output traces or filters = Normal decon output
 Apply a bandpass filter after decon? = No
 Re-apply trace mute after decon? = Yes

*** Bandpass Filter ***

TYPE of filter = Single Filter
 Type of filter specification = Ormsby bandpass
 PHASE of filter = Zero
 Domain for filter application = Frequency
 Percent zero padding for FFT's = 25.0
 Apply a notch filter? = No
 Ormsby filter frequency values = 3-6-80-120

Re-apply trace mute after filter? = Yes

*** True Amplitude Recovery ***

Apply spherical divergence corrections? = Yes
 Basis for spherical spreading = 1/(time*vel**2)
 Apply inelastic attenuation corrections? = No
 Get TAR velocity function from database? = Yes
 Should the velocity be treated as space variable? =
 Yes
 Select velocity parameter file = 307.vel02.smooth
 Apply dB/sec corrections? = No
 Apply time raised to a power corrections? = No
 APPLY function to data or REMOVE effect of amplitude
 corrections? = Apply
 Maximum application TIME = 14000.0
 Normalization reference TIME = 0.0

*** Normal Moveout Correction ***

Direction for NMO application = FORWARD
 Stretch mute percentage = 30.0
 Apply any remaining static during NMO? = No
 Long offset correction? = ALCHALABI
 Anisotropy correction parameter eta = 0.0
 Apply partial NMO? = No
 Get velocities from the database? = Yes
 SELECT Velocity parameter file = 307.vel02

*** Parallel End ***

*** Radon Velocity Filter ***

Has NMO already been applied? = Yes
 Number of P-values = 31
 Number of time gates = 5
 Minimum time of interest (ms) = 0.0
 Maximum time of interest (ms) = 2.0
 Minimum frequency of interest = 2.0
 Maximum frequency of interest = 90.0
 Pass modeled data or subtract from input? =
 SUBTRACT
 Type of transform to perform = Parabolic
 Reference offset for transform = 3929.7
 Low percentage of velocity to keep. = 15.0
 High percentage of velocity to keep. = 20.0
 Get velocities from the database? = Yes
 SELECT Velocity parameter file = 307.vel02.smooth
 Radon domain starting ramp length = 30.0
 Re-apply T-X trace mute after filter? = Yes
 Remove NMO after filtering? = No

*** Parallel Begin ***

Enter host name(s) for parallel execution = b3lx04,
 b3lx04, b3lx04, b3lx04
 Unit of data distribution/collection = Ensemble
 Data distribution/collection policy = Round-robin

*** Bandpass Filter ***

TYPE of filter = Single Filter
 Type of filter specification = Ormsby bandpass
 PHASE of filter = Zero
 Domain for filter application = Frequency
 Percent zero padding for FFT's = 25.0
 Apply a notch filter? = No
 Ormsby filter frequency values = 3-6-80-120
 Re-apply trace mute after filter? = Yes

*** CDP/Ensemble Stack ***

Sort order of input ensembles = CDP
 METHOD for trace summing = Alpha-trimmed Mean
 PERCENT of samples to exclude = 25.0

A.5A Exemplary processing work flow

Apply final datum statics after stack? = No
Has NMO been applied? = Yes

*** Bandpass Filter ***

TYPE of filter = Single Filter
Type of filter specification = Ormsby bandpass
PHASE of filter = Zero
Domain for filter application = Frequency
Percent zero padding for FFT's = 25.0
Apply a notch filter? = No
Ormsby filter frequency values = 3-6-80-120
Re-apply trace mute after filter? = Yes

*** Parallel End ***

*** Disk Data Output ***

Output Dataset Filename = 307.srme.second_stack
New, or Existing, File? = New
Record length to output = 0.0
Trace sample format = 16 bit
Skip primary disk storage? = Yes

Poststack Kirchhoff Migration:

*** Disk Data Input ***

Read data from other lines/surveys? = No
Select dataset = 307.srme.second_stack
Propagate input file history = Yes
Trace read option = Sort

Interactive Data Access? = No

Select primary trace header entry = CDP bin number
Select secondary trace header entry = No trace header
entry selected
Sort order list for dataset = */
Presort in memory or on disk? = Memory
Read the data multiple times? = No
Process trace headers only? = No
Override input data's sample interval? = No

*** Kirchhoff Time Mig. ***

CDP interval (feet or meters) = 6.25
Maximum frequency to migrate (in Hz) = 120.0
Migration aperture (feet or meters) = 6000.0
Maximum dip to migrate = 30.0
Avoid spatial aliasing? = Yes
Get RMS velocities from database? = Yes
Select RMS vs.time velocity file = 307.vel02.smooth
Change maximum memory usage? = No
Change the default tapering? = No
Re-apply trace mutes? = Yes
Re-kill dead traces? = Yes

*** Disk Data Output ***

Output Dataset Filename = 307.srme.second_khmig
New, or Existing, File? = New
Record length to output = 0.0
Trace sample format = 16 bit
Skip primary disk storage? = Yes

A.6 OBS STATION LIST, PROFILE BGR10-3R1

station number	latitude (°N)	longitude (°W)	depth (m)	profile name
450st001	73,3192	-64,9717	2301	AWI-20100450 / BGR10-3r1
450st002	73,3747	-64,5457	2062	AWI-20100450 / BGR10-3r1
450st003	73,4295	-64,1225	1516	AWI-20100450 / BGR10-3r1
450st004	73,4843	-63,6973	643	AWI-20100450 / BGR10-3r1
450st005	73,5388	-63,2698	598	AWI-20100450 / BGR10-3r1
450st006	73,5942	-62,8397	567	AWI-20100450 / BGR10-3r1
450st007	73,6497	-62,4098	579	AWI-20100450 / BGR10-3r1
450st008	73,7048	-61,9783	595	AWI-20100450 / BGR10-3r1
450st009	73,7602	-61,5460	577	AWI-20100450 / BGR10-3r1
450st010	73,8163	-61,1152	445	AWI-20100450 / BGR10-3r1
450st011	73,8702	-60,6728	551	AWI-20100450 / BGR10-3r1
450st012	73,9250	-60,2388	555	AWI-20100450 / BGR10-3r1
450st013	73,9805	-59,7972	513	AWI-20100450 / BGR10-3r1
450st014	74,0348	-59,3582	368	AWI-20100450 / BGR10-3r1
450st015	74,0893	-58,9140	228	AWI-20100450 / BGR10-3r1
450st016	74,1437	-58,4713	139	AWI-20100450 / BGR10-3r1
450st017	74,1992	-58,0252	598	AWI-20100450 / BGR10-3r1

A.7 OBS STATION LIST, PROFILE BGR10-3R2

station number	latitude (°N)	longitude (°W)	depth (m)	profile name
200st001	74,0953	-69,4368	1831	AWI-20100200 / BGR10-3r2
200st002	74,1565	-69,0723	1940	AWI-20100200 / BGR10-3r2
200st003	74,2187	-68,7083	2015	AWI-20100200 / BGR10-3r2
200st004	74,2783	-68,3450	2061	AWI-20100200 / BGR10-3r2
200st005	74,3393	-67,9817	2093	AWI-20100200 / BGR10-3r2
200st006	74,4017	-67,6067	2156	AWI-20100200 / BGR10-3r2
200st007	74,4617	-67,2500	2175	AWI-20100200 / BGR10-3r2
200st008	74,5217	-66,8833	2198	AWI-20100200 / BGR10-3r2
200st009	74,5843	-66,5048	2198	AWI-20100200 / BGR10-3r2
200st010	74,6457	-66,1298	1873	AWI-20100200 / BGR10-3r2
200st011	74,7072	-65,7543	1213	AWI-20100200 / BGR10-3r2
200st012	74,7690	-65,3768	540	AWI-20100200 / BGR10-3r2
200st013	74,8298	-64,9985	415	AWI-20100200 / BGR10-3r2
200st014	74,8918	-64,6142	343	AWI-20100200 / BGR10-3r2
200st015	74,9538	-64,2360	289	AWI-20100200 / BGR10-3r2
200st016	75,0148	-63,8522	158	AWI-20100200 / BGR10-3r2
200st017	75,0777	-63,4680	130	AWI-20100200 / BGR10-3r2
200st018	75,1372	-63,0838	153	AWI-20100200 / BGR10-3r2
200st019	75,1978	-62,6972	189	AWI-20100200 / BGR10-3r2
200st020	75,2593	-62,3037	594	AWI-20100200 / BGR10-3r2
200st021	75,3213	-61,9195	924	AWI-20100200 / BGR10-3r2
200st022	75,382	-61,5225	1187	AWI-20100200 / BGR10-3r2
200st023	75,4442	-61,1292	436	AWI-20100200 / BGR10-3r2
200st024	75,5057	-60,7362	394	AWI-20100200 / BGR10-3r2
200st025	75,539	-60,5087	472	AWI-20100200 / BGR10-3r2

A.8 OBS STATION LIST, PROFILE BGR10-3R3

station number	latitude (°N)	longitude (°W)	depth (m)	profile name
300st001	77,1048	-71,8112	857	AWI-20100300 / BGR10-3r3
300st002	76,9918	-71,6920	1048	AWI-20100300 / BGR10-3r3
300st003	76,8783	-71,5567	937	AWI-20100300 / BGR10-3r3
300st004	76,7655	-71,4315	777	AWI-20100300 / BGR10-3r3
300st005	76,6520	-71,3085	662	AWI-20100300 / BGR10-3r3
300st006	76,5390	-71,1833	491	AWI-20100300 / BGR10-3r3
300st007	76,4265	-71,0623	537	AWI-20100300 / BGR10-3r3
300st008	76,3133	-70,9410	642	AWI-20100300 / BGR10-3r3
300st009	76,1995	-70,8202	649	AWI-20100300 / BGR10-3r3
300st010	76,0870	-70,7020	609	AWI-20100300 / BGR10-3r3
300st011	75,9742	-70,5845	599	AWI-20100300 / BGR10-3r3
300st012	75,8608	-70,4617	572	AWI-20100300 / BGR10-3r3
300st013	75,7485	-70,3503	534	AWI-20100300 / BGR10-3r3
300st014	75,6342	-70,2355	545	AWI-20100300 / BGR10-3r3
300st015	75,5215	-70,1225	578	AWI-20100300 / BGR10-3r3
300st016	75,4085	-70,0087	637	AWI-20100300 / BGR10-3r3
300st017	75,2958	-69,8960	675	AWI-20100300 / BGR10-3r3
300st018	75,1827	-69,7835	702	AWI-20100300 / BGR10-3r3
300st019	75,0690	-69,6727	770	AWI-20100300 / BGR10-3r3
300st020	74,9560	-69,5608	975	AWI-20100300 / BGR10-3r3
300st021	74,8423	-69,4515	1292	AWI-20100300 / BGR10-3r3
300st022	74,7307	-69,3403	1563	AWI-20100300 / BGR10-3r3
300st023	74,6173	-69,2340	1716	AWI-20100300 / BGR10-3r3
300st024	74,5035	-69,1258	1792	AWI-20100300 / BGR10-3r3
300st025	74,3910	-69,0207	1863	AWI-20100300 / BGR10-3r3
300st026	74,2780	-68,9157	1947	AWI-20100300 / BGR10-3r3
300st027	74,1652	-68,8092	2011	AWI-20100300 / BGR10-3r3
300st028	74,0525	-68,7030	2040	AWI-20100300 / BGR10-3r3

A.9 OBS STATION LIST, PROFILE BGR10-3R4

station number	latitude (°N)	longitude (°W)	depth (m)	profile name
400st001	73,9805	-59,7972	513	AWI-20100400 / BGR10-3r4
400st002	73,8490	-59,8888	438	AWI-20100400 / BGR10-3r4
400st003	73,7180	-59,9758	373	AWI-20100400 / BGR10-3r4
400st004	73,5862	-60,0628	328	AWI-20100400 / BGR10-3r4
400st005	73,4568	-60,1490	340	AWI-20100400 / BGR10-3r4
400st006	73,3255	-60,2335	368	AWI-20100400 / BGR10-3r4
400st007	73,1942	-60,3180	309	AWI-20100400 / BGR10-3r4
400st008	73,0633	-60,4010	329	AWI-20100400 / BGR10-3r4
400st009	72,9325	-60,4873	411	AWI-20100400 / BGR10-3r4
400st010	72,8018	-60,5765	702	AWI-20100400 / BGR10-3r4
400st011	72,6705	-60,6545	719	AWI-20100400 / BGR10-3r4
400st012	72,5393	-60,7373	673	AWI-20100400 / BGR10-3r4
400st013	72,4083	-60,8160	645	AWI-20100400 / BGR10-3r4
400st014	72,2772	-60,8972	877	AWI-20100400 / BGR10-3r4
400st015	72,1465	-60,9785	1488	AWI-20100400 / BGR10-3r4
400st016	72,0155	-61,0575	1550	AWI-20100400 / BGR10-3r4
400st017	71,9333	-61,1087	1597	AWI-20100400 / BGR10-3r4

A.10 LIST OF LAND STATIONS

Station	Deployment	Recovery	Lat. (Heli)	Lon. (Heli)	Equipment
200stL1	15.08.2010 16:15	27.08.2010 15:57	75°33.90' N	58°35.24' W	geophone chains
300stL1	30.08.2010 14:47	03.09.2010 14:10	77°19.26' N	72°01.20' W	geophone chains
300stL2	30.08.2010 14:47	03.09.2010 13:50	77°19.26' N	72°01.20' W	seismometer
300stL3	30.08.2010 17:12	04.09.2010 13:00	77°25.58' N	72°06.97' W	geophone chains
450stL1	17.09.2010 11:34	22.09.2010 15:45	74°19.95' N	56°58.32' W	geophone chains
450stL2	17.09.2010 10:09	22.09.2010 14:38	74°21.13' N	56°41.82' W	seismometer

A.11 SONOBUOY STATION LIST

Station	Profile	Channel	Duration	Depth	Lat. (N)	Long. (W)	Deployment	Date	Time (UTC)
SB02	306a	88	8 h	30 m	73° 19.15'	62° 50.14'	helicopter	12.08.2010	15:11
SB03	305	88	8 h	30 m	74° 27.66'	64° 48.33'	helicopter	13.08.2010	19:07
SB04	307	88	8 h	30 m	73° 46.56'	64° 56.56'	helicopter	18.08.2010	16:10
SB05	309	88	8 h	30 m	72° 45.82'	60° 37.48'	helicopter	21.08.2010	11:11
SB06	309	56	8 h	30 m	73° 13.63'	60° 19.07'	helicopter	21.08.2010	17:09
SB07	310	88	8 h	30 m	74° 18.14'	59° 28.70'	ship	22.08.2010	06:27
SB08	311	88	8 h	30 m	73° 25.53'	64° 08.98'	helicopter	23.08.2010	14:29
SB09	313	96	4 h	30 m	73° 56.05'	68° 34.71'	ship	24.08.2010	12:50
SB10	302a	88	4 h	30 m	75° 09.66'	62° 55.71'	helicopter	28.08.2010	12:15
SB11	302a	88	4 h	30 m	74° 55.08'	64° 22.82'	helicopter	28.08.2010	18:00
SB12	305a	88	4 h	30 m	74° 44.85'	67° 56.94'	helicopter	29.08.2010	09:34
SB13	303a	88	4 h	120 m	74° 58.42'	69° 36.83'	helicopter	29.08.2010	19:00
SB14	303a	88	4 h	120 m	76° 03.40'	70° 39.42'	helicopter	30.08.2010	08:54
SB15	303a	88	4 h	66 m	76° 26.66'	71° 04.70'	helicopter	30.08.2010	13:39
SB16	314	88	4 h	120 m	74° 50.26'	72° 24.24'	helicopter	07.09.2010	21:28
SB17	314	88	4 h	66 m	75° 47.93'	73° 35.43'	helicopter	08.09.2010	10:51
SB18	314	88	4 h	300 m	76° 10.41'	74° 03.03'	helicopter	08.09.2010	14:45
SB19	316	88	4 h	66 m	79° 24.34'	66° 52.89'	ship	10.09.2010	08:25
SB20	316	96	4 h	66 m	79° 33.20'	67° 23.97'	ship	10.09.2010	10:38
SB21	316	88	4 h	66 m	79° 41.70'	67° 56.31'	ship	10.09.2010	12:47
SB22	316	2	4 h	66 m	79° 47.94'	68° 19.15'	ship	10.09.2010	14:19
SB23	317	88	4 h	66 m	80° 07.50'	68° 35.39'	ship	10.09.2010	19:57
SB24	317	96	4 h	66 m	79° 53.37'	68° 55.66'	ship	10.09.2010	22:57
SB25	317	88	4 h	66 m	79° 38.79'	69° 17.97'	ship	11.09.2010	02:04
SB26	317	2	4 h	66 m	79° 25.67'	69° 38.07'	ship	11.09.2010	04:55
SB27	317	88	4 h	66 m	79° 10.64'	70° 00.45'	ship	11.09.2010	08:14
SB28	321	88	4 h	66 m	75° 45.40'	67° 10.48'	helicopter	14.09.2010	20:36
SB29	321	88	4 h	66 m	75° 06.51'	69° 51.44'	ship	15.09.2010	07:37
SB30	321	96	4 h	66 m	74° 51.47'	70° 52.95'	ship	15.09.2010	12:09

A.12 HEAT FLOW STATION LIST

Station	Station-no.	Date/Time	Depth [m]	comments	T. Gradient [mK/m]
HG1	PS76/256 3r4	10.08./22:46 11.08./00:34	1854	No sensor 6	67.2
BGR10-3r2					
HG2	PS76/302	25.08./11:35-12:45	1772	No sensor 6	58.6
HG3	PS76/306	25.08./22:01-23:20	2069	No sensor 6	69.6
HG4	PS76/308	26.08./04:34-06:15	2124	No sensor 6	70.4
HG5	PS76/309	26.08./08:27-10:05	2136	No sensor 6	77.9
HG6	PS76/310	26.08./12:25-14:15	2132	No sensor 6	113
HG7	PS76/312	26.08./18:16-19:35	1172	No sensor 6	21.6 No distinct gradient
HG8	PS76/322	27.08./09:08-10:20	896	No sensor 6	No temperature Gradient
HG9	PS76/323	27.08./13:30-14:35	1150	No sensor 6	No temperature Gradient
BGR10-3r3					
HG10	PS76/352	01.09./00:50-02:20	1519	No sensor 6	55.4
HG11	PS76/353	01.09./03:36-05:05	1669	No sensor 6	58.6
HG12	PS76/354	01.09./06:12-07:45	1745	No sensor 6	55.4
HG13	PS76/355	01.09./08:53-10:30	1813	No sensor 6	59.9
HG14	PS76/356	01.09./11:38-13:15	1896	No sensor 6	37.4
HG15	PS76/357	01.09./14:25-16:05	1957	No sensor 6	58.1
HG16	PS76/394 3r2	06.09./05:11-07:03	1959	No sensor 6	49.8
HG17	PS76/397 3r3	06.09./11:08-12:52	1982	No sensor 6	51.5
HG18	PS76/398 3r3	06.09./14:08-15:53	2019	No sensor 6	59.4
HG19	PS76/399 LT	06.09./18:15-20:03	1909	No sensor 6	43.1
HG20	PS76/401 3r2	07.09./00:02-01:43	1658	No sensor 6	36.0
HG21	PS76/402 LT	07.09./04:16-05:55	1704	No sensor 6	49.0
BGR10-3r1					
HG22	PS76/415	16.09./09:46-11:41	2317	No sensor 3 5 bad	63.0
HG23	PS76/416	16.09./13:05-14:55	2241	No sensor 3 5 bad	63.9
HG24	PS76/417	16.09./16:11-17:43	2005	No sensor 3 5 bad	66.85
HG25	PS76/418	16.09./19:03-20:28	1470	No sensor 3 5 bad	23.7
BGR10-3r4					
HG26	PS76/446	18.09./06:42-08:10	1445	No sensor 3 2 and 8 bad	27.3
HG27	PS76/447	18.09./09:15-10:47	1506	No sensor 3	30.64
HG28	PS76/448	18.09./11:35-12:56	1548	No sensor 3	29.6
HG29	PS76/491	23.09./22:24-23:47	1587	No sensor 3 2 bad	37.15
HG30	PS76/492	24.09./00:54-02:18	1646	No sensor 3	41.0
HG31	PS76/493	24.09./03:17-04:45	1689	No sensor 3 5 bad	53.0
HG32	PS76/494	24.09./05:43-07:18	1777	No sensor 3 2 and 5 bad	50.5

A.13 CORING STATION LIST

Core label	Site	Latitude	Longitude	Water Depth (m)	Recovery (cm)	Coring date (dd:mm:yyyy)	on deck (hh:mm)	Remarks
PS76/248-04 GC	248	69° 41,52'N	64° 14,08'W	1928	131	08.08.2010	16:18	w/p
PS76/256-02 GC	256	71° 12,13'N	61° 38,07'W	1903	312	11.08.2010	02:01	w/p
PS76/280-01 GC	280	75° 11,94'N	62° 41,88'W	190	119	15.08.2010	14:03	w/p
PS76/282-01 GC	282	75° 19,27'N	61° 55,17'W	923	300	15.08.2010	16:24	w/p
PS76/284-01 GC	284	75° 26,65'N	61° 07,76'W	437	0	15.08.2010	18:33	w/p
PS76/286-01 GC	286	75° 33,98'N	60° 20,21'W	483	37	15.08.2010	20:40	w/p
PS76/290-01 GC	290	74° 01,34'N	69° 45,14'W	1718	83	17.08.2010	10:42	w/p
PS76/292-01 GC	292	74° 03,92'N	68° 38,54'W	2056	350	17.08.2010	14:22	w/p
PS76/293-01 GC	293	74° 13,52'N	68° 45,50'W	2002	386	17.08.2010	14:22	w/op
PS76/294-01 GC	294	74° 14,22'N	69° 36,58'W	1758	354	17.08.2010	16:37	w/op
PS76/361-01 GC	361	77° 05,77'N	71° 47,34'W	924	469	03.09.2010	14:15	w/op
PS76/363-02 GC	363	76° 52,92'N	71° 34,01'W	938	469	03.09.2010	19:35	w/op
PS76/365-02 GC	365	76° 39,04'N	71° 18,79'W	658	367	03.09.2010	23:03	w/op
PS76/367-02 GC	367	76° 26,84'N	71° 04,84'W	498	219	04.09.2010	02:29	w/op
PS76/369-02 GC	369	76° 11,94'N	70° 48,14'W	651	469	04.09.2010	06:04	w/op
PS76/371-02 GC	371	75° 58,24'N	70° 34,86'W	598	405	04.09.2010	09:08	w/op
PS76/373-02 GC	373	75° 44,74'N	70° 21,22'W	536	86	04.09.2010	12:03	w/op
PS76/383-02 GC	383	75° 17,69'N	69° 53,75'W	674	232	05.09.2010	10:16	w/op
PS76/387-02 GC	387	74° 50,42'N	69° 27,14'W	1300	332	05.09.2010	16:45	w/op
PS76/389-02 GC	389	74° 37,05'N	69° 13,75'W	1716	424	05.09.2010	21:00	w/op
PS76/391-02 GC	391	74° 23,36'N	69° 01,22'W	1864	427	05.09.2010	01:24	w/op
PS76/453-02 GC	453	73° 19,39' N	64° 57,70' W	2300	469	21.09.2010	12:28	w/op
PS76/456-01 GC	456	73° 25,02' N	64° 05,98' W	1526	370	21.09.2010	17:16	w/op
PS76/459-01 GC	459	73° 31,97' N	63° 16,19' W	594	50	21.09.2010	20:42	w/op
PS76/461-02 GC	461	73° 38,90' N	62° 24,66' W	575	335	21.09.2010	23:49	w/op
PS76/464-01 GC	464	73° 46,06' N	61° 28,19' W	570	235	22.09.2010	03:19	w/op

A.13 Coring station list

Core label	Site	Latitude	Longitude	Water Depth (m)	Recovery (cm)	Coring date (dd:mm:yyyy)	on deck (hh:mm)	Remarks
GC								
PS76/466-02 GC	466	73° 52,20' N	60° 40,45' W	551	284	22.09.2010	06:38	w/op
PS76/468-02 GC	468	73° 58,79' N	59° 47,76' W	511	61	22.09.2010	09:42	w/op
PS76/471-01 GC	471	74° 06,01' N	58° 48,05' W	223	3	22.09.2010	12:52	w/op
PS76/473-02 GC	473	74° 11,94' N	58° 01,45' W	599	198	22.09.2010	16:16	w/op
PS76/480-01 GC	480	73° 12,00' N	60° 17,97' W	309	68	23.09.2010	02:57	w/op
PS76/484-02 GC	484	72° 40,17' N	60° 39,24' W	719	260	23.09.2010	09:05	w/op
PS76/486-02 GC	486	72° 24,49' N	60° 48,82' W	645	469	23.09.2010	12:33	w/op
PS76/488-02 GC	488	72° 08,77' N	60° 58,77' W	1493	469	23.09.2010	17:05	w/op

w/p = with piston; w/op = without piston

A.14 GAS GEOCHEMISTRY SAMPLING LIST

Samples taken for adsorbed gas analyses.		Samples taken for free gas analyses.	
Core #	Interval/part	Core #	Interval/part
248	106-112	280	24
248	120-131	280	119
256	266-278	282	20
256	300-312	282	120
277	CC	282	210
280	100-114	282	250
282	295-300	282	270
282	300-310	282	280
282	090-100	282	290
284	CC	290	60
286	10-20	293	105
290	73-83	293	125
293	290-300	293	137
293	376-386	293	145
293	190-200	293	155
294	344-354	293	173
294	190-199	293	185
294	90-100	293	198
294	290-300	293	200
361	459-469	293	300
363	459-469	293	355
365	357-367	294	295
367	193-203	294	330
369	459-469	361	425
371	395-405	363	425
383	222-232	365	353
387	322-332	367	180
389	414-424	369	450
391	417-427	371	400
453	459-469	383	215
456	CC	387	315
456	360-370	389	380
459	CC	391	415
459	cutting shoe	393	170
464	CC	453	430
468	CC	456	350
471	CC	461	325
473	CC	464	320
480	CC	466	270
486	459-469	484	250
488	459-469	486	450
488	CC	488	457

A.15 ONSHORE ROCK SAMPLING LIST

Trip	Sample Point	Date (dd.mm.yy)	Latitude (dec min N)	Longitude (dec min W)	Elevation (m)	Locality
Meteorbugt 1	1	27.08.10	76°23.822	64°04.675	841	Meteorbugt
Meteorbugt 1	2a	27.08.10	76°16.933	64°29.898	718	Meteorbugt
Meteorbugt 1	2b	27.08.10	76°17.004	64°29.779	715	Meteorbugt
Meteorbugt 1	3a	27.08.10	76°08.887	64°40.360	335	near Saveqarfik
Meteorbugt 1	3b	27.08.10	76°08.632	64°40.800	246	near Saveqarfik
Meteorbugt 1	3c	27.08.10	76°08.787	64°40.655	270	near Saveqarfik
Meteorbugt 1	4	27.08.10	76°08.445	64°02.893	258	near Nugssuapaluk
Meteorbugt 1	5	27.08.10	76°04.323	64°59.006	204	Meteoritø
Meteorbugt 1	6	27.08.10	76°06.098	64°03.821	207	near Navdlortoq
Meteorbugt 2	7a	27.08.10	76°22.684	64°30.144	840	Meteorbugt
Meteorbugt 2	8a	27.08.10	76°01.671	65°06.769	303	Meteoritø, near Savigsivik
Meteorbugt 2	9	27.08.10	75°57.61	65°02.88	4	Bushnan
Meteorbugt 2	10	27.08.10	75°58.821	65°02.012	0	Bushnan
Crimson Cliffs 1	11a	28.08.10	75°55.304	66°32.732	331	Kap York, Peary Monument
Crimson Cliffs 1	11b	28.08.10	75°55.307	66°32.797	341	Kap York, Peary Monument
Crimson Cliffs 1	12a	28.08.10	75°56.520	66°33.334	297	W' Peary Monument
Crimson Cliffs 1	12b	28.08.10	75°56.503	66°33.267	289	W' Peary Monument
Crimson Cliffs 1	13	28.08.10	75°59.618	67°06.439	309	E' Sisússat
Crimson Cliffs 1	14a	28.08.10	76°01.942	67°29.593	380	between Sisússat and Sukaussat
Crimson Cliffs 1	14b	28.08.10	76°01.981	67°29.912	431	between Sisússat and Sukaussat
Crimson Cliffs 1	15	28.08.10	76°03.549	67°53.488	548	W' Sukaussat
Crimson Cliffs 1	16	28.08.10	76°03.794	68°05.927	525	near Súkat
Crimson Cliffs 2	17a	30.08.10	76°07.763	68°29.387	219	Parker Snow Bugt
Crimson Cliffs 2	17b	30.08.10	76°07.790	68°29.665	201	Parker Snow Bugt
Crimson Cliffs 2	18	30.08.10	76°09.715	68°40.849	333	Parker Snow Bucht, near Kap Dudley Digges
Crimson Cliffs 2	19	30.08.10	76°15.440	68°55.999	235	Nigarfivik, NW' Pitugfik glacier
Pitufik Land 1	20	30.08.10	76°17.986	69°11.558	289	SE' of Qaersorssuaq
Pitufik Land 1	21a	30.08.10	76°21.336	69°29.665	216	SE' of Kap Atholl
Pitufik Land 1	21b	30.08.10	76°21.362	69°29.819	210	SE' of Kap Atholl
Pitufik Land 1	22	30.08.10	76°22.991	69°37.063	191	near Kap Atholl
Pitufik Land 1	23a	30.08.10	76°24.710	69°32.388	388	Katitdlarnat
Pitufik Land 1	23c	30.08.10	76°24.657	69°32.975	379	Katitdlarnat
Steensby Land 1	24	31.08.10	76°49.437	70°13.534	7	Granville Fjord, Kap Peary
Steensby Land 1	25a	31.08.10	76°51.735	70°08.714	10	Granville Fjord
Steensby Land 1	25b	31.08.10	76°51.747	70°08.494	25	Granville Fjord

A.15 Onshore rock sampling list

Trip	Sample Point	Date (dd.mm.yy)	Latitude (dec min N)	Longitude (dec min W)	Elevation (m)	Locality
Steensby Land 1	26	31.08.10	76°56.220	69°54.787	3	Granville Fjord
Steensby Land 1	27	31.08.10	77°01.330	69°40.165	21	Granville Fjord
Steensby Land 1	28	31.08.10	76°58.226	69°34.261	606	Granville Fjord
Steensby Land 1	29	31.08.10	76°48.877	70°02.596	2	Granville Fjord
Pitufik Land 2	30	31.08.10	76°19.883	68°19.351	563	W' Freuchen Nunatak
Pitufik Land 2	31a	31.08.10	76°22.710	68°47.882	779	S' Thule Airbase
Pitufik Land 2	31b	31.08.10	76°22.711	68°47.865	775	S' Thule Airbase
Pitufik Land 2	32	31.08.10	76°21.938	68°48.036	753	S' Thule Airbase
Pitufik Land 2	33a	31.08.10	76°20.097	68°45.728	377	S' Thule Airbase
Pitufik Land 2	33b	31.08.10	76°20.080	68°45.677	371	S' Thule Airbase
Pitufik Land 2	34	31.08.10	76°17.628	68°45.493	356	N' Pitugfik glacier
Pitufik Land 2	35a	31.08.10	76°17.187	68°46.659	295	N' Pitugfik glacier
Pitufik Land 2	35b	31.08.10	76°17.207	68°46.973	333	N' Pitugfik glacier
Pitufik Land 2	36	31.08.10	76°16.927	68°49.888	321	N' Pitugfik glacier
Pitufik Land 2	37	31.08.10	76°15.216	68°51.463	19	Near igarfivik, NW' Pitufik glacier
Crimson Cliffs 3	38a	02.09.10	76°05.412	68°24.799	262	Crimson Cliffs
Crimson Cliffs 3	38b	02.09.10	76°05.434	68°24.888	261	Crimson Cliffs
Crimson Cliffs 3	39	02.09.10	76°04.987	68°14.975	208	Crimson Cliffs
Crimson Cliffs 3	40	02.09.10	76°02.192	67°38.207	395	Crimson Cliffs
Crimson Cliffs 3	41	02.09.10	76°01.353	67°16.388	294	Crimson Cliffs
Crimson Cliffs 3	42	02.09.10	76°00.188	67°08.963	331	Crimson Cliffs
Washington Land	43	11.09.10	80°27.685	66°42.699	133	Lafayette Bugt
Washington Land	44	11.09.10	80°27.666	66°42.262	136	Lafayette Bugt
Washington Land	45	11.09.10	80°27.677	66°42.826	108	Lafayette Bugt
Washington Land	46	11.09.10	80°27.684	66°42.765	128	Lafayette Bugt
Washington Land	47	11.09.10	80°21.219	67°22.066	243	Kap Jefferson
Washington Land	48	11.09.10	80°10.868	67°20.610	63	Morris Bugt
Prudhoe Land	50	11.09.10	77°46.915	71°18.033	380	Prudhoe Land (S)
Prudhoe Land	51	11.09.10	77°53.000	71°22.123	513	Fjord between Cap Powell & Cap Saumarez
Prudhoe Land	52	11.09.10	77°55.106	71°53.863	497	Kap Powell
Prudhoe Land	53	11.09.10	77°56.720	72°07.920	515	Kap Chalon
Prudhoe Land	54	11.09.10	78°00.151	72°01.279	713	Prudhoe Land
Prudhoe Land	55	11.09.10	77°02.957	69°45.958	231	Steensby Land
Prudhoe Land	56	11.09.10	77°04.505	69°39.925	551	Steensby Land
Steensby Land 2	57	12.09.10	77°05.052	69°46.320	591	Steensby Land

A.15 Onshore rock sampling list

Trip	Sample Point	Date (dd.mm.yy)	Latitude (dec min N)	Longitude (dec min W)	Elevation (m)	Locality
Steensby Land 2	59	12.09.10	77°12.661	70°14.490	858	Steensby Land
Steensby Land 2	60	12.09.10	77°10.260	70°36.376	187	Steensby Land
Steensby Land 2	61	12.09.10	77°11.486	70°51.596	281	Steensby Land
Bylot Sund	61X	12.09.10	76°17.092	68°58.321	334	Pitufik Land
Bylot Sund	62	13.09.10	76°19.012	69°05.577	234	Pitufik Land
Bylot Sund	63	13.09.10	76°20.694	69°18.501	140	Pitufik Land
Bylot Sund	64	13.09.10	76°22.508	69°32.543	299	Pitufik Land
Bylot Sund	65	13.09.10	76°25.042	69°58.029	278	Pitufik Land
Bylot Sund	66	13.09.10	76°24.248	70°02.289	13	Pitufik Land
Bylot Sund	67	13.09.10	76°27.126	70°09.887	15	Pitufik Land
Crimson Cliffs 4	68	13.09.10	76°02.693	67°41.977	1	Crimson Cliffs
Crimson Cliffs 4	69	13.09.10	76°00.639	67°18.022	2	Crimson Cliffs

A.16 SUMMARY OF HELICOPTER OPERATIONS

Flight time and fuel consumption ARK-XXV/3 30.07. - 10.10.2010					Date:	07.10.10
D-HANT			D-HLSZ			
Flight time	Fuel consumption	Average	Flight time	Fuel consumption	Average	
15:56 h	3276 ltr	205,6 ltr/h	121:37 h	24905 ltr	204,8 ltr/h	
Total fuel amount:		28181 ltr				
Average fuel consumption:		204,9 ltr/h				
Scientific flights:	162	130:52	11778 NM	21825 Km		
Aeromagnetics:	40					
Seismics:	26					
Geological sampling:	96					
Passenger flights:	8	5:36 h	504 NM	934 Km		
Training flights:	1	1:05 h	87 NM	161 Km		
Total flight hours:		137:33 h				
Total flight distance:		12369 NM	22919 Km			

A.17 WEEKLY MARINE MAMMAL OBSERVATION REPORTS

Marine Fauna Mitigation Weekly Report	CLIENT; BGR Germany	DECC Ref;	Project; EOM 1288
		Report No.; 1	Date; 16/8/10

DISTRIBUTION; As directed by client, plus all MMOs/PAM operators and RPS project manager

MMOs; Sarah Stelter
PAM Operators; N/A

Seismic Contractor; Dr. Volkmar Damm, Head of Unit Marine Seismics, BGR
Vessel; R/V POLARSTERN
Survey type; 2D Seismic

WEEKLY SUMMARY

Report period;	08/11/10 to 15/08/10
Total hours visual observation	81:23
Visual obs with guns	75:23
Total hours acoustic monitoring	00:00
Acoustic monitoring with guns	00:00
Total no. soft-starts during daylight/good visibility;	4
Total no. soft-starts during hours of darkness/poor visibility;	0
No. gun tests	0
No. visual pre-watch periods	4
No. acoustic pre-watch periods	0
No. cetacean sightings	0
No. acoustic detections	0
No. concurrent sighting/detections	4
No. mitigation actions initiated	0
Incidences of non-compliance	0

Weather conditions

Weather conditions for the week were variable. There were periods of intermittent fog which reduced visibility to less than 1km, throughout the day on most days. Cloud coverage was 90 - 100%, sea swells were less than 0.5 m, with Beaufort States averaging 1 - 2, and overall winds were less than 5 - 6 knots. Overall sighting conditions were good with periods of poor sighting conditions due to heavy fog. Twenty four hours of daylight persists during this time of year with a slight reduction of light between the hours of 03:00 to 05:00 UTC. Areas of large ice formations were observed ranging from large intermittent ice bergs to ice fields that covered large areas.

Soft-start procedures and compliance

The soft start procedures were conducted in Greenland waters according to the JNCC 2009 seismic guidelines. An initial 30 minute pre-shooting search was conducted by the MMO before commencement of airgun operations. After which time, the guns were ramped up gradually starting with one gun shooting for 22 shots then the next gun added after another 22 shot interval for a total of 6 guns total added to the ramp up until full power was reached which took approximately 33-35 minutes to full power. There were no compliance issues to report during this reporting period.

PAM Status

N/A

MMO Sightings

Ref	Species	Group size	Range (m)	Vessel status	Action / Comment
1	Harbor Seal	150	5	FullPower	No mitigation required
2	Seal UnID	1	150	Full Power	No mitigation required
3	Hooded Seal	1	200	Full Power	No mitigation required
4	Harbor Seal	1	100	Guns Off	

Marine Fauna Mitigation Weekly Report	CLIENT; BGR Germany	DECC Ref;	Project; EOM 1288
		Report No.; 2	Date; 23/08/10

DISTRIBUTION; As directed by client, plus all MMOs/PAM operators and RPS project manager

MMOs; Sarah Stelter
PAM Operators; N/A

Seismic Contractor; Dr. Volkmar Damm, Head of Unit Marine Seismics, BGR
Vessel; R/V POLARSTERN
Survey type; 2D

WEEKLY SUMMARY

Report period;	16/08/10 to 22/08/10
Total hours visual observation	149:01
Visual obs with guns	143:11
Total hours acoustic monitoring	N/A
Acoustic monitoring with guns	N/A
Total no. soft-starts during daylight/good visibility;	5
Total no. soft-starts during hours of darkness/poor visibility;	0
No. gun tests	0
No. visual pre-watch periods	7
No. acoustic pre-watch periods	0
No. cetacean sightings	0
No. acoustic detections	0
No. concurrent sighting/detections	5
No. mitigation actions initiated	0
Incidences of non-compliance	1

Weather conditions

Weather conditions for this weekly reporting period were variable. Conditions were mostly cloudy with 100% overcast. Winds ranged between 2 - 8 knots with Beaufort States of 1 on average. Swells were minimal of less than 1 m. Mostly ice free seas with scattered ice bergs. Sighting conditions ranged from good to poor depending on fog in the area and visiblility was highly variable from 500 m to the horizon.Polar twilight is starting to become darker during hours of 02:00-06:00 with visibility less than 500 m if significant cloud cover overhead.

Soft-start procedures and compliance

The soft start procedures were conducted in Greenland waters according to the JNCC 2009 seismic guidelines. An intial 30 minute pre-shooting search was conducted by the MMO before commencement of airgun operations. After which time, the guns were ramped up gradually starting with one gun shooting for 22 shots then the next gun added after another 22 shot interval for a total of 6 guns total added to the ramp up until full power was reached which took approximately 25-35 minutes to full power.

There was one incident of non compliance according to JNCC standards. On 18 August 2010 at 19:02 the airguns had lost a buoy from the top of the gun apparatus, and the guns stopped shooting for a period of 22 minutes. They resumed shooting at full power without the 20 minute ramp up. I addressed the situation and they are aware of the procedures.

PAM Status

N/A

MMO Sightings

Ref	Species	Group size	Range (m)	Vessel status	Action / Comment
5	Ringed Seal	1	250	Full Power	No Mitigation required
6	Hooded Seal	6	250	Full Power	No Mitigation required
7	UnID Seal	1	300	Full Power	No Mitigation required
8	Hooded Seal	1	220	Full Power	No Mitigation required
9	UnID Seal	3	250	Full Power	No Mitigation required

Marine Fauna Mitigation Weekly Report	CLIENT; BGR Germany	DECC Ref;	Project; EOM 1288
		Report No.; 3	Date; 30/08/10

DISTRIBUTION; As directed by client, plus all MMOs/PAM operators and RPS project manager

MMOs; Sarah Stelter
PAM Operators; N/A

Seismic Contractor; Dr. Volkmar Damm, Head of Unit Marine Seismics, BGR
Vessel; R/V POLARSTERN
Survey type; 2D

WEEKLY SUMMARY

Report period;	23/08/10 to 29/08/10
Total hours visual observation	87:12
Visual obs with guns	80:51
Total hours acoustic monitoring	N/A
Acoustic monitoring with guns	N/A
Total no. soft-starts during daylight/good visibility;	4
Total no. soft-starts during hours of darkness/poor visibility;	0
No. gun tests	0
No. visual pre-watch periods	5
No. acoustic pre-watch periods	0
No. cetacean sightings	0
No. acoustic detections	0
No. concurrent sighting/detections	4
No. mitigation actions initiated	0
Incidences of non-compliance	0

Weather conditions

Weather conditions for this weekly reporting period were variable. Conditions were mostly cloudy with 100% overcast during the beginning of the week but was clear skies by weeks end. Winds ranged between 2 - 8 knots with Beaufort States of 1 on average. Swells were minimal of less than 1 m. Mostly ice free seas with scattered ice bergs. Sighting conditions were generally excellent with periods of dense fog in areas and visibillity less than 2 km. Polar twilight is starting to become darker during hours of 02:00-06:00 with visibility less than 500 m if significant cloud cover overhead.

Soft-start procedures and compliance

The soft start procedures were conducted in Greenland waters according to the JNCC 2009 seismic guidelines. An intial 30 minute pre-shooting search was conducted by the MMO before commencement of airgun operations. After which time, the guns were ramped up gradually starting with one gun shooting for 22 shots then the next gun added after another 22 shot interval for a total of 6 guns total added to the ramp up until full power was reached which took approximately 25-35 minutes to full power.

No compliance issues during reporting period.

PAM Status

N/A

MMO Sightings

Ref	Species	Group size	Range (m)	Vessel status	Action / Comment
10	Ringed Seal	1	174	Full Power	No Mitigation required
11	UnID Seal	1	225	Full Power	No Mitigation required
12	Ringed Seal	1	5	Full Power	No Mitigation required
13	UnID Seal	1	150	Full Power	No Mitigation required

Marine Fauna Mitigation Weekly Report	CLIENT; BGR Germany	DECC Ref;	Project; EOM 1288
		Report No.; 4	Date; 06/09/10

DISTRIBUTION; As directed by client, plus all MMOs/PAM operators and RPS project manager

MMOs; Sarah Stelter
PAM Operators; N/A

Seismic Contractor; Dr. Volkmar Damm, Head of Unit Marine Seismics, BGR
Vessel; R/V POLARSTERN
Survey type; 2D

WEEKLY SUMMARY

Report period;	30/08/10 to 05/09/10
Total hours visual observation	75:52
Visual obs with guns	52:37
Total hours acoustic monitoring	N/A
Acoustic monitoring with guns	N/A
Total no. soft-starts during daylight/good visibility;	2
Total no. soft-starts during hours of darkness/poor visibility;	0
No. gun tests	0
No. visual pre-watch periods	2
No. acoustic pre-watch periods	0
No. cetacean sightings	0
No. acoustic detections	0
No. concurrent sighting/detections	0
No. mitigation actions initiated	0
Incidences of non-compliance	0

Weather conditions

Weather conditions for this weekly reporting period were very good. Conditions were mostly cloudy with 100% during the morning hours and cleared throughout the day. Winds ranged between 5 - 8 knots with Beaufort States of 1 on average. On 4 September, Beaufort States of 4 and winds of 20 kts were recorded creating poor sighting conditions in the early half of the day. Swells were minimal of less than 1 m. Mostly ice free seas with large scattered ice bergs. Sighting conditions were generally excellent with periods of dense fog in areas and visibility less than 2 km. Polar twilight is increasingly becoming darker during the hours of 02:00-06:00 with visibility less than 500 m.

Soft-start procedures and compliance

The soft start procedures were conducted in Greenland waters according to the JNCC 2009 seismic guidelines. An initial 30 minute pre-shooting search was conducted by the MMO before commencement of airgun operations. After which time, the guns were ramped up gradually starting with one gun shooting for 22 shots then the next gun added after another 22 shot interval for a total of 6 guns total added to the ramp up until full power was reached which took approximately 25-35 minutes to full power.

No compliance issues during reporting period.

PAM Status

N/A

Marine Fauna Mitigation Weekly Report	CLIENT; BGR Germany	DECC Ref;	Project; EOM 1288
		Report No.; 5	Date; 13/09/10

DISTRIBUTION; As directed by client, plus all MMOs/PAM operators and RPS project manager

MMOs; Sarah Stelter
PAM Operators; N/A

Seismic Contractor; Dr. Volkmar Damm, Head of Unit Marine Seismics, BGR
Vessel; R/V POLARSTERN
Survey type; 2D

WEEKLY SUMMARY

Report period;	06/09/10 to 12/09/10
Total hours visual observation	83:20
Visual obs with guns	57:00
Total hours acoustic monitoring	N/A
Acoustic monitoring with guns	N/A
Total no. soft-starts during daylight/good visibility;	5
Total no. soft-starts during hours of darkness/poor visibility;	0
No. gun tests	0
No. visual pre-watch periods	5
No. acoustic pre-watch periods	0
No. cetacean sightings	1
No. acoustic detections	0
No. concurrent sighting/detections	6
No. mitigation actions initiated	0
Incidences of non-compliance	0

A.17 Weekly marine mammal observation reports

Weather conditions

Weather conditions for this weekly reporting period were of mixed conditions. The week began with heavy seas of 3 m and gusts of 20 - 25 kts and sighting and visibility were poor. On 09 September, the storm peaked into 37 - 40 kts winds and sea states of 6 - 7 and seas 4 m. After shooting on 9 September, observations were halted due to bad weather and very poor sighting conditions. Skies were mostly cloudy with 100% during the morning hours and cleared throughout the day with variable fog. Temperatures ranged from -6 to -2 degrees C. Moving to the north, thick ice packs and icebergs covered 50 - 60 percent of the total sea area. Sighting conditions were generally excellent with periods of dense fog and visibility less than 2 km. Polar twilight is increasingly becoming darker during the hours of 02:00-07:00 with visibility less than 500 m.

Soft-start procedures and compliance

The soft start procedures were conducted in Greenland waters according to the JNCC 2009 seismic guidelines. An initial 30 minute pre-shooting search was conducted by the MMO before commencement of airgun operations. After which time, the guns were ramped up gradually starting with one gun shooting for 22 shots then the next gun added after another 22 shot interval for a total of 6 guns total added to the ramp up until full power was reached which took approximately 25-35 minutes to full power.

No compliance issues during reporting period.

PAM Status

N/A

MMO Sightings

Ref	Species	Group size	Range (m)	Vessel status	Action / Comment
14	Unidentified Seals	2	500	Full Power	None
15	Ringed Seal	1	300	Full Power	None
16	Hooded Seal	1	225	Full Power	None
17	UnID Seal	1	300	Full Power	None
18	UnID Baleen Whale	2	1200	Line Change	None
19	UnID Seal	1	350	Full Power	None

Marine Fauna Mitigation Weekly Report	CLIENT; BGR Germany	DECC Ref;	Project; EOM 1288
		Report No.; 6	Date; 20/09/10

DISTRIBUTION; As directed by client, plus all MMOs/PAM operators and RPS project manager

MMOs; Lead: Sarah Stelter
PAM Operators; N/A

Seismic Contractor; Dr. Volkmar Damm, Head of Unit Marine Seismics, BGR
Vessel; R/V POLARSTERN
Survey type; 2D

WEEKLY SUMMARY

Report period;	13/09/10 to 20/09/10
Total hours visual observation	75:41
Visual obs with guns	58:15
Total hours acoustic monitoring	N/A
Acoustic monitoring with guns	N/A
Total no. soft-starts during daylight/good visibility;	3
Total no. soft-starts during hours of darkness/poor visibility;	1
No. gun tests	0
No. visual pre-watch periods	3
No. acoustic pre-watch periods	0
No. cetacean sightings	0
No. acoustic detections	0
No. concurrent sighting/detections	0
No. mitigation actions initiated	0
Incidences of non-compliance	0

Weather conditions

Weather conditions for this weekly reporting period were generally good. The week began with mild seas of less than 2 m and gusts of 10 - 18 kts and sighting conditions and visibility were good to excellent. On 18 September, the seas rose from 14 kts winds and sea states of 4 and seas 2 m. Skies were mostly 100% cloudy throughout the day with some variable fog. Temperatures ranged from 1.2 to 1.9 degrees C. Moving back toward the south, very little icebergs were seen as the ship moved farther into the Baffin Bay. Sighting conditions were generally excellent and visibility extending to the horizon. Polar twilight is increasingly becoming darker during the hours of 23:20-01:30 with visibility less than 500 m.

Soft-start procedures and compliance

The soft start procedures were conducted in Greenland waters according to the JNCC 2009 seismic guidelines. An initial 30 minute pre-shooting search was conducted by the MMO before commencement of airgun operations. After which time, the guns were ramped up gradually starting with one gun shooting for 22 shots then the next gun added after another 22 shot interval for a total of 6 guns total added to the ramp up until full power was reached which took approximately 25-35 minutes to full power.

No compliance issues during reporting period.

PAM Status

N/A

Marine Fauna Mitigation Weekly Report	CLIENT; BGR Germany	DECC Ref;	Project; EOM 1288
		Report No.; 7	Date; 27/09/10

DISTRIBUTION; As directed by client, plus all MMOs/PAM operators and RPS project manager

MMOs; Lead: Sarah Stelter
PAM Operators; N/A

Seismic Contractor; Dr. Volkmar Damm, Head of Unit Marine Seismics, BGR
Vessel; R/V POLARSTERN
Survey type; 2D

WEEKLY SUMMARY

Report period;	20/09/10 to 26/09/10
Total hours visual observation	52:07
Visual obs with guns	28:07
Total hours acoustic monitoring	N/A
Acoustic monitoring with guns	N/A
Total no. soft-starts during daylight/good visibility;	0
Total no. soft-starts during hours of darkness/poor visibility;	2
No. gun tests	0
No. visual pre-watch periods	0
No. acoustic pre-watch periods	0
No. cetacean sightings	1
No. acoustic detections	0
No. concurrent sighting/detections	3
No. mitigation actions initiated	0
Incidences of non-compliance	0

Weather conditions

Weather conditions for this weekly reporting period were good to excellent. The week began with mild seas of less than 2 m and gusts of 10 - 18 kts and sighting conditions and visibility were good to excellent. On 23 September, the seas rose to a sea state of 4 with waves of 2 m. Skies were 100% cloudy throughout the days with some variable fog and light precipitation. Moving back toward the south, very little icebergs were observed and none were observed south of 72 degrees north. Sighting conditions were generally excellent and visibility extending to the horizon. 26 September had variable fog cover and rain with seas choppy with many whitecaps. Darkness is increasing by 15 to 20 minutes each day during the hours of 22:00-22:30 with visibility less than 500 m.

Soft-start procedures and compliance

The soft start procedures were conducted in Greenland waters according to the JNCC 2009 seismic guidelines. An initial 30 minute pre-shooting search was conducted by the MMO before commencement of airgun operations. After which time, the guns were ramped up gradually starting with one gun shooting for 22 shots then the next gun added after another 22 shot interval for a total of 6 guns total added to the ramp up until full power was reached which took approximately 25-35 minutes to full power.

No compliance issues during reporting period.

PAM Status

N/A

MMO Sightings

Ref	Species	Group size	Range (m)	Vessel status	Action / Comment
23	Unidentified Seal	1	500	Full Power	No mitigation required
24	Unidentified Seal	1	800	Full Power	No mitigation required
25	Minke Whale	1	5	Full	No mitigation required

A.18 LIST OF FIGURES AND TABLES

Fig. 1: Cruise track of R/V Polarstern during ARK-XXV/3	2
Abb.1. Fahrtverlauf von F/S Polarstern während ARK-XXV/3	2
Fig. 2.1: Geological map of northern Baffin Bay.....	8
Fig. 2.2: Location of seismic reflection and refraction lines, land based seismic stations, aeromagnetic surveying, heat flow measurements and geological sampling.....	13
Fig. 3.1: The seismic exploration vessel M/V Bergen Surveyor in the Melville Bay	16
Fig. 4.1: Sketch of R/V Polarstern with the locations of relevant equipment	24
Fig. 4.2 Scheme of the data acquisition installed during ARK-XXV/3	25
Fig. 5.1: Multi-beam data of the eastern part of BGR10-3r1	27
Fig. 5.2: CTD stations during expedition ARK-XXV/3	29
Fig. 5.3: CTD-workflow process on board R/V Polarstern.....	30
Fig. 5.4: Main research area of Northern Baffin Bay with track plot.	31
Fig. 5.5: Bathymetric data of profile BGR10-3r3	32
Fig. 6.1: HYDROMAP CONTROL, basic settings	34
Fig. 6.2: HYDROMAP CONTROL, receiver amplification	34
Fig. 6.3: HYDROMAP CONTROL, output sampling rate.....	35
Fig. 6.4: HYDROMAP CONTROL, depth source and penetration depth	35
Fig. 6.5: PARASTORE, acquisition and storage	36
Fig. 6.6: PARASTORE, new acquisition window.....	36
Fig. 6.7: PARASTORE, automatic delay and depth source	37
Fig. 6.8: PARASTORE, SEG Y storage	37
Fig. 6.9: REFLEXW menu, Import of raw SEG Y files.....	38
Fig. 6.10: GeoFrame IESX, projection of PARASOUND profile MCS profile	39
Fig. 6.11: Toplap structures due to glacial erosion in the eastern Baffin Bay.	40
Fig. 6.12: Cross-bedding structures in the distal Baffin Fan.....	40
Fig. 6.13: Slope instability and gravitational sliding in the eastern Baffin Bay.....	41
Fig. 6.14: Small basin infills in the Melville Trough.....	41
Fig. 6.15: Erosion and overcompacted sediments with little to no reflectivity in the Kane Basin.	42
Fig. 6.16: Incisions northwest of Disko Island, possibly iceberg scour marks.....	42
Fig. 6.17: Testing of different SLF frequencies.	43
Fig. 7.1: KSS31 gravimeter system on R/V Polarstern.	45
Fig. 7.2: Principle sketch of the gravity sensor GSS30 of the gravimeter system KSS31M.....	46
Fig. 7.3: Comparison of BEARB and KSS31M unfiltered free-air gravity anomalies along profile BGR10-3M01	47
Fig. 7.4: Location of the mooring site of R/V Polarstern in Reykjavik.....	50
Fig. 7.5: Location of the mooring site of R/V Polarstern in Bremerhaven	51
Fig. 7.6: Comparison of free-air gravity anomalies along profiles BGR10-302/302a and -3r2.....	52
Fig. 7.7: Crossover errors (COE) of the KSS31 free-air gravity anomalies	52
Fig. 7.8: Map of the free-air gravity anomalies in the survey area of cruise ARK-XXV/3	53
Fig. 7.9: Differences of the shipboard free-air gravity data and the gravity datasets derived from satellite altimetry.....	54
Fig. 7.10: Histogram of differences between shipboard KSS31 free-air gravity anomalies and the corresponding gravity datasets derived from satellite altimetry.	55
Fig. 7.11: Comparison of the ship-based KSS31M and satellite free-air gravity anomalies along profiles BGR10-302/302a and BGR10-3r3	57
Fig. 7.12: Map of the free-air gravity anomalies. The underlying gravity grid was compiled by merging ARK-XXV/3 and MSM09/3 shipboard gravity observations.	58
Fig. 7.13: Map of the free-air gravity anomalies. The underlying gravity grid was compiled by merging shipboard gravity observations and DNSC08 gravity data derived from satellite altimetry.	59
Fig. 7.14: Map of the free-air gravity anomalies of the ARK-XXV/3 survey area.	59
Fig. 7.15: Map of Bouguer gravity anomalies with no terrain corrections applied.	60

A.18 List of figures and tables

Fig. 7.16: Map of Bouguer gravity anomalies of the ARK-XXV/3 survey area with no terrain corrections applied.	61
Fig. 7.17: 2D density model explaining the free-air gravity anomalies along BGR10-306a.	62
Fig. 7.18: 2D density model explaining the free-air gravity anomalies along BGR10-307/307a.	63
Fig. 8.1: Schematic sketch of the towed gradiometer system setup.	64
Fig. 8.2: Components inside the fluxgate magnetometer tow fish.	65
Fig. 8.3: Installation of an experimental fluxgate sensor system in the helicopter.	67
Fig. 8.4: Calibration figure sailed on September 07, 2010.	68
Fig. 8.5: Result of the calibration pattern.	69
Fig. 8.6: Examples for removal of magnetic variations from the magnetic records.	72
Fig. 8.7: Magnetic anomalies acquired with the marine gradient magnetometer system.	73
Fig. 8.8: Magnetic anomalies acquired during the aeromagnetic measurements.	75
Fig. 8.9: Magnetic lines (shipborne and aeromagnetic) acquired during cruise ARK-XXV/3.	77
Fig. 8.10: Aeromagnetic and shipborne magnetic lines acquired during cruise ARK-XXV/3 and marine magnetic lines from cruise MSM09/3.	78
Fig. 8.11: Magnetic anomaly from one scalar sensor and reconstructed from the gradient related to an extremely high gravity anomaly on line BGR10-306a.	79
Fig. 8.12: Aeromagnetic lines acquired in the Kane Basin.	79
Fig. 8.13: Magnetic anomalies over the western flank of the Reykjanes ridge.	80
Fig. 9.1: Marine seismic methods.	81
Fig. 9.3: Sketch of the G-Gun pattern.	84
Fig. 9.4: The AWI G-Gun cage hanging from the A-Frame close before deployment.	85
Fig. 9.5: DigiCOURSE System 3 bird with compass.	86
Fig. 9.6: Streamer configuration used.	87
Fig. 9.7: Signal flow diagram for BGR's reflection seismic data acquisition system.	89
Fig. 9.8: A sonobuoy before and directly after deployment from the ship.	90
Fig. 9.9: The AWI Ocean bottom seismometer LOBSTER during deployment.	92
Fig. 9.10: Connecting the LOBSTER to an external GPS clock.	92
Fig. 9.11: Set up of land station 300stL2 equipped with a broadband seismometer.	94
Fig. 9.12: Set up of the seismometer of land station 450stL2.	94
Fig. 9.13: Hardware setup scheme for seismic ProMAX processing.	95
Fig. 9.14: Acquisition geometries for the seismic reflection lines - ice free conditions.	97
Fig. 9.15: Acquisition geometries for the seismic reflection lines - ice conditions.	98
Fig. 9.16: Acquisition geometries for the seismic reflection lines - Kane Basin.	98
Fig. 9.17: Example of a velocity analysis done at a CDP supergather after applying srme multiple reduction.	102
Fig. 9.18: Example of the interval velocity field based on the velocity analysis.	102
Fig. 9.19: Java CVS tool: Stack of the entire section with all velocity picks and semblance result of the selected time slice.	103
Fig. 9.20: Java CVS tool: Switch between the stack view and the color coded velocity view.	104
Fig. 9.21: Java CVS tool: Velocity picking.	104
Fig. 9.22: Example from line BGR10-309 for application of MASWEMR.	106
Fig. 9.23: Comparison between a raw stack section and the section after applying the above introduced processing sequence.	108
Fig. 9.24: Frequency spectrum of five shots of line BGR10-309 with the AWI source array.	109
Fig. 9.25: Frequency spectrum of five shots of line BGR08-304 with the BGR source array.	110
Fig. 9.26: Comparison of the migrated seismic sections of BGR10-309 and BGR08-304.	110
Fig. 9.27: Frequency power spectrum of 5 shots at different streamer towing depths.	112
Fig. 9.28: Two records, without (left hand side) and with own shot (right hand side). Note the regular linear noise, coming from the M/V Bergen Surveyor.	112
Fig. 9.29: Location map of the northern Baffin Bay. Red dots mark the positions of sonobuoys, black lines show the range of seismic shots with identified refracted arrivals at the station.	113
Fig. 9.30: Location map of the Kane Basin. Red dots mark the positions of sonobuoys, black lines show the range of seismic shots with identified refracted arrivals at the station.	114
Fig. 9.31: Seismic section from Sonobuoy 29, located on profile BGR10-321.	115

Fig. 9.32: Velocity depth model for SB 29	115
Fig. 9.33: OBS and land stations deployed during ARK-XXV/3.	118
Fig. 9.34: OBS and land stations deployed on the line AWI-20100450/BGR10-3r1	119
Fig. 9.35: OBS and land stations deployed on the line AWI-20100200/BGR10-3r2	120
Fig. 9.36: OBS and land stations deployed on the line AWI-20100300/BGR10-3r3	121
Fig. 9.37: Seismic record section of OBS 300st004 (hydrophone channel)	121
Fig. 9.38: Seismic record section of station 300st022 (hydrophone channel).....	122
Fig. 9.39: OBS and land stations deployed on the line AWI-20100400/BGR10-3r4	123
Fig. 9.40: Data example of the hydrophone component of OBS 400st006	123
Fig. 9.41: Five OBS with new 120 sec prototype seismometers deployed on a test network in the deep sea area.	124
Fig. 9.42: Band-pass (10-33 sec) filtered seismograms (vertical components) of the M=6.3 Aleutian Island earthquake from 03-Oct-2010 11:16 UTC.....	125
Fig. 10.1: BGR - hard ground heat flow probe	128
Fig. 10.2: BGR – hard ground probe deployment and recovery.....	128
Fig. 10.3: Heat flow measurement HG21 with the temperature of the 6 working sensors	129
Fig. 10.4: Estimation of the temperature gradient by linear regression for 3 stations.	130
Fig. 10.5: Map of the stations with measured temperature gradients in mK/m.	131
Fig.11.1: Symbols used for visual core description (VCD) and sediment nomenclature applied.	133
Fig.13.1: Pore water extraction in 1 m core sections and rhizons moistened in MilliQ water prior to be used.....	137
Fig. 14.1. Onshore sampling areas of cruise ARK-XXV/3.....	141
Fig. 15.1: Interpreted seismic line BGR10-306a	143
Fig. 15.2: Interpreted seismic line BGR10-307	144
Fig. 15.3: Interpreted seismic line BGR10-307a	145
Fig. 15.4: Interpreted seismic line BGR10-302	147
Fig. 15.5: Interpreted seismic line BGR10-302a	147
Fig. 15.6: Interpreted seismic line BGR10-309	151
Fig. 15.7: Interpreted seismic line BGR10-311	152
Tab. 5.1: Statistics of CTD measurements	28
Tab. 7.1: Observation report of the gravity tie measurements in Reykjavik and Bremerhaven	48
Tab. 8.1: Date and time of aeromagnetic helicopter flights and associated data file names	70
Tab. 9.1: Summary of all MCS lines	107

Die "**Berichte zur Polar- und Meeresforschung**" (ISSN 1866-3192) werden beginnend mit dem Heft Nr. 569 (2008) ausschließlich elektronisch als Open-Access-Publikation herausgegeben. Ein Verzeichnis aller Hefte einschließlich der Druckausgaben (Heft 377-568) sowie der früheren "**Berichte zur Polarforschung**" (Heft 1-376, von 1982 bis 2000) befindet sich im Internet in der Ablage des electronic Information Center des AWI (**ePIC**) unter der URL <http://epic.awi.de>. Durch Auswahl "Reports on Polar- and Marine Research" auf der rechten Seite des Fensters wird eine Liste der Publikationen in alphabetischer Reihenfolge (nach Autoren) innerhalb der absteigenden chronologischen Reihenfolge der Jahrgänge erzeugt.

To generate a list of all Reports past issues, use the following URL: <http://epic.awi.de> and select the right frame to browse "Reports on Polar and Marine Research". A chronological list in declining order, author names alphabetical, will be produced, and pdf-icons shown for open access download.

Verzeichnis der zuletzt erschienenen Hefte:

Heft-Nr. 609/2010 — "Daten statt Sensationen - Der Weg zur internationalen Polarforschung aus einer deutschen Perspektive", by Reinhard A. Krause

Heft-Nr. 610/2010 — "Biology of meso- and bathypelagic chaetognaths in the Southern Ocean", by Svenja Kruse

Heft-Nr. 611/2010 — "Materialparameter zur Beschreibung des zeitabhängigen nichtlinearen Spannungs – Verformungsverhaltens von Firn in Abhängigkeit von seiner Dichte", by Karl-Heinz Bässler

Heft-Nr. 612/2010 — "The Expedition of the Research Vessel 'Polarstern' to the Arctic in 2009 (ARK-XXIV/1)", edited by Gereon Budéus

Heft-Nr. 613/2010 — "The Expedition of the Research Vessel 'Polarstern' to the Antarctic in 2009 (ANT-XXV/3 - LOHAFEX)", edited by Victor Smetacek and Syed Wajih A. Naqvi

Heft-Nr. 614/2010 — "The Expedition of the Research Vessel 'Polarstern' to the Antarctic in 2009 (ANT-XXVI/1)", edited by Saad el Naggat and Andreas Macke

Heft-Nr. 615/2010 — "The Expedition of the Research Vessel 'Polarstern' to the Arctic in 2009 (ARK-XXIV/3)", edited by Wilfried Jokat

Heft-Nr. 616/2010 — "The Expedition of the Research Vessel 'Polarstern' to the Antarctic in 2009 (ANT-XXV/4)", edited by Christine Provost

Heft-Nr. 617/2010 — "The Expedition of the Research Vessel 'Polarstern' to the Amundsen Sea, Antarctica, in 2010 (ANT-XXVI/3)", edited by Karsten Gohl

Heft-Nr. 618/2010 — "Sozialhistorische Studie zur Polarforschung anhand von deutschen und österreich-ungarischen Polarexpeditionen zwischen 1868-1939", by Ursula Rack

Heft-Nr. 619/2010 — "Acoustic ecology of marine mammals in polar oceans", by Ilse Van Opzeeland

Heft-Nr. 620/2010 — "Cool Libraries in a Melting World - Proceedings of the 23rd Polar Libraries Colloquy 2010 June 13-18, 2010, Bremerhaven, Germany", edited by Marcel Brannemann and Daria O. Carle

Heft-Nr. 621/2010 — "The Expedition of the Research Vessel 'Polarstern' to the Arctic in 2010 (ARK-XXV/3)", edited by Volkmar Damm